Development and Testing of a Mobile Pilot Plant for the Advancement and Scale-up of the Hydrophobic-Hydrophilic Separation Process

Chad Michael Sechrist

Dissertation submitted to the faculty of the Virginia Polytechnic Institute and State University in partial fulfillment of the requirements for the degree of

Doctor of Philosophy
In
Mining Engineering

Christopher Aaron Noble, Chair
Roe-Hoan Yoon
Kaiwu Huang
Rick Q Honaker

April 28, 2023
Blacksburg, Virginia

Keywords: Ultrafine Particle Separation, Hydrophobic-Hydrophilic Separation, High-Value Carbon, Process Design

Copyright © 2022, Chad M Sechrist

Development and Testing of a Mobile Pilot Plant for the Advancement and Scale-up of the Hydrophobic-Hydrophilic Separation Process

Chad M Sechrist

Academic Abstract

Fine particle separation is a grand challenge in the mining and mineral processing industry. The industry standard process, froth flotation, is extremely robust and adaptable; however, it is inefficient for particles less than 20 microns. Owing to this limitation, some mining sectors, such as coal, opt to discard the ultrafine particles to waste impoundments as the costs to recover and dewater these materials are prohibitive. The Hydrophilic Hydrophobic Process (HHS) is one alternative to flotation that uses a recyclable solvent, rather than air bubbles, to selectively recover fine hydrophobic particles. Prior laboratory, proof-of-concept, and demonstration-scale testing has shown that the HHS process is extremely efficient, having no effective size limitation. The purpose of this research was to continue the development and improvement of the HHS process, through the design, construction, and testing of a mobile pilot plant. The pilot plant would in turn be used to demonstrate the robustness of the HHS process through a systemic study of multiple coal sources and ranks. In addition, the pilot plant would serve as a testbed for inquiry-based process intensification, the development and evaluation of design criteria for the various unit operation.

Through the course of this research, a 50 lb./hr. (product rate) pilot plant was constructed and commissioned. Initial investigations focused on the shakedown and design of key unit operations, including the agglomeration and de-emulsification (i.e. Morganizing) steps. Studies showed that the initial design of these units, namely pump induced mixing in agglomeration and packed bed emulsification in the Morganizer, were not adequate to meet production demands, and as such, these stages were redesigned after appropriate fundamental evaluations. After implementing the design changes, the pilot plant was successfully operated over a 7-month period,

routinely producing bituminous products with less than6% ash and less than 10% moisture as well as anthracite products with less than 3% ash and less than 4% moisture.

This study also evaluated a new approach to de-emulsification using a jig based Morganizer in place of the standard oscillating column Morganizer. The jig utilizes a pulsing mechanism to move liquid to break up agglomerates versus the mechanical disk stack. Preliminary results showed that the jig Morganizer was comparable to the oscillating unit at more than half the size. This new design provides a pathway for reduced cost, footprint, and improved scalability.

Lastly, this study evaluated both the HHS process and dual-scan X-ray based particle sorting as means of increasing the REE content of coal-based materials. Data from a pilot-scale x-ray sorter showed the unit was capable of preconcentrating REEs to over 300 ppm, while data from the HHS similarly showed the process was capable of REE recoveries of 85-90% and of preconcentrating REEs above 300 ppm. Altogether, these results indicate That both of these technologies are capable of efficiently and cost effectively preconcentrate REEs from wastes streams at operating coal preparation plants.

Development and Testing of a Mobile Pilot Plant for the Advancement and Scale-up of the Hydrophobic-Hydrophilic Separation Process

Chad M Sechrist

GENERAL AUDIENCE ABSTRACT

The mining sector has traditionally been a large producer of waste, with the vast majority of this waste being ultrafine particles that are unable to be recovered using conventional technologies. These particles are often disposed of in large surface impoundments, which are an environmental and social liability in many mining districts. This study has evaluated a novel method of fine particle separation, the hydrophobic-hydrophilic separation (HHS) process. The HHS process uses a recyclable oil to selectively agglomerate fine particles, which are subsequently dispersed and recovered. The oil is then filtered and recycled within the process creating an approach that is both efficient and environmentally friendly. In this study, a mobile pilot HHS plant was constructed and tested, with the results showing that the HHS can effectively recover fine carbon from waste coals, thus turning an environmental liability into a potential value stream for high-end applications. In addition, the study showed that the process can be further improved to reduce costs while improving overall efficiency. Overall, this study has provided the data needed to further commercialize the HHS process. If widely deployed, the HHS process has the potential to both reduce the current amount of waste fines being generated and reclaim the existing impoundments.

Acknowledgements

I would like to express my sincerest gratitude to my adviser, Dr. Aaron Noble, for his masterful guidance, criticisms, and priceless insight throughout my research project. Without his support and push, this accomplishment would not have been possible. Additionally, the valuable insight and support of my committee members, Dr. Rick Honaker, Dr. Kaiwu Huang, and Dr. Roe-Hoan Yoon are also gratefully acknowledged.

Three individuals need to be thanked for their support and motivation throughout this project. First is Dr. Serhat Keles. Without his support and friendship, the research project would have been a much more arduous process. His knowledge of processing and control systems was instrumental in making everything a success. Second is Mr. Robert (Bob) Bratton. Bob's endless knowledge and experience was instrumental in taking many of the half-baked ideas we had for design of the pilot plant and making them a reality. I hope that after this project, he can finally "retire." Third, is Mr. Glen Brock. His industry experience helped to facilitate the ease of completion of many challenges we faced working on this project. His friendship was also valuable to be there as support, to bounce ideas off, and to keep me grounded. I also acknowledge the staff at the Department of Mining and Minerals Engineering, particularly Mrs. Lori Andrews and Mrs. Annie Lawrence. They made sure we had whatever we needed to complete the objectives on this project and provided support in every way possible.

I would like to thank my parents, Mr. and Mrs. Jan and Kyna Sechrist for their unconditional support of a son who decided to change careers at this point in their life as well as every point in my life leading up to this accomplishment. Without their love and support, this process would have been virtually impossible.

Finally, I would like to thank my family. Without the support of my beautiful wife, Dawn Sechrist, I would not be in this position today. She has been my rock through this process and has kept me focused on the end goal. And I cannot forget my two sons, William, and Xavier, for reminding me every day why I am doing this and why this process will be worth it.

This material is based upon work supported by the U.S. Department of Energy under Award Number DE-FE0031711 and DE-FE0027035. Disclaimer: This report was prepared as an account of work sponsored by an agency of the United States Government. Neither the US

Government nor any agency thereof, nor any of their employees, makes any warranty, express or implied, or assumes any legal liability or responsibility for the accuracy, completeness, or usefulness of any information, apparatus, product, or process disclosed, or represents that its use would not infringe privately owned rights. Reference herein to any specific commercial product, process, or service by trade name, trademark, manufacturer, or otherwise does not necessarily constitute or imply its endorsement, recommendation, or favoring by the US Government or any agency thereof. The views and opinions of authors expressed herein do not necessarily state or reflect those of the US Government or any agency thereof.

In addition, the technical and financial support from Mineral Refining Company, LLC (Evan Energy, LLC) is acknowledged as being instrumental to the success of this project. Conflict of interest disclosure: Roe-Hoan Yoon has an ownership/equity interest in MRC.

Table of Contents

Acknowledgements ..... **iii**

Chapter 1. Background and Literature Review **1**

1.1. Background 1

1.2. High Value Carbon Rich Products 3

1.3. Variations on Froth Flotation 5

1.4. Background on the Dewatering of Coal 6

1.5. Methods for Drying 7

1.6. Introduction of a jig-type Morganizer 11

1.7. The Hydrophobic-Hydrophilic Separation Process 12

1.8. The HHS Process 15

1.8.1. Initial Research 15

1.8.2. Cleaning and Dewatering Fine Coal Using Hydrophobic Displacement 15

1.8.3. Low Temperature Drying of Ultrafine Coal 16

1.8.4. Development of the HHS Process 16

1.8.5. Introduction of the Morganizer 16

1.8.6. Development of a Novel Fine Coal Cleaning and Dewatering Technology 17

1.8.7. Advancement of the Hydrophobic-Hydrophilic Separation Process. 20

1.8.8. Hydrophobic-Hydrophilic Separation Process for the Recovery of Ultrafine Particles 24

1.8.9. Summary of Prior Research 25

1.9. Proposed Research 26

1.9.1. Research Objectives 26

1.9.2. Dissertation Organization 27

Chapter 2. Design and Construction of the HHS Pilot Plant **28**

2.1. Process Overview 28

2.1.1. Design Concept 28
2.1.2. Preconcentration 29
2.1.3. Agglomerate Formation 30
2.1.4. Agglomerate Recovery 30
2.2. Hydrophobic Displacement 31
2.2.1. Solvent Recovery/Recycle 31
2.3. Pilot Plant Design, Construction, and Shakedown 32
2.4. Process Feed 37
2.4.1. Final Design 37
2.4.2. Design Modifications during Test Campaigns 38
2.5. Agglomeration 38
2.5.1. Final Design 38
2.5.1. Design Modifications during Test Campaigns 47
2.6. Flotation 48
2.6.1. Final Design 48
2.6.1. Design Modifications during Test Campaigns 50
2.7. Morganizer 51
2.7.1. Final Design 51
2.7.1. Design Modifications during Test Campaigns 56
2.8. Solvent Recovery 57
2.8.1. Final Design 57
2.8.1. Design Modifications during Test Campaigns 62
2.9. Automation and Control 63
2.10. Safety Equipment 64
2.11. Additional Design Considerations 66

2.11.1. Pilot Plant Foundation/Early Build 66

2.12. Summary and Conclusions 68

Chapter 3. The Hydrophobic-Hydrophilic Separation (HHS) Process for Ultrafine Coal Recovery 70

3.1. Abstract 71

3.2. Introduction 71

3.2.1. Background 71

3.3. HHS Process Description 73

3.4. Materials and Methods 75

3.4.1. Materials 75

3.4.2. Laboratory-Scale Testing 76

3.4.3. Pilot-Scale Design and Construction 79

3.4.4. Sample Preparation/Analysis 80

3.5. Results and Discussion 81

3.5.1. Bituminous Pilot Plant Trial Results 81

3.5.2. Anthracite Pilot Plant Trial Results 85

(1) Laboratory-scale Tests 85

3.5.3. Pilot-scale tests 86

3.6. Summary and Conclusions 87

Chapter 4. Development of the Pilot Scale Column Morganizer 89

4.1. Introduction 89

4.2. Use of Oscillating Columns in the HHS Process 92

4.3. Study Objectives 94

4.4. Materials and Methods 95

4.4.1. Coal Samples 95

4.4.2. Oscillating Column Design 96

4.5. Methods and Procedures 100
4.5.1. Test Initiation 100
4.5.2. Column Feed 101
4.5.3. Column Level Control 102
4.5.4. Sampling Procedure 103
4.5.5. Sample Analysis Procedure 104
4.5.6. Test Result Analysis 105
4.5.7. Test Run Length 106
4.5.8. Steady State Establishment 106
4.6. Results and Discussion 106
4.6.1. Modifications derived from trials. 106
4.6.2. Column Profile Data 109
4.6.3. Oscillating versus packed column results 121
4.6.4. Influence of Column Shell Material 122
4.6.5. Influence of Internal Design 126
4.7. Material Balance 127
4.8. Theoretical Reactor Size Determination 128
4.9. Number of Discs Required for Necessary Hydrophilic Surface Area 130
4.10. Power Required to Operate Column 131
4.11. Scaling Parameters Determined from Pilot Plant Trials 134
4.11.1. Scale up #1: Reactor Diameter 135
4.11.2. Scale up #2: Number of plates needed within the column: 136
4.11.3. Scale up #3: Motor HP rating necessary to operate column: 137
4.12. Conclusions and Design Recommendations 139
Chapter 5. Development of a Column Jig Type Morganizer 140

5.1. History of Jigging 140
5.2. Use of Jig in the HHS process 142
5.3. Materials and Methods 144
5.3.1. Pilot Scale Jig Scale Up and Design 144
5.3.2. Materials 147
5.3.3. Procedures 148
5.4. Results and Discussion 149
5.4.1. Laboratory Jig Results 149
5.4.2. Evaluation of Ragging 150
5.4.3. Shakedown Trials 155
5.4.4. Glass jig Testing 157
5.4.5. Material Balance for Jig Morganizer 161
5.4.6. Future Testing, Scale up, and Design Considerations 161
5.5. Planned future testing. 163
5.6. Jig Scaleup 164
5.7. Summary and Conclusions 166
Chapter 6. Preconcentration of Coal-Based Rare Earth Element Feedstocks using X-Ray Sorter Technology 167
6.1. Abstract 168
6.2. Introduction 168
6.2.1. Ore Sorter Technology 170
6.3. Experimental 171
6.3.1. Sample Collection 171
6.3.2. Channel Sample Evaluation 171
6.3.3. Coarse Refuse Preconcentration 172

6.3.4. Sample Analysis..... 173

6.4. Results and Discussion 173

6.4.1. Channel Sample Results 173

6.4.2. Coarse Refuse Results..... 177

6.5. Summary 179

Chapter 7. Use of the HHS Process for Preconcentrating Coal-based Resources for Rare Earth Element Extraction 180

7.1. Introduction:..... 180

7.2. Materials and Methods..... 180

7.2.1. Materials 180

7.2.2. Pilot Plant Modification and Operation. 180

7.2.3. Results and Discussion 184

7.2.4. Discussion/Comparisons with X-ray sorting 191

7.3. Summary and Conclusions 192

Chapter 8. Conclusions and Recommendations..... 193

References 196

Appendix 202

List of Figures

Figure 1-1. Comparison of Non-Evaporative Dewatering Methods (Nikhil Gupta et al. 2014). ... 8
Figure 1-2. Cost of Dewatering Coal ($/ton) Versus Particle Size (Nikhil Gupta et al. 2014). .. 13
Figure 1-3. Representation of the HHS Process (R.-H. Yoon et al. 2016). 14
Figure 1-4. Estimated drying costs per ton for low heated air (left) and high heated air (right) (Freeland et al. 2010). 16
Figure 1-5: Summary of results from tests conducted by Jones (Jones, Yoon, and Noble 2019). 23
Figure 2-1. Simplified HHS block flow diagram. 29
Figure 2-2: Initial Concept Design of Mobile Pilot Plant. 33
Figure 2-3. Pilot plant "front end" schematic. 34
Figure 2-4. Pilot plant "back end" schematic. 35
Figure 2-5. Mass flow sheet for process. 36
Figure 2-6. Feed equipment schematic, equipment list, flow rates. 37
Figure 2-7. Design Considerations for High Shear Tank. 39
Figure 2-8. High shear design worksheet. 40
Figure 2-9. Low shear tank design schematic. 42
Figure 2-10. Low shear tank design worksheet. 43
Figure 2-11. Example of serrated impeller (R) and marine type impeller (L). 45
Figure 2-12. Agglomeration portion of HHS plant schematic. 46
Figure 2-13. Original Agglomeration Setup (Left) and Current Agglomeration Setup (Right). .. 48
Figure 2-14. Sieve screen and flotation cells. 49
Figure 2-15. New column jig Morganizer post fabrication (L) and installed on pilot plant (R). . 51
Figure 2-16. Pulsing mechanism for jig Morganizer. 52
Figure 2-17. Launder tops for new column jig Morganizer. 53
Figure 2-18. Close up of perforated oscillating disc. 54
Figure 2-19. Extraction column schematic. 55
Figure 2-20. Solvent recycle tank and pump. 60
Figure 2-21. Solvent recovery and vacuum filter/coal production. 61
Figure 2-22. Current thermal dryer configuration. 63
Figure 2-23: Mobile Pilot Plant PLC, VFD, and touchscreen. 64
Figure 2-24: Pneumatic component controls. 64

Figure 2-25: Conspec monitoring box, floor gas monitor, and onboard fire suppression bottle.. 66
Figure 3-1. Schematic representation of HHS process. 74
Figure 3-2. Contact angle of n-alkane hydrophobic liquids with surface of coal particles, Yoon, R-H, Eraydin, M, and Freelend, C., (2011). 75
Figure 3-3. Laboratory Oscillating Column..... 77
Figure 3-4. Laboratory HHS Testing Summary Results: Product Ash. Dashed lines show upper threshold limits for super-clean (5%) and ultra-clean (1.5%) products..... 78
Figure 3-5. Laboratory HHS Testing Summary Results: Product Moisture. Dashed lines show upper threshold limits for moisture objective. 78
Figure 3-6. Laboratory HHS Testing Summary Results: Combustible Recovery..... 79
Figure 3-7. Updated high shear tank with mixer. 82
Figure 3-8 Pilot plant test results: product ash. Dashed line at day 65 indicates change in high-shear mechanism..... 84
Figure 3-9. Pilot plant test results: product moisture. Two data series reflect modification to high-shear mechanism. 85
Figure 4-1. Photos showing a typical plate stack (L) and arrangement of perforated and baffle plates (R) (A. E. Karr 1980)..... 90
Figure 4-2. Vibrating screen setup from POC plant. 94
Figure 4-3. Piece of structured packing used in original 4" column..... 96
Figure 4-4: Settling velocities for particles in water/Isohexane. 98
Figure 4-5. Stack of oscillating discs (L) and steel insert baffles(R) for extraction column..... 99
Figure 4-6. Original 4” carbon steel column, current oscillating column configuration with 1/2" sample ports (R)..... 100
Figure 4-7. PVC standpipe..... 102
Figure 4-8. Image showing the pressure sensor and pneumatic valve used in interface level control. 103
Figure 4-9. A vacuum filter pump and filter pads are used for sample processing. 104
Figure 4-10. A&D MF-50 Moisture Analyzer used in analyzing pilot plant samples. 105
Figure 4-11. Leco TGA701 used in analyzing pilot plant samples. 105
Figure 4-12: Test 1 column profiles with product containing 10.1% moisture and 8.0% ash. .. 112

Figure 4-13. Test 2 column profiles with product containing 7.7% moisture and 7.0% ash..... 113
Figure 4-14. Test 3 column profiles with product containing 7.5% moisture and 6.2% ash..... 113
Figure 4-15. Test 4 column profiles with product containing 7.0% moisture and 6.4% ash..... 114
Figure 4-16. Test 5 column profiles with product containing 15.0% moisture and 9.5% ash.... 114
Figure 4-17. Test 6 column profiles with product containing 16.0% moisture and 8.2% ash.... 115
Figure 4-18. Test 1 column profiles with product containing 6.0% moisture and 8.7% ash..... 115
Figure 4-19. Test 1 column profiles with product containing 9.2% moisture and 8.9% ash..... 116
Figure 4-20. Test 9 column profiles with product containing 10.3% moisture and 7.8% ash.... 116
Figure 4-21. Test 10 column profiles with product containing 8.3% moisture and 10.5% ash.. 117
Figure 4-22. Test 11 column profiles with product containing 6.0% moisture and 5.1% ash.... 117
Figure 4-23. Test 12 column profiles with product containing 9.5% moisture and 4.4% ash.... 118
Figure 4-24. Test 13 column profiles with product containing 9.2% moisture and 8.9% ash.... 118
Figure 4-25. Test 14 column profiles with product containing 10.1% moisture and 3.8% ash.. 119
Figure 4-26. Test 15 column profiles with product containing 9.0% moisture and 4.1% ash.... 119
Figure 4-27. Test 16 column profiles with product containing 8.7% moisture and 4.3% ash.... 120
Figure 4-28. Test 17 column profiles with product containing 7.9% moisture and 3.9% ash.... 120
Figure 4-29. Test 18 column profiles with product containing 9.1% moisture and 4.1% ash.... 121
Figure 4-30. Test 19 column profiles with product containing 9.5% moisture and 3.9% ash.... 121
Figure 4-31:Comparison of structured packing column vs. oscillating column product moistures. 122
Figure 4-32. Diagrams showing the internal profiles of test configurations with the all-steel column..... 123
Figure 4-33:Diagrams showing the internal profiles of test configurations with the PVC column shell. 125
Figure 4-34: Material Balance for Column Type Morganizer as tested. 128
Figure 5-1. Photo of a small two stage mineral jig (Michaud 2016). 141
Figure 5-2. Coal cleaning technology use in the top 5 coal producing countries. 142
Figure 5-3. Laboratory jig Morganizer and diaphragm metering pump. 143
Figure 5-4. Concept drawing of U-tube pilot scale jig type Morganizer. 144
Figure 5-5. Completed base of U-tube pilot scale Morganizer. 145

Figure 5-6. Completed pilot scale Morganizer installed on pilot plant. 146
Figure 5-7. 3D printed screen support. 146
Figure 5-8. Jig actuator valve..... 147
Figure 5-9. Images of feldspar ragging (L) and spherical ceramic ragging (R) in the Morganizer. 153
Figure 5-10: Contact angles of various materials with water. 156
Figure 5-11. Steel insert and 3D printed flange. 157
Figure 5-12. Concept design for new jig Morganizer. 158
Figure 5-13. Modified jig pulsing mechanism (L) and new jig launder tops (R). 160
Figure 5-14. New jig Morganizer post fabrication (L) and jig Morganizer installed on pilot plant (R) 160
Figure 5-15: Material Balance for Jig Type Morganizer 161
Figure 6-1. Schematic of the X-ray sorting process. 171
Figure 6-2. X-ray baggage scanner (L) and Pilot-scale DriJet^{tm} x-ray sorter system. 172
Figure 6-3. Correlation between ash content and TREE concentration for different layers of coal seam strata from a channel sample. 175
Figure 6-4. Images from an x-ray inspection scanner of powdered samples from different layers of coals seam strata. 176
Figure 6-5. Associations of ash content, TREE concentration and x-ray response for different layers of strata from a coal seam channel sample. 177
Figure 6-6.Elemental upgrade ratios obtained using the pilot-scale x-ray sorter. 178
Figure 7-1. Large agglomerates 181
Figure 7-2. New flotation launder design 183
Figure 7-3. Recovery of combustible matter to the clean product and REEs to the REE product (high-ash tails) (L) and Ash contents of the clean product and REE product (high-ash tails) (R) 187
Figure 7-4. Element concentration versus ash content for selected elements..... 188
Figure 7-5. Element concentration versus ash content for selected elements..... 189
Figure 7-6. Element concentration versus ash content for selected elements..... 190
Figure 7-7. Element-by-element recoveries achieved during decarbonization testing. 191

List of Tables

Table 1. Energy Consumption of Different Coal Drying Methods (Karthikeyan, Zhonghua, and Mujumdar 2009). 10
Table 2. Lab and Proof of Concept Results of HHS tests (N. Gupta et al. 2016)..... 17
Table 3. Results from the POC trials (Nikhil Gupta et al. 2014). 20
Table 4. Process objectives and the purpose of testing each. 28
Table 5. Feed equipment and flow rates. 37
Table 6. Selection trials looking at impeller HP and tip speed. 45
Table 7. Agglomeration equipment list and flow rates. 47
Table 8. Screen/Flotation equipment and flow rates. 50
Table 9. Extraction column equipment list and flow rates. 56
Table 10. Solvent recycle equipment list and flow rates. 60
Table 11. Solvent recovery equipment/flow rates. 62
Table 12. Dry coal production equipment/flowrates. 62
Table 13. Salient Statistics for Coal Samples Utilized in Study. 76
Table 14. Pilot Plant Test Results for Super-Clean Product Production 85
Table 15:Results obtained in laboratory-scale tests. 86
Table 16:Results obtained in pilot-scale tests on the Silt Pond Sample 87
Table 17: Results obtained in pilot-scale tests on the Fine Clean Anthracite Sample..... 87
Table 18.Experimental Results from Column Profile Testing..... 111
Table 19. Laboratory HHS jig Morganizer results. 149
Table 20. Results from limited trials with jig Morganizer..... 159
Table 21. List of Rare Earth Elements..... 169
Table 22. Stratigraphic data for the West Kentucky channel/core sample. 174
Table 23. Pilot-scale sorter test data. 177
Table 24. Decarbonization data from five series of detailed HHS test runs. 185
Table 25.REE concentration data from five series of detailed HHS test runs. 186

Chapter 1. Background and Literature Review

1.1. Background

The recovery of ultrafine particles is a grand challenge for the mining and minerals sector. For the specific case of coal, the processing of fine coal has been a significant challenge to mine operators ever since the introduction of modern wash plants. While technical innovation has successfully reduced the lower particle size limit, most operations still do not recover material less than 45 microns due to the vast energy requirement needed for separation and dewatering. Currently, operators let these particles travel out with the waste streams from the plant and dispose of them in impoundments. These impoundments then create environmental and safety hazards as metals and other elements can leach from the coal contained within and their potential for failure could set billions of gallons of waste material free. A technical solution to recover these ultrafine particles would not only eliminate the need for these massive impoundments, but it would also provide the opportunity to recover significant amounts of saleable product. Moreover, since finer particles often exhibit higher degrees of liberation, selective separation of these finer sizes has the potential to yield higher purity products suitable for high-value carbon markets.

The definition of the sizes for ultrafine particles can vary depending on which industry is studying the particulates. In terms of air quality, the United States Environmental Protection Agency (EPA) defines ultrafine particles as those less than 0.1 microns. As for fine particles, the EPA defines them as those less than 2.5 microns (Chang et al. 2004). For the polyurethane nano fiber-based filter industry, ultrafine particles are those that range from 0.02 microns to 0.4 microns (Sambaer, Zatloukal, and Kimmer 2012). In coal processing, the sizing conventions are not as strictly defined and generally what are considered ultrafine particles are larger than other industries. Some coal processing researchers define ultrafine particles as those less than 25 microns (Honaker, Yoon, and Luttrell 2005) while others give them a range from 30 to 50 microns (Jones, Yoon, and Noble 2019). One school of thought is that fine particles can be considered the size of particles fed to a flotation cell which can be significantly larger all the way up to 2 – 3 mm (R. H. Yoon, Luttrell, and Asmatulu 2002). Ultrafine particles would then be considered the product of a desliming cyclone which has an upper limit of 45 microns. If this is

being used as a breaking point in sizes, the conventions used by previous researchers fit the criteria.

The ability to recover low ash ultrafine coal particles would provide a reliable source for the manufacture of high-value carbon-rich products. These products would be used by manufacturers and the high-tech energy industries to create materials vital to many industries. Some of these uses include:

- Graphite(K. Li, Rimmer, and Liu 2018)
- Carbon Fiber (Banerjee, Chandaliya, and Dash 2021)
- Nanotube Carbon Needle Coke (Zhu et al. 2019)
- Graphene(S.-Y. Lee and Mahajan 2021)
- Super capacitors

In order produce the low ash coal in sufficient quantities for evaluation in these industries, suitable feed stock needs to be found and tested. The coal should be tested in the lab to see if the product parameters can be met as well as what recovery method is best suited. Once the method is determined, work can be done to scale the procedure up to a pilot scale level and then eventually the commercial scale level.

Methods to recover these ultrafine particles have been developed and one such method, froth flotation, has been used to great success. However, while being a very effective recovery technique froth flotation does have some drawbacks that limit its capabilities. Flotation has a lower particle limit level and any particles below the 30 – 50-micron size range are lost, as they generally lack the inertia needed to penetrate the thin liquid film surrounding the air bubbles. Additionally, in flotation the ultrafine particles tend to follow the fluids as they move around the bubbles avoiding collision (R. H. Yoon and Luttrell 1989). To overcome these issues, researchers at Virginia Tech came up with a novel method called Hydrophobic-Hydrophilic Separation (HHS) (R.-H. Yoon et al. 2016) that not only can recover the ultrafine particles missed by flotation but can also dewater the process concentrate thus reducing the large amounts of energy required. The HHS and froth flotation recovery methods will be discussed in the next section to help better explain the principles and characteristics of each.

1.2. High Value Carbon Rich Products

Recent market trends for consumer electronics, lithium-ion batteries, and other technology have prompted unprecedented demand growth for numerous mineral and material resources (IEA 2021). While typically not included in official critical mineral lists, one material of growing interest and demand is carbon, which is utilized in advanced composite materials as well as advanced electronics. Government agencies, including the US Department of Energy, are seeking reliable domestic sources of these materials which would not be dependent on foreign trade and diplomatic relations with other countries. Below is a list of some high-value carbon products and some of their uses:

- Graphene: Composite material filler, super capacitors, batteries, interconnects, field emitters (Geim 2009).
- Graphite: lithium-ion batteries.
- Carbon Fiber: carbon-reinforced composite materials.
- Nanotube Carbons: polymers, plastics, and batteries.
- Needle Coke: graphite electrodes for electric arc steel furnaces (Dagle et al. 2017).
- Carbon Dots/nanomaterials: Optical sensors, light-emitting diodes, catalysis, photovoltaics, super- capacitors (Liu, Li, and Yang 2020).
- Marine fuel additive

As with many other critical minerals, high purity carbon is critical to produce many electronic components and communication devices. Having a reliable source for these materials domestically would help keep manufacturing costs down, which would help keep the end products affordable for consumers. In addition, it would insulate the costs of these materials from a vast number of influences coming from sources external to the United States.

Given this need, the US Department of Energy has recently initiated the Carbon Ore Processing program, which seeks to develop pathways to convert coal into high value products while remediating legacy environmental wastes associated with historic coal production. According to some estimates, there are more than 2 billion of tons of fine waste coal sitting in impoundments around the United States that that could be recovered without incurring new mining costs. Recovering this material will not only cost the operators less to process than raw coal but it will help clean up potentially hazardous installations while adding an income stream

where there was none before (R.-H. Yoon et al. 2016). Previous research at upgrading coal has focused on the use for thermal power generation and the creation of synthetic fuels. The source for the ultrafine coal is still from waste impoundments, but the coal is cleaned using various flotation methods and is then pelletized for shipment to generating facilities (E V Manlapig, C Green 2001).

Generally, the conversion processes for high value carbon products (e.g., coal to graphite, coal to graphene, coal to carbon fibers, etc.) rely on relatively high-quality coal sources, as the post-conversion impurity removal costs can be prohibitive. Moreover, conventional petroleum-based carbon precursors have very low levels of impurity, making them more attractive from both a cost and waste handling perspective. As such, pre-concentration or pre-cleaning is a critical component of the value chain, which must be optimized to successfully reduce high impurity waste coals to levels needed for carbon conversion.

Following pre-cleaning, there are several methods to upgrade coal precursors into carbon products. For the case of graphene, the production route can be classified into two categories either bottom-up or top-down. One of the bottom-up methods is chemical vapor deposition which can take a low molecular hydrocarbon and synthesize the graphene into large sheets. The issue with CVD is that it is expensive which can make it cost prohibitive for large scale production of graphene (S. Y. Lee and Mahajan 2021). The other top-down methods require a source of highly ordered graphite to use some sort of exfoliation to recover the graphene. Unlike CVD, this method creates flakes of graphene versus one solid sheet but is being considered more likely to be utilized in mass production (S. Y. Lee and Mahajan 2021). Recently, researchers have developed a method to exploit this process to reliably create graphite oxide from an anthracite coal sample. In their findings, they estimated that the mass losses from the coal during the conversion to graphite oxide was about 30 %. These losses were primarily in the form of CO_2 and CO (S. Y. Lee and Mahajan 2021).

In 2020, the average annual sales price for a ton of anthracite coal was $98.68 and bituminous coal was $50.05 (EIA 2020). When compared to other sources used to create graphene such as raw graphite, coal is a much more cost-effective source. Raw graphite is commonly used in many of the top-down methods of creating graphene. Some sources estimate that raw graphite can cost anywhere between $800 and $3,500 per ton (Critchley 2020). Current

North American pricing for graphite can range between $400/ton up to $2,250/ton depending on the particle size. However, there is no standard, and the spot market is also non-existent. Prices rely on negotiations between buyers and sellers (Northern Graphite Pricing 2021). So, while there is a large range and uncertainty of the cost for a ton of graphite, prices are all much higher than the cost of a ton of coal. Being able to clean and dewater coal to a level where it can be converted into graphene offers operators a chance to gain a highly profitable cash flow from something that was otherwise going to waste. Additionally, having a domestic source of graphene will lower dependence on foreign producers and possibly lower costs and prices.

The carbon fiber market is a $28 billion business and has been growing at a rate of 15 % to 20 % each year. Presently non-aerospace grade carbon fiber has a cost of around $21.5/kg and is driven by the source material Polyacrylonitrile (PAN). To transform the source material requires high manufacturing costs which translates to the price of the carbon fiber. It is predicted that the market for carbon fiber could expand greatly if the cost is able to come down (Shama et al. 2018). Because of this lower cost sources, such as coal, are being examined. To produce carbon fiber from coal, the coal is distilled to create a pitch which is the source material the manufactured into carbon fiber (Keboletse, Ntuli, and Oladijo 2021). Looking at the source materials, PAN costs about $4-$5/lb. while pitch derived from coal is about $1.50/lb. The carbon content is about 50 % for PAN and for the pitch the carbon content is about 85 % (Black 2017).

1.3. Variations on Froth Flotation

Froth Flotation is a mature particle-particle separation process used throughout the minerals industry and in the coal industry. Froth flotation relies on differences in surface wettability, or hydrophobicity, often explicitly defined by the contact angle, which is a thermodynamic property of surfaces. In flotation, an agitated slurry is mixed with fine air bubbles. These bubbles selectively attach to hydrophobic mineral surfaces, and the increased buoyancy of the bubble-particle aggregate causes it to float to the surface forming a mineralized froth. Hydrophilic particles are not collected and remain in the liquid phase prior to discharge. Flotation has a strong dependency on particle size and is optimal within a narrow range of particles, typically between 20 microns and 200 microns, with the specific range varying between different minerals (Trahar and Warren 1976). For most coal-based resources, other

processing options are available for particles outside the upper end of this range (e.g. spirals, dense medium cyclones, water only cyclones, reflux classifiers, etc.); however, no commercial options exist for particles below the lower particle size limit. Due to its particle size limitations, there have been several variations of the process developed to help increase its ability to collect fine particles.

Two methods that are similar in nature are selective flocculation-flotation and hydrophobic flocculation-flotation. Both methods involve the use of an agent being added to the process to aggregate the fine particles. In Selective Flocculation-Flotation, a long-chain organic polymer is used to gather the fine particles. These polymers are more commonly referred to as flocculants. In hydrophobic flocculation-flotation, some form of oil is used to gather particles, but the gangue material can become trapped. This issue can be resolved using multi-stage cleaning (Rubio and Marabini 1987). However, if an operator is looking to reduce their overall operating and capital costs, installing a cleaning loop may be cost prohibitive.

Other methods include carrier flotation, oil agglomeration, and two-liquid flotation. Like the two methods above, these improved recovery of particles in flotation but they all had some drawbacks that prevented them from achieving acceptable recoveries for industry.

1.4. Background on the Dewatering of Coal

This section will review the methods used to thermally dry coal after it has been processed and the energy requirements to do so as well as methods for drying coal that do not use thermal energy. Many end users of coal products have limits on the amount of moisture the product is being sent to them. Typically, these limits are written in the sales contracts between the coal provider and the user. These limits can vary based on the end use. For thermal coals, the amount of moisture presents after being washed can be up to 11 % and in coking coals the moisture after being washed can be as much as 15 %. This high moisture can account for almost 10 % of the fuel consumed when being burned for steam generation just to drive off the moisture. In addition to affecting the efficiency of the power plant, the moisture can affect the power consumption, flue gas flow rate, and add higher maintenance costs (Karthikeyan, Zhonghua, and Mujumdar 2009). On top of the problems that high moisture can cause at power plants and coking facilities, moisture can cause a litany of materials handling issues. High moisture coals add unnecessary weight for shipping. This means that operators are shipping less

actual coal to their customers. In cold regions, the high moisture can cause freezing in the railway cars making them difficult or impossible to unload. High moistures reduce friability which affects blending, efficient separation, classification, and transportation of fine coals through pneumatic means (Karthikeyan, Zhonghua, and Mujumdar 2009). Because of these issues, it is essential to dry coal out as much as possible after cleaning and processing it. In some lignite powered power generation stations, using waste heat to dry incoming fuel before combustion saw a 6 % reduction in moisture which resulted in an almost $2 Million savings in operating costs for one year (Karthikeyan, Zhonghua, and Mujumdar 2009).

1.5. Methods for Drying

Dewatering of coal is typically achieved by an evaporative or non-evaporative method. Evaporative drying methods employ the use of thermal dryers. Thermal dryers can be classified by several different parameters such as drying method, method of heat transference, coal drying media, and heat source (Nikolopoulos et al. 2015). Non-evaporative dewatering methods use some sort of mechanical means to dewater the coal. This can be achieved through gravity, centrifugal force, vibration, or vacuum pressure. While these methods may use less energy than the evaporative processes, they fail to effectively dewater fine coal particles. Figure 1-1 below shows a comparison of non-evaporative drying methods based on the particle size range they can operate with and the achievable product moisture. As shown in the figure, the non-evaporative methods that can reach moisture contents levels below 10 % are only able to do so with particle sizes greater than 100 mesh or 149 microns. The methods that can work with particle sizes smaller than 100 mesh down to passing 325 mesh or 44 microns are not able to achieve moistures below 10 %. Before now, thermal dryers were the only methods that were able to drive moisture content levels below 10 % in coal products consisting of fine particles.

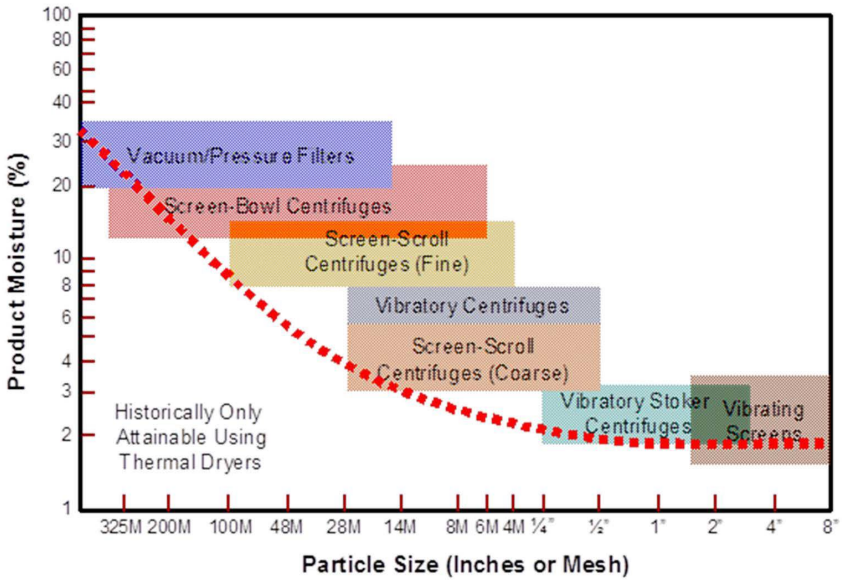


Figure 1-1. Comparison of Non-Evaporative Dewatering Methods (Nikhil Gupta et al. 2014).

Where these non-evaporative methods fail to dewater fine coal, particles are due to the capillary action and pressure during the dewatering. As the coal is being dewatered, capillaries form within the particles allowing the water to be removed. However, not all the capillaries are the same size the water tends to preferentially drain through the larger capillaries. This causes a short circuit of the dewatering due to the low capillary pressure in the large capillaries. The smaller capillaries will have a much higher capillary pressure which will tend to hold the water in place and not let it drain out (Keles et al. 2010). There has been some work looking at introducing air pressure to centrifuge dewatering equipment to lower the amount of water that was not removed by the centrifugal forces. For this to work, the air pressure needs to be sufficient to overcome the capillary pressure of the filter cake.

In the area on Figure 1-1 for particle sizes less than 48 microns and under 6 % moisture is found to be where thermal drying methods are successful. Thermal drying of coal products has been well established and is utilized to effectively dewater coal of varying particles sizes. In thermal methods, the main drying mechanism is either hot air, combustion gases, or superheated steam. In addition to the drying medium, the dryers can be categorized by being either direct or indirect, fixed, or fluid bed, rotary kilns, or some sort of entrained system (Karthikeyan, Zhonghua, and Mujumdar 2009).

Rotary dryers are some of the most common thermal dryers found in coal preparation plants. These dryers typically are of a simple design with a main cylindrical tub mounted on rollers that allow it to spin at a slow speed. One end of the dryer is usually higher so coal will move gradually down slope while it is being dried. The use of lifters inside the tubs helps to increase the efficiency of the drying as coal particles are lifted and therefore tumble allowing the heated gases to get between particles (Osman et al. 2011). Rotary dryers can be set up in a direct or indirect drying method. For direct drying, the coal particles must come in direct contact with the heated air, gas, or steam. The hot gases are pushed into the tube through a gas inlet so they can flow around the coal particles. Indirect drying involves the use of a double wall on the tube where the heated medium is circulated between the inner and outer jacket of the cylinder. One benefit to indirect drying is a lower chance of explosion or fire as the heat source is not in contact with the coal and dust particles. However, compared to direct rotary drying, indirect has a much lower efficiency. This is primarily due to the small surface area that contacts the coal particles at any one time (Osman et al. 2011). To overcome these inefficiencies, operators have developed improvements that are able to increase the contact surface areas thus increasing the overall drying efficiency of certain dryers. To illustrate the amount of energy needed by thermal drying methods,

In addition to direct and indirect dryers, some of the other thermal drying methods used to dry coal include Chamber Dryers, Pneumatic Dryers, Fluid Bed Dryers, and the Fleissner Process. Chamber dryers consist of a sealable vessel in which shelves or trays full of product are placed to be dried. These dryers are typically divided into those that use a forced circulation system or a system in which the air moves based on its volumetric weight and the differences in the hot and cold states (Lukianov, Lozovaya, and Lozovoy 2018). While these dryers can be useful in some industries, since they are a batch system, they are not well suited for drying coal where a continuous system is preferred. Pneumatic dryers function using heated air to push the particles being dried vertically through a tube. At the top of the tube, a cyclone can be used to separate the solids from the heated gas. This method is well suited for materials that are heat sensitive or even explosive due to the short residence time the particles spend in the heated gas (Baeyens, van Gauwbergen, and Vinckier 1995). Fluid Bed Dryers (FBD) work by pushing air into a body of particles through a porous area so that the particles begin to behave as a fluid. Where this method has an advantage is it allows for a large surface area for contact between the

solids and the drying gas. This ensures a rapid heat transfer which can reduce drying time. Where FBD fall short is their ability to scale up easily. There are no mathematical models available that allow for scaling from a lab setup. Usually, these dryers are scaled up by empirical models based on a specific material being dried (Daud 2008). The Fleissner Process uses superheated saturated steam and is introduced to the coal under high pressure. This process can dry out the coal without damaging the coal particles. One advantage to this method is that the superheated steam can change the coal's form which in some cases increases the heating value of the coal (Harrington *et al*., 1942). To illustrate the differences in energy usage, Table 1 below lists the above evaporative drying methods and how much energy they consume to dry a kilogram of coal. Energy consumed to drive off water is significantly less for the methods that utilize superheated steam. The ability of superheated steam to drive off moisture effectively has provided inspiration for new research on how it can be incorporated into other drying methods.

Table 1. Energy Consumption of Different Coal Drying Methods (Karthikeyan, Zhonghua, and Mujumdar 2009).

Dryer Type	**Energy Consumed for Each Kilogram of Water Removed (kJ/kg H20)**
Rotary Dryer	3,700
Rotary Tube Dryer	2,950 – 3,100
Chamber Dryer	3,150
Pneumatic Dryer	3,100
Fluid Bed Dryer	3,100 – 4,000
Fleisnner Process – Superheated Steam	130 – 1,750
Fluid Bed – Superheated Steam with Heat Recovery	450

The HHS process has been proven to be able to produce a low moisture ultrafine coal product with moisture values consistently below 5 %. Since the solvents being used in the process have a higher affinity for coal than water does, they easily replace water (Qiao, Rui, Noble, Aaron, Yoon 2021). What is left is a product that has residual organic solvent with coal. Depending on the end use of the coal, the solvent may need to either be removed or at least lowered to an acceptable limit based on environmental regulations and customer specifications. In addition, this recovered solvent can easily be recycled and reused in the process of saving operators money. Traditionally, the preferred method to recover the solvent would be using a

thermal dryer. The downside to these dryers is that they consume a large amount of energy on a commercial scale, unlike the evaporative dryers mentioned earlier. One difference with thermal dryers used for solvent recovery is that due to the lower vapor point of the solvents, they only need to heat up to 60 – 80 degrees Celsius (Qiao, Rui, Noble, Aaron, Yoon 2021).

Researchers at Virginia Tech have begun preliminary lab scale research to look at a novel method of removing the imbedded organic solvent using different carrier gases. The setup for the tests conducted at Virginia Tech is an insulated steel cylinder with a mesh filter on the bottom connected to a computer measuring internal temperatures as well as the amount solvent removed. A coal-solvent slurry is put into the cylinder and a compressed gas is pushed into the top of the apparatus. Carrier gases chosen for the tests are Nitrogen and steam which will be heated to a predetermined temperature designed to vaporize the solvent in the cake (Qiao, Rui, Noble, Aaron, Yoon 2021). Compressed atmospheric air is not considered for this concept because the introduction of Oxygen into a solvent rich environment can significantly increase the chance of ignition of the organic solvent and carbon rich coal. Even on a lab scale, the pressure filter chamber could act as a pipe bomb if the mixture inside combusted.

The results of this experiment show that the use of superheated steam can be used to drive off residual organic solvent out of filter cakes formed from a coal-solvent slurry. With this method, product moisture results like thermal drying are achievable with a significantly lower amount of energy input. What is promising about the method is that it shows that it can be potentially paired with existing filtering technologies on a commercial scale. Being able to be paired with existing technology will significantly lower capital costs to operators who would potentially adopt the technology (Qiao, Rui, Noble, Aaron, Yoon 2021). The next step for testing this method would be to construct a pilot scale testing unit that will collect data used to determine the characteristics needed to scale the process up to a commercial scale.

1.6. Introduction of a jig-type Morganizer

Jigging equipment has been around for centuries and is one of the oldest forms of coal cleaning in existence. In fact, the use of jigs can be traced back to the sixteenth century as described by Agricola for use by miners to separate metal ore and waste materials (Agricola, Hoover, and Hoover 1912). The main benefit of jigs is that they are very effective in dealing with large particles. In the United States, the Baum jig was introduced to the coal industry in the

1920's and by the 1930's over a third of all US coal production was cleaned with a jig (Yancey et al. 1938). The Baum jig utilized an injection and exhausting of air from a closed end of a U-shaped tube. This injection and exhaustion would create a pulsing motion of the water through the particle bed (Daemen 2004). The typical installation of this jig utilized a particle layer called ragging. This layer allowed the larger particles to settle out and finer particles to remain on the top and report to the overflow (Falconer 2003).

One major benefit that jigging enjoys is that the equipment is mechanically simple with very few moving parts making them cheaper to build/operate. However, the jigs main limitation is the lower particle size where it cleans efficiently is typically above the ultra-fine particle size class. This research project will look at designing a jig type Morganizer that will be efficient in recovering ultra-fine coal particles and be a viable replacement for the oscillating column type Morganizer.

1.7. The Hydrophobic-Hydrophilic Separation Process

Due to the drawback of already existing methods, researchers at Virginia Tech worked to develop a method that cleans ultrafine particles and in the same process dewater the particles. The basis for the HHS process was born out of another process developed at Virginia Tech by Dr. Yoon and Dr. Luttrell. They had patented a method for dewatering fine coal particles called dewatering-by-displacement (DBD) (Roe-Hoan Yoon; Gerald H. Luttrell 1995). The two researchers began work on this new method after studying a method patented over a decade before, the Otisca T-Process. This process utilized chloro-fluoro carbon (CFC) and agglomerated it with ultrafine coal particles. These agglomerates were then dispersed in a large volume of CFC allowing any mineral matter to sink to the bottom while the coal remained with the CFC. The CFC could then easily be recovered through thermal drying at low temperature heat and collected for further use. The development of the DBD method eventually became the HHS process through advancements in the technologies used to make the agglomerates. Where HHS stands out against the other recovery methods is that it can simultaneously clean the coal particles and dewater them (Jones, Yoon, and Noble 2019). The HHS process is currently licensed to Minerals Refining Company of Richmond, VA.

The HHS process takes advantage of typically hydrophobic coal particles and typically hydrophilic mineral matter. Since coal is hydrophobic, it will tend to prefer to attach itself to a

hydrocarbon droplet. When the hydrocarbon encounters the coal particle, it displaces the surface moisture of that particle essentially dewatering the coal. Where this has an advantage over previous methods is that the energy required to dewater the coal is minimal with HHS. In conventional methods, thermal drying is used to strip the moisture off layer by layer. Meanwhile, HHS can directly replace the bottom moisture layer and can be considered thermodynamically spontaneous (Roe-Hoan Yoon; Gerald H. Luttrell 1995). The mineral matter will then remain with the displaced water droplets which will coalesce and flow out of the bottom of the process. Figure 1-2 below illustrates the cost of dewatering coal on a per ton basis compared to particle sizes. It shows that the cost of dewatering exponentially increases as the sizes drop below 1 millimeter.

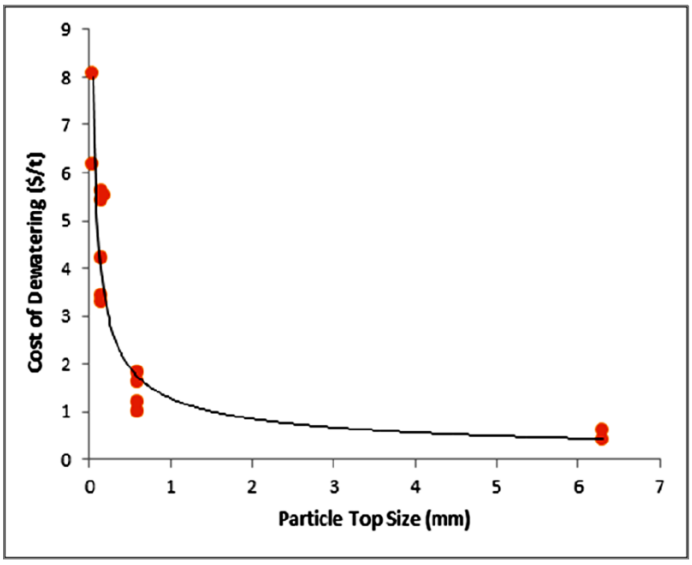


Figure 1-2. Cost of Dewatering Coal ($/ton) Versus Particle Size (Nikhil Gupta et al. 2014).

The feed slurry used for the HHS process typically comes from equipment used to remove fines in a preparation plant prior to standard flotation such as a de-sliming cyclone. The slurry is then collected from either a thickener or off a decanter where particles are allowed to settle, and water is removed. The feed slurry for HHS is then mixed with an organic solvent and mixed in a high shear environment. The high rate of agitation from pumps or mixing blades allows for a fine dispersion of the solvent so it has a greater chance of attaching to the coal particles (Jones, Yoon, and Noble 2019). The goal of the high shear step is to allow coal particles and solvent to clump together and form agglomerates separating the coal from the water. After high shear, the agglomerates are subjected to a period of slow mixing commonly

referred to as the low shear stage. The purpose of the low shear stage is to allow the coal agglomerates to grow larger thus collecting the bulk of the carbon material in the slurry. The next step is a phase separation where the coal agglomerates are separated from the liquid phase. This separation can be achieved through conventional flotation cells or through screens set up specifically for the size of agglomerates being created. After separation, the agglomerates are fed to a de-emulsification stage (often colloquially denoted a *Morganizer)* where the agglomerates are further mixed with a large volume of solvent under gentle agitation. The agitation breaks the agglomerates which releases any entrained water and promotes the coalescence water droplets to be discharged. The water droplets will then fall out of the process taking the remaining mineral matter with them. The coal from the broken agglomerates will be dispersed in the solvent and will flow out of the process as a product stream. In most embodiments, the agitation is achieved via stationary packing or via oscillating internal mechanisms. The coal-solvent mixture can then be dried to recover and recycle the solvent for future use (Jones, Yoon, and Noble 2019). Figure 1-3 gives a visual representation of the key operations within the HHS process. The figure illustrates the coal particles moving from water into oil where agglomerates are formed and then as they are broken up the water and mineral matter fall out of the bottom while the coal and oil flow out the top of the system.

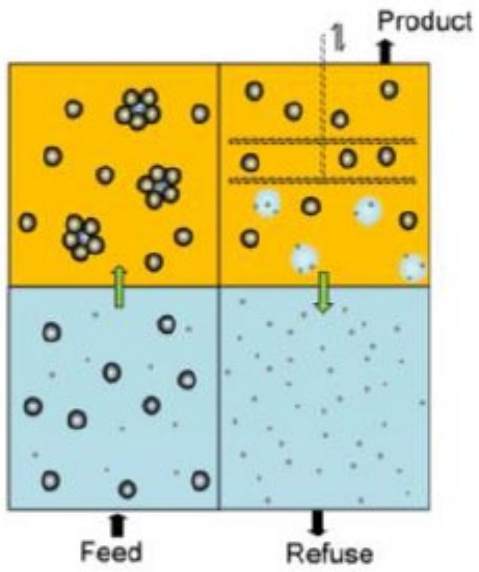


Figure 1-3. Representation of the HHS Process (R.-H. Yoon et al. 2016).

1.8. The HHS Process

In past research, the HHS process has been utilized in studying how effective it is with the processing of coal. In particular, the dewatering of steam and metallurgical coal. Outside the processing of coal, limited studies have been conducted with the use of HHS to process copper ore. While the cleaning of coal was discussed, ash content values below 3 % were achieved but none achieved ash contents considered to be ultra-clean or below 1.5 %.

1.8.1. Initial Research

Otisca patented a process in the early 1980's that used chloro-flouro carbon (CFC) to agglomerate with coal that had been micronized. These agglomerates would be put into a bath of CFC to disperse the coal from the mineral containing mineral matter. CFC like organic solvents has a low boiling point so it could be recovered easily with low heat (Keller 1982). They sought to develop a method that would dewater coal in an energy efficient way for ultrafine particles that did not require the high energy consumption of thermal drying. Dewatering by Displacement (DBD) was developed and patented as a method using a hydrophobic liquid to displace water in the coal particles. As the method is described as thermodynamically spontaneously, the only energy that is really required is to recover the residual hydrocarbon liquid (Roe-Hoan Yoon; Gerald H. Luttrell 1995).

1.8.2. Cleaning and Dewatering Fine Coal Using Hydrophobic Displacement

In 2008, K. Smith investigated different methods of breaking apart agglomerates after they were formed. Six de-emulsification methods were tested to determine how efficient they were at cleaning and dewatering. These include hand shaking, screening, air classification, centrifugation, filtration, and displacement. The first five methods were performed using oil agglomeration to displace water and the last method used hydrophobic displacement (K. E. Smith 2008). Of all the methods, screening produced the lowest moistures but also had extremely low recoveries and the screen was prone to blinding. Centrifugation produced single digit moistures but were not below 7 %. The other methods all produced double-digit moistures (K. E. Smith 2008). Smith concluded that further work should be conducted, in particular on dewatering by displacement as it offered to be the most promising cleaning and dewatering method.

1.8.3. Low Temperature Drying of Ultrafine Coal

Research on the low temp drying process tested with three different devices. The first was a static breaker, the second was the air jet conveyor, and the third was the centrifugal fan. The research focused on cleaning coal samples using both froth flotation and oil agglomeration. However, unlike current HHS research the goal was not to produce a low ash product but rather remove clay materials to aid in the dewatering process (Freeland et al. 2010). In addition to evaluating these three methods, the potential cost per ton to dry the material was investigated. Below in Figure 1-4 the cost per ton to dry coal for two of these methods is shown.

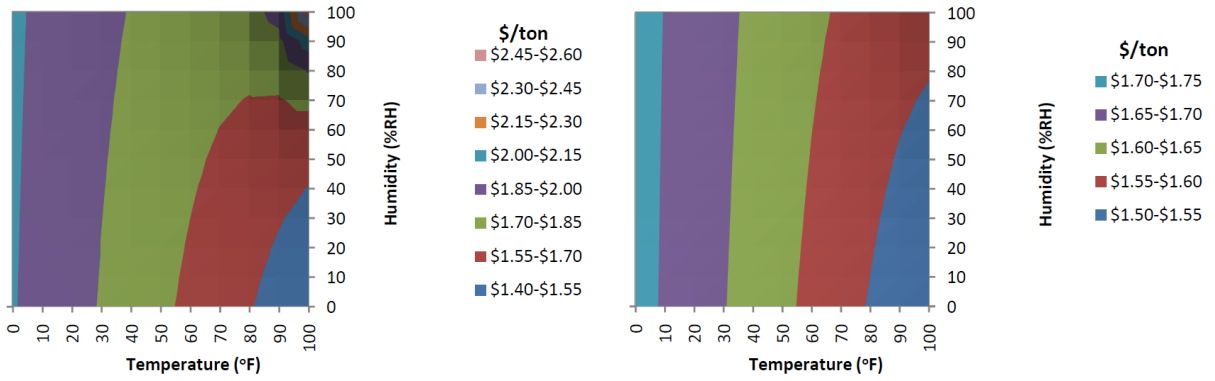


Figure 1-4. Estimated drying costs per ton for low heated air (left) and high heated air (right) (Freeland et al. 2010).

1.8.4. Development of the HHS Process

Building from previous research in agglomeration, S. Smith was the first to use a cylindrical reactor for testing as a continuous process which could then be scaled up. In addition to the cylinder, Smith tested two different methods for breaking the agglomerates: an ultrasonic probe and a series of vibrating screens. The metallurgical results of both methods were similar; however, the ultrasonic probe was not used in further testing for scale up due to the high energy consumption (S. A. Smith 2012). Rather the findings for the vibrating screen were used as the basis for further scale-up in the de-emulsification stage.

1.8.5. Introduction of the Morganizer

In 2016, the HHS method was developed to use short chain hydrocarbons to clean and dewater coal. The sample chosen to be used for the next round of HHS tests was a desliming cyclone overflow. After agglomerate formation, the material was fed into a new de-emulsifying device called the Morganizer. Inside this device the stable emulsions or agglomerates were

destabilized by mechanical means. This caused the mineral matter and water to fall out of the bottom and the coal along with the solvent flowed out of the top of the unit (N. Gupta et al. 2016).

Table 2 below shows the results of the research in both lab scale tests and larger scale proof of concept tests.

Table 2. Lab and Proof of Concept Results of HHS tests (N. Gupta et al. 2016).

Test	Lab Tests		Proof of Concept Tests	
	% Moisture	% Ash	% Moisture	% Ash
1	1.82	3.4	5.3	2.5
2	1.42	4.76	8.5	3.4
3	2.08	4.34	4.9	5.0
4	2.21	3.72	3.8	2.1
5	2.73	4.55	3.8	3.1

1.8.6. Development of a Novel Fine Coal Cleaning and Dewatering Technology

The primary goal of this research was the testing and scale up of the HHS process to develop a Proof of Concept (POC) pilot plant that can produce data to scale up to a commercial application. To test this concept coals from northern and central Appalachian coalfields were chosen to process in the lab and the new pilot plant. These coals were chosen because they were low-volatile bituminous coals which are very hydrophobic in nature. Initial tests used ultra-sonic energy to try and disperse the agglomerates. Did not work over longer runs and stable emulsions proved difficult to break with the ultrasonic energy. Testing evolved into using less oil and increased residence time to form spherical agglomerates. Retention time was later reduced by having a short high shear mixing step then a longer low shear mixing step. For these tests, a kitchen blender was used to do the mixing in the high shear and low shear stages. The agglomerates in this configuration proved much easier to disperse in a column of pentane. Agglomerates from these tests were put on a 60-mesh screen to remove free water and mineral matter. The agglomerates were again put into a column with water and pentane and an ultrasonic probe was used to disperse the coal into the liquid. The issue with these tests is that over a longer test run, the ultrasonic probe would heat up and boil the water.

The next step was to create a semi-continuous bench scale system to duplicate the results achieved in the previous batch system. Since the glass mixing vessels would not withstand the high shear stage, the agglomerates were premade in a kitchen blender and then fed into the bench system. The bench system employed a column type phase separator. Testing of this system showed that the height of the solvent water interface was important to control to prevent the formation of stable emulsions. Product from the phase separator was sent to a settling vessel where the extra solvent could be drawn off and the remaining solvent in the coal could be evaporated off. Using this method, decent recoveries (above 80%) were achieved, and product moistures were below 6%.

The next step was to test a device designed to aid in breaking up of agglomerates and aiding in the coalescence of water. The research looked at a simple device submerged in a tank of milk that moved up and down a small distance at 2Hz (Richardson and Thorpe 1995). This device was capable of aiding milk fat particles to find each other and coagulate. So, a similar device was designed for use with the coal agglomerates. The device's design consisted of two mesh discs attached on a thin shaft approximately 1 inch apart. The shaft was connected to an electro–dynamic shaker that could operate at a 0 – 60 Hz frequency range. Testing began with the new dispersion tool. As with prior tests, agglomerates were formed in a kitchen blender and then fed to the dispersion vessel with the screen oscillating. Results with the new method were positive. Results were similar to using the ultrasonic probe, but the process was much safer as it generated no heat to boil the liquids. One of the more important findings of these tests is that the throughput was much higher which allowed the processing of larger quantities of sample (Nikhil Gupta et al. 2014).

Testing moved onto screenbowl effluents taken from Consol Mines in Pa and Virginia as well as Arch plants in West Virginia. The Pennsylvania and West Virginia mines provided bituminous samples and the Virginia plant is an anthracite sample. Results were very favorable with the Buchanan and Beckley samples achieving product ashes of 3% and less and recoveries of 98%. The Sentinel and Bailey samples also produced low product ash (3.3% - 6.4%) and recoveries above 90% (Nikhil Gupta et al. 2014). After screenbowl effluent, the next sample tested was from deslimer overflows. As with the effluent, the results were favorable, and the process was shown to be able to recover carbon from this waste stream.

One thing pointed out is that solvent dosage increases as the particle size decreases. For the screenbowl effluent, solvent dosage ranged around 25-30% by weight while for the flotation feed is 10-15% by weight. This is driven by the increase in total surface area as particle size decreases (Nikhil Gupta et al. 2014).

The second part of research was to scale the batch process up to a POC pilot plant. The pilot plant was designed to be able to process 100 pounds per hour of (.15mm x 0) raw dry feed (Nikhil Gupta et al. 2014). There were not a lot of resources available about being able to scale up many of the different portions of the HHS process. So, calculations were made using known relationships and constants to best scale up the mixers and tanks.

For the POC project, a thermal dryer was selected to remove remaining solvent from the coal product. Feeding the thermal dryer was a thickened product that came from a thickener tank that collected the Morganizer product. This thickener helped to have excess solvent flow out of the tank to be recycled while the coal settled at the bottom to be pumped to the dryer. The work on this POC and the flow of material through the plant became the basis for the design of future processing plants applying this technology. Table 3 below summarizes the test runs with the POC unit. The research was able to produce low moisture products as well as very low ash values. Even though the ash values were low, there were no results below 2 %.

Table 3. Results from the POC trials (Nikhil Gupta et al. 2014).

Test Number	Feed	Product		Reject	Combustible Recovery%	%Ash Rejection	Separation Efficiency
	Ash%	*% Moisture*	*Ash%*	*Ash %*	***R***	***J***	***R+J-100***
Shakedown #6	7.0	4.2	2.1	64.0	97.0	71.8	68.8
		3.8	2.1	64.8	97.1	71.9	69.0
Pilot Test #1	55.7	4.6	2.2	89.4	85.3	98.4	83.7
		5.3	2.5	89.8	86.0	98.3	84.3
		8.5	2.5	89.3	85.2	98.3	83.5
Pilot Test #2	66.2	5.9	3.3	86.0	68.6	98.8	67.4
		5.2	3.3	86.1	68.8	98.8	67.6
Pilot Test #3	67.5	6.8	3.8	88.3	72.9	98.6	71.5
		9.6	3.6	86.9	69.2	98.8	68.0
Pilot Test #4	60.5	12.5	2.7	90.6	84.4	98.5	82.9
	77.3	9.8	2.7	88.7	56.8	99.5	56.3
Pilot Test #5	53.0	8.5*	3.4	84.4	79.7	97.5	77.2
Pilot Test #6	50.9	14.0*	3.3	85.7	83.2	97.3	80.5
		14.5*	3.2	78.7	72.6	97.7	70.3
Pilot Test #7	28.5	16.6*	5.5	78.9	90.8	86.8	77.6
	29.1	12.9*	5.0	82.2	92.2	88.3	80.5

** Combined percentage of moisture and pentane is reported.*

1.8.7. Advancement of the Hydrophobic-Hydrophilic Separation Process.

Following success in the POC plant, further research sought to identify the processing limits of the HHS through a longitudinal study of coals from various sources (Jones, Yoon, and Noble 2019). The goal of this study was to see how the process compares to froth flotation for recovery metals. Coal samples were collected from flotation tailings, raw coal cyclone overflow, and decanter feed to a thickener. A second set of metallurgical coal samples were collected from screen bowl effluent and deslime cyclone overflow. Additional steam samples were collected from screen bowl effluent and deslime cyclone overflow. Impoundment samples were also collected from the companies providing samples for the project. Some of the samples had appeared to be oxidized which affected their performance with HHS. Reagents would need to be used to make the coal hydrophobic again. For these samples, Sorbitan Monooleate (SMO) was utilized to increase the hydrophobicity.

Similarly, to the work that Gupta had done, this research used a lab setup that included mills for size reduction, mixing vessels to form agglomerates, a lab scale Morganizer, and a

thermal dryer to remove residual solvent from the coal product. Some samples received were very course and they needed to be ground to reduce their size in order to be used in the HHS process. The grinding also helped to reduce the ash of middling samples where the particles initially consist of mineral matter entrained in the coal.

One difference in the lab tests conducted was the means of creating the agglomerates. Gupta's work used a blender to create the agglomerates but in the new lab tests a Denver flotation cell was primarily used to agglomerate. If some of the coal samples were difficult to agglomerate, the blender was used to add higher energy. The lab Morganizer used for these tests was the same glass tube column type that was used in previous research. Thermal drying was also done in the same method of a glass jar with vent ports set inside of a hot water bath.

For most of the samples, the HHS process was successful in producing a coal product with low as and moisture values. Product ashes were predominantly under 5 % and moisture ranged from 1 % to 10 %. One sample that did not produce a low ash coal product was a middling sample from one of the West Virginia preparation plants. For this sample, the product ash did not get below 12 %. HHS also proved to be successful in processing the impoundment samples and produced product ash values under 4 %. One important factor that was determined in this research is that samples with extremely high ash values were difficult to agglomerate. This was due to the low population of coal particles which greatly reduced the opportunity for the coal to collide with the solvent and then with other coal particles.

While previous research proved that the HHS process was capable of cleaning and dewatering coal streams from processing plants, new research expanded the capability of the process to waste streams, impoundments, and middling products. Products produced in this process were consistently under 10 % in moisture which is the threshold of high value coal products. Moreover, this research showed that for various coal streams how effective HHS is at dewatering coal. The results of the tests showed single digit product moistures consistently which is something that is normally only achievable with thermal drying. Froth Flotation was also tested with these coal samples to compare how efficient it is in separation with HHS. Based on the results, it is clear that the separation efficiency of HHS is much higher than that of flotation. This is a measure of the recovery of the desired material minus the recovery of the

waste material. One of the most significant findings of these tests is that HHS can be effectively used to process waste streams and impoundment material.

The second goal of this research project was to test HHS as a method of pre-concentrating materials containing Rare Earth Elements (REEs). According to Zhang, nearly 50 % of the world's REEs reserves are associated with coal and its byproducts (Zhang et al. 2015). This combined with the fact that REEs tend to be very small particles the HHS process seems very well suited to recover the material. A similar process to that being used to recover coal from impoundments or waste streams will be used and be modified slightly.

Testing for this portion consisted mainly of fine coal samples that are typically treated as waste streams. Additionally, middling samples that had been found to have larger concentrations of REEs would be tested as well. The first step of the process is to use HHS to remove the carbon from the slurry. The tailings from the decarbonization process are then ground to reduce particle size to less than 10 microns. The sample after grinding is then put into a vessel to condition. Conditioning utilized a reagent mixed together with the sample that would depress the recovery of the gangue material. Following conditioning, collectors were mixed into the slurry in order to increase the hydrophobicity of the REE minerals. The difference in the REE agglomeration versus coal agglomeration is that for REEs, emulsions are formed to collect the minerals. This is accomplished by adding a significant amount of oil more than with regular oil agglomeration. The large amount of oil is needed due to the small population of REE particles in the slurry feed. The agglomerates are then filtered out in a separatory funnel and then more oil is added after the water is removed. The addition of the oil was necessary to change the oil in water emulsions to water in oil emulsions which are less stable and tend to release the entrained mineral matter to the water phase.

Testing showed that the HHS process is successful in upgrading low-value middlings and waste products into a high-value coal product and at the same time produces REE feedstock from the process's tailings. Figure 1-5 below summarizes the product moistures and ash values from the tested coal samples.

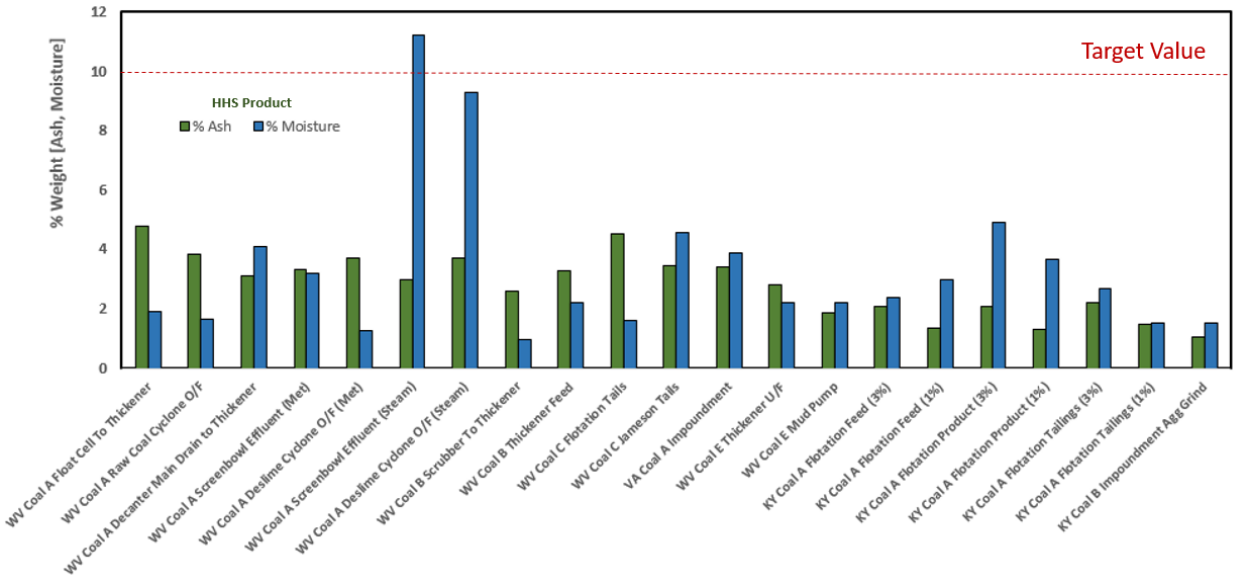


Figure 1-5: Summary of results from tests conducted by Jones (Jones, Yoon, and Noble 2019).

The next area HHS was to be tried out on was in metallic ore recovery. With increasing global demands and lower production, new means of recovering more particles from copper processing plants is increasingly important. Flotation tails are the majority of tailings stream from copper plants. In these streams, the recoverable particle size is less than 30 microns (Mankosa et al. 2016) which is favorable for the HHS process to be successful. For this round of tests, samples were provided from copper producers from within the US. Each of the samples needed to be processed in order to reduce the particle size to be effective in the HHS process.

The copper HHS process was similar to the REE process. The copper ore was conditioned with a collector to increase the hydrophobicity of the particles. Organic solvent is added to the slurry, and it is agitated to create oil-in-water emulsions. After the emulsions were formed, there were two methods to do the phase separation. The first method used a separatory funnel and the second used a new lab Morganizer design. One difference in this round of HHS testing is that heptane was used instead of pentane. It cannot be as easily recovered by thermal energy, so it was filtered out using a laboratory pressure filter. The new Morganizer design used a stationary structured packing inside of the column instead of the vibratory screens. The packing provided two important aspects. The first was enough restriction to generate the energy necessary to break the emulsions. The second aspect was that it provided the necessary surface area for water drops to coalesce and grow on and then fall out with the tails. An upward flow of

solvent was added to the column at a predetermined velocity capable of carrying the copper ore particles upwards and not letting them settle out.

The testing with copper ores and waste streams showed that the HHS process with the addition of a new Morganizer design coupled with a phase inversion stage to be effective at recovering high grade concentrates. Once again, the results show that HHS outperforms flotation in this application. These changes to the HHS process should be able to help increase the grades of REEs put through the process.

1.8.8. Hydrophobic-Hydrophilic Separation Process for the Recovery of Ultrafine Particles

The first part of the research was to look at the ability of HHS to agglomerate chalcopyrite. Initial tests looked at an artificial mixture of chalcopyrite and silica in order to help better understand how much solvent to use, agitation speed, and agitation time. With the decline of raw ore grades around the globe, increasingly finely ground ores are needed to achieve the amount of liberation necessary for recovery (Calvo et al. 2016). This increase in fine particle population presents a problem for current flotation techniques as they typically struggle with recovering ultrafine particles in particular smaller than 30 microns for chalcopyrite particles (Mankosa et al. 2016). Previous research looking at oil agglomeration and copper ore typically only used kerosene and other heavy oils. In order to make the process more industry scalable, an organic solvent such as heptane was looked at since it is much more easily recycled from the process.

The experimental process was similar to previous tests looking at coal recovery. A kitchen blender was utilized to add in the shear energy. A stand mixer was used to condition the slurry before the high shear agitation and agglomeration. The mixer was used again to help the agglomerates grow before screening, drying, and analysis. Using this method, ultrafine chalcopyrite particles were able to be recovered successfully with recoveries up to 96 %. However, to achieve this high of a recovery, agitation time was around 90 minutes, and it took at least 70 minutes of agitation to achieve recoveries above 90 %. In addition to agitation time, solvent dosage, and stirring speed were looked at to find the optimal points for recovery of the chalcopyrite. The optimal stirring speed was found to be 900 RPM. Any speed above 900 RPM the recoveries began to drop off. It was determined that at higher speeds the agglomerates would

start to break faster than they could form, and recovery dropped. These tests were then repeated using the hydrophobic polymer PX-1 which is used to influence the contact angle. Tests showed that contact angles increase with increasing dosages of PX-1 which correlates with an increase of recoveries. Similarly, Hydrophobizing agent KAX was tested to see how it impacted agglomeration and recoveries. It was also found to increase recoveries with increased dosages and not using it at all produced very poor recoveries.

These tests showed that recoveries above 90 % of ultrafine chalcopyrite particles is possible with HHS. However, the agglomeration process took an extremely long time without the aid of conditioning agents and hydrophobic polymers.

Initial work for the recovery of ultrafine chalcopyrite began with Li's research. In this research a brand new Morganizer was built specifically designed for use with heavy mineral particles.

1.8.9. Summary of Prior Research

Recent previous research on agglomeration and with the HHS process has mainly focused on methods for effectively dewatering coal slurries. Additionally, the research tested to see how effective the process is when dealing with heavier material types such as copper ore.

1. K. Smith investigated different methods for the breaking of agglomerates and the use of displacement to break them apart as well as dewatering the coal.
2. Freeland investigated mechanical methods to dewater coal after being agglomerated by oil.
3. S. Smith investigated methods to break up agglomerates effectively by using ultrasonic probes and with vibrating screen plates. Smith found that the vibrating screen plates to be the most effective and applicable to industry.
4. Gupta investigated the development of a scaled-up proof of concept pilot plant to test the commercial scalability of the HHS process.
5. Jones looked at the ability of the HHS process to not only upgrade coal waste streams but create a potential feed stock for REE from a domestic source.
6. Li used HHS to show it is possible to recover ultrafine particles from other materials such as copper ore and developed a new type of Morganizer to accommodate these ores.

All of the tests conducted with HHS on coal were done with bituminous coal samples and while upgrading the coal was considered in some of the research, dewatering was the primary focus. None of the research tested to see how the HHS process would be effective when processing anthracite samples. Finally, the previous research did not push how low in product ash the HHS process could produce from any type of coal sample for the use in industries outside that of premium fuels.

1.9. Proposed Research

1.9.1. Research Objectives

Given the current state of technology development for the HHS process, the goal of this research is to design, develop, and test, a mobile pilot-scale embodiment of the process to provide a testbed for inquiry-based process intensification and the evaluation of design criteria for the various unit operations. The process is to be implemented on a sufficient scale so as to generate product quantities suitable for downstream testing, and the modular integration of process unit operations will allow testing of various process improvements in a range of feedstocks. Specific sub-objectives of this work include:

1. Design, construct, and commission a mobile pilot HHS process capable of producing 50 lb/hr of product.
2. Investigate the process design of the agglomeration unit operation and determine the design criteria needed to produce high quality carbon products (nominally <4.5% ash and <8% moisture) across a range of coal types and ranks.
3. Investigate the process design and design criteria of the column-type de-emulsification (Morganizer) unit operation and evaluate how mechanical and operational variables effect column performance.
4. Design, construct, and test alternative Morganizer configurations, including a jig-type Morganizer for the purpose of process intensification (i.e. larger performance range at reduced cost and reduced footprint).
5. Investigate the utility of the HHS in decarbonizing fine coal for the purpose of REE recovery. Compare this performance against that of other nascent technologies, such as dual-scan x-ray sorting.

1.9.2. Dissertation Organization

The body of this dissertation is organized into eight chapters with the technical chapters being organized standalone papers (some of which have been submitted as proceedings articles). A comprehensive reference list and appendix are included at the end of the documents.

Chapter 1 includes a review of the state-of-the-art of fine particle separation and coal preparation, including a detailed history of the technical development of the HHS process. The chapter also details the knowledge and technical gaps that prompted this research.

Chapter 2 describes the design, construction, and shakedown of the pilot-scale HHS process, including the process engineering and mechanical engineering deliverables that aided the design process. This chapter also describes design modifications and improvements that were made through the course of the pilot campaign.

Chapter 3 is a conference paper that describes the development of design criteria for the agglomeration unit operation as well the results of a detailed pilot testing campaign that sought to produce high quality carbon products from both bituminous and anthracite feedstocks.

Chapter 4 describes the testing and scale-up of the column-type Morganizer, including a detailed investigation of the influence of mechanical and operational parameters on the solids profile within the column. Design recommendations for the column-type Morganizer are provided herein.

Chapter 5 describes the development, construction, and testing of a jig-type Morganizer, including the integration of the unit with the existing pilot plant and performance comparisons against the column-type Morganizer.

Chapter 6 is a conference paper that describes a novel method of REE preconcentration from coal refuse using dual scan x-ray sorting. This process was tested and the pilot-scale, and this chapter includes detailed performance results and analysis.

Chapter 7 shows similar data describing the capability of the HHS in decarbonizing fine coal refuse for the purpose of REE concentration.

Chapter 8 summarizes the key findings of the work and provides recommendations for further research and development.

Chapter 2. Design and Construction of the HHS Pilot Plant

As discussed in the literature review, through prior research and development efforts, the HHS process has been successfully scaled from the bench-scale to the proof-of-concept scale (POC) to a large one ton per hour demonstration. To support the further development and commercialization of the process, the current effort sought to design, construct, and test a mobile pilot plant for the purpose of developing definitive design criteria while also providing a modular platform for process intensification of high cost/low efficiency unit operations. Process objectives for the mobile pilot plant are summarized in Table 4 and include provisions for process throughput, product quality, and other key design features.

Table 4. Process objectives and the purpose of testing each.

Process Objective	Target	Justification
Product Capacity	50 lb/hr product	Sufficient to generate product lots for downstream verification.
Plant Feed	Clean and/or waste coals of bituminous or anthracite origin	Integrated robustness for a range of feed materials.
Product Ash	Objective: 4-5% Stretch: 1.5%	Objective target suitable for fuel additives/steam market. Stretch target suitable for high-value carbon markets
Product Moisture	6-8%	Suitable for a variety of product markets
Platform	Self-contained trailer/mobile	Suitable for on-site testing for plant trials
Integration	Fully integrated including separation and solvent recovery modules	Allow high fidelity cost estimation for scale-up purposes.

2.1. Process Overview

2.1.1. Design Concept

Baseline design considerations for the mobile pitot plant were based off of the information gathered from previous pilot plant designs as well as a larger demonstration plant. From these two processes, an overall flowsheet and initial process design for the mobile plant was developed. Figure 2-1 below outlines the simplified block flow diagram showing the

arrangement of unit operations and process flows. As shown in the figure, the process is broken into five distinctive sub-processes, with each inclusive of several unit operations. Subprocesses and the critical factors influencing performance are described in further detail below.

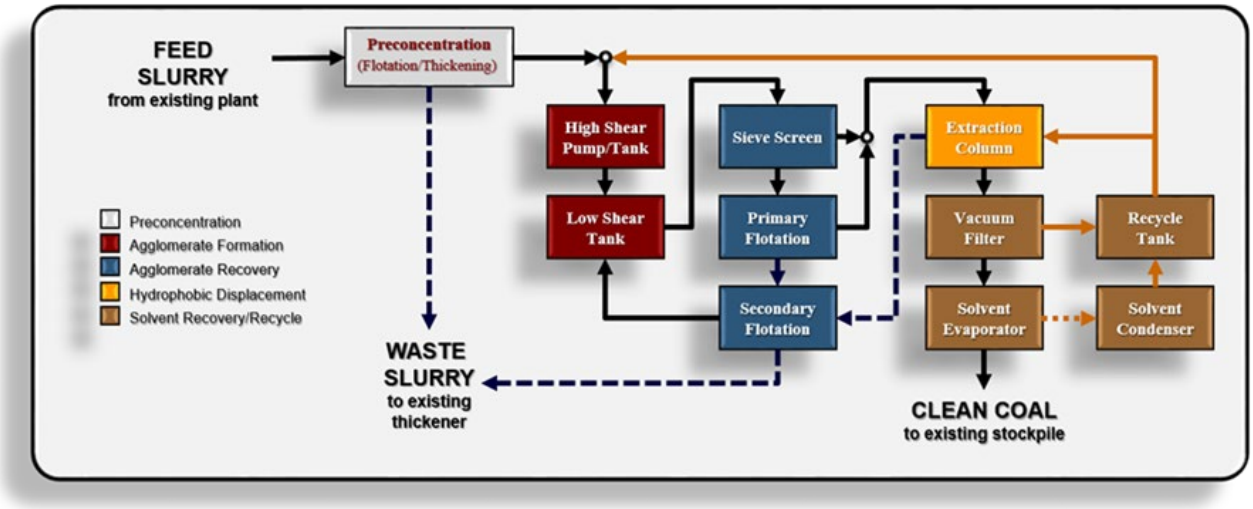


Figure 2-1. Simplified HHS block flow diagram.

2.1.2. Preconcentration

Depending on the nature and source of the feed material, a preconcentration step is often needed prior to the core HHS process operations. This preconcentration step is crucial to ensure that the feed slurry entering the system is at a consistent solid commensurate with the design value, often 6% to 8% by mass. Preconcentration can be obtained with the use of a thickening vessel in cases where feed material is too diluted, or the thickener can be replaced by water-addition large mixing tanks in cases where the feed is too concentrated. The final unit of the preconcentration process is a progressive cavity pump coupled with a flow meter and pneumatic pinch valve. The flow meter and pinch valve will be installed to maintain a constant feed rate to the process. The progressive cavity pump is going to be utilized due to its ability to provide a constant flow rate independent of how much feed remains in the mixing vessel. A consistent flow rate is extremely important to the performance of the system as inconsistencies can cause issues with agglomerate formation and extraction column performance.

2.1.3. Agglomerate Formation

The agglomerate formation operation is a critical unit that has significant influence on the balance of the plant. Without effective agglomerate formation, the subsequent portions of the process will not be able to perform as designed, leading to extremely low process yields and inferior product quality. Respecting those constraints, the overall objective of this subprocess is to generate moderately sized, well-formed coal-oil agglomerates. This agglomerate formation is typically conducted in two stages: a high-shear step where high energy dissipation is used to nucleate the agglomerates and a low-shear step where the retention time is carefully controlled to optimize agglomeration growth. The method of high-shear mixing can vary according to specific process designs and include: (1) overhead mixing, (2) static mixing, (3) inline pump mixing (e.g., a Silverson pump), (4) overhead mixing with a recirculation pump, and (5) combinations of the aforementioned. In addition, overhead mixing can be achieved using one of several impeller types, including a serrated impeller, a Rushton-type impeller, or a propeller. The method of energy inundation was evaluated through the course of this study, and the overall power intensity (e.g., HP/gpm) is a key variable impacting performance. Conversely, low shear mixing of often accomplished in a simple agitated tank, with the tank size dictating the retention time.

2.1.4. Agglomerate Recovery

Following their formation, the agglomerates are separated from the bulk of the aqueous phase. The main goal of the next step in the process is to remove as much free water as possible before the agglomerates are dispersed in the extraction column. Reducing the amount of water introduced to the extraction column helps the overall performance of the column and reduces the chances of stable emulsions forming. As agglomerates and free water leave the low shear tank, they flow over a sieve screen. Prior research had shown that agglomerates over 1mm in size were well formed and performed well in the HHS process. The screen chosen will have a nominal opening size of 1mm in order to remove agglomerates that had already grown to this size. The fully formed agglomerates flow over the screen and report to the extraction columns feed pump. The underflow of the screen collects all of the free water and any coal from under formed agglomerates. This material is sent to a set of flotation cells where the coal can be skimmed off the top and sent either for re-agglomeration or to the column for recovery. Well-

formed agglomerates tend to plug up piping and chutes due to the low moisture content. To help aid in moving these agglomerates, the first cell's overflow can be used to facilitate the moving of the dry agglomerates to the extraction column. For feeding the column progressive cavity pump will be used to feed the extraction column as it can handle a variety of solids easily and provide a constant flow rate.

2.2. Hydrophobic Displacement

Following agglomerate recovery, the enriched product is fed to hydrophobic displacement stage where additional solvent is added to disperse the agglomerates and prompt phase inversion. The agglomerates are then subject to mechanical impact, which prompts agglomerate breakage. After breakage, the entrained water is released and coalesces with other droplets or hydrophilic surfaces and drains out of the oil phase along with any entrained hydrophilic gangue. Colloquially, this unit is often denoted as a *Morganizer*, with process designs either being a column-type or jig-type. In the column-type Morganizer, agglomerates are pumped into a tall extraction column where solvent is introduced from the bottom to prompt upward flows product. In the column Morganizer, mechanical impact can be applied either through a fixed bed of packing (Jones, Yoon, and Noble 2019) or via oscillating screens (Nikhil Gupta et al. 2014). In the column type Morganizer, the upward solvent velocity must be carefully selected so as to lift the largest particles in the system without overdiluting the product, thus prompting larger downstream solvent recovery operations. Thus, in a column-type Morganizer, an economical limit often dictates the maximum effective particle size. Moreover, the hydrophilic surface area from the column walls and internals is a key design variable, which must be carefully addressed during scale up. Alternatively, in a jig-type Morganizer, mechanical impact is applied through a pulsating bed of hydrophilic ragging material. An air diagram pump can be used to control the rate and stroke of pulsation.

2.2.1. Solvent Recovery/Recycle

The final stage in the process is designed to recover as much of the solvent from the agglomeration and displacement portions of the process and recycle it for the continuous process. Coal laden solvent overflows the extraction column and enters into a cone bottomed thickening tank. The coal settles into the coal of this vessel and the excess solvent are decanted from the top back into the solvent storage tank. The settled coal is pumped into the vacuum drum filter where

the vacuum pressure removes the liquid solvent and produces a cake of mostly coal and residual solvent. This solvent is primarily on the particles' surfaces, so it is easily removed by a dual screw thermal dryer following the filter. The dryer temperature is set to be between 150 – 180 degrees Fahrenheit. This temperature is high enough to gently boil off the volatile solvent but much lower than the energy required to evaporate water. After the residual solvent is removed, the coal exits the dryer through a rotary valve and into a screw conveyor for collection.

2.3. Pilot Plant Design, Construction, and Shakedown

The design and construction of the pilot plant was an iterative process whereby design changes were made implemented after test campaigns in an effort to improve operability and overall process performance. The final iteration was able to consistently meet the process objectives described above for a range of feedstock types. The following section describes both the initial design as well as design modifications leading to the final plant iteration.

Figure 7 shows the general plant layout and the physical location of all unit operations on the mobile trailer. Likewise, Figure 2-3 shows the plant P&ID, including the location of all pumps, valves, and sensors of the "front end" of the pilot plant which includes the feed, agglomeration, screening/flotation, and extraction column. Figure 2-4 shows a similar schematic for the "back end" of the pilot plant which includes the solvent recovery and vacuum filters equipment used to recover the coal product. Detailed in the document below are the different operations portions of the process in their final form and a description of the testing and work completed to arrive at the present state. Figure 2-5 shows the mass flow sheet for the process.

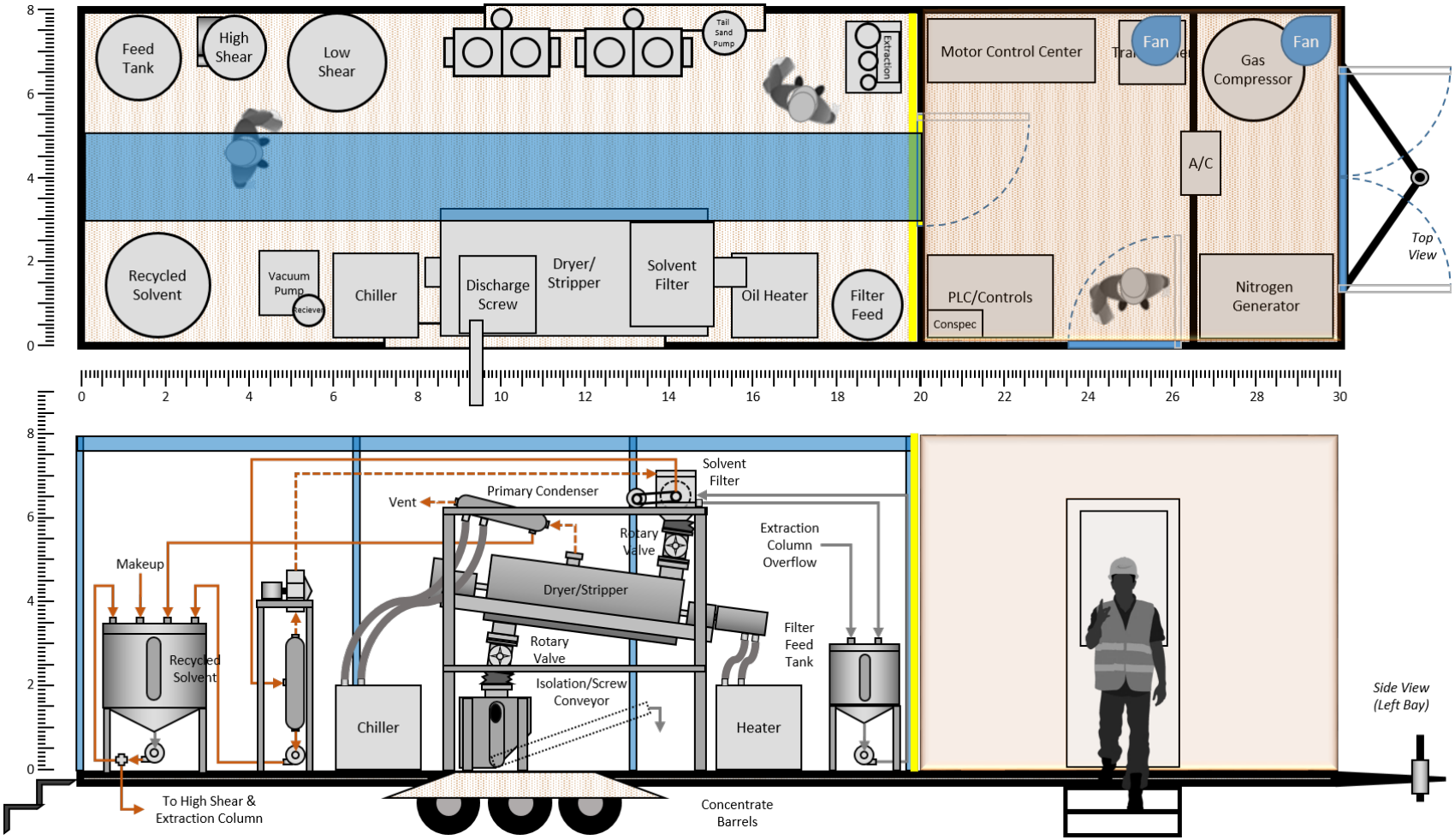


Figure 2-2: Initial Concept Design of Mobile Pilot Plant.

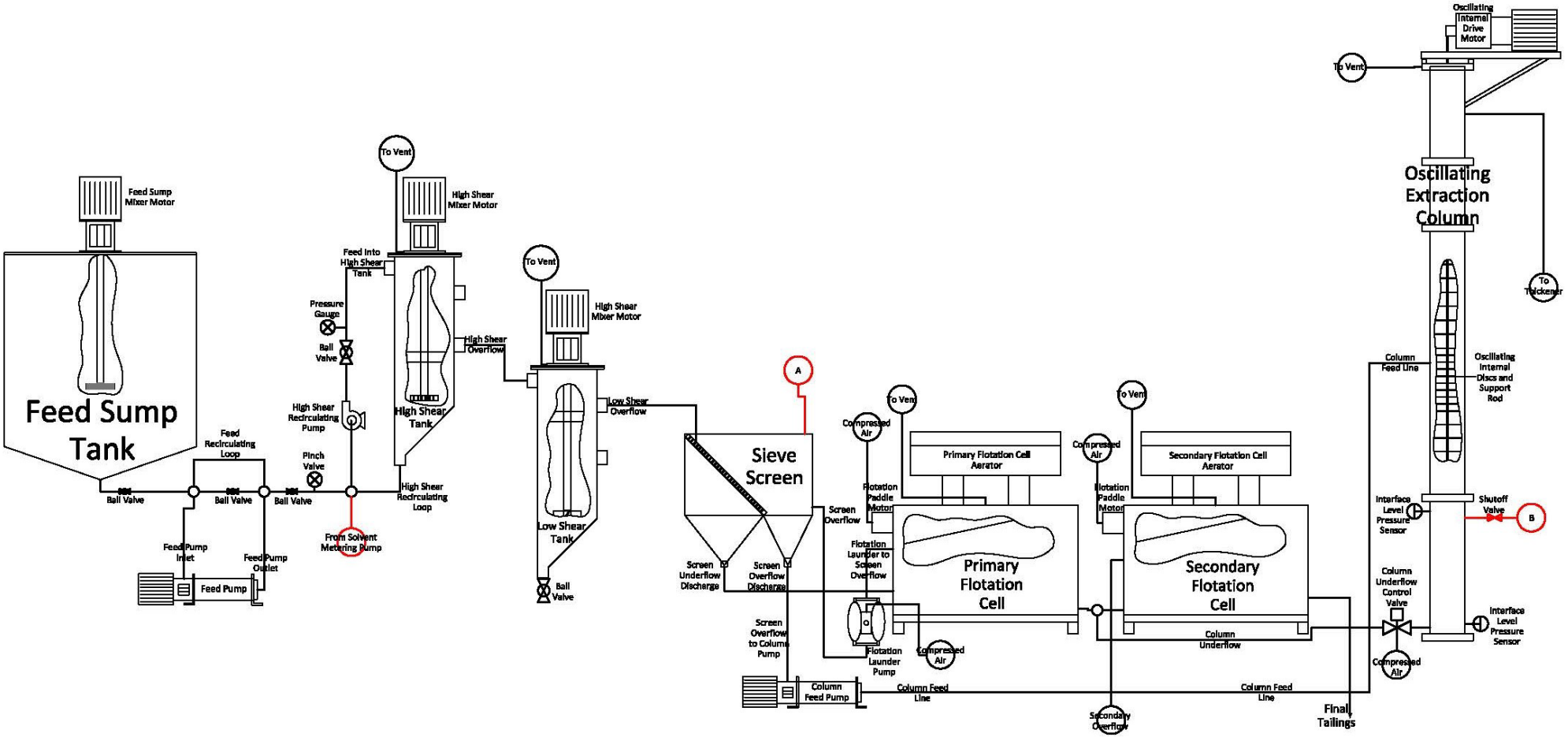


Figure 2-3. Pilot plant "front end" schematic.

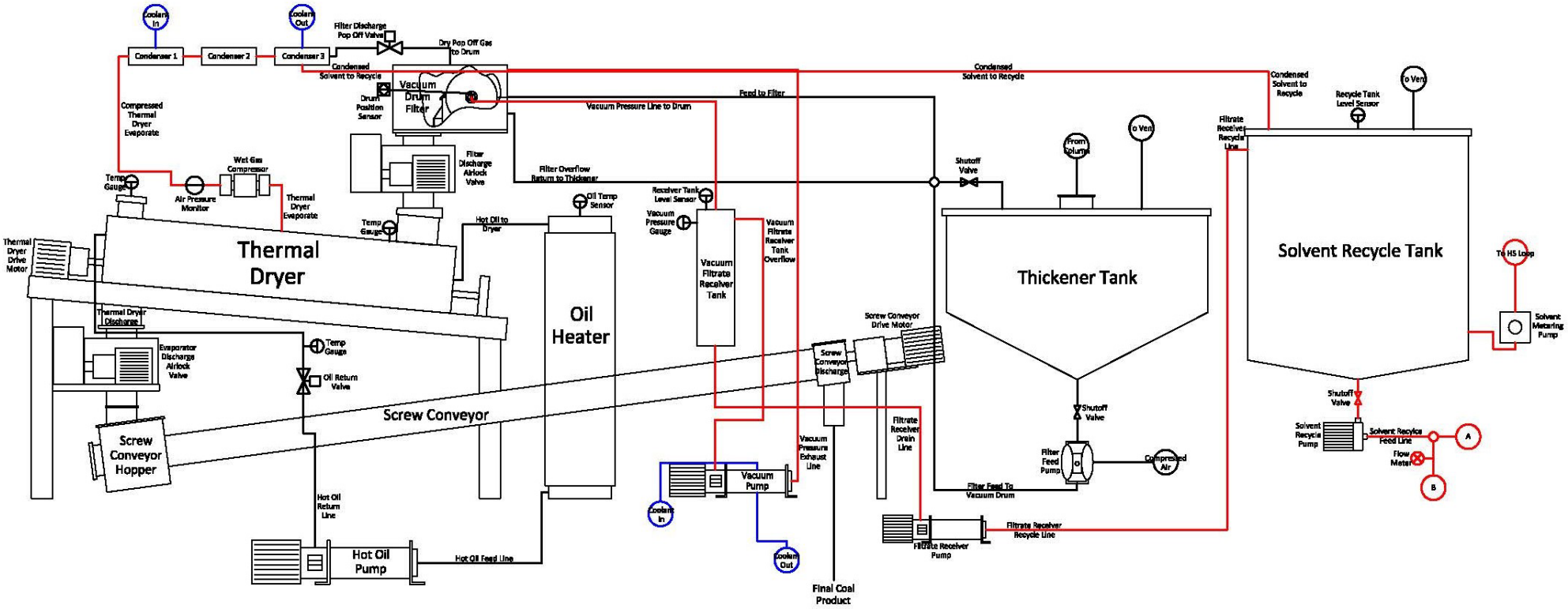
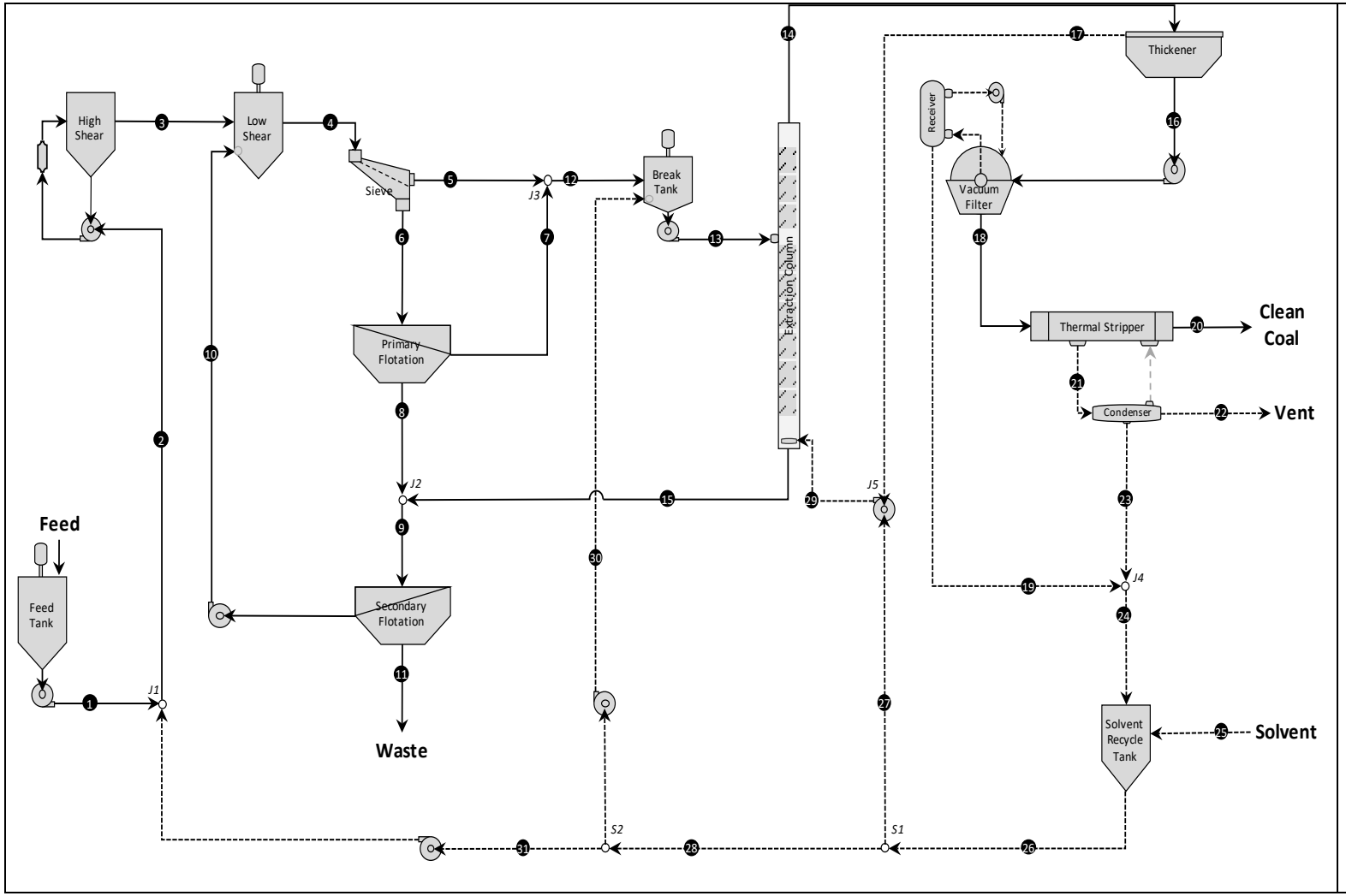


Figure 2-4. Pilot plant "back end" schematic.



STREAM	Feed (gpm)	Strm (gpm)
1	2	2.0
2	0	2.6
3	0	2.6
4	0	5.1
5	0	3.0
6	0	2.0
7	0	1.2
8	0	0.8
9	0	4.2
10	0	2.5
11	0	1.7
12	0	4.2
13	0	4.8
14	0	5.0
15	0	3.4
16	0	4.0
17	0	1.0
18	0	3.2
19	0	0.8
20	0	2.9
21	0	0.3
22	0	0.0
23	0	0.3
24	0	1.1
25	2.6	2.6
26	0	3.7
27	0	2.6
28	0	1.1
29	0	3.6
30	0	0.6
31	0	0.6

Figure 2-5. Mass flow sheet for process.

2.4. Process Feed

2.4.1. Final Design

The process is fed from a 200-gallon mixing vessel located outside of the storage facility where the mobile is located. The slurry from this tank is fed into the process by means of a progressive cavity pump. This pump was chosen as it will provide a constant feed rate independent of how much feed is in the mixing vessel and independent of air pressure. The pump is plumbed into a loop with a recirculation line to help handle excess flow rate in trials where the full rate of the pump is not needed. The main feed line from the pump passes through an air-controlled pinch valve. This pinch valve limits the flow rate into the system allowing precise control over the flows into the various parts of the system. Figure 2-6 below shows the flow diagram for the feed portion of the system. Table 5 shows the feed system equipment and flow rates.

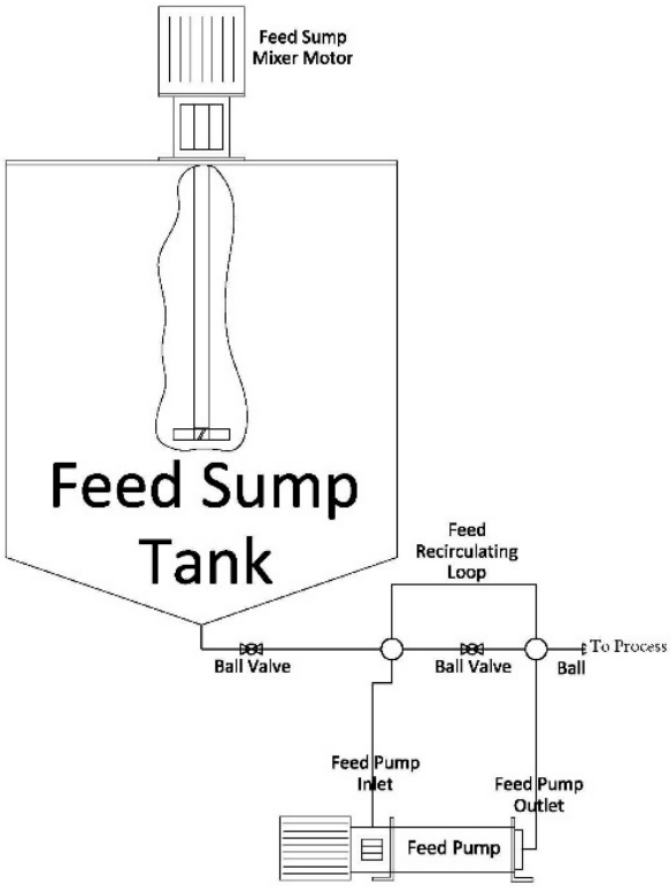


Table 5. Feed equipment and flow rates.

Feed Equipment List:
200 Gallon Stainless Tank
3/4 HP 120V AC Mixer Motor
1 HP 207V AC Progressive Cavity Pump
1" Steel Piping
3 - 1" Balls Valves

Flow Rates:
Recirculating Loop: up to 9 gpm
Feed to Process: 2 gpm

Figure 2-6. Feed equipment schematic, equipment list, flow rates.

2.4.2. Design Modifications during Test Campaigns

Previously the process was fed in a similar fashion be first a centrifugal pump and then followed by a pneumatic peristaltic pump. Initial trials with the centrifugal met with issues maintaining consistent feed rate. As the trials proceeded over an hour each time, the feed volume in the mixing vessel was drained down which reduced the hydrostatic head pressure. This reduction in pressure lowered the rate at which the pump could supply feed consistently and prohibited the pinch valve from functioning normally. While this would not be a problem for short trials, many of the initial trials were designed to be longer to test the various portions of the process. After the issues were brought to life with the centrifugal pump, a pneumatic peristaltic pump was chosen. This type of pump was chosen due to the ability to deliver a constant feed rate independent of the amount of feed in the tank. Initial trials were promising but problems also began to develop with this pump. First was the tubing that the pump used. The pump relies on a set of rollers to pinch the tube in a sequence to draw in fluids and push away from the pump head. After prolonged use the hose can develop weak spots and either burst or become too pliable to pump consistently. Second, the pneumatic pumps required a large amount of air pressure. This consumption combined with the other air driven units on the mobile plant soon over drew the system's air compressor which would lead to a decline in feed rate. It was these issues that guided the project to use a progressive cavity Seepex pump. After installation of this new pump, the plant has enjoyed consistent feed rates without interruption that have allowed the mobile pilot plant to meet all of its required product grades.

2.5. Agglomeration

2.5.1. Final Design

The current agglomeration setup utilizes two small mixing vessels: one dedicated to high-shear mixing and a second for low-shear. The current high shear tank has a volume of 4 gallons and two overflow ports that allow varying retention times based on the feed rate. The tank has a centrifugal pump plumbed into the bottom and a high-speed mixer mounted on the lid. The pump helped to create the necessary one minute of retention time by circulating the slurry through the vessel before the coal agglomerated large enough to pass to the low shear tank. The one minute of retention time was estimated to be the optimal time the agglomerates needed to form without spending too much time in the tank and growing too large. The mixer added a

greater amount of energy which greatly increased the oil dispersion. Figure 2-7 below shows the design considerations that went into the construction of the high shear tank. Figure 2-8 shows the design criteria and calculations used to design the new high shear tank.

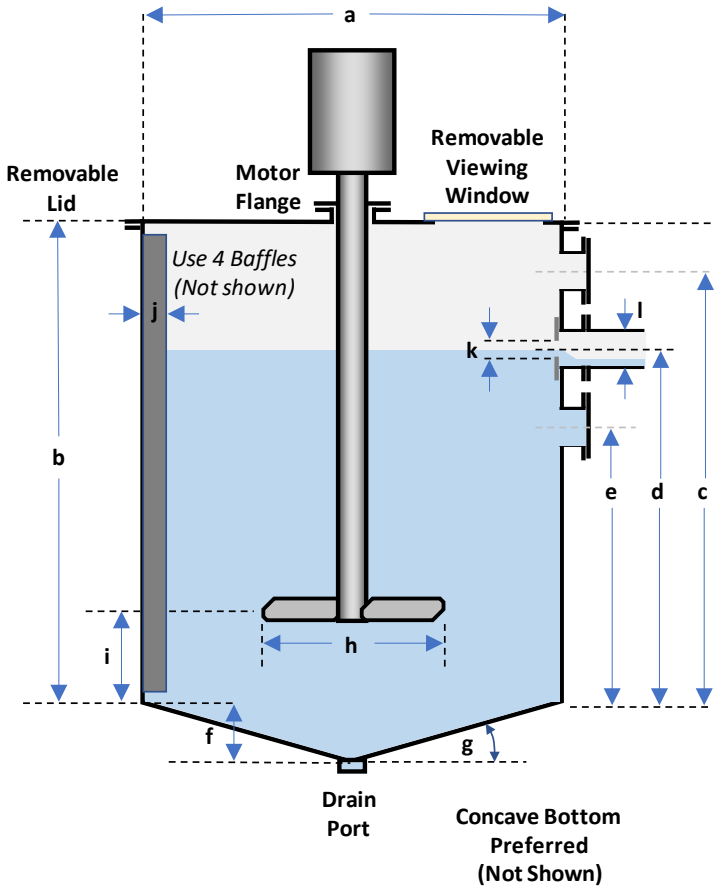


Figure 2-7. Design Considerations for High Shear Tank.

HIGH SHEAR TANK DESIGN RECOMMENDATIONS (MOBILE RIG)							
Feed Flow Rate	GPM	ID	2.00				
Tank Geometry							
-Cylinder Diameter	inch	a	8.000				
-Cylinder Area	ft^2	--	0.349				
-Cylinder Height	inch	b	12.000				
Liquid Levels							
- Upper Port Basis	inch	c	10.000	*based on 1:1.25 ratio			
- Middle Port Basis	inch	d	8.000	*based on 1:1 ratio (ideal)			
- Lower Port Basis	inch	e	6.000	*based on 1:0.75 ratio			
Cylinder Volume							
- Upper Port Basis	gal	--	2.18				
- Middle Port Basis	gal	--	1.74				
- Lower Port Basis	gal	--	1.31				
Cone Geometry							
-Height	inch	f	0.44	*based on 1/18 of tank diameter			
-Angle	degrees	g	6.34				
-Volume	gal	--	0.10				
Total Liquid Volume							
- Upper Port Basis	gal	--	2.27				
- Middle Port Basis	gal	--	1.84				
- Lower Port Basis	gal	--	1.40				
Retention Time							
- Upper Port Basis	min	--	1.14	*Otisca recommends <2-3 minutes			
- Middle Port Basis	min	--	0.92	*Otisca recommends <2-3 minutes			
- Lower Port Basis	min	--	0.70	*Otisca recommends <2-3 minutes			
Impeller							
-Diameter	inch	h	2.667	*based on 1/3 of tank diameter			
-Circumference	ft	--	0.698				
-Tip Velocity	ft/s	--	16	*based on Otisca 5 m/sec (i.e., 16 ft/s)			
-Rotation Speed	RPM	--	1375				
Impeller Position							
- Upper Port Basis	inch	--	3.333	*based on 1/3 off bottom			
- Middle Port Basis	inch	i	2.667	*based on 1/3 off bottom			
- Lower Port Basis	inch	--	2.000	*based on 1/3 off bottom			
Baffles							
-Width	inch	j	0.667	*based on 1/12 of tank diameter			
-Number	--	--	4	*standard recommendation			
Overflow Orifice (Insert)							
-Overflow Rate	GPM	--	2.00		→	126.2	cm^3/s
-Orifice Diameter	inch	k	2.00		→	5.08	cm
- Overflow Diameter	inch	l	3.00		→	7.62	cm
-Gravitational Accel.	ft/s^2	--	32.2		→	980.8	cm/s^2
-Fractional Full (est)	--	--	0.42	(target 0.4)	→	0.42	--
-Fractional Full (calc)	--	--	0.42		→	0.42	--
-Discharge Coeff (Cw)	--	--	0.59		→	0.59	--
-Overflow Depth	inch	q	0.84		→	2.14	cm
-Back-Check Flow**	GPM	--	3.01		→	190.1	L/s

Figure 2-8. High shear design worksheet.

The low shear tank originally was designed to be larger than the high shear tank to provide longer retention time in the agglomeration portion. However, this larger size created much longer than necessary retention times and agglomerates grew too large and sank. The tank was then redesigned to be the same diameter as the high shear tank with retention time set by overflow port positioning. The retention time the low shear tank was designed to have at a 2 gallon per minute feed rate was two minutes. As with the high shear, this time was determined to be the optimal time before agglomerates grew too large and began to sink. These times were calculated based on previous trials with larger tanks and longer retention times where large agglomerate growth and sinking was observed. Similarly, to the high shear, the low shear tank has a mixer mounted on the lid which rotates at lower speeds than the prior. This gentler mixing allowed agglomerates formed in the high shear to pick up more coal particles and grow larger in size. Once the agglomerates grow and leave the low shear tank, they flow over a sieve screen which primary purpose is to separate the coal particles from the bulk of the mineral matter and water from the feed slurry. Figure 2-9 shows the design considerations that went into the construction of the low shear tank. Figure 2-10 shows the design criteria and calculations used to design the new low shear tank.

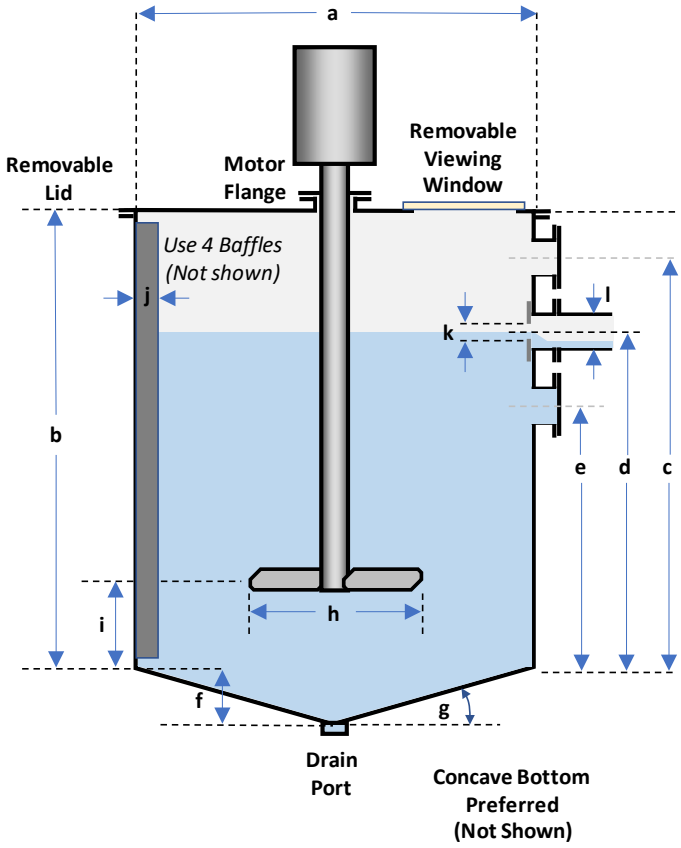


Figure 2-9. Low shear tank design schematic.

LOW SHEAR TANK DESIGN RECOMMENDATIONS (MOBILE RIG)							
Feed Flow Rate	GPM	ID	2.00				
Tank Geometry							
-Cylinder Diameter	inch	a	8.000				
-Cylinder Area	ft^2	--	0.349				
-Cylinder Height	inch	b	12.000				
Liquid Levels							
- Upper Port Basis	inch	c	10.000	*based on 1:1.25 ratio			
- Middle Port Basis	inch	d	8.000	*based on 1:1 ratio (ideal)			
- Lower Port Basis	inch	e	6.000	*based on 1:0.75 ratio			
Cylinder Volume							
- Upper Port Basis	gal	--	2.18				
- Middle Port Basis	gal	--	1.74				
- Lower Port Basis	gal	--	1.31				
Cone Geometry							
-Height	inch	f	0.44	*based on 1/18 of tank diameter			
-Angle	degrees	g	6.34				
-Volume	gal	--	0.10				
Total Liquid Volume							
- Upper Port Basis	gal	--	2.27				
- Middle Port Basis	gal	--	1.84				
- Lower Port Basis	gal	--	1.40				
Retention Time							
- Upper Port Basis	min	--	1.14	*Otisca recommends <2-3 minutes			
- Middle Port Basis	min	--	0.92	*Otisca recommends <2-3 minutes			
- Lower Port Basis	min	--	0.70	*Otisca recommends <2-3 minutes			
Impeller							
-Diameter	inch	h	2.667	*based on 1/3 of tank diameter			
-Circumference	ft	--	0.698				
-Tip Velocity	ft/s	--	16	*based on Otisca 5 m/sec (i.e., 16 ft/s)			
-Rotation Speed	RPM	--	1375				
Impeller Position							
- Upper Port Basis	inch	--	3.333	*based on 1/3 off bottom			
- Middle Port Basis	inch	i	2.667	*based on 1/3 off bottom			
- Lower Port Basis	inch	--	2.000	*based on 1/3 off bottom			
Baffles							
-Width	inch	j	0.667	*based on 1/12 of tank diameter			
-Number	--	--	4	*standard recommendation			
Overflow Orifice (Insert)							
-Overflow Rate	GPM	--	2.00		→	126.2	cm^3/s
-Orifice Diameter	inch	k	2.00		→	5.08	cm
- Overflow Diameter	inch	l	3.00		→	7.62	cm
-Gravitational Accel.	ft/s^2	--	32.2		→	980.8	cm/s^2
-Fractional Full (est)	--	--	0.42	(target 0.4)	→	0.42	--
-Fractional Full (calc)	--	--	0.42		→	0.42	--
-Discharge Coeff (Cw)	--	--	0.59		→	0.59	--
-Overflow Depth	inch	q	0.84		→	2.14	cm
-Back-Check Flow**	GPM	--	3.01		→	190.1	L/s

Figure 2-10. Low shear tank design worksheet.

To aid in the design of the two mixing vessels a workbook was created that used established tank design criteria. Using this criterion, the workbook can calculate dimensions for the tank as well as the impeller and the overflow ports. The overall liquid level is determined by a ratio of the level to the diameter of the tank. The ideal ratio of level to tank diameter is in the region of 0.8 – 1.0. In general, if the ratio is too low (<0.6) the design should be avoided and if it increases (>1.4) dual impellers should be used. For the use of a cylindrical tank baffles should be installed to prevent swirling and any round or conical bottoms should be kept small in order to eliminate dead spots provide for good mixing (James 2015). Baffles installed should be 1/12 of the tank diameter in width. Typically, 3 – 4 baffles are used in designing tanks with 4 baffles being the ideal number. Adding more than 4 baffles does not show any significant improvement to the mixing efficiency (James 2012). Impellers are typically designed to be 1/3 of the overall tank diameter and for best mixing efficiency should be located at one impeller diameter for the tank bottom (Hennis 2017). Impellers were chosen for each tank based on the required action inside the particular tank. The high shear tank needs an impeller that will create high shear forces that will widely disperse the solvent into the coal particles. For this tank a serrated impeller was chosen. Serrated impellers created intense shear forces at the tips of the blade which aid in rapid dispersion (Greaves 2023). Trials conducted by Otisca had determined that in oil agglomeration complete dispersion is achieved when impeller tip speeds range from 10 – 18 m/s (Keller 1982). Table 6below shows a selection of trials looking at the high shear section of the process. The table shows that the tip speed of the impellers was well within this range and would signify that complete dispersion was being achieved in the high shear tank. The table also shows the horsepower calculated on the mixer shaft which ranged from 0.4 Hp to 0.66 Hp depending on the rotational speed of the high shear pump. However, the data shows that the performance of the high shear mixer in producing on spec moisture products and recoveries >80% was largely not influenced by the high shear pump. This is most likely due to the mixer taking the bulk of the dispersion responsibilities and the pump mainly recirculating the feed through the high shear loop.

Table 6. Selection trials looking at impeller HP and tip speed.

Test	Coal Slurry Feed Rate	Coal Slurry Conc.	High Shear Pump Speed (rpms)	High Shear Shaft Horsepower	High Shear Tip Speed (ft per sec)	High Shear Tip Speed (m per sec)	High Shear Tailings Ash	Extraction Column Solids	Extraction Column Moisture	Final Tailings Ash
1	3.6 gpm	4%	2800	0.4	44.3	13.50	54.86	7.0	6.0	86.3
1	3.6 gpm	4%	3200	0.45	50.6	15.42	50.05	7.0	6.0	
2	3.6gpm	4%	3600	0.62	56.9	17.34	56.54	8.1	5.7	87.9
2	2.0gpm	4%	2800	0.45	44.3	13.50	40.87	7.1	6.8	
2	2.0gpm	4%	3200	0.45	50.6	15.42	50.43	4.3	1.9	
2	2.0gpm	4%	3600	0.62	56.9	17.34	44.36	7.5	5.2	
3	2.0 gpm	8%	2800	0.41	44.3	13.50	15.96	8.3	6.1	85.3
3	2.0 gpm	8%	3200	0.49	50.6	15.42	16.14	7.8	6.6	
3	2.0gpm	8%	3600	0.66	56.9	17.34	25.11	--	--	
4	2.0 gpm	8%	3200	0.51	50.6	15.42	22.74	7.0	6.2	
4	2.0 gpm	8%	3600	0.66	56.9	17.34	36.37	6.8	5.5	
5	2.0 gpm	8%	3200	0.45	50.6	15.42	49.32	7.4	5.7	89.7
5	2.0 gpm	8%	3600	0.62	56.9	17.34	60.03	8.0	8.8	
6	2.0 gpm	8%	2800	0.41	44.3	13.50	61.51	7.7	6.2	90.8
6	2.0 gpm	8%	2800	0.31	44.3	13.50	44.87	7.3	12.8	
6	2.0 gpm	8%	2800	0.41	44.3	13.50	--	7.5	9.1	
8	2.0gpm	8%	3200	0.51	50.6	15.42	63.27	6.0	6.5	89.7
8	2.0gpm	8%	3200	0.51	50.6	15.42	45.34	6.0	6.5	
8	2.0gpm	8%	3200	0.51	50.6	15.42	63.42	6.0	65	

In the low shear, the tank needs to be evenly mixed to allow the agglomerates to contact each other and grow. For this application, an axial flow marine propeller type impeller was chosen. The axial flow design keeps solids in suspension and marine style provides for efficient mixing (James, 2013). Figure 2-11 below shows an example of a serrated impeller and a marine type of impeller.



Figure 2-11. Example of serrated impeller (R) and marine type impeller (L).

The screen has openings that are approximately one millimeter in size. The overflow from the screen is then fed into the Morganizer to be dispersed and broken down to separate the

carbon from the remaining water and mineral matter. The underflow from the screen is fed into a flotation cell where the remaining coal can potentially be recirculated into the beginning of the agglomeration portion. The water taken from the flotation cells is used to help move the agglomerates to the Morganizer where it falls out in the underflow and the remaining portion overflows to the secondary flotation recovery and then final tailings. Figure 2-12 below shows the basic agglomeration setup diagram as it is currently being tested without the flotation cells and sieve screen. Table 7 lists the equipment pieces and flow rates associated with this portion.

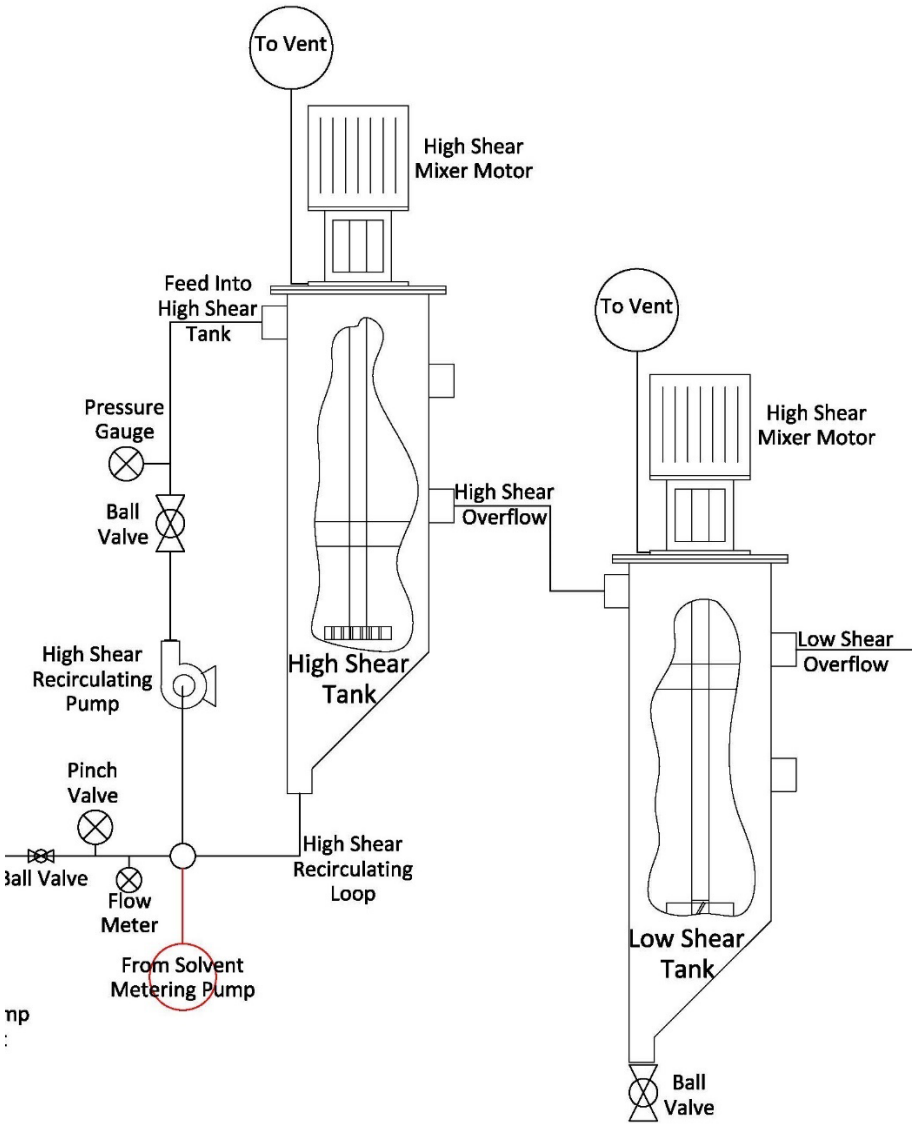


Figure 2-12. Agglomeration portion of HHS plant schematic.

Table 7. Agglomeration equipment list and flow rates.

Agglomeration Equipment List:
2.27 Gal Carbon Steel Custom Tank x 2
1.5 HP 480V AC Mixer Motor x 2
1.5 HP 480V AC Centrifugal Pump
1 HP 480V AC Progressive Cavity Pump
2.667" Shear Type Mixing Impellar
2.667" Axial Flow Type Mixing Impellar
1/2" Mass Flow Meter
1/2" pneumatic pinch valve
2" Steel Piping for Overflows
1" Steel Piping
3 - 1" Balls Valves
1" Stainless Mixing Shaft x 2
1/4" Low Pressure Gauge
Flow Rates:
Recirculating Loop: 11 gpm
Feed to Agglomeration: 2 gpm
Solvent Inflow: 350 ml/min
High Shear Overflow: 2 gpm
Low Shear Overflow: 2 gpm

2.5.1. Design Modifications during Test Campaigns

Previous to the current agglomeration setup, the portion went through several iterations. Changes before the final setup were minor with the low shear tank being replaced and a mixer being added to the high shear tank. The previous tank was much larger which gave long retention times. The problem with these longer retention times was that the agglomerates would grow too large and prevent them from passing from the tank into the Morganizer. The mixer in the high shear tank greatly improved agglomerate formation and provided for more consistent results. Once the agglomeration became consistent, product ash and moisture values were able to hit project targets reliably. Prior to the high shear tank with a pump and mixer, the agglomeration was attempted to be formed solely with a pump called the Silverson pump. This pump is commonly used for cutting up emulsions by spinning a special rotor in a drilled stator at a very high speed. The intent was to add high energy quickly dispersing the solvent in the feed slurry. Data showed that this method of energy dissipation was inconsistent, with product quality varying dramatically through the course of a trial. While some trials resulted in decent

agglomeration formation, most trials struggled to form good agglomerates with this set up. It was determined that the pump while adding large amounts of energy, only allowed for a very small retention time and longer retention times are crucial for well-formed agglomerates Chapter 3 describes this design modification in further detail along with the attendant results. Figure 2-13 shows the original agglomeration setup (L) and the current agglomeration setup (R).



Figure 2-13. Original Agglomeration Setup (Left) and Current Agglomeration Setup (Right).

2.6. Flotation

2.6.1. Final Design

The mobile plant utilizes two flotation cells in series. The two cells sit next in line after a sieve screen that separates the newly formed agglomerates from the bulk of the mineral laden free water. The free water passes through the screen and through the underflow enters the primary flotation cell. The flotation cell takes any coal that makes it through the screen and then passes it along to a pump which can send the coal to any point in the agglomeration portion. Currently agglomerate formation is very efficient so there is very little coal that passes through the screen. Any coal and excess water that make it to the pump are then used to wash the agglomerates through the screen overflow and into the pump that feeds the Morganizer. The secondary cell produces the final tailings as well as recovering any coal and solvent that exits the underflow in the Morganizer. The water, coal, and solvent enter the cell and the carbon and oil are overflowed to a pump which can also be sent to any portion of the agglomeration process. Currently the overflow of this cell is pumped into barrels for recovery. Depending on the coal

sample and its ability to form good agglomerates can greatly affect what enters the secondary cell. With slurries that are easy to agglomerate, there is little coal and solvent that make it into the flotation cell. If the slurry is a difficult sample, emulsions will form and report to the cell. Because of this and due to testing different slurries frequently, the decision was to pump the overflow into the drums so as not to impact the system. However, trials were conducted where the underflow was pumped into the Morganizer which has shown its ability to handle the emulsions and extra solvent without disrupting the process. Figure 2-14 shows the flow diagram of the current setup with the sieve screen and two flotation cells. Table 8 lists the screening and flotation equipment and flow rates.

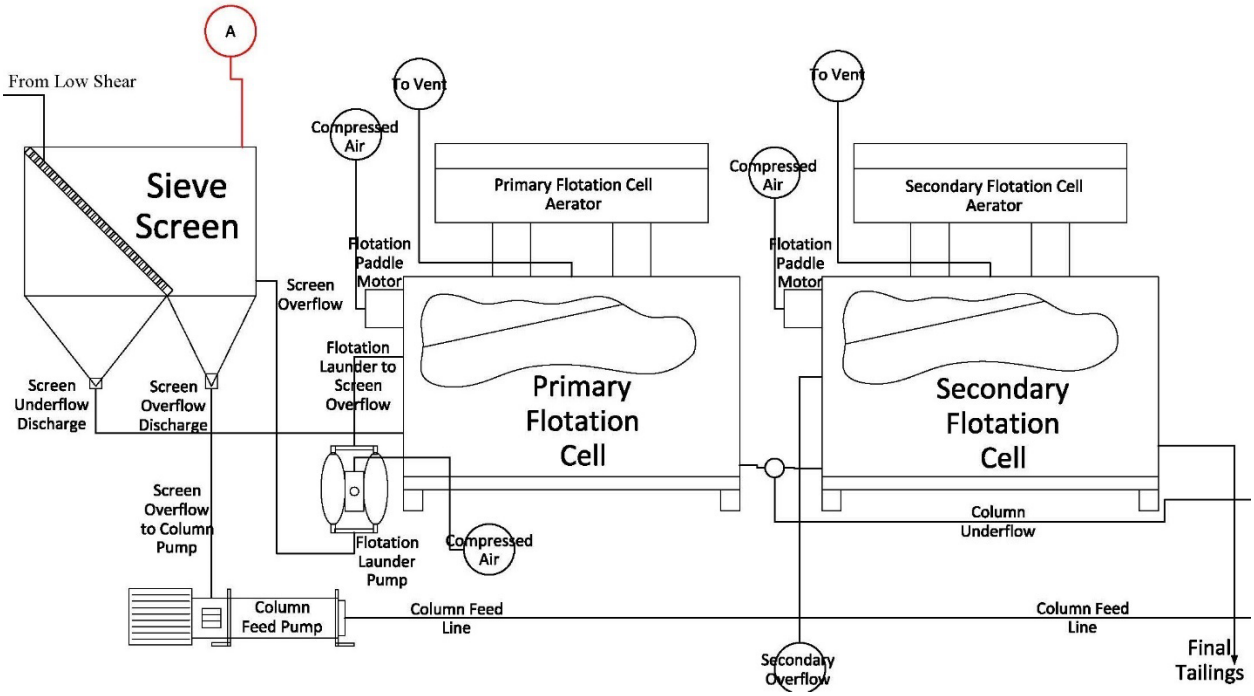


Figure 2-14. Sieve screen and flotation cells.

Table 8. Screen/Flotation equipment and flow rates.

Screening/Flotation Equipment List:
Enclosed Stainless Sieve Screen w/ 1mm openings
Titan Flotation Cells x 2
1 HP 480V AC Progressive Cavity Pump
1" Pneumatic Diaphragm Pump
1/2 Hp Pneumatic Paddle Motor x 2
3/4 Hp 480V AC Aerator Motor x 4
2" Steel Piping for Screen Under/Overflow
1" Steel Piping
1" Reinforced PVC Tubing
Flow Rates:
Solvent Inflow (A): 1 gpm when needed
Feed to Column: 4.8 gpm
Primary Flot Overflow: 1.2 gpm
Secondary Flot Overgflow: 2.5 gpm
Final Tailings: 1.7 gpm

2.6.1. Design Modifications during Test Campaigns

The flotation cells have primarily remained unchanged since their initial installation on the mobile pilot plant. In several trials the floatation overflow from the secondary has been tested being fed into different portions of the process but it is currently being sent to a 55-gallon drum for collection. The most notable change to this part of the process was the addition early on of the sieve screen which allowed for the easy removal of the bulk of freed water from the system. At first the underflow would just report to the flotation cells and eventually to the tailings stream. However, as agglomerate formation in the process improved it was found that the dryer better formed coal agglomerates would plug up the screen's overflow chute. Once the chute plugged in, the trial had to be stopped and the plug cleared. To aid in keeping this cute open, the screen underflow as before went into the primary cell. As this material built up it would overflow the cell into its launder and then would be pumped into the screen's chute. This extra water stream helped to keep agglomerates from building up and helped to pump them into the Morganizer. The amount of water was found to not be enough to affect the extraction column's performance.

2.7. Morganizer

2.7.1. Final Design

The equipment described in the previous section was used to create the agglomerates which were then fed to the crucial part of the process. The pilot plant utilized two variations of the column type Morganizer to handle the dispersion of the newly formed coal agglomerates. The first type tested consisted of a taller column with mechanical internals used to break apart the agglomerates. This column was used for the bulk of the test trials so most of the data within this document was generated with this piece of equipment. The second type of Morganizer which was the last piece installed and tested on the pilot plant was a smaller column which used compressed air to creak the necessary motion needed to break apart the agglomerates.



Figure 2-15. New column jig Morganizer post fabrication (L) and installed on pilot plant (R).

The latest de-emulsifier consists of two parts; the compressed air actuated pulsing mechanism and the launder topped column which contained a layer of ceramic sphere ragging suspended on a screen. The air mechanism uses compressed air fed to a valve block with two solenoid valves. These valves are controlled by a simple plc logic control box that has them operating at opposite timing of each other. The output of this valve is connected to a pneumatic

cylinder that drives a piston. The valves allow the air to push and pull the cylinder back and forth creating the pulsing action. Needle valves on the discharge of the solenoids grant the ability to increase or decrease the length of the stroke in the pulsating motion. The control box has a timing control that connects a timing dial to each solenoid valve. Adjusting these dials can increase or decrease the number of pulses the valves can create with the pneumatic cylinder. Figure 2-16 shows the pneumatic cylinder, valve block, and piston.

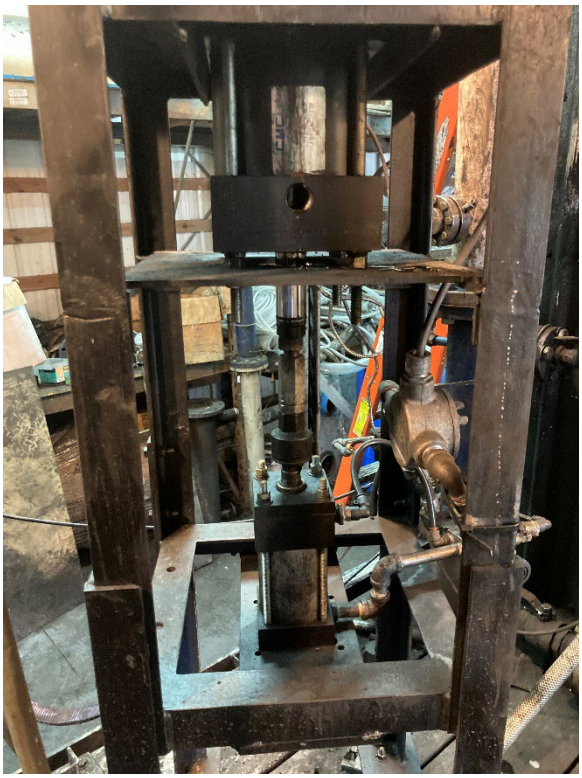


Figure 2-16. Pulsing mechanism for jig Morganizer.

The upper portion of the Morganizer is constructed using four-inch diameter piping. The main body of the column is built using large glass tubing connected in the middle by four-inch carbon steel pipe fittings. Both glass and steel are hydrophilic materials, so they are chosen to help water coalesce and fall out of the system. The reason glass is chosen is to help researchers visually see what is happening within the Morganizer without sacrificing performance as what would happen with Plexiglas. Inside of the metal connector between the two glass sections is a stainless screen which is approximately 1.5 inches below the glass/metal interface. This distance allows the Morganizer feed to be pumped into the ragging layer while keeping the pipe fittings in the metal section and not compromising the integrity of the glass when attached to hoses etc. a

launder top constructed out of Plexiglas which collects the column overflow and funnels it to a one-inch fitting that is plumbed into the pilot plant's thickener. At the base of the column there is a one-inch fitting with a gate valve that controls the underflow leaving the Morganizer. The lower section of glass allows for operators to easily see where the oil/water interface is without the need to install a level control system. While a level control system would be ideal, they are both costly and have proven to be problematic with a small column like this version of the Morganizer when the pulsing mechanism is operating. Figure 2-17 shows the upper portion on this version.



Figure 2-17. Launder tops for new column jig Morganizer.

Both halves of the Morganizer are joined together on a stand which is built to allow easy removal of the upper portion from the lower portion which keeps the rest of the system intact. The pulsing mechanism is bolted to the upper portion inline. This allows the full force of the pulse to travel directly straight up the column to interact with the ragging and agglomerates in a smooth motion. Previous tests showed that attempting to have the pulsing force enter the column from a perpendicular angle to the column just created an unstable wave motion in the column.

The previous version of the Morganizer is much larger than the new version and utilized a different mechanical action to break up the agglomerates. This version of the de-emulsifier used a motor driven gearbox with an offset spindle. This spindle pushed and pulled on a long rod inserted into the center of the column. This rod had a series of perforated discs spaced along its length. These discs being pulled up and pushed down inside the length of the column would create the mechanical energy necessary to break apart the agglomerates. Compared to the current version, this Morganizer was much taller and stood approximately ten-feet tall from the base up to the top mounted oscillating motor. The oscillating column Morganizer consists of three sections. The base section is where the underflow exits the column as well as the extra solvent flow is introduced to help with the lifting of coal particles. The next section is where the oscillating plates are positioned as well as where the feed is introduced to the column. The top section includes a twelve-inch section where there are no plates and the column overflows which drains into the thickener. Figure 2-18 shows a close up of one of the perforated oscillating discs.



Figure 2-18. Close up of perforated oscillating disc.

The spacing on the discs within the column has been determined through multiple trials where the distances between each disc were changed and then tested. Areas of concern were the spacing around where feed enters the column as well as spacing above and below this point. Concerns about spacing are due to it being too tight in the wrong areas which could actually end

up pushing released water upwards instead of letting it fall into the underflow. Figure 2-19 shows the as tested flow diagram for the extraction column or Morganizer. Table 9 lists the equipment associated with the extraction column and the associated flow rates.

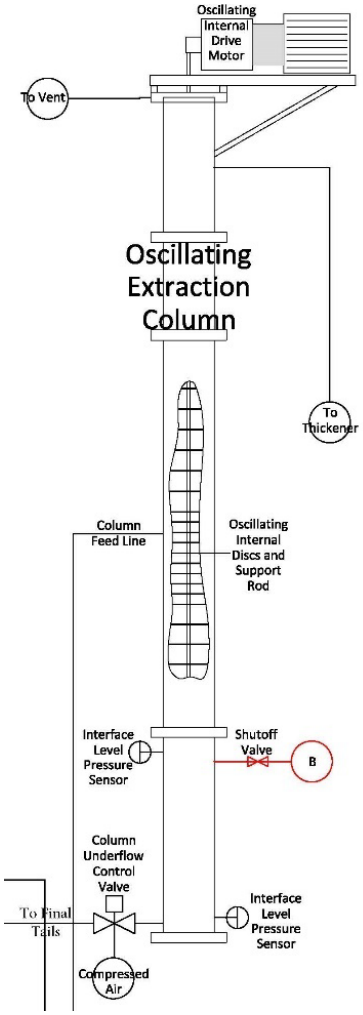


Figure 2-19. Extraction column schematic.

Table 9. Extraction column equipment list and flow rates.

Eaxtraction Column Equipment List:
4" Steel/PVC Custom Extraction Column
1/2 Hp 120V AC Motor and Oscillating Gear Box
1/4" Stainless Rod - 72"
2.5" Perforated Discs x 24
1" Ball Valve x 1
1/2" Pressure Differential Sensors x 2
1" Pneumatic Pinch Valve
1" Steel Piping
1" Reinforced PVC Tubing
Flow Rates:
Column Overflow: 5 gpm
Column Underflow: 3.4 gpm

2.7.1. Design Modifications during Test Campaigns

The previous version of the column Morganizer utilized a stack of stainless-steel packing to break up agglomerates. The packing consisted of several strips of very thin stainless steel welded and pinned together to form a four-inch cylinder that would fit tightly inside the inner diameter of the column. The theory behind the packing was that the spaces created in between the strips of metal create turbulence as fluid flowed through it. This turbulence was intended to break up the agglomerates and the steel would provide a hydrophilic surface for the newly freed water particles to attach to and coalesce. The larger drops would then be free to fall down and out of the system.

Initial trials with the packed column showed mixed results. Even though many of these trials occurred before the agglomeration setup was improved with the high shear mixer, overflow moisture was not consistent and often above spec. One difficulty with the trials was evident with samples comprised with higher percentage solids. Samples with higher solids contents often would overwhelm the tight spaces between the pieces of packing and end up with the column becoming plugged. Another downside to the packed column is that it was susceptible to contamination from heavy oils and other materials that inhibit the hydrophilic surface properties of the metal. These contaminations were proved in several trials to not only lower performance of the Morganizer but also increased the possibility of the column becoming packed with solids

materials. Due to these operational problems, the decision was made that the packed column was ineffective, and the move was made to develop the oscillating column.

2.8. Solvent Recovery

2.8.1. Final Design

The ability to recover solvent back from the process is a key factor in keeping the operating costs at a minimum. In order to accomplish this task, the mobile pilot plant utilizes a system that contains a thermal dryer as the center piece. Following the Morganizer, the coal/solvent product flows into a thickener tank. The coal particles settle quickly in this vessel and any excess solvent overflows back to the solvent recycle tank.

Settling velocity for the coal particles can be calculated using Stoke's Law.

Equation 2-1

$$v = \frac{d^2 * g * (\rho_s - \rho_f)}{18 * \mu}$$

Where v = settling velocity (m/s), d = diameter of the coal particle, g = acceleration due to gravity, ρ_s = density of coal (1.35), ρ_w = density of the fluid (0.653), and μ is viscosity of the fluid ($4.21e^{-7}$ m^2/sec). For the calculation assume a particle passing through a 325-mesh screen 44 microns ($4.318x10^{-5}$m) in diameter. While Stokes law is typically valid for free settling and not for concentrated particles, in this case it is valid for the system due to the solids concentrations being very low.

Equation 2-2

$$v\ (m/s) = \frac{4.318x10^{-5\ 2} * 9.8\ m/sec^2 * (1.35 - 0.653)}{18 * 4.21x10^{-7}}$$

$$v\ (m/s) = \frac{4.318e^{-5\ 2} * 9.8\ m/sec^2 * (1.35 - 0.653)}{18 * 4.21x10^{-7}}$$

$$v\ (m/s) = 0.00168$$

$$v\ (ft/min) = 3.94$$

In order to obtain this upward velocity, the necessary feed rate of solvent was determined. The calculation of the feed rate is shown below.

$$Q = A * v$$

Where Q is the flowrate inside the column, A is the cross-sectional area of the column, and v is the upward velocity of the solvent in the column.

Equation 2-3

$$Q(ft^3/min) = (\Pi * r^2) * v$$

$$Q(ft^3/min) = 0.35$$

$$Q\left(\frac{gal}{min}\right) = 0.35 * 7.48$$

$$Q\left(\frac{gal}{min}\right) = 2.61$$

Based on the above calculation, the solvent will need to be fed into the column at around 2.6 gallons per minute in order to achieve an upward velocity of at least 4 feet per minute.

The underflow from this tank is pumped into a vacuum drum filter where the remaining excess solvent is extracted from the coal particles as it rotates, and the carbon material forms a filter cake. The filter cake drops from the drum through a rotary airlock into the bottom of the thermal dryer. The thermal dryer utilizes the heat generated by circulating hot oil through the body of the dryer by means of a hot oil pump. A set of augers pushes the material through the center of the dyer. The circulating hot oil raises the internal temperature of the dryer to above 150 degrees Fahrenheit. This temperature is above the vaporization temperature of iso-hexane (140 degrees Fahrenheit) which allows residual solvent to be driven off to be collected. This lower temperature helps to reduce the amount of overall energy the thermal dryer needs to operate. The difference in energy required to evaporate isohexane versus water is calculated below. Using the formula for the heat of vaporization of a liquid:

Equation 2-4

$$Hv = q / m$$

Where Hv (J/g) is the heat of vaporization which is the energy required to evaporate a liquid, and q (J) is total heat of the liquid at the vaporization point, and m (g) is the total mass of the liquid. Solving equation 1 for q:

Equation 2-5

q = mHv

For water: Assume 100g sample.

Hv(w) = 2,260 J

m(w) = 100 g

q(w) = 100 g * 2,260 J/g

q(w) = 226,000 J

For Isohexane: Assume 100g sample.

Hv(iso) = 323.625 J/g

m(iso) = 100 g

q(iso) = 100 g * 323.625 J/g

q(iso) = 32,363 J

Comparing the two heat values calculated it shows that water takes a significantly larger amount, almost 7 times more, to evaporate than isohexane. This shows why a drying method that does not involve evaporating water is desirable especially for plant operators where energy can constitute a large portion of operating costs.

The solvent driven off from the coal particles in the thermal dryer are collected and compressed using a wet gas compressor. This compressed mixture is sent through a series of three condensing units being cooled by a glycol chiller unit. The chiller circulates an ethylene glycol mixture through the condensers at around 30 degrees Fahrenheit. The combined pressure and cold temperature turn the vaporized solvent back into a liquid which is collected and returned to the solvent holding tank. The pressurized gasses leftover after the solvent is removed are then regulated to about 20 psi at a solenoid valve connected to the drum filter and are utilized in pushing the built off cake from the drum and into the dryer. The solenoid valve is controlled by a magnetic sensor fastened near the drive shaft for the drum filter. A series of metal tabs attached to the shaft are read by the sensor and counted by the system's programming for it to fire the valve after six tabs have been read.

After leaving the thermal dryer, the coal material passes through another rotary airlock into a screw conveyor. This conveyor is equipped with dual butterfly valves at its discharge to eliminate any vapors from leaving the screw. A nitrogen line is plumbed into the discharge of this screw conveyor to push any remaining vapors back to the dyer to be collected. The screw conveyor is insulated to help eliminate temperature drop which would result in the condensing of any vapors back into the coal product. Following the screw conveyor, the dry coal product leaves the double valves and is collected into drums. Figure 2-21 illustrates the flow diagram for the solvent recovery system which utilizes a drum filter and thermal dryer. Figure 2-20 and Table 10 lists the equipment and flow rates associated with the solvent recycle tank and solvent recycle pump. Table 11 and Table 12 list the equipment and flow rates associated with the solvent recovery and dry coal production.

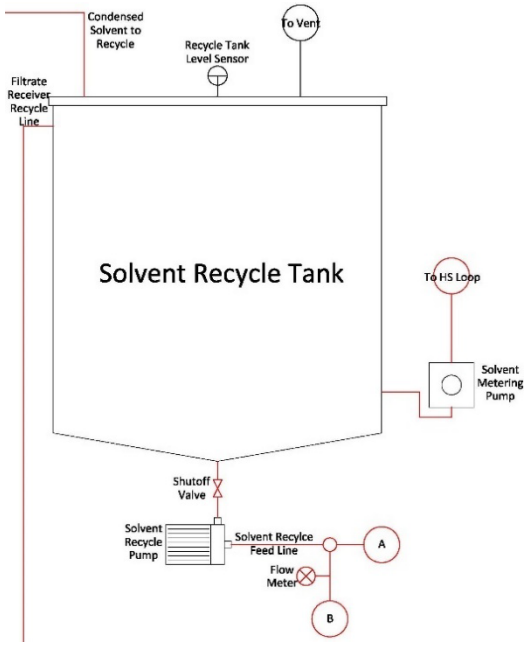


Figure 2-20. Solvent recycle tank and pump.

Table 10. Solvent recycle equipment list and flow rates.

Solvent Recycle Equipment List:
90 gallon ceramic coated steel tank
LMI Metering Diaphragm Pump
1.5 HP 480V AC Centrifugal Pump
1/2" Mass Flow Meter
Rosemount level sensor
1/4" Reinforced PVC Tubing
3/4" Reinforced PVC Tubing
1" Ball Valve x 1
Flow Rates:
Solvent Flow to Column (B): 2.6 gpm
Solvent Outflow (A): 1 gpm when needed
Solvent Inflow from Filtrate Receiver: 0.8 gpm
Solvent Inflow from Condensors: 0.3 gpm

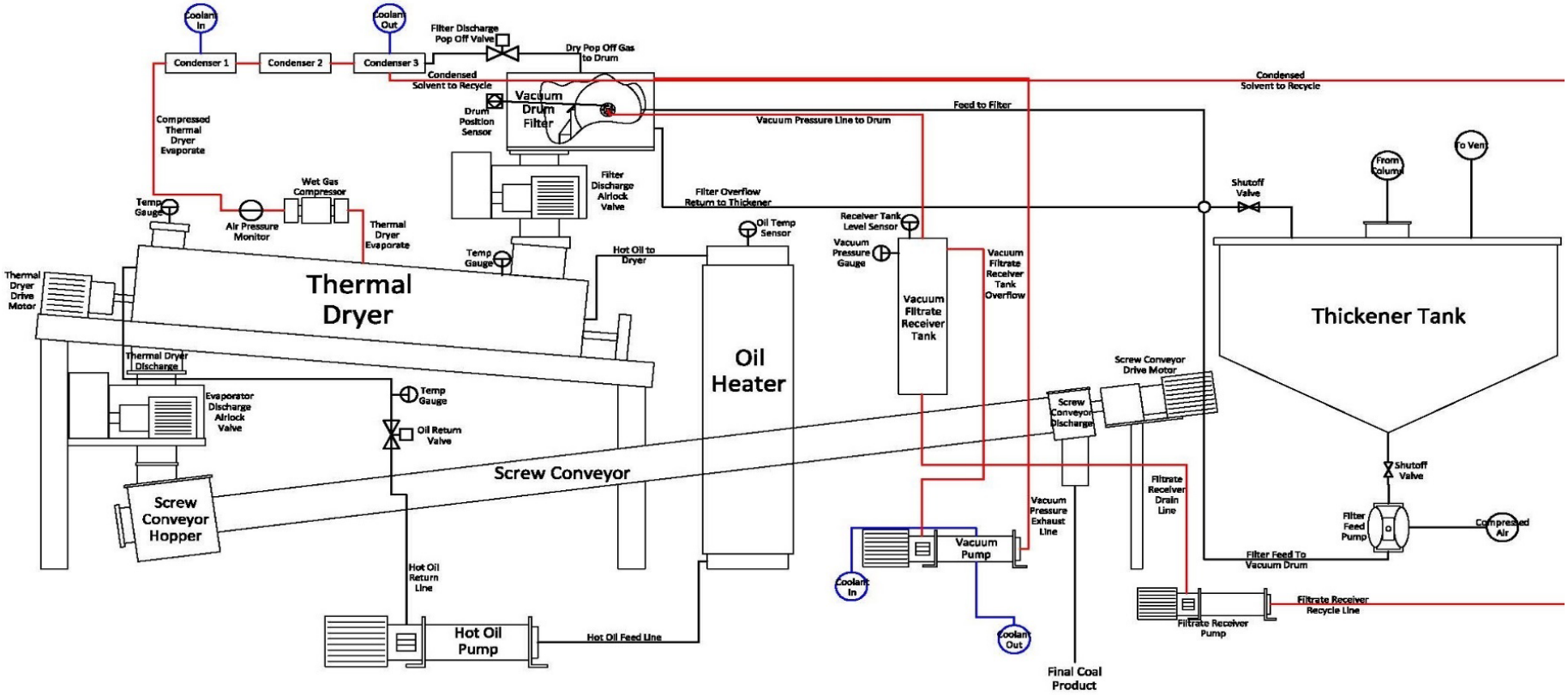


Figure 2-21. Solvent recovery and vacuum filter/coal production.

Table 11. Solvent recovery equipment/flow rates.

Solvent Recovery Equipment List:
480V AC Water Sealed Vacuum Pump
Oil Heated Twin Screw Evaporator Dryer
480V AC Rotary Valve Airlocks x 2
480V AV Oil Heater
Gylcol Cooled Condensors x 3
480V AC Wet Gas Compressor
1 HP 480V AC Progressive Cavity Pump x 2
1/2" Air Pressure Sensor
DC Pneumatic Discharge Valve
5 Gallon Custom Stainless Tank
3/8" Reinforced PVC Tubing
1/2" Reinforced PVC Tubing
1" Reinforced PVC Tubing
1" Steel Piping
1/2" Shutoff Valve
1/4" Vacuum Pressure Gauge
480V AC Glycol Chiller
Flow Rates:
Vacuum Receiver: 0.8 gpm
Condenser Recycle: 0.3 gpm
Hot Oil Circulation: 3 gpm

Table 12. Dry coal production equipment/flowrates.

Dry Coal Production Equipment List:
480V AC Rotary Valve Airlocks x 2
Custom Enclosed Rotary Drum Vacuum Filter
85 gallon Conical Bottom Ceramic Coated Stee
1/2" Pneumatic Diaphragm Pump
Custom Screm Conveyor with 1/2 Hp Drive
1/4" Temperature Gauge x 3
1" Ball Valve x 1
Flow Rates:
Coal Product: 50 tph
Filter Feed: 4 gpm
Filter Overflow: 1 gpm

2.8.1. Design Modifications during Test Campaigns

The solvent recovery system is one of the few systems in the mobile pilot plant that have been relatively untouched. Other than some minor changes primarily to aid in access to points prone to clogging, the system has not been changed. Proposed for a future research project is a solvent recovery system that will not utilize thermal drying. The system is proposed to eliminate the need for the energy intensive thermal dryer and replace it with a method which utilizes super-heated steam to drive off residual solvent.

Figure 2-22 shows the current setup for the thermal dryer and solvent recovery.



Figure 2-22. Current thermal dryer configuration.

2.9. Automation and Control

Electrical control for the mobile pilot plant is run from the motor control room built on the front of the trailer. Inside this control room is housed the electrical breakers, pneumatic controls, air monitoring system, variable frequency drive units (VFDs), and the programmable logic control (PLC) system. Almost all of the pilot plant's electrical motors and pumps are connected to VFDs that are tied to the PLC. The PLC being utilized in this setup is an Allen-Bradley Compact Logix L33ER powered by an Allen-Bradley 1606-XL 24V DC power supply. Commands from the PLC are communicated to the VFDs through an Allen-Bradley Stratix 5700 communication hub. For this pilot plant, Allen-Bradley PowerFlex 525 VFDs are being used for motor and pump control. Figure 2-23 below shows the PLC, an example of one of the VFDs being used, and the touch screen interface. Operators can interface with the system through an Allen-Bradley Panelview Plus 7 touch screen where motor speeds, level controls, and motor operations can be easily controlled. Figure 2-23: Mobile Pilot Plant PLC, VFD, and touchscreen. shows the touch screen interface.



Figure 2-23: Mobile Pilot Plant PLC, VFD, and touchscreen.

In addition to the electrical components, the PLC unit also controls the functions of the pneumatic components of the pilot plant. Air is supplied to the plant from an Ingersol-Rand R37ie rotary screw air compressor and enters the control room through a ½ inch steel line. Air is then divided amongst the component controls through an air distribution block. Each pneumatic component is controlled by a current-to-pressure (I/P) transducer. These transducers take the signals sent from the PLC and convert it to an air pressure value allowing the components to operate at the proper pressure when needed. Figure 2-24 shows the controls mounted on the inside of the control room for the pneumatic components.

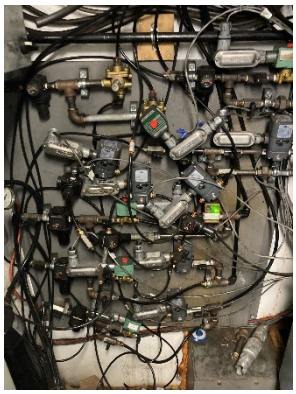


Figure 2-24: Pneumatic component controls.

2.10. Safety Equipment

Safety is a large concern for the operators of the mobile pilot plant, so several systems are in place to help prevent dangerous situations from developing and to help mitigate problems if they occur. The plant employs two monitoring systems. The first monitors gas levels on the trailer in different points as well as inside the common ventilation system through hoses

connected to The Conspec ERT. The Conspec uses a pump to systematically cycle through the sample points and draw in an air sample to analyze it for oxygen and solvent vapor contents. Alert thresholds are set for high solvent vapor content and for high oxygen content. Ideally inside the ventilation system, the oxygen levels should be low as nitrogen is introduced to help keep the environment inert. In the presence of solvent vapors, high oxygen levels could create the potential for ignition. The second monitoring system is a set of Honeywell Sensepoint XCD gas detectors set on the floor around the pilot plant. The vapors produced from evaporating iso-hexane are heavier than air and tend to accumulate in low places. Therefore, the sensors on the floor are able to alert operators to a dangerous buildup of vapor which could end up growing large enough to interact with a piece of electrical equipment that is not designed to be operated in an intrinsically safe environment. All of the motors selected for use in the pilot plant have been rated for use in a hazardous environment. Meaning they are sealed, and all connections are secured so that vapors are not capable of reaching electrical current. Any motors that are not intrinsically safe are kept at safe distances away from the pilot plant or sealed in the climate-controlled utility room.

In the event there is an ignition on the pilot plant, a fire suppression system has been installed. Four Safecraft LT fire suppression bottles are mounted on the trailer with activation handles on both the outside perimeter and the inside walkway. Each bottle has flexible steel line plumbed into them and terminated by dispersion nozzles over each major electrical component. Upon activation, a dry chemical will dispense covering the impacted area and smothering any flames. In addition to these on-board units, the building enclosing the pilot plant is equipped with type ABC dry chemical fire extinguishers to support the suppression system or be used in areas not covered by it. Figure 2-25 below shows the Conspec monitoring system box, one of the floor gas monitors, and one of the fire suppression system's bottles.



Figure 2-25: Conspec monitoring box, floor gas monitor, and onboard fire suppression bottle.

Finally, to keep the area clear of any potentially dangerous vapor buildup, the storage building containing the pilot plant is equipped with a ventilation system. The system consists of two ¾ horsepower exhausting fans. The one fan is located near the solvent storage tank and product discharge chute. The second is located in the wall adjacent to the back end of the trailer. A positive airflow is introduced through a set of two large misting fans installed in the wall adjacent to the front of the trailer. The wall of the building had been cut allowing these two fans to draw fresh air into the building to sweep away any vapor and pushing them towards the exhaust fans.

2.11. Additional Design Considerations

2.11.1. Pilot Plant Foundation/Early Build

Learning from another project that utilized a similar trailer, the decision was made to construct the control room and utility room out of modular uni-strut. The control room on the other trailer was constructed out of a modified shipping container which had been cut and reduced to an overall length of ten feet. Even though the size of the container was reduced to approximately half of the original, the weight of the remaining piece proved to be problematic for the overall weight of the plant and ease of transportation. Constructing the enclosed portions of the trailer and roof system would provide a strong and stable structure while greatly reducing weight. Uni-strut bases were bolted to the outer metal frame of the trailer. Specialty corner brackets and “Tee” couplers would allow the upper frame to tie the legs into bases completing

the outer frame. After the framework for the two rooms was completed, the interior and exteriors walls could be installed.

The control room was divided into two halves. The first half houses the electrical equipment and process controls. The drive motors for the pumps and processing equipment are controlled by variable frequency drives that allow users to change the speed that they rotate, or the amount of power delivered to the motor. These values from the drive motors would be essential to the scaling up of the pilot plant to a commercial scale. In addition to electrical equipment, the first half of the control room housed the transducers which control the air flow and pressure to the air driven motors and diaphragm pumps used in the plant. Finally, the first half contains the Conspec system which is used to detect and motor gas levels at monitoring points around the trailer. The system monitors for solvent, oxygen, and nitrogen to ensure that dangerous gas mixtures are not building up in areas not easily accessed. The second half contains the pilot plant's air and chilling systems. A 200-gallon piston air compressor would provide air for all of the necessary functions on the trailer. Coupled with the air compressor was a nitrogen generator which would provide inert gas to be pumped into the vent system as well as any vessel where the organic solvent would be located. The inert gas would prevent oxygen from being present and possibly creating an explosive environment. The final piece of equipment in the second half was the glycol chiller unit. This unit was used to circulate coolant at near freezing temperatures through the pilot plants condensers used to recover solvent from the gasses in the thermal dryer. A plywood and uni-strut framed wall divided the two rooms and provided a surface on which to mount the electrical boxes. Since the trailer would be utilizing a highly volatile organic solvent, the control room would need to have a firewall between the process side of the trailer and the two halves of the control room. The firewall was constructed using fire rated drywall with an air gap between two drywall sheets and covered by an outer metal wall. The entire control room was covered in metal siding on the walls and on the roof. In both halves any gaps between the joints of the walls, roof, and floor were sealed with a fire rated expanding foam. The purpose of the sealing was to prevent any vapors from the solvent leaking back into the control room and possibly igniting on any of the mechanical and electrical equipment. Another safety precaution added to the control room was to install two ventilation blower fans on the front end of each half of the control room. The main purpose of these fans was to put positive air pressure into each half of the room to prevent vapors from entering. The

floor in the control room was left as the bare trailer decking and the gaps between the boards were left open. The gaps were left in to allow the air from the fans to exit out of the bottom of the room and push air out of the lowest place in the control room. This would ensure that any vapors present would be pushed out as they are heavier than air and would be at the bottom of the air column.

2.12. Summary and Conclusions

The research set out to construct a mobile pilot plant with a prescribed throughput of 50 lbs/hr and a product grade of less than 10% moisture and less than 8% ash. The goal was met and included several improvements to some of the crucial potions of the circuit. Two of the most important, the agglomeration and Morganizer, received special attention. The agglomeration step started with a design that was incapable of producing consistent results within the targeted ash and moisture parameters. This was problematic for the process as this step was crucial as it dictated the results of the remaining portions. Through a series of improvements, this step was improved to a point where it was capable of producing on spec repeatable results. The stable well-formed agglomerates would help to improve the downstream pieces.

The Morganizer started as a design utilizing structured packing in order to disperse the agglomerates. Through its evolution it became a unit utilizing a stack of oscillating discs that would effectively break apart the agglomerates and disperse the coal particles into the iso-hexane. Using this Morganizer, the product specs set forth for the project were met. This design became the basis for the design of the first commercial scale HHS plant to be built. Further evolution of the Morganizer saw it take the form of a pulsing jig column Morganizer. This design is much simpler and has a smaller profile than the oscillating column. While this version only had limited trials conducted on it, it showed promise as being as capable as the larger oscillating column Morganizer.

The work completed on this pilot plant was able to show that the HHS process could be turned into a continuous process producing at least 50 lbs/hr of dry carbon product. The work also showed that the process could be scaled up to a commercial size operation capable of handling waste streams from a full-size coal wash plant. Undoubtedly future improvements on the designs of the equipment on the pilot plant will prove the process's efficacy with a multitude of commercial waste streams.

Chapter 3. The Hydrophobic-Hydrophilic Separation (HHS) Process for Ultrafine Coal Recovery

C. Sechrist[1], S. Keles[1], N. Youmans[1], K. Huang[1], J. Reyher[2], A. Jones[2], A. Noble[1], R.H. Yoon[1]

1: Department of Mining and Minerals Engineering
Virginia Tech
Blacksburg, VA 24061

2: Minerals Refining Company
Richmond, VA 23230

Portions of this chapter were published as proceedings paper for the 2022 CoalProTech Conference. C. Sechrist's primary contributions include the design, construction, and testing of the pilot-scale process. C. Sechrist also contributed to the formal analysis and manuscript writing. Laboratory testing and analysis was performed by N. Youmans and K. Huang.

Citation: Sechrist, Chad, Serhat Keles, Nathan Youmans, Kaiwu Huang, James Reyher, Alan Jones, Aaron Noble, and Roe-Hoan Yoon. (2022). "The Hydrophobic-Hydrophilic Separation (HHS) Process for Ultrafine Coal Recovery. CoalProTec 2022. Lexington, KY, April 2022.

3.1. Abstract

The recovery of ultra-fine particles, particularly those less than 44 microns, is a longstanding challenge for the coal industry. Conventional separation processes, such as flotation, are unable to effectively upgrade this material, and as a result, many operators discard coal fines to slurry impoundments creating environmental liabilities. Some estimates show that the amount of coal currently stored in impoundments in the US exceeds 6 billion tons. To address this challenge and provide a pathway for converting this liability into a valuable resource, Virginia Tech, and Minerals Refining Company (MRC) have jointly developed the Hydrophobic-Hydrophilic Separation (HHS) process. Unlike flotation, this novel process has no lower particle size limit and produces a dry product. Testing of this process with coal in both the laboratory and pilot plant scale testing has demonstrated that the technology is effective and an economically positive option for recovering fine coals from various waste streams. Some of the waste streams tested to date include deslime cyclone overflow, thickener underflow, and screenbowl effluent. This paper describes the most recent laboratory testing of the HHS process and then the scaling of those tests into a 50 lb/hr pilot plant. Results to date on bituminous and anthracite coals show that the process can produce coal products with less than 1.5% ash and 2% moisture. Opportunities for new product markets for this rich carbon product will also be discussed.

3.2. Introduction

3.2.1. Background

Coal has been a staple over the past centuries in the development of human society. From its humble beginnings as a fuel for heating the production of stronger tools, coal has been a driver for progress (Olney 2020). Starting in the 1800's, the world saw the largest advances during the industrial revolution thanks in part to coking coal for iron making and the advent of coal steam power (Turner 2021). Since this period, millions upon millions of tons of coal have been mined for both the making of steel and for the generation of electricity (IEA 2022). Though political factors and the shift to alternative fuel sources have caused the coal industry to slow (Kolstad 2017), it remains a vital piece of society. Coal still provides a large portion of the fuel for energy generation, and it remains a crucial piece in steel making (IEA 2022).

While the search for alternative uses of coal is not a new topic, recent changes in the global energy mix have hastened the development of these alternative markets (Gagarin et al. 2020). Domestically, the US has very few sources for high value carbon used in manufacturing and high technology. Most of the current providers are foreign, which places domestic producers at the mercy of many factors that can drive supplies low and prices high. Often in these markets, there are no pricing standards and no spot markets. Graphite which is used in the production of graphene can cost anywhere from $400/ton up through $2,250/ton compared to bituminous coal at $50/ton and anthracite at $100/ton (Critchley, 2020) (IEA, 2020). Carbon fiber derived from materials such as Polyacrylonitrile (PAN) can cost up to $28/kg, which is primarily driven by the cost of the material. In this application, the source material costs approximately $4-5/lb, while pitch derived from coal costs about $1.50/ton (Black, 2017). This pitch can also be used to produce carbon fiber. With the carbon fiber industry being a billion-dollar industry with an annual growth of over 15%, this data shows large potential for lowered product costs allowing expansion into more markets (Shama, Simha, T, G, Rao, K, & Kumar, Ravi, G, V, 2018).

In addition, operators, and federal agencies, such as the US Department of Energy, are seeking ways to utilize waste coals, which are currently an environmental liability. The current availability of waste coals is due to technological limitations. In particular, the cleaning and dewatering of ultrafine coal is a longstanding challenge for industry. In general, coal cleaning is done at coarser sizes, as both the costs and process inefficiencies increase with decreasing particle sizes. On the other hand, the processing of ultrafine coal has the potential to produce higher quality products, including those best suited for alternative end uses, due to the improved liberation of mineral matter from the organic constituents.

Unfortunately, the best available technology for fine particle recovery, flotation, is ineffective for particles less than 44 microns. These small particles lack the inertia to stick to air bubbles and are often washed out in the flotation tailings and non-selectively entrained into the flotation product (R. H. Yoon & Luttrell, 1989). Additionally, ultrafine particles are exceptionally difficult to dewater, requiring high pressure filtration or thermal drying, which is costly and environmentally prohibitive. As a result of these issues, ultrafine particles are often discarded to impoundments, thus leading to product loss and environmental liabilities. In the U.S. alone, there is estimated to be 4 to 6 billion tons of fine coal refuse stored in impoundments. Currently, producers are not only losing large amounts of valuable material, but they are creating large waste

management facilities that exist as environmental liabilities and adversely affect public opinion of the industry and operators (McSpirit et al. 2007). As the political environment continues to change, it will be increasingly harder to permit new facilities, therefore limiting the lifespan of current mining operations. To combat this, a method that can help to clean up these legacy waste facilities as well as capture the fine coal particles before they even leave the processing plant is needed.

To address the particle size limitations and inefficiencies imposed by flotation, researchers at Virginia Tech invented the Hydrophobic-Hydrophilic Separation (HHS) process (R.-H. Yoon et al., 2016). This novel approach uses oil droplets, rather than air bubbles, to simultaneously recover and dewater fine particles. By recovering and recycling the oil from the product streams, the overall process cost can be minimized while prompting higher separation efficiencies and lower energy requirements when compared to conventional fine particle cleaning and dewatering techniques. The ability to efficiently recover ultrafine coal particles provides a unique opportunity to generate extremely low ash coal products suitable for high value carbon markets while also solving the environmental issues associated with legacy impoundments. In this manuscript, we describe the development and demonstration of the HHS process as a potential solution for this challenge. To date, the HHS process has been successfully tested in three distinct pilot campaigns, and the current work will highlight the design, construction, and testing of a 50 lb./hr. pilot scale embodiment of the process including the accompanying laboratory data collection and analysis. Coincident with this pilot testing campaign, the HHS licensee, Minerals Refining Company (Richmond, VA) has also designed and constructed the first commercial HHS plant in Southern Appalachia. Discussion on process scale up and lessons learned will also be described.

3.3. HHS Process Description

The HHS process relies on the hydrophobic properties of coal and the hydrophilic properties of the ash containing mineral matter in slurries. Figure 3-1 shows a schematic representation of the HHS process at a microscopic level. In the first step, a small amount of oil is added to a coal slurry consisting of hydrophobic (i.e., coal) and hydrophilic (i.e. reject materials). Due to thermodynamic favorability of oil on the coal surface (i.e., $\Delta Gt < 0$), the oil spontaneously displaces the surface water and binds to the coal particles forming oil-in-water emulsions stabilized by small hydrophobic particles. These coal-oil agglomerates are then mixed with additional oil to convert the oil-in-water emulsion to a water-in-oil emulsion through phase inversion. The oil

slurry is then gently agitated to destabilize the emulsion and liberate any entrained water and hydrophilic refuse. These deleterious components are removed through settling, and the residual solvent is recovered from the product via filtration and evaporation. This evaporated liquid can then be condensed and recycled for use in the continuing process.

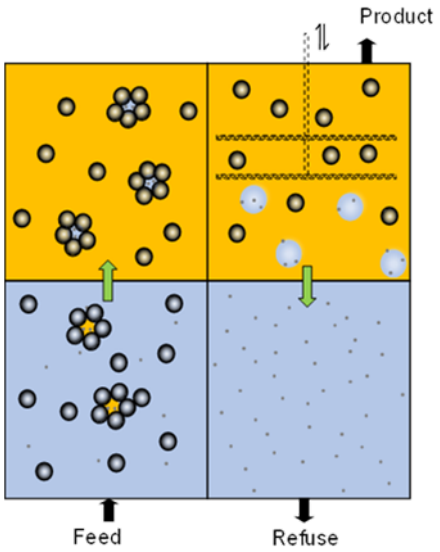


Figure 3-1. Schematic representation of HHS process.

The HHS process takes advantage of the contact angles of short hydrocarbon chains. Figure 3-2 shows the contact angle for molecules with carbon chains between 4 – 10, which vary from 90° to over 110°. As a comparison, the contact angle for air bubbles attaching to bituminous coals is only 65° (Gutierrez-Rodriguez & Aplan, 1984). The significantly higher contact angle for particle-oil contact thus necessitates a higher attractive force, which in turn prompts a greater collection efficiency for hydrophobic particles, particularly ultrafine particles. Moreover, the use of a solvent, rather than air negates the deleterious influence of the van der Waals force, which is attractive for solvents but attractive or air bubbles (Gupta et al., 2016). The much higher contact angles formed with hydrocarbon chains create much higher attractive forces which greatly increases collection efficiency. This is particularly effective with ultrafine particles. Additionally, using solvent versus using air to collect fine particles helps to negate the deleterious influences of van der Waals forces which are attractive for oils/solvents but not for air bubbles (Nikhil Gupta et al. 2014).

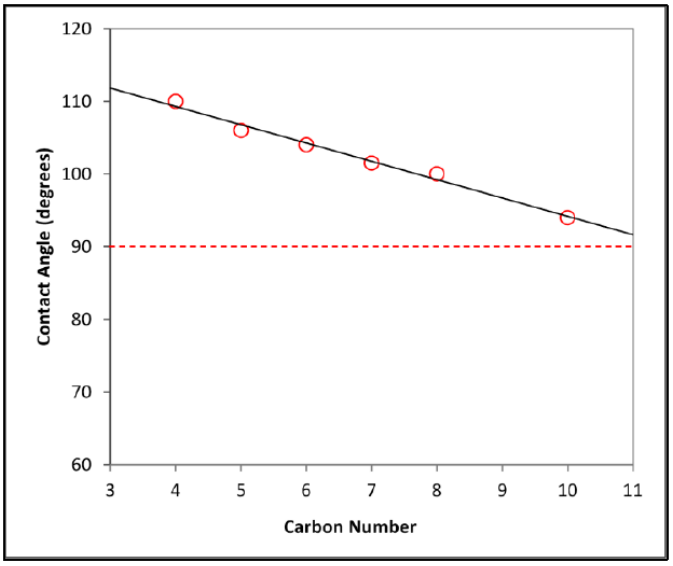


Figure 3-2. Contact angle of n-alkane hydrophobic liquids with surface of coal particles, Yoon, R-H, Eraydin, M, and Freelend, C., (2011).

Given the prior success in the testing of the HHS, the current effort sought to continue development through the design and construction of a one-skid mobile pilot plant capable of producing 50 lb./hr. of clean coal product. To evaluate the limits of the process with respect to cleaning potential, the process objectives for the one-skid unit testing were to evaluate multiple coal feedstocks while producing either a super-clean coal that has an ash content of 4 – 5% and a moisture of 6 – 8% or an ultra-clean coal product that has an ash content of less than 1.5% and a moisture of 6 – 8%.

3.4. Materials and Methods

3.4.1. Materials

Samples evaluated in the current study were sourced from three coal basins in the US, namely Southern Appalachia, Central Appalachia, and Northern Appalachia. Salient data on the samples is shown in Table 13 for the three areas where samples were sourced. Sample ID-1 was the primary material used throughout the trials; however, other samples were also tested to evaluate the robustness of the process. In all, ten different samples from the three operating regions were tested in the lab. Samples were typically shipped to the pilot plant location in sealed 55-gallon barrels and stored on-site until ready for testing.

Table 13. Salient Statistics for Coal Samples Utilized in Study.

Sample ID	Source	Plant Stream	Rank	Nominal Feed Ash (%)
1	Southern Appalachia	Screenbowl Effluent	LV Bituminous	15%
2	Central Appalachia	Thickener Underflow	LV Bituminous	15% - 60%
3	Northeast PA	Silt Pond Impoundment	Anthracite	50% - 60%

3.4.2. Laboratory-Scale Testing

Prior to pilot testing, potential candidate materials were tested in the laboratory to determine the optimal process parameters needed to produce the various product quality specifications. Laboratory testing generally followed the general processing steps of the HHS pilot plant, albeit in a batch-wise manner. After any pre-processing, high shear agglomeration was conducted in a laboratory blender for a set period of time. Next, the agglomerates were agitated in the same blender at a lower speed to promote low shear agglomerate growth. After agglomeration, the blender contents were screened on a laboratory sieve, and the product was then transferred to a laboratory Morganizer, which consists of a glass tube with an overflow launder at the top, a drain valve at the bottom, and several side feed ports. Figure 3-3 below shows the laboratory oscillating column. Gentle agitation was applied in the Morganizer by a set of circular screens attached to an oscillating motor. After loading the agglomerates into the Morganizer, a peristaltic pump was used to provide a steady inflow of fresh solvent thus providing a net upward flow that carried the clean coal to the overflow launder. After testing, the products were analyzed for moisture and ash to complete a mass balance.



Figure 3-3. Laboratory Oscillating Column.

In total, more than 100 successful HHS tests were conducted on 11 distinct samples. The feed materials assessed in this study were sourced from Southern Appalachia, Central Appalachia, and Northern Appalachia and included both bituminous and anthracite coals. Feed ashes typically varied from 10% to 20%; however, some waste coals with ashes as high as 62% were also successfully processed in the HHS process. Figure 3-4, Figure 3-5, and Figure 3-6 show summary results from this testing campaign for product ash, product moisture, and combustible recovery, respectively. As shown, the product ash typically met the super-clean requirement (5% to 6%), with the two exceptions being coal H and coal K. It should be noted, though, that after optimization, coal H was able to produce a 1.7% ash product and coal K was able to produce a 6.5% product. Coals C, D, E responded very well to the process, often meeting the ultra-clean specification of 1.5% ash. In fact, two of the best results in the campaign were achieved in coals C and E, which produced 0.50% and 0.47% ash products, respectively. Product moisture values consistently met the 8% product threshold, and the higher values were often due to poor parameter selection in the test process. Lastly, combustible recoveries were generally quite high, typically exceeding 90% and often exceeding 95% under optimal conditions.

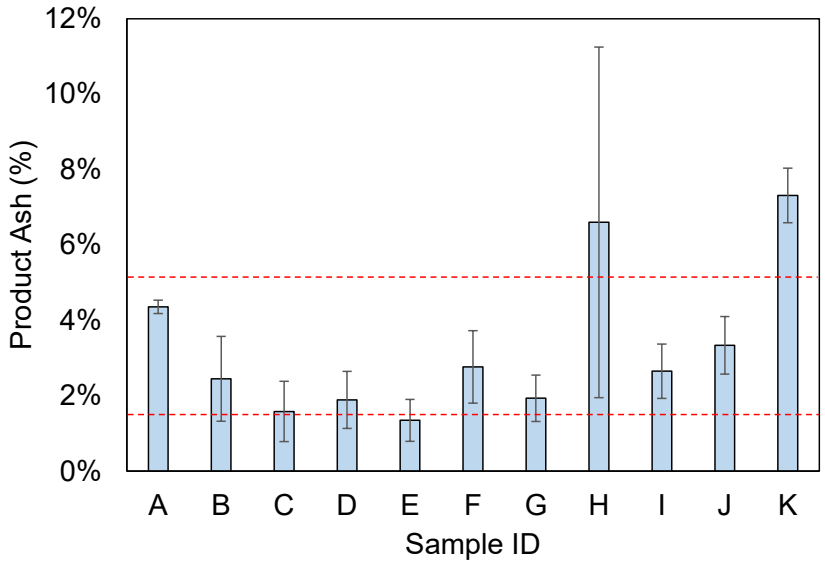


Figure 3-4. Laboratory HHS Testing Summary Results: Product Ash. Dashed lines show upper threshold limits for super-clean (5%) and ultra-clean (1.5%) products.

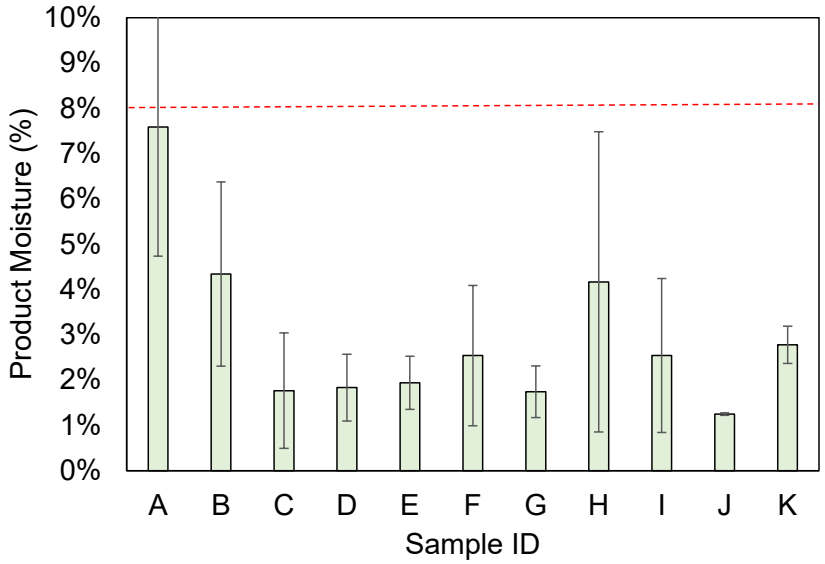


Figure 3-5. Laboratory HHS Testing Summary Results: Product Moisture. Dashed lines show upper threshold limits for moisture objective.

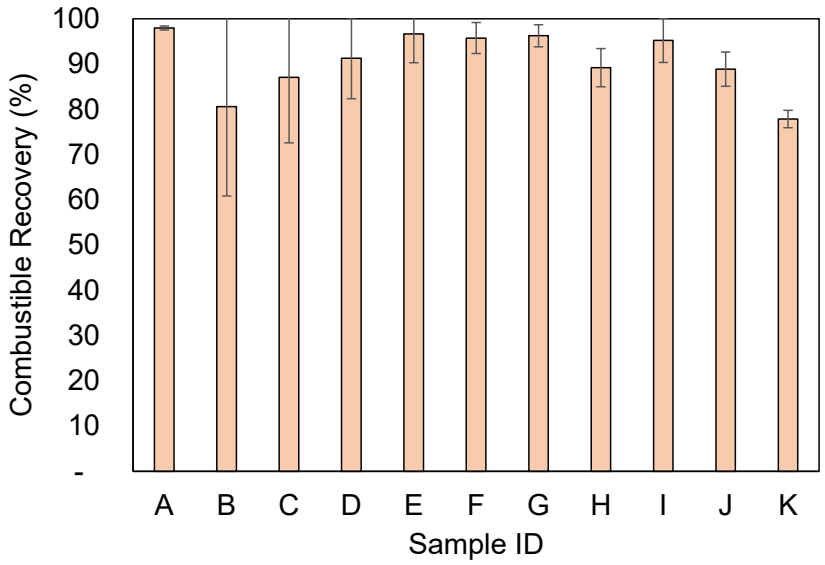


Figure 3-6. Laboratory HHS Testing Summary Results: Combustible Recovery.

3.4.3. Pilot-Scale Design and Construction

To further advance the team's testing capability and facilitate larger production runs, a 50 lb./hr. mobile pilot plant embodiment of the HHS was designed and constructed. Details on the design, construction, and shakedown of the pilot plant are described in the previous chapter on the design and construction of the mobile pilot plant. This pilot plant would allow for longer test runs to change operating parameters and observe how these changes affect the final product. The design of the pilot plant was inspired by the previous POC and demonstration plants. The aim was that the design and function of the pilot plant would translate directly into the first commercial HHS plant.

Construction and shakedown of the pilot plant was conducted over a 9-month period. The process equipment included both new and used items as well as some materials refurbished from the earlier POC and demonstration plants. The final plant included two equipment lines for the separations and solvent recovery operations; a control room with integrated PLC controls, data logging, and touch screen HMIs; and integrated gas monitoring, fire suppression, and other miscellaneous safety equipment. Upon assembly and startup, the key units were first tested with water only to ensure plumbing connects and equipment operability. After troubleshooting the major issues, production runs commenced.

3.4.4. Sample Preparation/Analysis

Samples used in the pilot plant trials were primarily sourced from a bituminous coal processing plant. While the underflows from thickening units were initially considered, the decision was made to use the effluent stream from the screen bowl centrifuges. The decision was based on the inherent solids and ash content of the screen bowl effluent versus the thickener underflows. For this instance, the effluent had an average solids content of 4-5% and an ash content of 15% versus 15% and 60% for the thickener respectively. Sample material was collected from the effluent stream leaving the centrifuges. A diversion valve was installed to allow 55-gallon drums to be filled and shipped to the pilot plant for testing. Typically, tranches of 36 to 40 drums were sent at one time. Prior to test trials, up to four drums of sample were added to the feed sump and allowed to mix properly. The feed rate was typically set at 2 gallons per minute which allowed for easier retention time calculations for the various mixing vessels in the process. Based on research completed by Otisca, optimum retention time should be less than 2-3 minutes. In order to calculate the retention time in the vessels, the volume at each outlet would need to be calculated and divided by the feed rate. An example is shown below.

Equation 3-1

$$t\ (\text{min}) = \frac{TLV\ (gal)}{Flow\ Rate\ (gpm)}$$

TLV = Total Liquid Volume for the vessel at the outlet.

For an 8-inch diameter tank with a cone bottom with discharge port 10 inches from bottom of cylinder portion of tank:

Equation 3-2

$$TLV\ (gal) = Cylinder\ Volume\ (gal) + Cone\ Volume(gal)$$

$$TLV\ (gal) = \Pi * r^2 * h * 7.48\ \left(\frac{gal}{ft^3}\right) + \Pi *\ r^2 * \frac{h}{3} * 7.48\ (gal/ft^3)$$

$$TLV\ (gal) = 2.21$$

Substituting Equation 3-2 into Equation 3-1:

$$t\ (\text{min}) = \frac{2.21\ (gal)}{2\ (gpm)}$$

$$t\ (\text{min}) = 1.10$$

This shows that using the upper discharge port on the mixing vessel will give the slurry a little over one minute of retention time in the tank for mixing. This is less than the recommended 2 -3 minutes which keeps agglomerates from growing too large to leave the tank while growing large enough to be screen in the next stages of the process. Additionally, this feed rate provided for trial runs that lasted for up to 90 minutes which would be sufficient to allow for steady state to be reached and multiple samples to be taken.

During the trials, samples were collected in 1-liter plastic jars from points around the plant including the feed, tailings from the primary and secondary flotation cells, and final process tails. Each of these source points had a valve that allowed the stream to briefly be diverted into the jar for collection. In addition to these samples, extraction column overflow samples were collected via a diversion valve into a graduation cylinder. These samples would be weighed to calculated percent solids in the overflow and then any clear solvent poured off. The remaining coal/solvent mixture was poured into an aluminum sample pan to allow residual solvent to evaporate. The final sample collected was the dry coal produced by the drum filter and thermal dryer. This sample was also collected into an aluminum sample pan. The column overflow and dry coal product would both be analyzed for moisture content using a WYS moisture analyzer. The samples collected in jars would be vacuum filtered and then dried in a laboratory oven. Final analysis of all samples collected was accomplished in a TGA ash analyzer to determine the ash content of each.

3.5. Results and Discussion

3.5.1. Bituminous Pilot Plant Trial Results

Data from the pilot testing has consistently confirmed the laboratory findings and shown that the HHS can produce both super-clean (5% ash) and ultra-clean (1.5% ash) products with low moisture content. Through all testing campaigns, more than 120 pilot testing trials were

conducted, many of which have met the performance objectives and goals described above. Results from these tests are shown in Figure 3-8, Figure 3-9, and Table 14.

Figure 3-8 shows the product ash contents as measured from the daily composite product sample for each individual test run. As shown, the initial product ash values were extremely variable and averaged 7.6%, which exceeded the threshold target. A detailed investigation of the system design showed that the design high-shear mixing loop was not supplying enough energy for agglomerate formation. The system was thus rebuilt using a modified overhead stirring mechanism, thus improving the energy transfer to the working fluid. The impacts of this process modification were immediately evident as the product ash became less volatile and within the target specification for the super-clean product. Nearly 60 productions were conducted under this new configuration, all of which were within specification. Figure 3-7 image showing the high shear tank with the new mixer installed. Previously this tank appeared the same as it does in the image except there was nothing on the lid of the tank.



Figure 3-7. Updated high shear tank with mixer.

Looking further into what was happening within the process, the improvement came down to combination of retention time and dispersion of solvent. The volume of the head of the pump is approximately 265ml or 0.07 gallons. Due to this small volume, the coal slurry only has

about a 2 second window where it is exposed to a high-shear environment with a 2 gallon per minute feed rate.

Equation 3-3

$$t\ (\text{min}) = \frac{TLV\ (gal)}{Flow\ Rate\ (gpm)}$$

TLV = Total Liquid Volume of the pump head.

$$t\ (\text{min}) = \frac{0.07\ (gal)}{2\ (gpm)}$$

$$t\ (\text{min}) = 0.035$$

$$t\ (\text{sec}) = 2.1$$

The volume inside the high-shear tank can vary depending on which overflow port being used. Using the bottom port, the tank has a volume of 1.34 gallons. While using the top port the tank has a volume of 2.21 gallons. This gives the residence times inside the high-shear tank at 0.67 minutes for the bottom port and 1.10 minutes with the top port when operating with a 2 gallon per minute feed. The addition of the mixer greatly increased the window where the slurry is in a high-shear environment from 2 seconds to over a minute. The retention time for the high shear tank is the same as the calculation above for the 8-inch diameter tank.

This increased time allows for the coal particles to more chances to collide with solvent droplets. Additionally, the serrated mixing blade created a more intense high-shear environment which allowed the solvent to disperse more quickly and more widely within the slurry. This high dispersion and longer time allowed for agglomerates to properly form before moving on to the low shear tank.

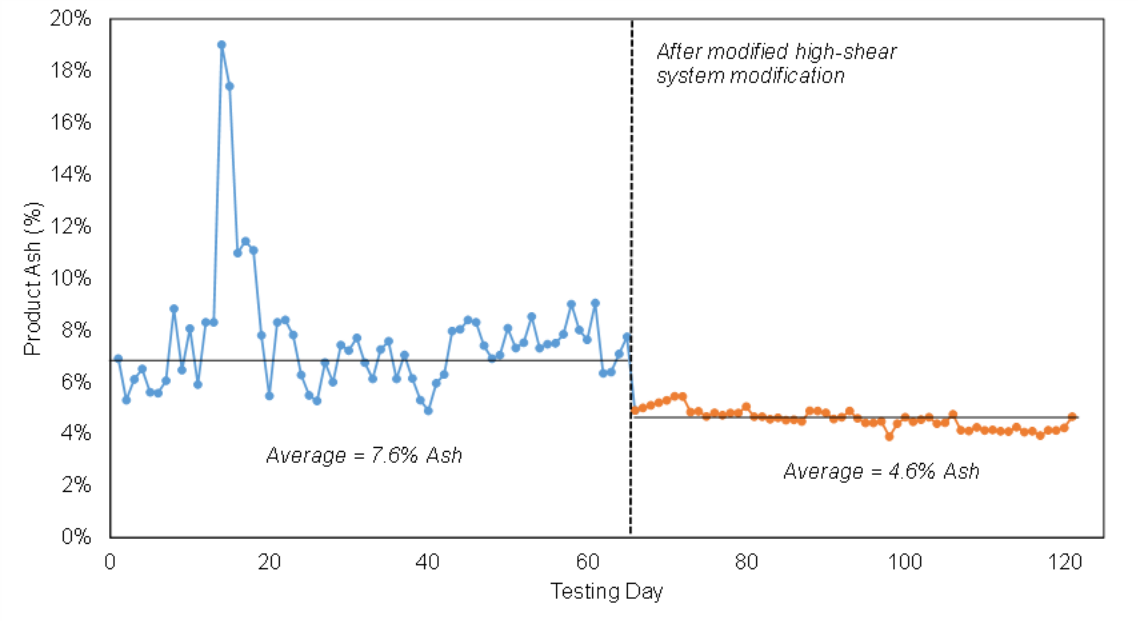


Figure 3-8 Pilot plant test results: product ash. Dashed line at day 65 indicates change in high-shear mechanism.

Figure 3-9 shows the trial results with respect to product moisture. While the high-shear modification did show some improvement to mean product moisture, the results were not found to be statistically significant (single paired t-test p value = 0.11) and were less dramatic than the changes to the ash content. This result is anticipated, as the moisture content is more significant to the Morganizer design rather than the high-shear design. It should be noted that some of the higher moisture values, >15% are due to anomalous test conditions. When properly optimized the pilot plant routinely produced product moisture <8%.

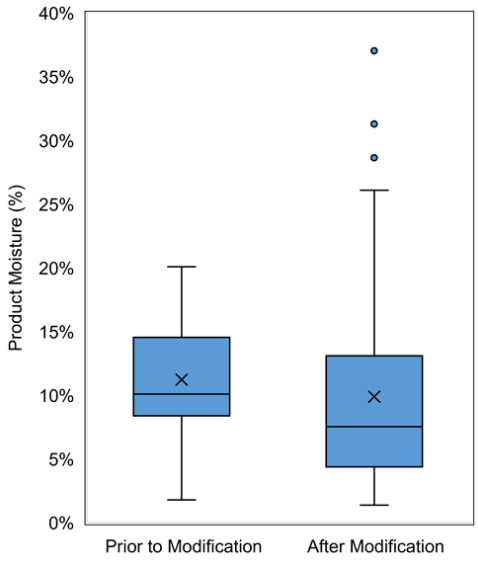


Figure 3-9. Pilot plant test results: product moisture. Two data series reflect modification to high-shear mechanism.

While these initial tests focused on the production of a super-clean (<5%) ash product, additional trials addressed the production of an ultra-clean product assaying 1.5% ash. TABLE shows the results of testing for this objective using the Central Appalachian coal source. As shown, after several initial optimization runs, the latter runs, particularly run S-4 produced extremely low ash and moisture values. These products are currently being evaluated for use in various high purity carbon applications.

Table 14. Pilot Plant Test Results for Super-Clean Product Production

Pilot Test ID	Product Ash	Product Moisture
S-1	2.26%	3.25%
S-2	2.20%	20.1%
S-3	1.66%	2.70%
S-4	1.46%	2.80%
S-5	1.64%	12.7%

3.5.2. Anthracite Pilot Plant Trial Results

(1) Laboratory-scale Tests

Before the pilot-scale tests, a series of laboratory tests were conducted to identify the best approaches for producing low-ash carbon feedstocks. For the silt pond sample, a short period of

grinding was necessary to create fresh surfaces to minimize the detrimental effects of surface oxidation, followed by a flotation pre-concentration step. The preconcentrate obtained by flotation was then subjected to a single-stage HHS test to obtain low-ash clean anthracite products. The results presented in

Table 15 show that 58.42 % of the carbon was recovered by flotation during the preconcentration stage. The carbon recovery was 87.20% for the HHS tests. The combined recovery between the flotation and the HHS tests was 50.94%.

With the coarse clean anthracite sample, oil agglomeration was used to process to remove the easy-to-remove mineral matter to obtain a clean anthracite product with 6% ash at a 95.91% carbon recovery. The clean anthracite product was ground to a smaller particle size before subjecting the mill product to the HHS process. The product ash was reduced to 1.46% at a carbon recovery of 93.56%. The overall recovery was 89.73%. With the fine clean anthracite sample, the final ash content was 2.20 % at an overall recovery of 91.10%.

Table 15:Results obtained in laboratory-scale tests.

Sample ID	Pre-concentration Recovery (%)	HHS Yield (%)	Product Ash (%)	Product Moisture (%)	Carbon Recovery (%)	Overall, Carbon Recovery (%)
Silt Pond	58.42[1]	75.69	2.80	1.23	87.20	50.941
Coarse Clean Anthracite	95.91[2]	88.55	1.46	2.93	93.56	89.732
Fine Clean Anthracite	99.02[2]	79.00	2.20	3.80	92.00	91.102

[1] flotation; [2]oil agglomeration.

3.5.3. Pilot-scale tests

For the pilot-scale tests, the silt pond sample was first ground in an attrition mill, where the particle size was reduced to $d_{80} < 12$ μm. Then, the ground material was precleaned in a floated column cell at a feed rate of 250 lbs/hr. The flotation product was then subjected to the pilot-scale HHS tests. The results of this series of tests are presented in Table 16. As can be seen, apart from one outlier data point, the final product ash values ranged between 1.7-2.0% and the product moisture ranged between 3.9-4.1%. These results are consistent with the result obtained in the laboratory-scale test (See Table 15).

Table 16:Results obtained in pilot-scale tests on the Silt Pond Sample

Flotation Preconcentration						
Feed Rate (TPD)	Feed Rate (lbs/hr)	Feed Ash (%)	Concentrate Ash (%)	Tails Ash (%)	Yield to Concentrate (%)	Carbon Recovery (%)
3.0	250.0	56.2	8.3	60.9	8.9	18.6
HHS Pilot Plant Test						
Sample No.	Feed Rate (GPM)	Solids Content (%)	Moisture Content (%)	Ash Content (%)	Final Tails Ash (%)	Carbon Recovery (%)
1	0.83	0.27	3.9	2.0	48.3	92.2
2*	0.83	0.35	12.6	2.4	--	--
3	0.83	0.46	4.3	1.8	--	--
4	0.83	0.40	3.9	1.7	--	--
5	0.83	0.45	4.1	1.7	--	--
					Overall Recovery (%):	17.2

Of the two clean anthracite samples tested in our lab tests, we chose to use the fine clean anthracite sample for pilot-scale tests. The sample was ground using an attrition mill to produce a particle size distribution with $d_{80} < 8$ µm. Then, the ground material was precleaned by agglomeration as had been done in our lab tests and then subjected to the HHS pilot-scale tests. The results of these tests are given in Table 17. As can be seen, the final product ash content ranged between 1.8-2.1% with moistures ranging between 4.1-6.0% at an overall carbon recovery of 95.9%.

Table 17: Results obtained in pilot-scale tests on the Fine Clean Anthracite Sample

Agglomeration Preconcentration					
Sample No.	Feed Rate (GPM)	Feed Ash (%)	Product Ash (%)	Tails Ash (%)	Carbon Recovery (%)
0	2	15.15	3.4	80.2	96.4
HHS Pilot Plant Test					
Sample No.	Feed Rate (GPM)	Moisture Content (%)	Ash Content (%)	Final Tails Ash (%)	Carbon Recovery (%)
1	2	6.0	1.8	75.7	99.4
2	2	4.1	2.1	--	--
				Overall Recovery (%):	95.9

3.6. Summary and Conclusions

The hydrophobic-hydrophilic separation (HHS) process is a novel technology used in the cleaning of fine coal with no lower particle size limit. The advantage of this process is that it

simultaneously dries and cleans the coal particles. Both laboratory and pilot scale testing has proven that this process, which uses oil droplets, is thermodynamically superior to the use of air bubbles in conventional flotation. The pilot scale configuration, the process has been able to produce a super-clean (<5% ash) and ultra-clean (<1.5% ash) product from both bituminous and anthracite coal sources. Laboratory testing was used to screen potential coal sources and to help identify the optimal process configuration to achieve target thresholds. Of the 11 samples tested in the battery of laboratory tests, 10 were able to routinely meet the super-clean 5% ash threshold, while 3 were able to meet the ultra-clean 1.5% threshold. All 10 coal samples were able to produce below target moisture values, with the best results producing just over 1% moisture. These results were later recreated in pilot scale trials using the 50 lb./hr. mobile one-skid pilot plant. First rounds of testing with the one-skid pilot plant prompted a needed change with the high-shear agglomerate formation loop. After this change, product ash qualities were consistently below the 5% ash threshold. Over a period where more than 60 pilot plant trials were conducted, the product ash averaged around 4.6% and this was all due to the modification of the high shear loop. Although limited trials were conducted, additional testing proved that the one-skid plant was able to produce ultra-clean coals with product ash less than 1.5%.

Chapter 4. Development of the Pilot Scale Column Morganizer

The Morganizer is the colloquial name for one of the crucial components in the Hydrophilic Hydrophobic Separation process (HHS) which is a means of mechanically de-emulsifying coal slurries. The iteration of the Morganizer tested in the lab and in pilot plant scale is a variation of the Karr column. The Karr column has been used in the extraction industry since the 1950's. While fundamentally the same as previous versions, the new extraction column performed its separation in a manner that opposed gravity rather than utilizing it. The new design was tested to find its efficacy with coal agglomerates as well as how to scale up to a commercial scale. Column features that were tested included different internal components and their configuration to see how they would affect the quality of the product. This would be accomplished by testing two internal component makeups as well as the overall layout and spacing of the pieces. Additionally, the columns height, feed port placement, overflow port placement, and interface level would be tested to see how they contributed to the overall quality of the product. Of the two main configurations, the oscillating column proved to be the more reliable and efficient design. Using this configuration as the base, varying internal plate spacing layouts were tested along with changes in the ports, heights, etc. to find the most complimentary setup. This setup would then be used to test the pilot plant in producing low ash and low moisture coal products which could become feedstocks for high value carbon industries.

4.1. Introduction

Extraction columns as used in modern applications have their roots in the late 1950's with the development of the Karr column (K. H. Smith, Bowser, and Stevens 2008). Karr recognized that extraction columns designed with rotating impellers or column utilizing pulsing fluids were difficult to scale up. Additionally, he recognized pulsed columns were difficult to scale up due to channeling of the different liquids as diameter increased instead of being evenly distributed across the cross section (Andrew E Karr 1959). Karr set out to develop an extraction column that would be effective and at the same time scalable. The first column was designed to employ the use of a series of plates suspended on a central shaft inside the shell of the column.

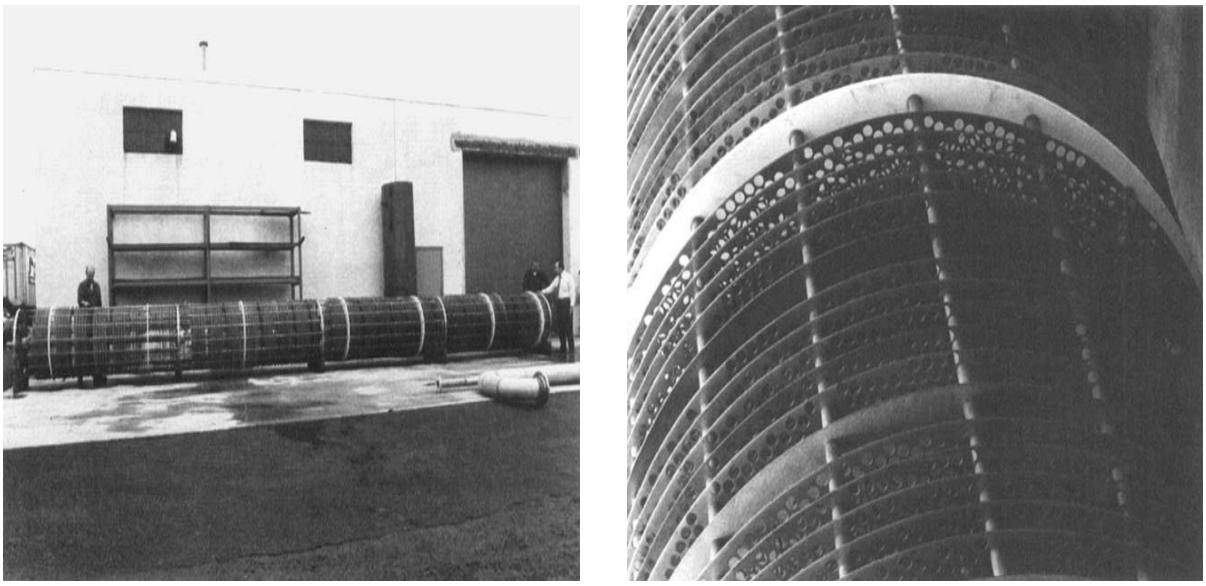


Figure 4-1. Photos showing a typical plate stack (L) and arrangement of perforated and baffle plates (R) (A. E. Karr 1980)

These plates would be reciprocated inside the column by means of a variable speed drive motor and drive mechanism mounted above the column. The plates were designed to have large openings which had a few benefits over small closely spaced openings. First the large openings would offer minimal resistance which would allow the capacity of the column to be maxed. Second, the large openings would eliminate the need for the tolerances between the column wall and plates to be larger therefore eliminating bypassing and allowing particles to fall freely through the openings. Most importantly, the large openings allowed for a uniform dispersion within the column's cross section which would allow for a straightforward scale up (Andrew E Karr 1959). Figure 4-1 shows a typical stack layout and a close up of the perforated plates in a Karr column.

Following these tests, the reciprocating plate extraction column was shown to be effective at high volumes at industrial sizes including 12-inches and 36-inches in diameter. Because of this, the columns were being employed extensively in labs, industrial plants, and pilot plants particularly in the chemical extraction industry (A. E. Karr 1980). Some of the main characteristics of these column included large open areas inside typically around 55%, large hole diameters typically around 9/16", stroke length around ¾", and plate spacing ranging from 1" – 8" with the typical spacing around 2" (A. E. Karr 1980). Typical extraction applications can be found in chemicals, metals/mining, polymer processing, biochemical, inorganic chemicals, and other industries. Specifically, they are used acid recovery and washing, metal production and

recovery, separation of catalysts from reaction products, carboxylic acid recovery from broths, and purification of phosphoric acid (Glatz and Cross 2020). Other researchers such as Baird studied the hydrodynamic characteristics of the reciprocating plate column. Baird would develop a set of empirical equations that helped to better understand how parameters such as liquid densities, agitation speeds, and column diameters affect the performance of the column (Baird 1976). Further studying Baird's equations, Karr was able to determine that many of the physical properties vary in different parts of the column. The solution to this would be to vary the agitation in the different lengths of the column. However, since agitation is a fixed parameter for the length of the column, the solution for this is to vary the spacing of the plates (A. E. Karr 1980).

Later researchers would again test the scale up of the Karr oscillating extraction column specifically looking at the hydrodynamic and mass transfer performance. Karr's scaleup equations are as follows:

Equation 4-1

$$\frac{(HETS)_{D_{C2}}}{(HETS)_{D_{C1}}} = \left(\frac{D_{C2}}{D_{C1}}\right)^{0.38} \quad (1)$$

Equation 4-2

$$\left(\frac{f_2}{f_1}\right) = \left(\frac{D_{C1}}{D_{C2}}\right)^{0.14} \quad (2)$$

Equation 1 relates to the pilot scale column developed by Karr and equation 2 relates to the larger column diameter. Dc is representative of the column diameter and f is the frequency at which the reciprocation is set. HETS relates to the height equivalent at which it reaches the stage for desired separations (A. E. Karr 1980). The 0.38 exponent is set at a default for a difficult high interface tension in a system of 0-xylene, acetic acid, and water. These exponents can range from 0.169 to 0.36 (Othmer, Baird, and Rao 1991). The 0.38 has been considered a recommendation for safety (K. H. Smith, Bowser, and Stevens 2008).

For these tests, the column's diameter would be increased in order to see what its effect is on these indicators. What was found during these tests was that while increasing the column diameter had no effect on the holdup, mass transfer coefficient, and specific interfacial area for mass transfer. They would conclude that previous scale up calculations were too conservative and that when scaling up the diameter, the overall height should decrease and agitation increase.

This finding is contrary to what Karr had previously concluded. The relationship was then changed to:

Equation 4-3

$$\left(\frac{(H_{ox})_{D_{c2}}}{(H_{ox})_{D_{c1}}}\right) = \left(\frac{D_{c2}}{D_{c1}}\right)^{0} \neq \left(\frac{D_{c2}}{D_{c1}}\right)^{0.38} \quad (3)$$

Equation 4-4

$$\frac{f_2}{f_1} = \left(\frac{D_{c1}}{D_{c2}}\right)^{0} \neq \left(\frac{D_{c1}}{D_{c2}}\right)^{0.14} \quad (4)$$

In this new relationship, H_{ox} is the overall height of the transfer unit. What the authors showed in their work determining this relationship is that in order to scale up a column it is more important to increase the agitation rates and reduce the overall height which is the opposite of what Karr originally proposed (K. H. Smith, Bowser, and Stevens 2008).

Karr columns became widely used due to the advantages they had over already existing technology. The main advantage the column had is that it could perform the necessary extraction in one pass while other technology typing took multiple steps. This simplification could help to minimize the overall investment and maintenance, minimize solvent usage and losses, and minimize costs for power and labor (A. E. Karr, Gebert, and Wang 1980). While many researchers have tested the scaling of the Karr column and used it to test various hydrodynamic properties, the column design has primarily remained unchanged for decades. The design still consists of a set of oscillating plates suspended depending on their diameter from a number of rods inside a column shell. The column shell can consist of a variety of materials, but glass is primarily used in the chemical extraction industry (Andrew E Karr 1959). These suspended plates are oscillated up and down by a drive motor attached to a special mechanism that can be used to vary the frequency and amplitude of the oscillation.

4.2. Use of Oscillating Columns in the HHS Process

As described in the previous chapter concerning the design and construction of the pilot plant, the current commercial embodiment of the HHS utilizes a modified version of the Karr column as a de-emulsification step after agglomeration but prior to solvent recovery. This unit operation, often called an extraction column or *Morganizer*, is used to break the coal-oil agglomerates, which leads to higher product purities with lower moisture. Smith's (2012)

research represented one of the earliest attempts to utilize a column-type de-emulsification stage in the HHS process. Here, Smith used a cylindrical reactor to test a continuous process and experimented with two methods of breaking agglomerates. The first utilized an ultrasonic probe, while the second utilized a set of vibrating screens. While both methods produced similar results, the ultrasonic probe was abandoned due to the heat it created and the large amount of energy needed to operate(S. A. Smith 2012).

Following Smith's (2012) effort, continued development of the HHS utilized oscillating screens in the Morganizer (B. Li and Luttrell 2019). Laboratory tests, bench-scale continuous, proof-of-concept (POC), and pilot scale trials were all conducted with this design (see Chapter LITERATURE REVIEW for a detailed description of the HHS technology development timeline). Similar to the lab setup, the oscillating column in the POC plant utilized two mesh screens suspended on a central shaft inside a mixing vessel. Screens were spaced on a support rod and a modified pneumatic reciprocating saw was used to drive the shaft. The oscillating frequency was adjustable from 0 – 30 Hz and was testing with a constant amplitude of 1.125 inches (Nikhil Gupta et al. 2014). Figure 4-2 below shows the screens and power unit of the vibrating screens for the POC. During testing, the POC was able to produce low ash and low moisture coal products, proving that a pilot scale continuous HHS process is possible. Data collected from batch tests of the dispersion vessel was then used to determine scaling up parameters which would be later used to help design a large-scale demonstration plant.

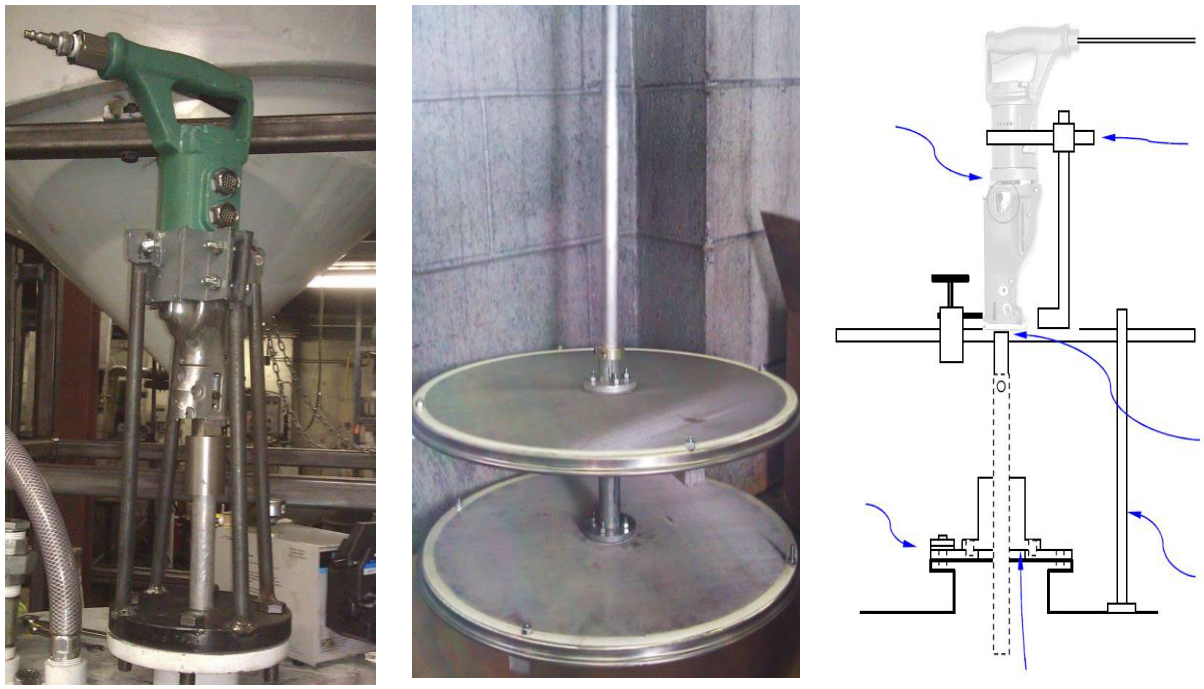


Figure 4-2. Vibrating screen setup from POC plant.

Following the success in the POC plant, a larger demonstration scale HHS unit was constructed and tested. In this unit, a 12-inch column was utilized, which allowed a designed production rate of 1 tph. Rather than using oscillating internals, the demonstration plant utilized a fixed bed of stainless-steel structured packing. The packing consisted of metal strips bonded together in order to form a structure that would fill the annulus of the column. The small spaces between the strips would create a pressure differential that would help to break apart the agglomerates as they flowed upwards. The surface of the stainless steel would provide a hydrophilic area for water to attach to and coalesce. Using this type of column, the demonstration plant successfully ran for 2 years before being decommissioned in 2017.

4.3. Study Objectives

Preliminary testing of the mobile pilot plant utilized the same structured packing design that was used in the demonstration plant; however, this design led to several operability and material concerns and was ultimately deemed infeasible. First, extended production runs caused clogging/plugging within the packed bed, which could only be rectified through complete dismantling and specialized cleaning. Second, the stainless packing would slowly build a thin layer of solvent coating, which prohibited water from coalescing on the surface. This problem

led to high product moistures as free water would flow with the upward solvent rather than with the discharge tailings.

Given these irreconcilable challenges, the structured packing design was abandoned, and the mobile pilot plant process was adapted to utilize the reciprocating plat column, modeled after the Karr design. Since the conventional Karr design is intended for liquid-liquid extraction, the conventional design and scale-up criteria are not readily applicable for the HHS application, which is solid-liquid emulsification. The addition of solid particles into the column provides additional design constraints and process criteria, as the upward solvent flow rate must be carefully managed to balance the competing influence of particle size dispersion and copious solvent addition. In addition, the energy transfer from the column must be sufficient to break the coal-oil agglomerates without re-emulsifying the constituents. Given the lack of scientific understanding on these parameters, a detailed investigation was conducted on the design and operation of the oscillating column utilized in the mobile pilot HHS process. Specific objectives of this study are as follows:

- Design, construct, and test a pilot-scale oscillating column-type Morganizer (nominally 4" diameter, 50 to 75 lb/hr coal product) with sufficient instrumentation and sampling capabilities to fully diagnose column performance with internal geometric resolution.
- Evaluate the influence of materials of construction, feed port location, baffle design, and other column properties on metallurgical performance.
- Evaluate the influence of oscillating frequency, disc number, disc spacing, and other internal design features on metallurgical performance.
- Synthesize the results of the study to prescribe the design recommendations for a full-scale oscillating column design.

4.4. Materials and Methods

4.4.1. Coal Samples

All tests were conducted using a low vol bituminous coal sample sourced from the Southern Appalachia coal basin. This sample was recovered from the screen bowl effluent of an operating plant and delivered to the Virginia Tech laboratory facility in sealed 55-gallon drum. Prior to testing in the column, the samples were first processed through the agglomeration and screening circuit in the pilot plant. Agglomeration was completed by sending the feed through a

high-speed pump after iso-hexane was introduced to the slurry line. The high-speed shearing action of the pump was designed to distribute the solvent equally throughout the coal slurry so it could interact with the carbon particles and begin to form agglomerates. This mixed feed went into the high shear tank where it was recirculated for a minimum of one minute to allow the agglomerates to grow in size. After the agglomerates leave the high shear tank, they moved onto the low shear tank for another two minutes where the slow agitation of the mixer would cause the agglomerates to grow in size. The agglomerates went through a screening process and then were pumped to the extraction column.

4.4.2. Oscillating Column Design

Throughout the test campaign, the column underwent several major design modifications, resulting in at least three test versions. As described above, Version 1 utilized the structured packing with no oscillating internals. This version was tested in 16 trials before being deemed infeasible for future use. Figure 4-3 shows a section of the structured packing after use in the first iteration of the extraction column. This version of the column can be seen in the first image in Figure 4-6. Following this test work, the research team worked with a major equipment vendor to design Version 2, which would utilize a 3-inch diameter column with approximately 3” diameter internal oscillating plates. The plates were supplied by the vendor, who would also be responsible for designing the oscillating mechanism in the commercial unit. {need to explain the physical design – pictures, locations of input and output ports, general flow balance, etc.).



Figure 4-3. Piece of structured packing used in original 4" column.

Shakedown testing of this design showed unpromising results, and further analysis showed that typical Karr columns have a lower void fraction than structured packing (55% vs >90%). This lower void fraction lowers the overall capacity of a Karr column and the 3-inch

column as tested only has a capacity for 0.8 GPM total. So, this was determined to be the primary reason that water was reporting to the product stream because the column was past capacity to work properly. With this knowledge, column Version 3 was designed utilizing a 4-inch column along with stationary rings to prevent the channeling of agglomerates along the annulus of the column. These rings would force any falling agglomerates back into the set of oscillating rings to be broken up.

Column Version 3 was originally constructed completely out of 4-inch diameter carbon steel piping. It was divided into 3 sections and bolted together with flanges to help facilitate dismantling and cleaning. The bottom section of the column was approximately 2-feet tall and had 1-inch fittings for the underflow of the column as well as the fresh solvent feed to the column. In order to have the solvent carry the coal particles up through the column, it would have to be fed at a sufficient rate to overcome the settling velocity of the particles. Using stokes law for coal particles in isohexane and water, the settling velocities for a range of particle sizes were calculated. These are shown below in Figure 4-4.

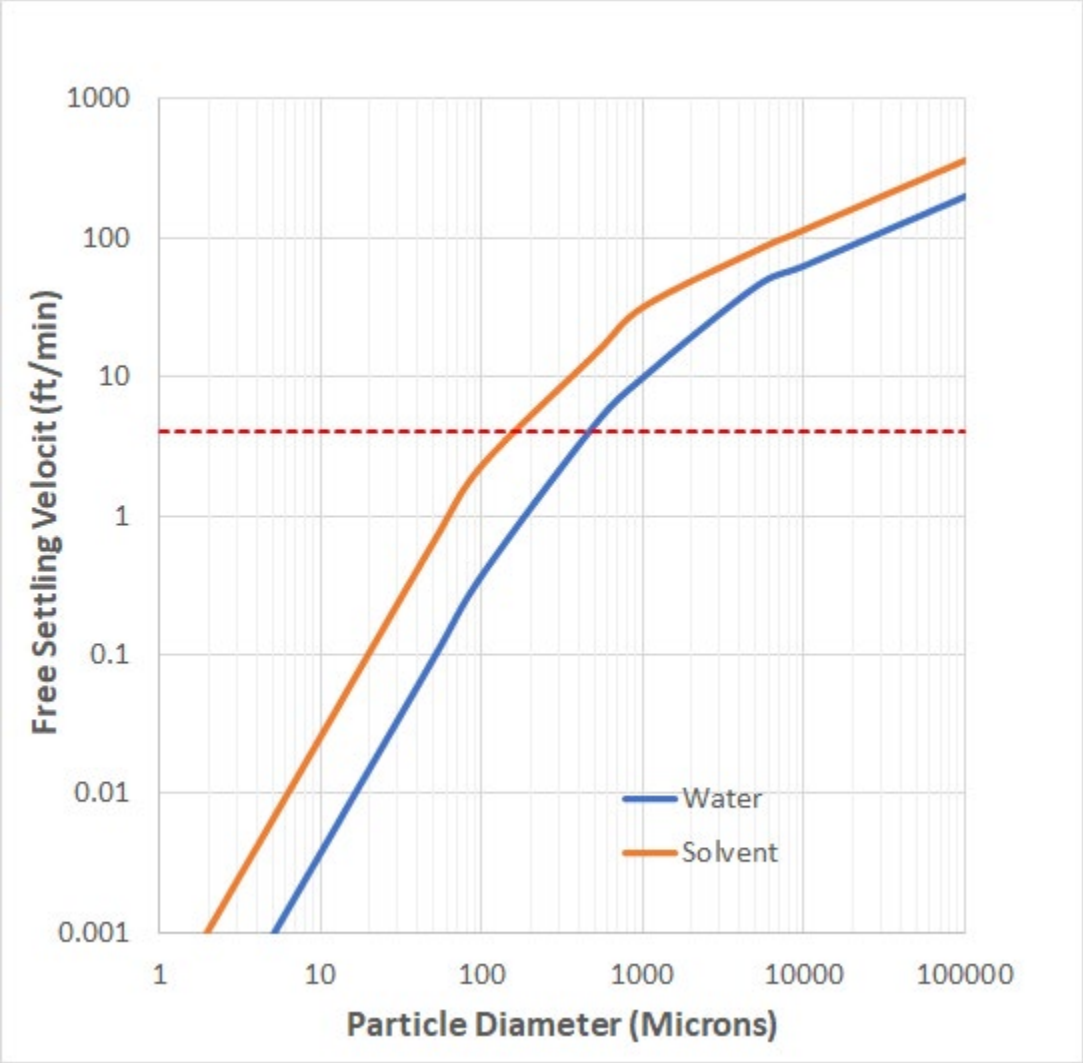


Figure 4-4: Settling velocities for particles in water/Isohexane.

The focus of the trials would be on particles capable of passing through 325 mesh or 44 microns or less. Observing the solvent line on the chart, particles around 44 microns in size would require an upward solvent velocity of approximately 4 feet per second to overcome the particles settling velocity and move it upward.

The middle section was the tallest at around 6-feet and housed the baffle rings and oscillating discs. Figure 4-5 shows images of the oscillating discs used in the column as well as the steel baffles inserted into the column to mimic surface area with the plastic shell. Several ports were added in the side of this section to test how performance changed by feeding the column at different heights. The top section had the product overflow port as well as a port so any vapor could be reported to the pilot plant ventilation system. Finally, the top of the column

had a modified flange that allowed the shaft for the oscillating internals to pass through and be connected to the drive motor mounted above. Along the height of the column, half-inch ports were installed so that samples could be taken of the entire column while operating to better understand what was happening inside at each level. Figure 4-6 below shows the current column configuration with the ½" sample ports used to take samples along the height of the unit. These samples would allow the creation of column profiles that aided in determining the optimal plate spacing and feed entry point. Figure 4-6 also shows the original four inch all carbon steel column installed on the pilot plant and the current version of the four-inch column with the PVC upper.



Figure 4-5. Stack of oscillating discs (L) and steel insert baffles(R) for extraction column.



Figure 4-6. Original 4" carbon steel column, current oscillating column configuration with 1/2" sample ports (R).

4.5. Methods and Procedures

4.5.1. Test Initiation

Trials on the pilot plant started with a planning meeting to discuss results from previous tests and what would be changed for the next trial. After any necessary modifications were made to the column, the feed was prepared to the prescribed solids content. The feed pump, the pilot plant, and the air compressor were powered up and allowed to run until the system was ready to go and the full air pressure of 120 psi was reached. Following startup, the feed pump began operating and the feed was sent through a recirculation loop plumbed in after the feed control pinch valve. This allowed the feed rate to stabilize to whatever feed rate was prescribed for the trial. The majority of the trials were conducted with a feed rate of two gallons per minute. After the feed rate stabilized, the recirculation loop would be closed allowing feed to enter the agglomeration equipment. Simultaneously, solvent would start pumping to the agglomeration equipment.

4.5.2. Column Feed

After material left the agglomeration portion of the process it passed over the sieve screen. The screen overflow would drop into the feed port on a progressive cavity pump. This mixture of coal and water would then be pumped up to and above the column through a length of one-inch reinforced PVC tubing. At the highest point above the column the tube passed through a t-connection which acted as an air break. This break would ensure that any extra air would exit the feed and not make it to the column. Air entering the system could disrupt the dispersion of the coal particles and could help to send water up to the overflow when it normally would have sunk in the system. Following the air break, the feed material would flow through another length of one-inch reinforced tubing to the feed point on the column. Based on the pilot plant's two gallon per minute feed rate, the column would be receiving around 65 pounds of coal per hour. The calculation below shows how the amount of coal entering the column was determined.

Feed Rate: 2 gpm Feed Ash: 17% Feed Solids: 8% Recovery: 95%

Equation 4-5

$$Feed\ Rate\ L/\min = 2\frac{g}{min} * \ 3.7854\ L/gal$$

$$Feed\ Rate\ L/\min = 7.5708$$

Equation 4-6

$$\text{Solids Feed Rate (kg/min)} = Feed\ Rate\ (lpm) * Slurry\ Density * Feed\ Solids$$

$$\text{Solids Feed Rate (kg/min)} = 7.5708 * 1.028 * 0.008$$

$$\text{Solids Feed Rate (kg/min)} = 0.6226$$

$$\text{kg per minute in Feed (kg/min)} = Solids\ Feed\ Rate\ (kg/min) * (\ 1 - Feed\ Ash)$$

$$\text{kg per minute in Feed (kg/min)} = 0.6626 * (\ 1 - 0.17)$$

$$\text{kg per minute in Feed (kg/min)} = 0.51678$$

Equation 4-7

$$\text{kg per hr in Column (kg/hr)} = kg/\min\ in\ feed * Recovery * 60\ min/hr$$

$$\text{kg per hr in Column (kg/hr)} = 0.51678 * 0.95 * 60$$

$$\text{kg per hr in Column (kg/hr)} = 29.46$$

$$\text{Using the conversion factor: 1 } kg = 2.2lbs$$

$$\text{lbs per hr in Column (lbs/hr)} = 29.46 * 2.2$$

$$\text{lbs per hr in Column (lbs/hr)} = 64.81$$

4.5.3. Column Level Control

The interface in the column where the oil phase meets the water phase has an important role in the operation of the column. If the interface is allowed to climb too high in the column, excess water can report to the overflow and create high product moisture. If the interface drops too low in the column recovery can suffer as coal will start to be lost in the tails. To control this interface a standpipe constructed out of PVC was fabricated and plumbed into the underflow of the column. This standpipe resembled a ladder with several cross pipes with valves connecting the inlet and outlet side of the standpipe. To control the interface, the valves in the cross pipes were opened or closed to raise and lower the level in the standpipe to match the column's level. The standpipe was effective at controlling the interface level however it kept constant monitoring throughout the trial. The standpipe was also prone to plugging after prolonged use, so it needed to periodically clean out. Figure 4-7 shows a view of the PVC standpipe.

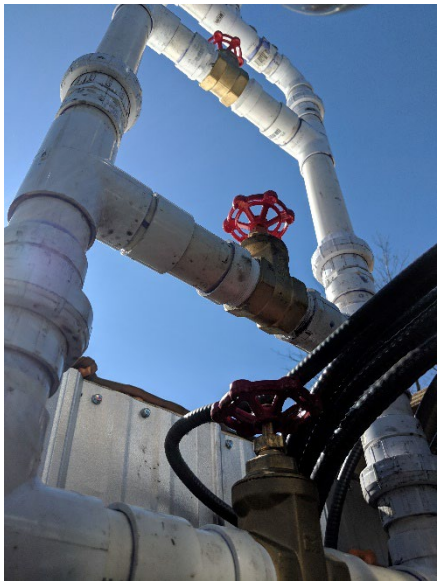


Figure 4-7. PVC standpipe.

To alleviate the manual inspection, a computer-controlled level monitoring system was designed and implemented. A set of differential pressure monitors were drilled and tapped into the lower section of the column. These samples measured the pressure difference between two points in the water column several times a second and took the average of these measurements. These measurements were fed to the pilot plants PLC which controlled a pneumatic pinch valve. The pinch valve opened and closed to control the tailings outflow therefore controlling the interface level. Figure 4-8 below shows one of the pressure sensors and the pneumatic pinch valve.

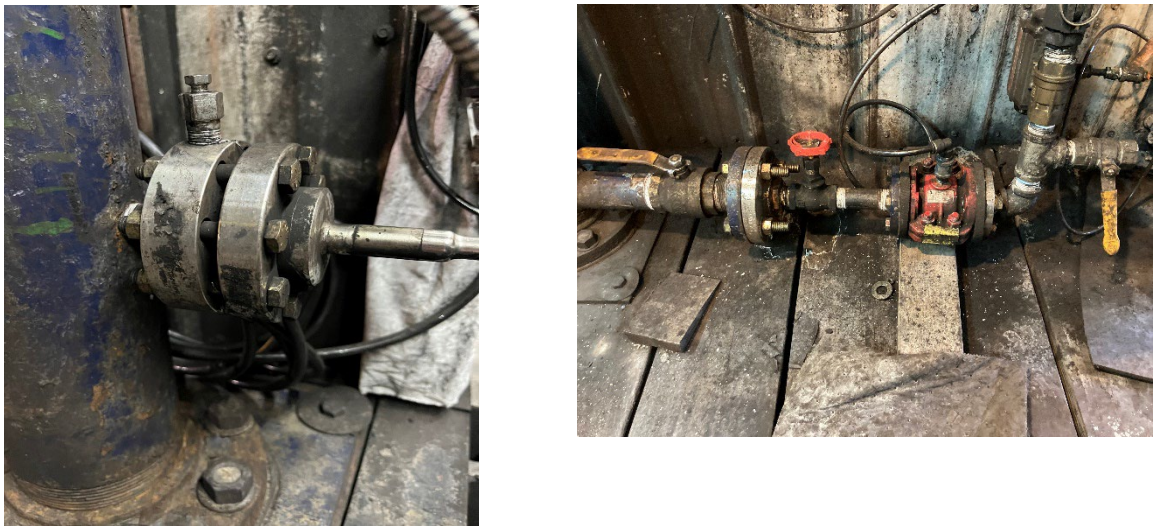


Figure 4-8. Image showing the pressure sensor and pneumatic valve used in interface level control.

4.5.4. Sampling Procedure

Sample ports were an important consideration in the pilot plant build. Due to the number of process portions being tested, sample ports were installed before and after each step in the plant. The sample ports were comprised of 3-way ball valves where applicable or else a pair of straight ball valves. Samples were taken by actuating the valves to divert the process flow into one liter labeled sample jars. For trials testing similar parameters, the same samples were collected for each trial. At a minimum for every trial, a feed, primary flotation tails, secondary flotation tails, final tails, and extraction column overflow samples were taken. Depending on the length of the trial, multiple samples were taken at each point. During a typical 60 – 90-minute run, 3 three sets of samples would be taken at each point if no parameters were changed.

For the oscillating column trials, a series of ½ inch ports were installed along the height of the oscillating column. These sample ports were set approximately 12 inches apart and a total of 15 were installed. During the trials, samples from each port ascending the height of the column from the bottom port were collected into one liter labeled sample jars.

4.5.5. Sample Analysis Procedure

After the completion of each trial, samples collected from the feed and tailings ports were weighed before being vacuum filtered. The vacuum filter used was a Nash water seal vacuum pump set up with 3 Sepor 12-inch vacuum pads utilizing Whatman 202 33 cm filter. The samples were dried following vacuum filtering and weighed to calculate the percent solids of each feed stream. Samples taken from the oscillating column ports were analyzed in the same manner. Figure 4-9 shows the vacuum filter setup.



Figure 4-9. A vacuum filter pump and filter pads are used for sample processing.

Samples taken from the column overflow were weighed in solution and then poured into aluminum pans to allow the bulk of the solvent to evaporate. These pans would be placed in direct sunlight on days when weather allowed or else placed near a low temp heater to drive off the residual solvent without evaporating any water moisture. A representative portion of these

samples would be placed on an A&D MF-50 moisture analyzer to determine the amount of moisture left with the coal following the process. The A&D analyzer is below in Figure 4-10.



Figure 4-10. A&D MF-50 Moisture Analyzer used in analyzing pilot plant samples.

A representative portion of all samples from each trial would be placed into a Leco TGA701, shown in Figure 4-11 below, in order to determine the ash content of each stream. The analyzer ran a test profile that would gently heat up to 23423 degrees first to drive off any moisture. Since the trial samples were already dried, this step served to ensure that any moisture accumulated onto the material from atmosphere etc. would be driven off.

.



Figure 4-11. Leco TGA701 used in analyzing pilot plant samples.

4.5.6. Test Result Analysis

The main purpose of the HHS process is to produce a clean low moisture carbon product. Therefore, the results from the TGA and the moisture analyzer were the primary focus. Results from each trial would be compared to previous results from trials testing the same parameters. The comparison would indicate whether a process change produced a lower grade and needed to

be relooked at or if it produced a higher grade. The improved grade would be compared to the project specs to verify how close it was to the range and what modifications would be needed to improve it further.

4.5.7. Test Run Length

Pilot plant tests could range anywhere from 30 minutes up to 90 minutes long. This usually depended on what needed to be tested on the plant and how much feed there was available. The feed sump for the plant was 200 gallons when completely full. Feeding the plant at the normal two gallons per minute meant this tank could provide running times up to 100 minutes. However, the trials were capped at 90 minutes due to the liquid level in the feed sump would drop below the bottom mixing impeller around this time and the solids content could start to vary. A 30-minute run time would allow for the process to reach a steady state and for the collection of at least one round of samples.

4.5.8. Steady State Establishment

Steady state for the process was estimated as 3 times the retention time of the agglomeration portion. Prior to the redesign of the agglomeration portion the residence time was approximately 5 minutes which meant it would take approximately 15 minutes to reach a steady state. After the redesign, the time to reach steady state was reduced to 9 minutes which was 3 times the combined 1 minute of retention if the high shear tank and 2 minutes of retention in the low shear tank.

4.6. Results and Discussion

4.6.1. Modifications derived from trials.

During the trials several design changes were made to the extraction column. The first change came early in the trials. The surface area of the pilot scale column was calculated to begin determining the dimensions of the scaled up commercial column shell. After the desired commercial size was determined, the surface area was calculated and unfortunately it was not equivalent to a scale up of the pilot column. The surface area of the scaled-up pilot column in relation to diameter was found to be much higher than what would be feasibly possible on a commercial size structure. This discrepancy would lead to any data collected on column performance does not correlate to potential performance of the commercial plant.

Below is an example of how this was determined. The proposed commercial plant would theoretically process 36,800 lbs of coal per hour and the pilot plant was processing 63 lbs of coal per hour. The diameter of the pilot plant column was 4 inches, and the height of the total column was approximately 10 feet.

Equation 4-8

$$\frac{lb}{sqft}/hr_{\square} = \frac{MF_{coal}}{2 * \pi * r * h}$$

$$\frac{lb}{sqft}/hr_{\square} = \frac{63_{lb/hr}}{2 * \pi * 2/12 * 10}$$

$$\frac{lb}{sqft}/hr_{\square} = 6.02$$

Using this factor to scale up:

Equation 4-9

$$6.02\frac{lb}{sqft}/hr_{\square} = \frac{36{,}800}{2 * \pi * r * h}$$

$$r * h = \frac{36{,}800}{2 * \pi * 6.02}$$

$$r * h = 973.545\ ft^2$$

Substituting in a proposed height 25' would give a diameter of nearly 39' and vice versa substituting in a proposed diameter of 22' would give a height of 45'. Both of these would be beyond the scope of what would be physically possible to construct at the site. Additionally, the corresponding internals that would need to be constructed for each design case would be too large and heavy for a reasonable motor size to be purchased.

So, the decision was made to replace the long metal section with a plastic shell and insert a metal structure. The structure would be designed and constructed to simulate the surface area that would equal the surface area of the scaled up commercial extraction column.

Based on available motor sizes and consultation with column manufacturers, the commercial plant was planned to be around 22' in circumference and 15' tall in order to process the 36,800 lbs of coal an hour. Below shows how the new PVC column was to be modified to mimic this design criteria.

Equation 4-10

$$\frac{lb}{sqft}/hr_{\square} = \frac{MF_{coal}}{2 * \pi * r * h}$$

$$\frac{lb}{sqft}/hr_{\square} = \frac{36{,}800}{22 * 15}$$

$$\frac{lb}{sqft}/hr_{\square} = 111.5$$

Substituting this into the pilot plant's column feed:

Equation 4-11

$$111.5\frac{lb}{sqft}/hr_{\square} = 63/SA_{column}$$

$$SA_{column} = \frac{63}{111.5}$$

$$SA_{column} = 0.565$$

Assuming the length of the column where the surface area needed to be adjusted to be 5', the width of the new pieces would be 0.565 sqft/5ft = 0.113 feet or 1.36 inches. Therefore, strips of metal measuring approximately 0.7 inches by 5 ft would be sufficient to mimic the performance of the proposed commercial column.

The second design change came after repeated observations of high moisture in the product overflow. In the initial design the top of the oscillating internals was only a few inches away from the overflow port. In lab trial set up, the oscillating screens were much lower than the overflow port. The theory was that the extra space between the screens and the overflow allowed any residual water droplets to enter a relatively calm area. This area of non-movement allowed any remaining free water droplets to stop moving upward and fall back down towards the water phase. To recreate this in the pilot scale column, a new 12-inch section of column was constructed and inserted in between the oscillation section and the top piece. Trials conducted after the introduction of this column extension showed lower moisture results similar to those achieved in the lab setup.

4.6.2. Column Profile Data

In total, 32 tests were conducted over a period of period of 7 months (inclusive of a 3-month shut down due to COVID-19). Through the tests, the following variables were adjusted a modified: column shell material, coal loading, solvent flowrate, oscillating frequency, agglomerate feed pot location, oscillating disc number, oscillating disc spacing, disc design, and vertical baffle number.

Table 18 shows the summarized results from all tests. In addition, Figure 4-12 through Figure 4-30 show profiles of the column obtained from the detailed column sampling. These profiles were able to show the effect on the location and spacing of the internal components as well as the feed point location and overall column height on its performance in producing a clean dry coal product. Testing of the column's internal configuration ended after the 32nd trial with the results stabilizing with a product ash content around 4% and a product moisture less than 10 percent. This was based on a decanter effluent feed with a solids content of around 4% and a feed ash content of 15% as this would be the primary feed stream used to feed the then proposed first commercial plant. Subsequent demonstration trials produced similar results with other waste feed streams. However, more testing would be needed to determine if the final configuration would be applicable to all coal seams or if revisions would need to be made to achieve the best possible results. The effect of the placement and spacing of the column internal pieces on the results is discussed in section 4.1.5 below.

Table 18.Experimental Results from Column Profile Testing

Test	Column Shell	Coal (lb/hr)	Solvent Flow (gpm)	Oscillating Freq.	Agg. Feed Port	Oscillating Discs No.	Oscillating Discs - Spacing	Baffle Discs	Vertical Baffle No.	Overflow Solids (%)	Overflow Moist. (%)	Overflow Ash (%)	OF Org. Rec (%)	UF Ash (%)
1	CS		2.3	5 hz	28"	36	2 "	Fixed	--	8	10.1	7.5	90.7	85.3
2	CS		2.3	3 hz	19"	36	2"	Fixed	--	7	7.7	7.1	93.7	84.8
3	CS		2.3	3 hz	28"	36	2"	Fixed	--	7.5	7.5	6.2	94.4	85.7
3	CS		2.3	3 hz	19"	36	2"	Fixed	--	7.5	7	6.4	92.5	85.3
5	CS		2.3	1 hz	28"	36	2"	Fixed	--	8	15	9.5	90.6	78
6	CS		2.3	3 hz	19"	18	4"	Fixed	--	6.1	16	8.2	95.6	83.8
7	CS		2.3	3 hz	19"	24	12-2", 12-4"	Fixed	--	7.1	6	8.7	95.8	85.1
8	CS		2.3	3 hz	19"	24	12-2", 12-4"	OP	--	6.5	9.2	8.9	90.4	82.1
9	CS		2.3	3 hz	19"	24	12-2", 12-4"	OP	--	8.1	10.3	7.8	86.7	87.1
10	CS		2.3	3 hz	19"	24	12-2", 12-4"	OS	--	6.7	8.3	10.5	90.9	86.4
11	CS		2.6	3 hz	19"	24	12-2", 12-4"	OS	--	7	8.8	7.9		
12	CS		3	3 hz	19"	24	12-2", 12-4"	OS	--	8	15.9	7.9		
13	CS		2.6	3 hz	19"	24	12-2",12-4"	OS	--	9	8.1	6.3		
14	CS		2.6	3 hz	19"	24	12-2",12-4"	OS	--	10	9.3	6.8		
15	CS		2.6	3 hz	19"	21	12-2", 9-4"	OS	--	8	7.5	6		
16	CS		2.6	3 hz	19"	21	12-2", 9-4"	OS	--	8	5.1/8.4	4.2		
17	CS		2.6	3 hz	19"	21	12-2", 9-4"	OS	--	8	7.3	4.2		
18	PVC	35	2.3	2 hz	28"	24	12-2", 9-4"	OS	--	5	9.9			
19	CS		2.6	3 hz	19"	24	12-2", 9-4"	OS	--	6.5	6.1			
20	PVC	35	2.3	2 hz	28"	35	31- 1", 4-6"	OS	--	4.7	5.5			
21	PVC	52.5	2.3	2 hz	28"	35	31- 1", 4-6"	OS	--	7	6.2			
22	PVC	63	2.6	2 hz	28"	35	31- 1", 4-6"	OS	--	7.4	8.5			
23	PVC	63	2.6	2 hz	28"	35	31- 1", 4-6"	OS	--	7.4	6	5.14	99.3	86.68
24	PVC	80.5	3	2 hz	28"	35	31- 1", 4-6"	OS	--	7.6	14.0/20.0			
25	PVC	63	2.6	2 hz	19"	35	31- 1", 4-6"	OS	--	7	9.5	4.4	99.2	88
26	PVC	63	2.6	2 hz	28"	35	1-4", 25-1",5-2",4-6"	OS	--	6.5	9.2	8.9	90.4	82.1
27	PVC	63	2.6	2 hz	28"	35	1-4", 25-1",5-2",4-6"	OS	--	7.6	10.1	3.8	99.2	79.87
28	PVC	63	2.6	2 hz	28"	35	24-1", 3-2", 1-4", 3-3", 2-4", 2-5"	SS	4	8.5	9	4.14	99.5	80.5
29	PVC	63	2.6	2 hz	28"	34	24-1", 3-2", 1-4", 3-3", 2-4", 2-5"	SS	4	7.7	8.7	4.3	97.2	79.9
30	PVC	63	2.6	2 hz	28"	34	24-1", 3-2", 1-4", 3-3", 2-4", 2-5"	SS	8	7.5	7.9	3.95	98.8	81.07
31	PVC	63	2.6	2 hz	28"	34	24-1", 3-2", 1-4", 3-3", 2-4", 2-5"	SS	3	7.1	9.1	4.1	99.5	84.8
32	PVC	63	2.6	2 hz	39.5"	26	8-2", 9-1", 3-2", 1-4", 3-3", 2-4"	SS	3	8.2	9.5	3.9	97.96	77.8

CS: Carbon Steel
OP: Oscillating/Perforated
OS: Oscillating/Solid
SS: Stationary/Solid

Test 1 - 5 Hz Oscillation and 28 Inch Feed Port

Note: Red = Feed Inlet; Blue = Solvent Inlet; Green = Ring; Gray Bars @ Zero = Oscillating Disc Locations

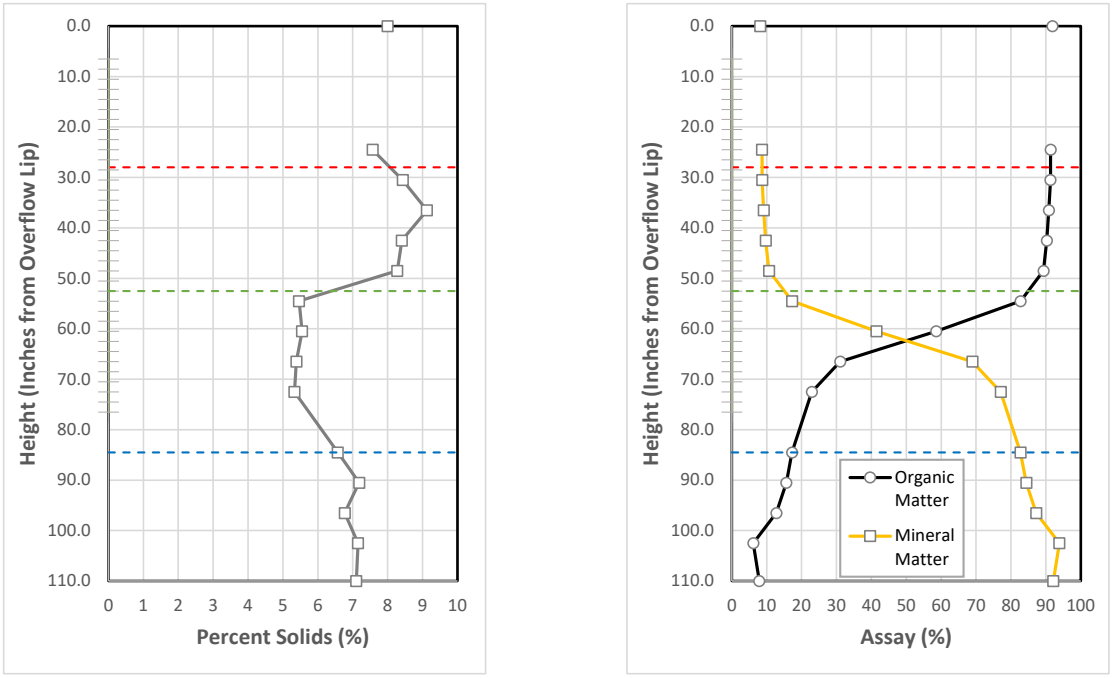


Figure 4-12: Test 1 column profiles with product containing 10.1% moisture and 8.0% ash.

Test 2 - 3 Hz Oscillation and 19 Inch Feed Port

Note: Red = Feed Inlet; Blue = Solvent Inlet; Green = Ring; Gray Bars @ Zero = Oscillating Disc Locations

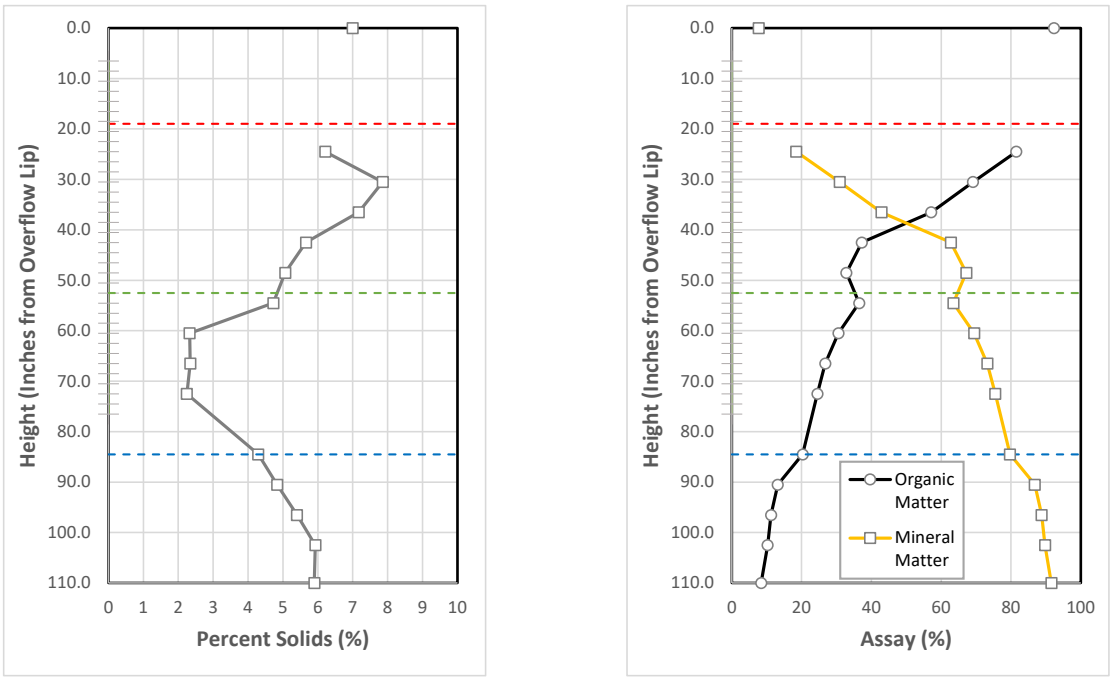


Figure 4-13. Test 2 column profiles with product containing 7.7% moisture and 7.0% ash.

Test 3 - 3 Hz Oscillation and 28 Inch Feed Port

Note: Red = Feed Inlet; Blue = Solvent Inlet; Green = Ring; Gray Bars @ Zero = Oscillating Disc Locations

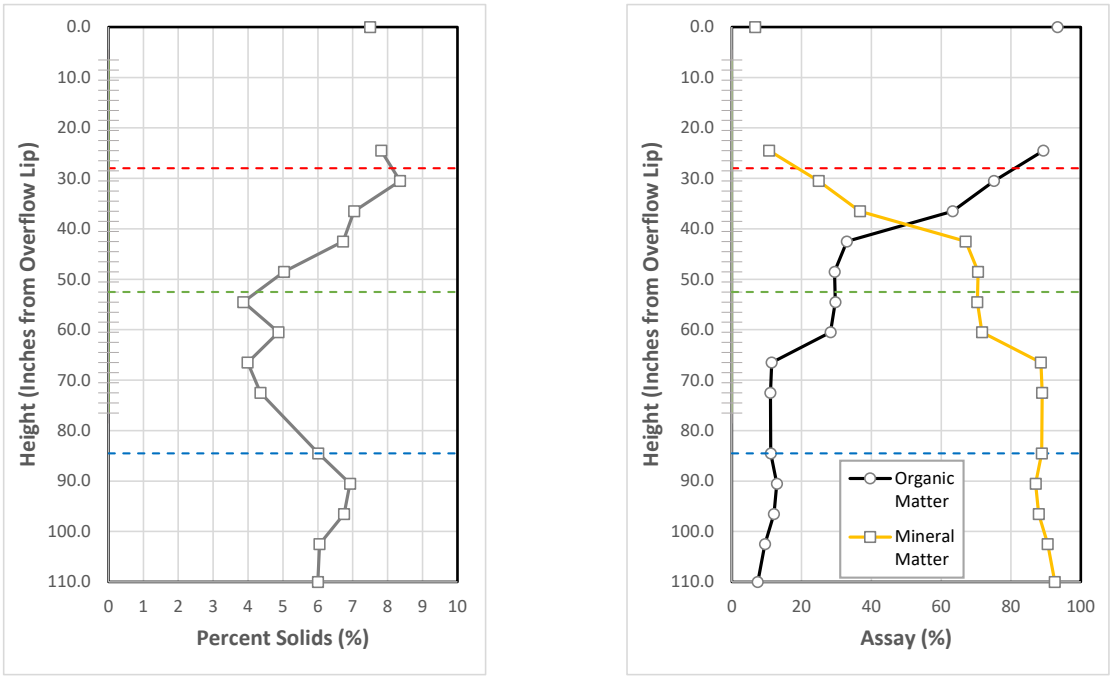


Figure 4-14. Test 3 column profiles with product containing 7.5% moisture and 6.2% ash.

Test 4 - 3 Hz Oscillation and 19 Inch Feed Port

Note: Red = Feed Inlet; Blue = Solvent Inlet; Green = Ring; Gray Bars @ Zero = Oscillating Disc Locations

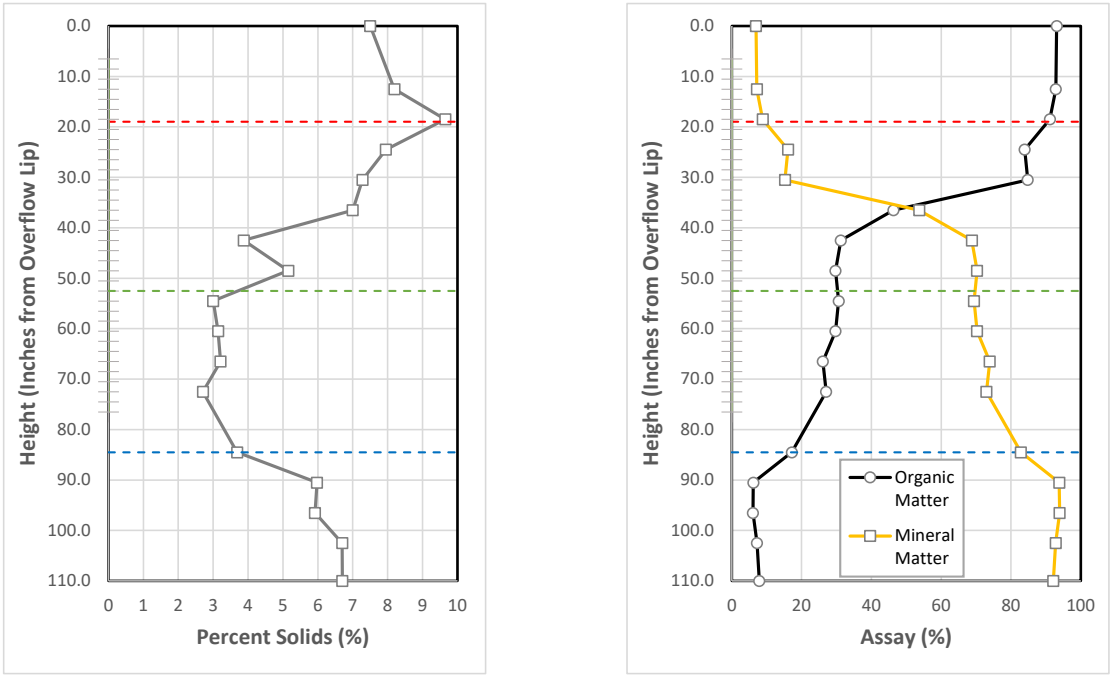


Figure 4-15. Test 4 column profiles with product containing 7.0% moisture and 6.4% ash.

Test 5 - 1 Hz Oscillation and 28 Inch Feed Port

Note: Red = Feed Inlet; Blue = Solvent Inlet; Green = Ring; Gray Bars @ Zero = Oscillating Disc Locations

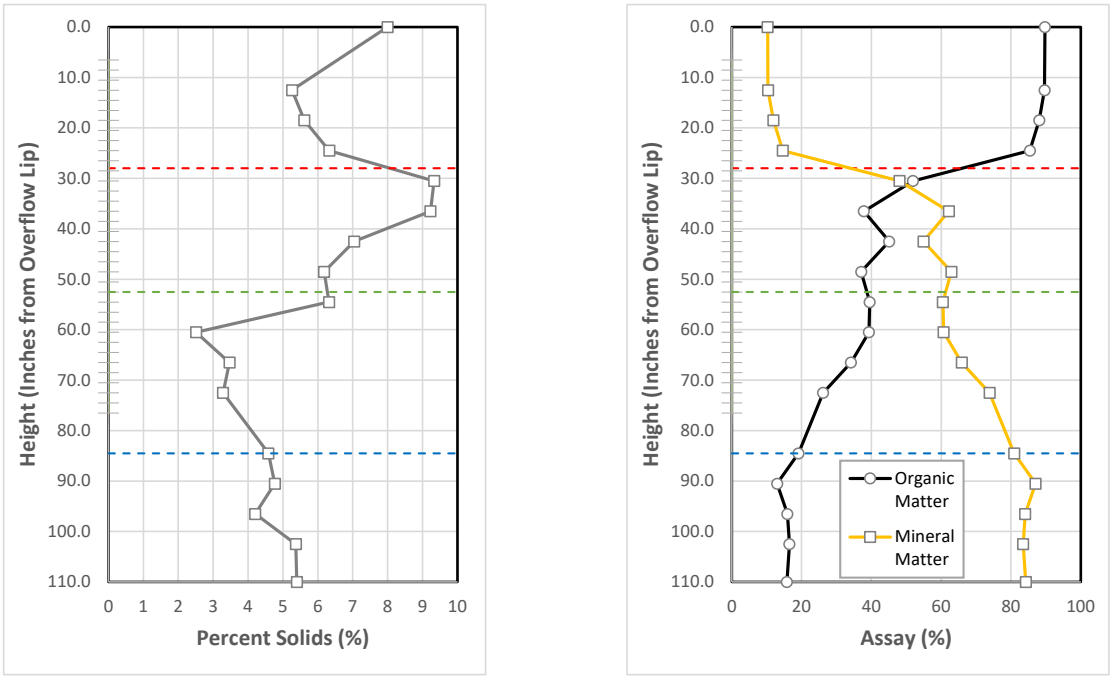


Figure 4-16. Test 5 column profiles with product containing 15.0% moisture and 9.5% ash.

Test 6 - 3 Hz Oscillation and 19 Inch Feed Port

Note: Red = Feed Inlet; Blue = Solvent Inlet; Green = Ring; Gray Bars @ Zero = Oscillating Disc Locations

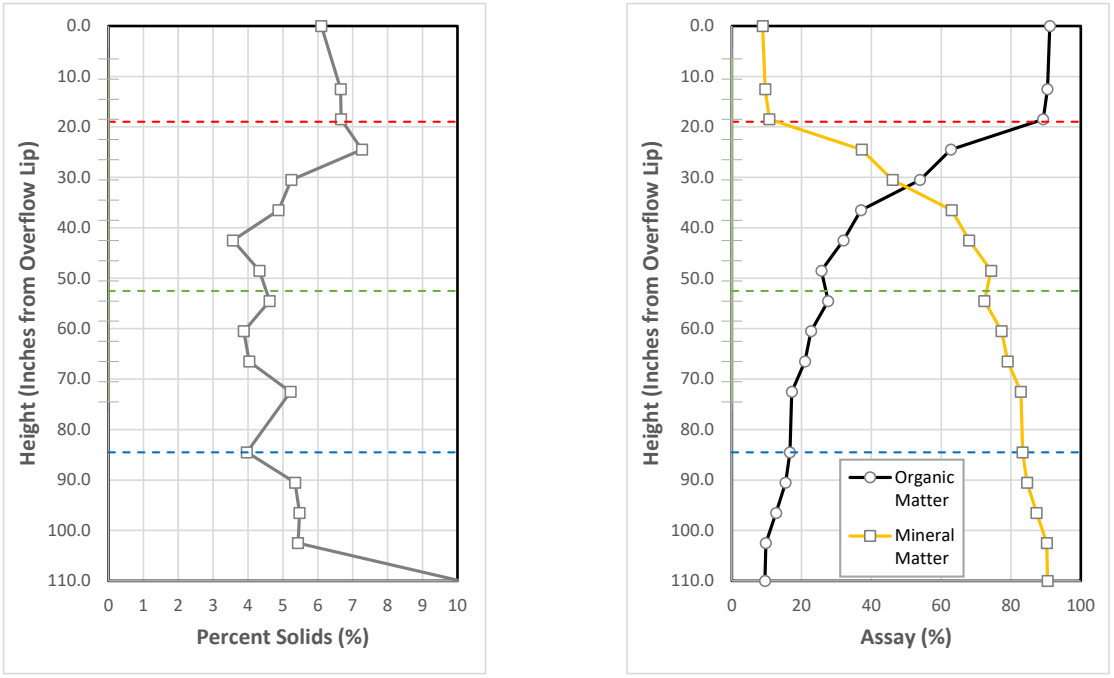


Figure 4-17. Test 6 column profiles with product containing 16.0% moisture and 8.2% ash.

Test 7 - 3 Hz Oscillation and 19 Inch Feed Port

Note: Red = Feed Inlet; Blue = Solvent Inlet; Green = Ring; Gray Bars @ Zero = Oscillating Disc Locations

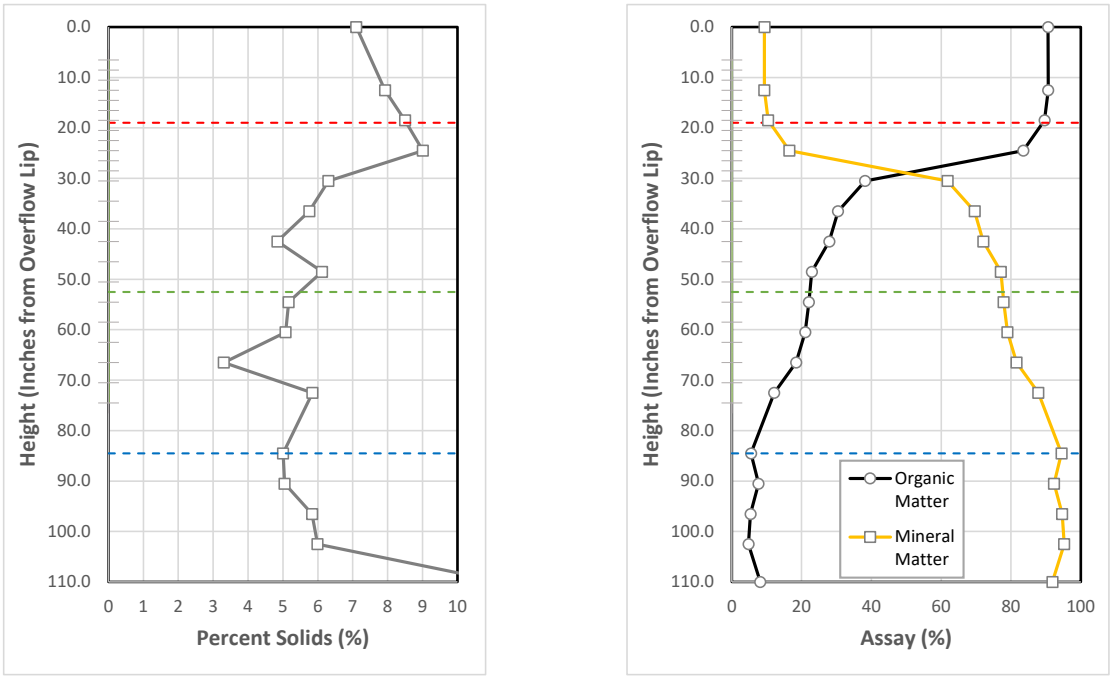


Figure 4-18. Test 1 column profiles with product containing 6.0% moisture and 8.7% ash.

Test 8 - 3 Hz Oscillation and 19 Inch Feed Port

Note: Red = Feed Inlet; Blue = Solvent Inlet; Green = Ring; Gray Bars @ Zero = Oscillating Disc Locations

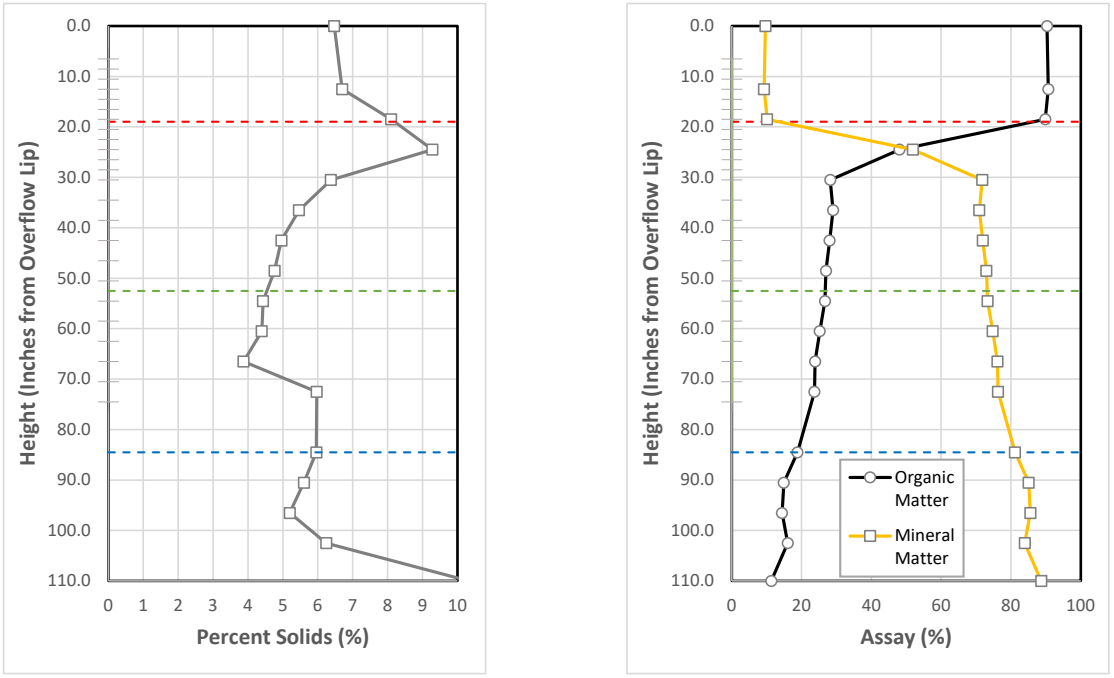


Figure 4-19. Test 1 column profiles with product containing 9.2% moisture and 8.9% ash.

Test 9 - 3 Hz Oscillation and 19 Inch Feed Port

Note: Red = Feed Inlet; Blue = Solvent Inlet; Green = Ring; Gray Bars @ Zero = Oscillating Disc Locations

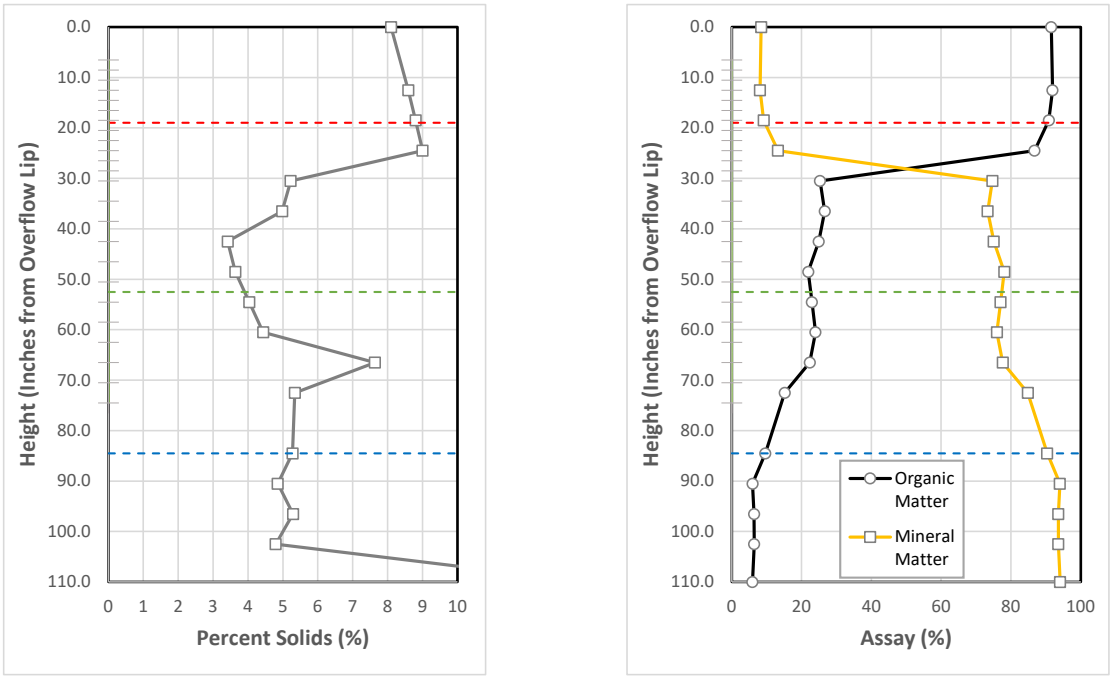


Figure 4-20. Test 9 column profiles with product containing 10.3% moisture and 7.8% ash.

Test 10 - 3 Hz Oscillation and 19 Inch Feed Port

Note: Red = Feed Inlet; Blue = Solvent Inlet; Green = Ring; Gray Bars @ Zero = Oscillating Disc Locations

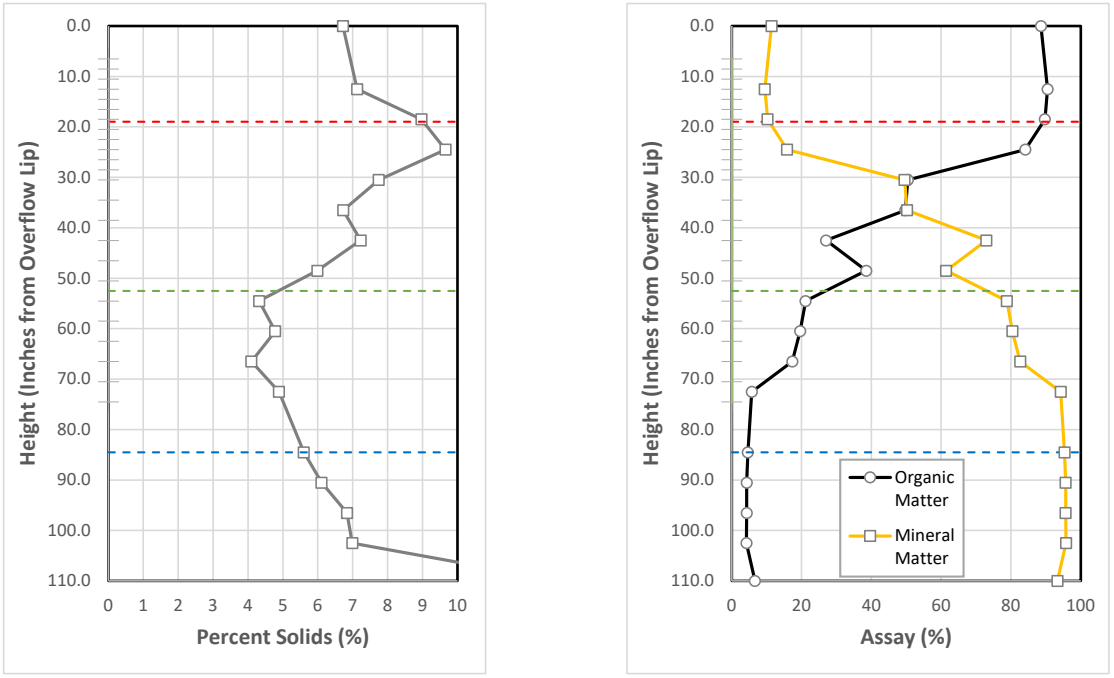


Figure 4-21. Test 10 column profiles with product containing 8.3% moisture and 10.5% ash.

Test 11 - 2 Hz Oscillation and 28 Inch Feed Port

Note: Red = Feed Inlet; Blue = Solvent Inlet; Green = Ring; Gray Bars @ Zero = Oscillating Disc Locations

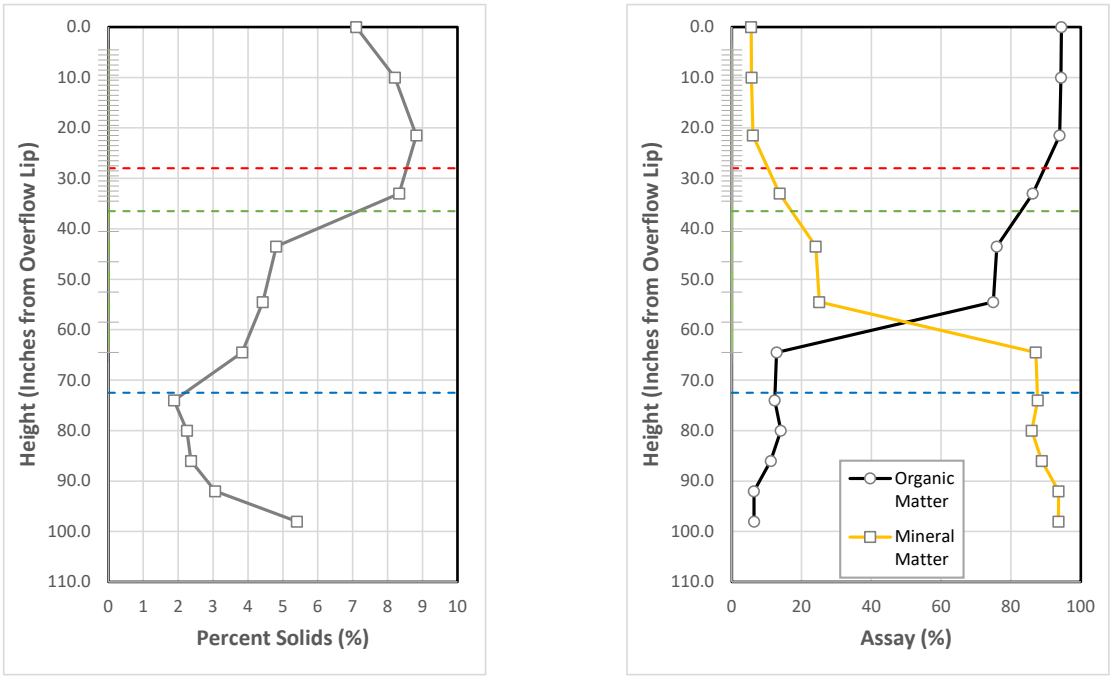


Figure 4-22. Test 11 column profiles with product containing 6.0% moisture and 5.1% ash.

Test 12 - 2 Hz Oscillation and 19 Inch Feed Port

Note: Red = Feed Inlet; Blue = Solvent Inlet; Green = Ring; Gray Bars @ Zero = Oscillating Disc Locations

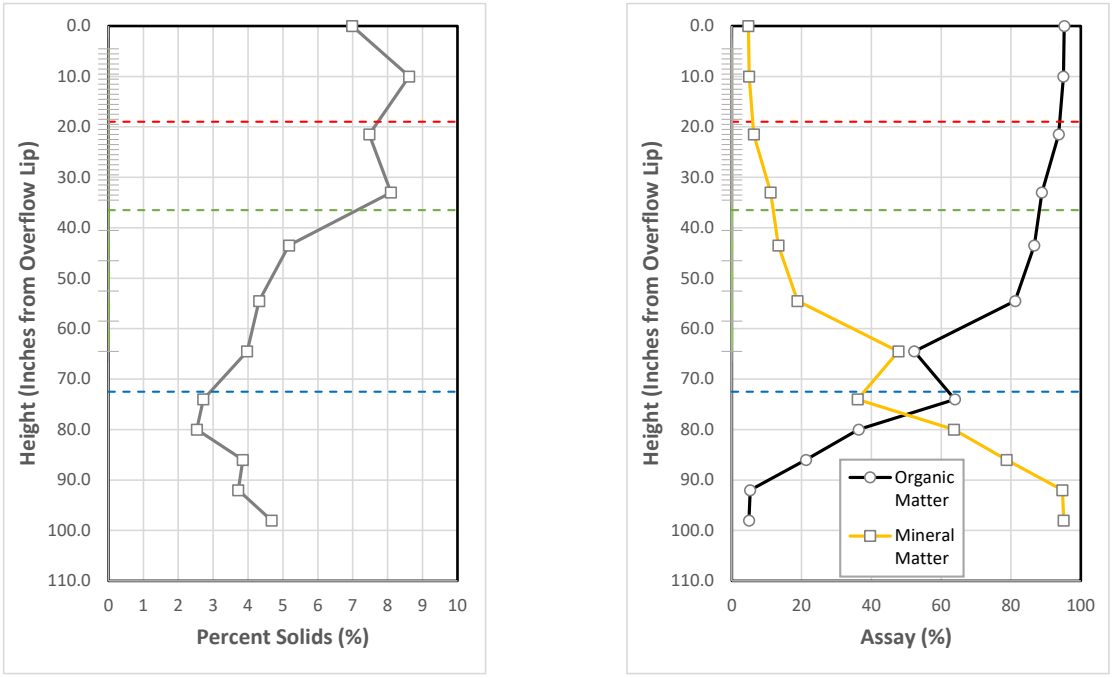


Figure 4-23. Test 12 column profiles with product containing 9.5% moisture and 4.4% ash.

Test 13 - 2 Hz Oscillation and 28 Inch Feed Port

Note: Red = Feed Inlet; Blue = Solvent Inlet; Green = Ring; Gray Bars @ Zero = Oscillating Disc Locations

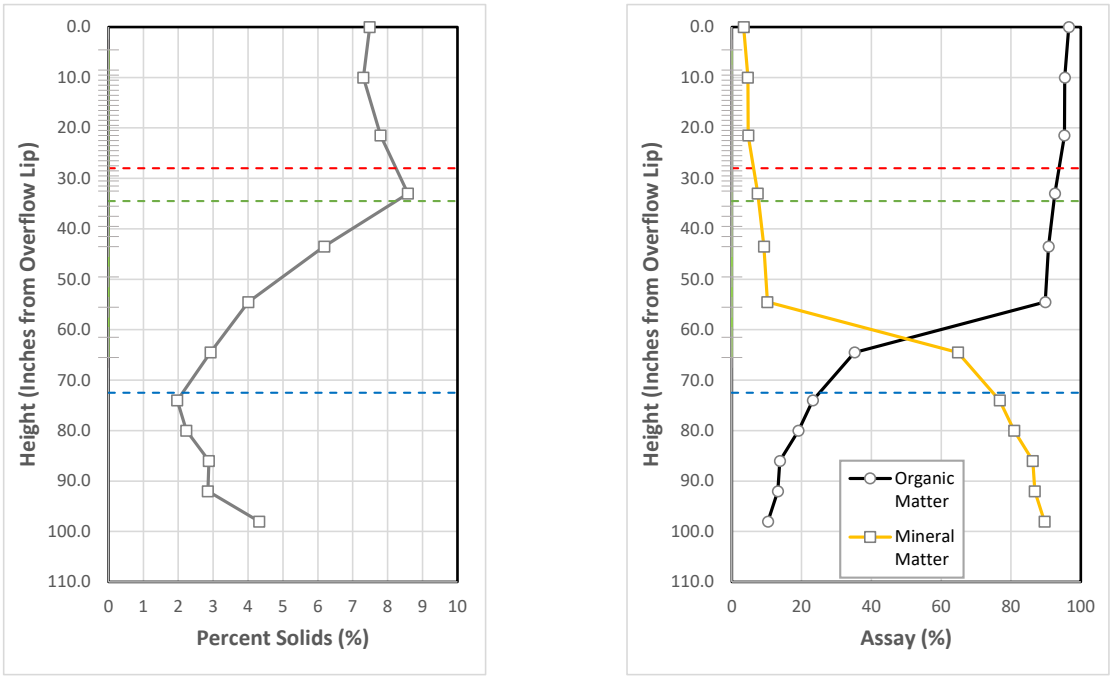


Figure 4-24. Test 13 column profiles with product containing 9.2% moisture and 8.9% ash.

Test 14 - 2 Hz Oscillation and 28 Inch Feed Port

Note: Red = Feed Inlet; Blue = Solvent Inlet; Green = Ring; Gray Bars @ Zero = Oscillating Disc Locations

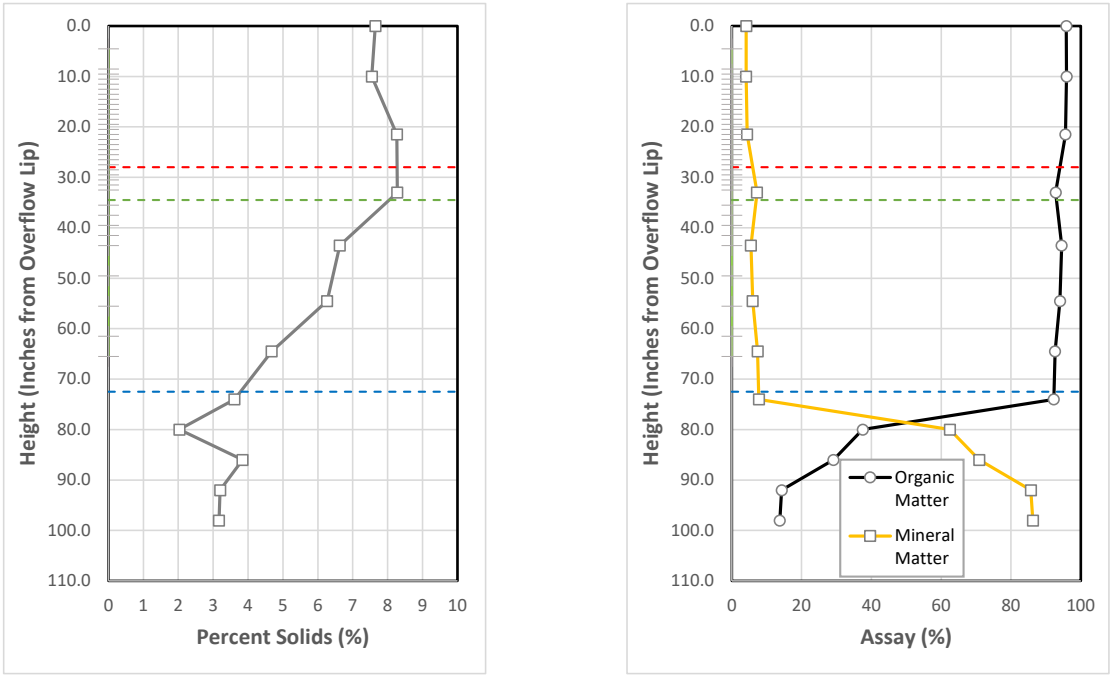


Figure 4-25. Test 14 column profiles with product containing 10.1% moisture and 3.8% ash.

Test 15 - 2 Hz Oscillation and 28 Inch Feed Port

Note: Red = Feed Inlet; Blue = Solvent Inlet; Green = Ring; Gray Bars @ Zero = Oscillating Disc Locations

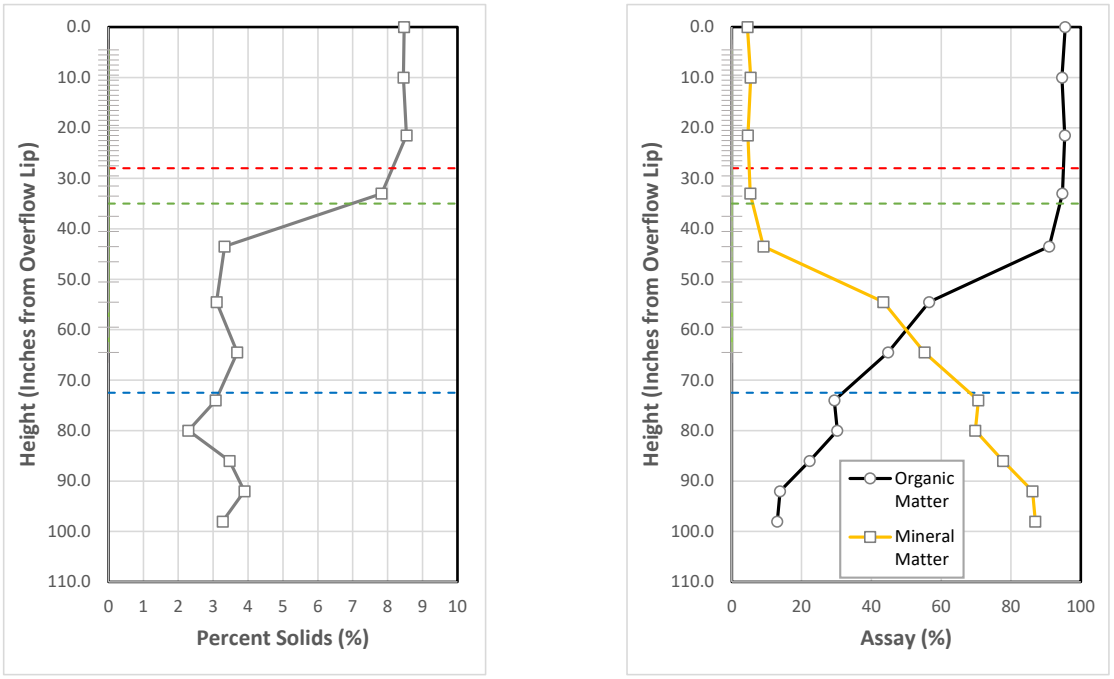


Figure 4-26. Test 15 column profiles with product containing 9.0% moisture and 4.1% ash.

Test 16 - 2 Hz Oscillation and 28 Inch Feed Port

Note: Red = Feed Inlet; Blue = Solvent Inlet; Green = Ring; Gray Bars @ Zero = Oscillating Disc Locations

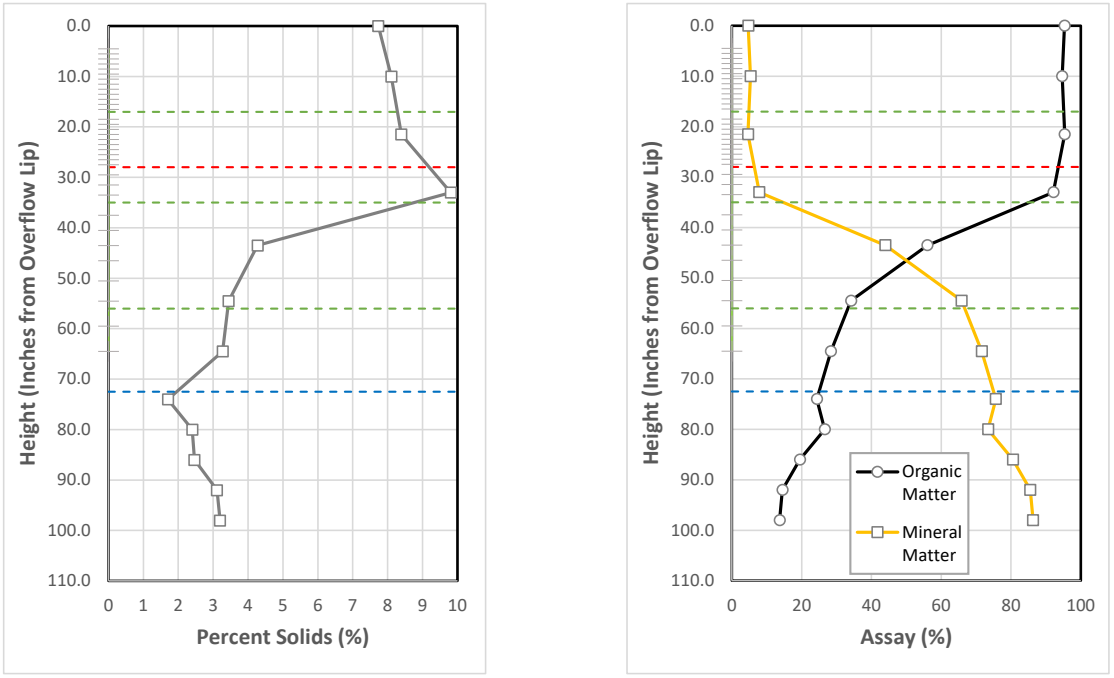


Figure 4-27. Test 16 column profiles with product containing 8.7% moisture and 4.3% ash.

Test 17 - 2 Hz Oscillation and 28 Inch Feed Port

Note: Red = Feed Inlet; Blue = Solvent Inlet; Green = Ring; Gray Bars @ Zero = Oscillating Disc Locations

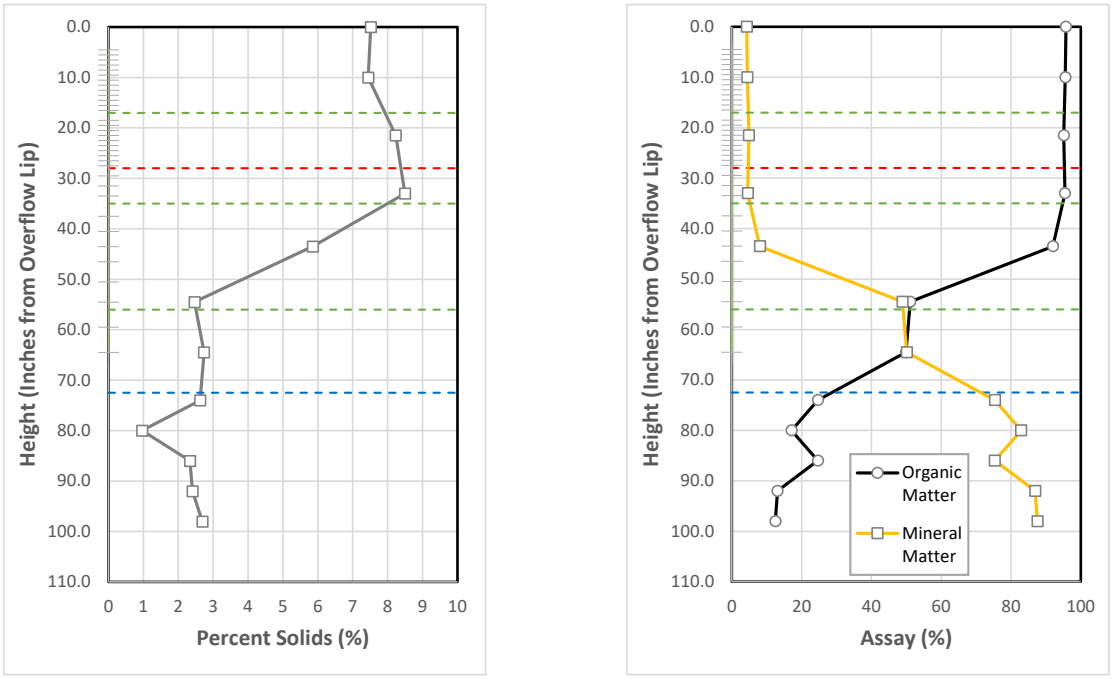


Figure 4-28. Test 17 column profiles with product containing 7.9% moisture and 3.9% ash.

Test 18 - 2 Hz Oscillation and 28 Inch Feed Port

Note: Red = Feed Inlet; Blue = Solvent Inlet; Green = Ring; Gray Bars @ Zero = Oscillating Disc Locations

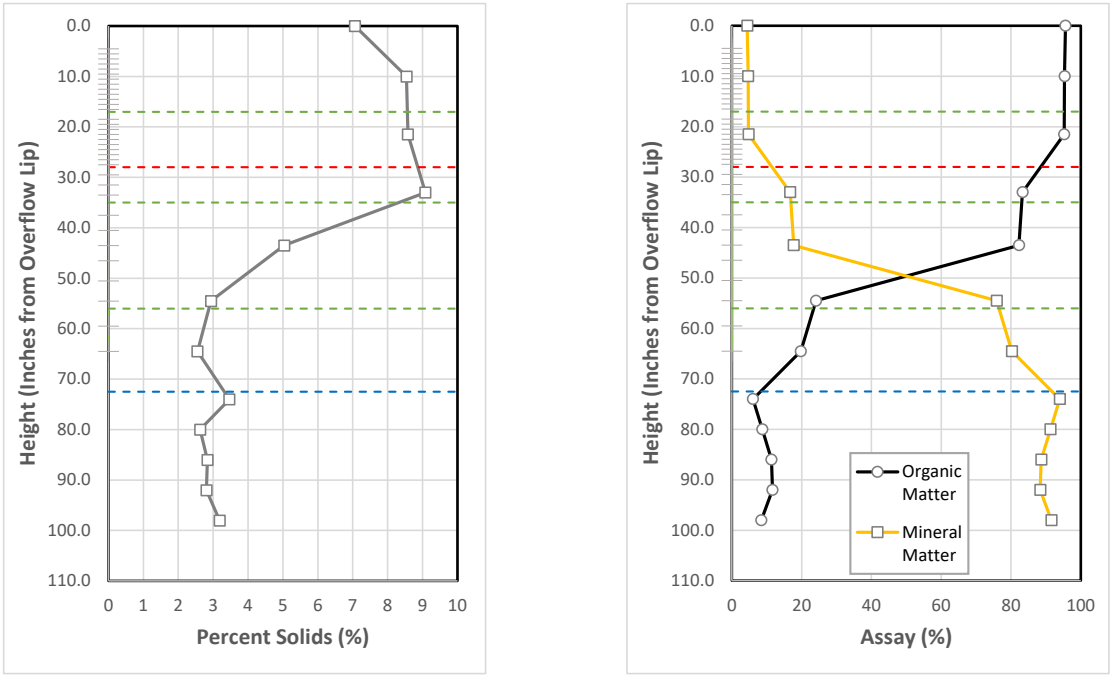


Figure 4-29. Test 18 column profiles with product containing 9.1% moisture and 4.1% ash.

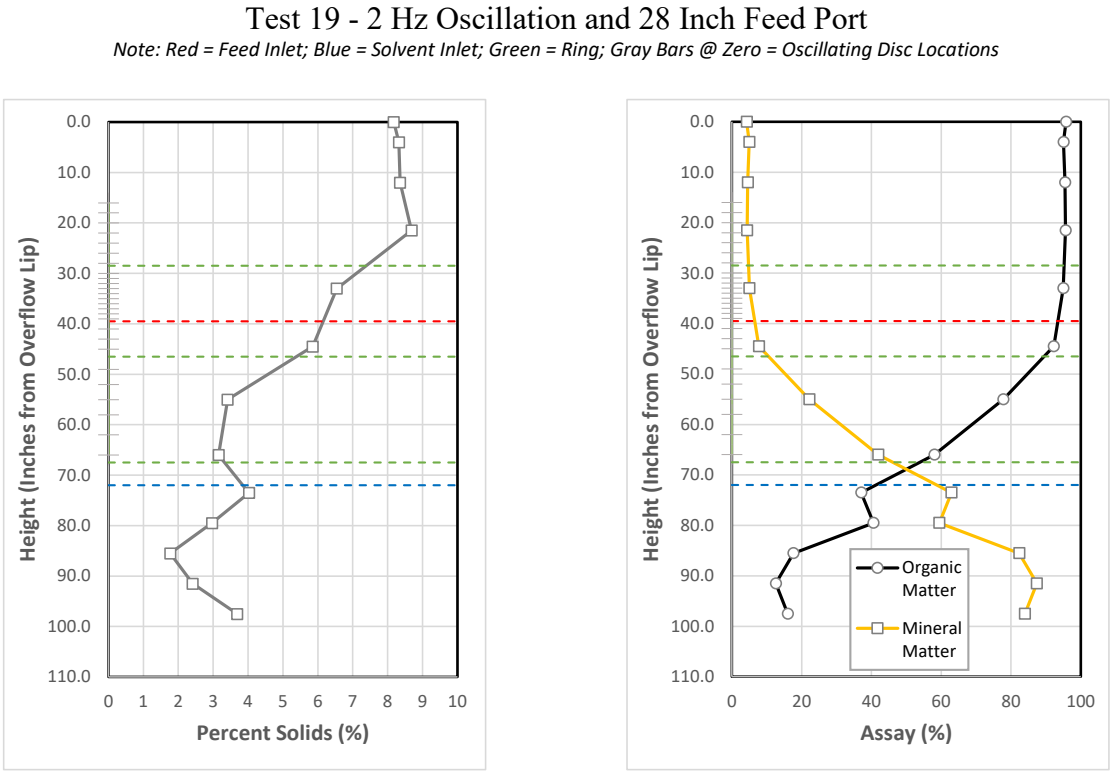


Figure 4-30. Test 19 column profiles with product containing 9.5% moisture and 3.9% ash.

4.6.3. Oscillating versus packed column results

The structured packing first testing in the column quickly showed it was prone to operational issues. The small pathways between the metal strips were easily clogged by coal agglomerates. The packing needed to be removed frequently to clean out the buildup of coal material which would be impractical on a commercial scale. Additionally, the stainless steel was also prone to collecting heavy oils that leaked into the system which would render its hydrophilic surface hydrophobic.

Overall, the structured packing was able to produce similar product moisture values to the oscillating internals column. Figure 4-31 below shows the product moistures of trials conducted with structured packing compared to trials conducted with the oscillating column. For the structured packing trials the high product moisture was almost exclusively attributed to plugging issues withing the column and the packing material. The transition to the oscillating internals eliminated plugging within the column. After this change, high product moisture would be attributed to poor agglomeration formation or plugging within the system feeding the column or

screen. This would be important for the commercial design as this would mean less downtime for cleaning obstructions inside the column.

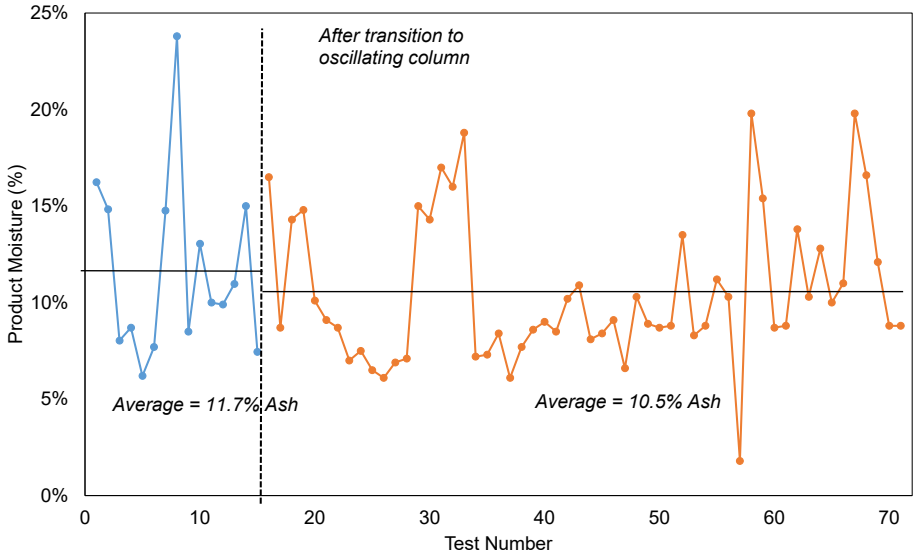


Figure 4-31:Comparison of structured packing column vs. oscillating column product moistures.

4.6.4. Influence of Column Shell Material

The material that the column Morganizer is comprised of is as important to the process as the chemistry. The water separated by the dispersion of the agglomerates will begin to fall out of the system. Constructing the column out of hydrophilic material provides surface area for water to adhere to and coalesce. The coalescence of the water allows the water droplets to fall out at a faster rate due to their increased size and weight. The upward flow of solvent would not be fast enough to carry the larger particles to the overflow.

The lab oscillating column was constructed out of glass. The glass tube provides an excellent surface for water droplets to coalesce on. However, using glass as a building material in a pilot plant scale unit can present problems due to its fragile nature. Scaling the unit up to commercial scale would be virtually impossible. Another material that has excellent hydrophilic properties is carbon steel and it is widely used as a structural and construction material. As so the pilot plant extraction column was constructed out of carbon steel pipe and pipe fittings. The internals for both the oscillating and packed columns were fabricated out of stainless steel. While the all steel column performed well with the static packing and the oscillating discs, an issue was brought up when calculations estimating the scaling to commercial scale were

tabulated. The issue discovered was that the surface area of the column shell proportional to the size of the oscillating discs could not be scaled up to a commercial unit. This ratio would in practice not be able to be duplicated on a large scale. The full-size column shell would have less equivalent surface area as shown in section 4.6.1 than the pilot scale, therefore, the data from the pilot trials would not be an indication of how the commercial plant would perform. Figure 4-32 below shows a selection of the tests performed with the all steel column and the profile of the internal configurations used.

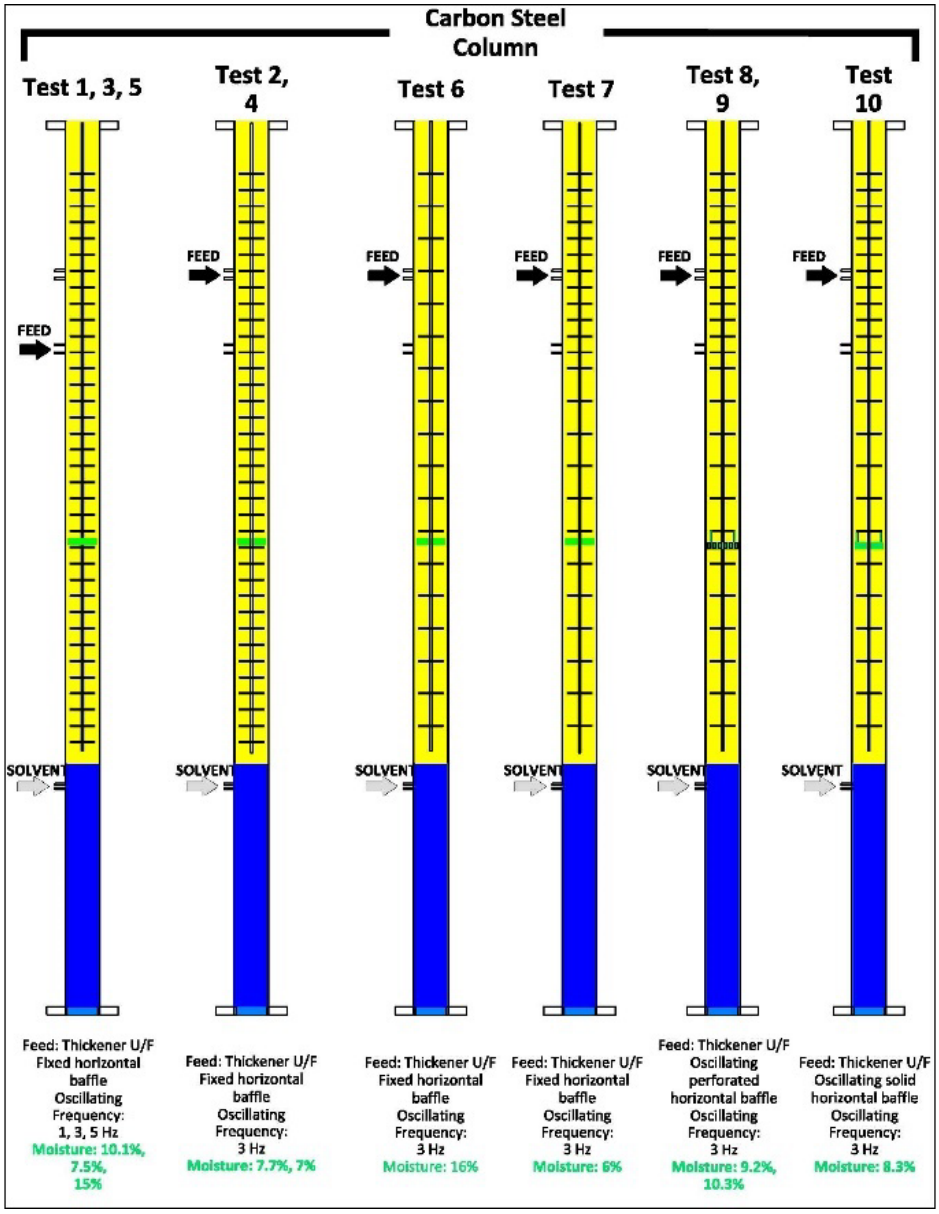


Figure 4-32. Diagrams showing the internal profiles of test configurations with the all-steel column.

An extraction column would need to be designed which could test the effectiveness of the column and produce data that would be directly scalable to a commercial plant. The key would be finding a design that had a hydrophilic surface area capable of being scaled. The design settled upon utilized a PVC shell with vertical carbon steel baffles around the inner wall of the pipe. These baffles were fabricated to have a surface area that would be realistically scalable as shown in section 4.6.1. The PVC was chosen as the base material as it is hydrophobic and would not influence the performance of column. Figure 4-33 shows a selection of test configurations with the PVC shell column and the profiles of the internal setups used. Note in tests 19 – 21 the overall height of the column was increased by 12 inches. This was to test the efficacy of a zone not influenced heavily by the movement of the oscillating discs on the overall product moistures. As described above the zone helped reduce the product moisture by providing a buffer for droplets to lose the upward momentum and to begin to fall out.

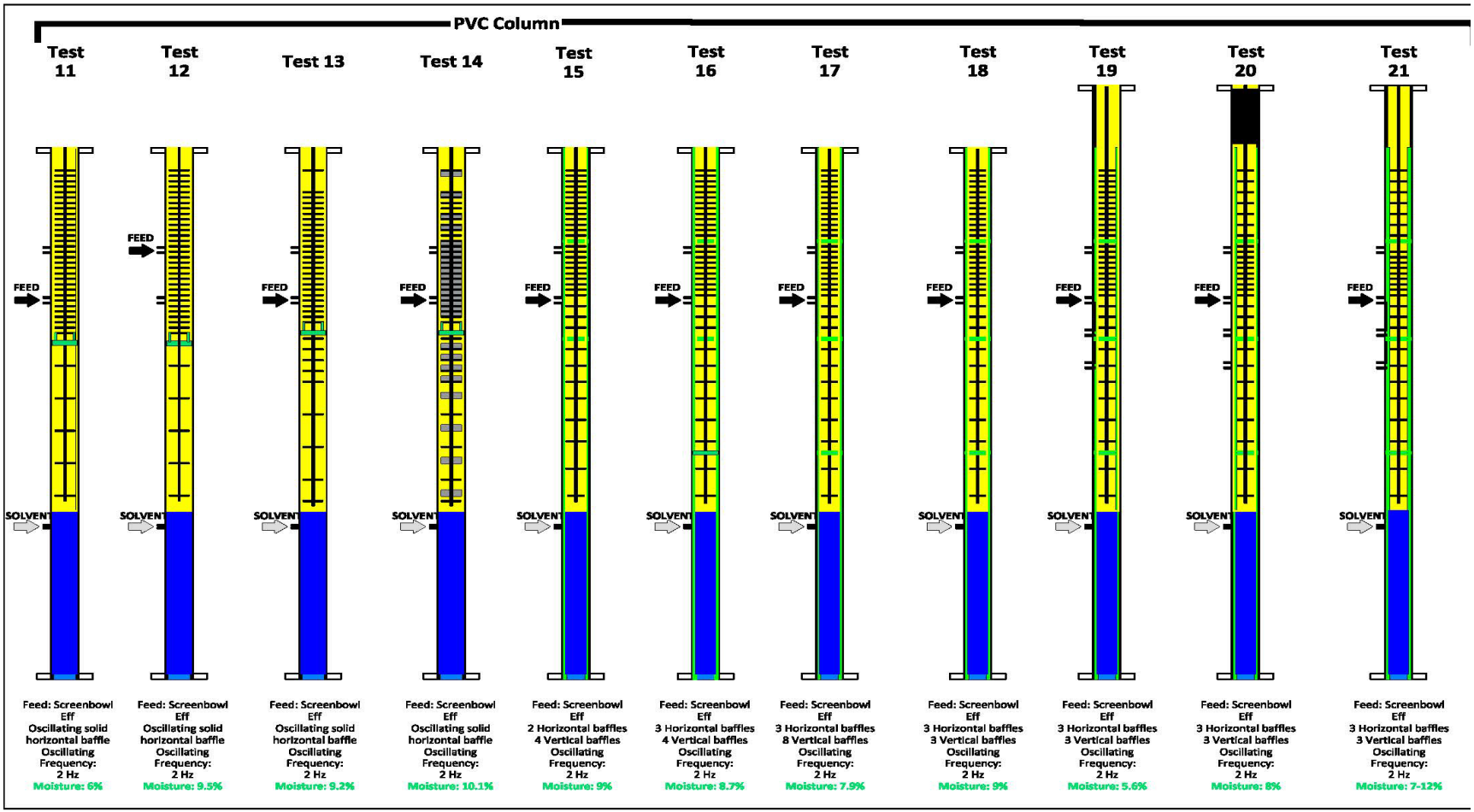


Figure 4-33:Diagrams showing the internal profiles of test configurations with the PVC column shell.

Figure 4-32 and Figure 4-33 show that the columns constructed out of the two materials performed similarly in regard to moisture content. Extremes in the product moisture typically were a result of poor agglomerate formation, plugging of a feed line, or inconsistent feed to the column. The introduction of the vertical baffles into the PVC shell increased the hydrophilic surface area which led to a small improvement in product moistures. The final improvement to the overall product came with the addition of a 12-inch section of carbon steel pipe above the oscillating section.

4.6.5. Influence of Internal Design

The internal configuration of the extraction column looked at several variables which included the type of internal part, how many were included in the design, and how they were spaced in relation to each other and the other parts. Also contributing to the effectiveness of the unit would be at what frequency the internals would have to oscillate. The configurations tested can be seen in Figure 4-32 and Figure 4-33 above.

The first design for the oscillating discs was with the discs spaced evenly at two inches apart along the center support. Several tests were conducted with this configuration and with varying the feed inlet. The results were similar in these trials and the only factor that seemed to change the output was the oscillating frequency. Based on early trials the decision was made to keep the frequency set to 3 Hz for the remaining trials. Below 3 Hz tended to have poor dispersion and led to the creation of emulsions which produced high overflow moisture. Over 3 Hz led to high moisture as it would essentially pump water and emulsions up to the overflow and not allowing them the time to sink in the column.

Keeping with the trend of having the discs evenly spaced, a trial was run with the discs four inches apart. The theory behind the increased spacing was that on a commercial scale having less discs would mean the internals would weigh less. Subsequently, the unit powering the oscillating motion would not need to be as big to operate the column, which would save initial capital as well as operating expenses. The next four trials looked at having the discs at a closer spacing in the upper half around where the feed inlet was located and the bottom half with the higher spaced discs. These trials showed that on spec results could be achieved with a lower number of discs. Following this test, the remaining trials were conducted with configurations

with shorter disc spacing in the upper portion of the column and a variation of wide spacing in the lower portion. Further refinement would see short one inch spacing just above the feed inlet with discs evenly spaced at two inches above and a mixture of three and four inch spacing below the feed inlet. Using this configuration, product moistures were routinely below 10% and product ash contents averaged around 4% which met the product grade prescribed for the project.

The final internal component that was studied was a solid stationary ring attached to the inner wall of the column called a baffle ring. The need for these rings was determined after early trials showed that the tailings contained a large amount of coal. What was theorized to be happening was agglomerates and emulsions were traveling down the annulus of the column between the outer edge of the discs and the inner column wall. Typically, the oscillating rings would have a tighter tolerance with the column wall, but the discs used in these trials were initially designed for the three-inch oscillating column. The meant the discs had up to a ¼ inch gap between their edge and the column. The baffle rings remedied this by forcing any undispersed agglomerates or emulsions out into the center of the column and back into the oscillating discs where they had a chance to break up. Trials started with one ring about halfway up the oscillating section, and they ended with three rings installed. The bottom ring was about six inches above the last oscillating disc, the middle ring was in the middle of the disc stack, and the top ring was above the feed port where the spacing transitioned from one inch to two inches.

The use of baffle rings has implications for potential commercial scale plants. The rings would allow for the oscillating discs to be smaller in diameter, not having to reach the column wall. This would save on the capital necessary for fabrication and installation as well as savings on the necessary drive unit and power usage.

4.7. Material Balance

Below in Figure 4-34 is a representation of the mass balance on the column type Morganizer as tested on the pilot plant with optimal spacing on the oscillating internals. The feed conditions are representative of the samples tested during the majority of the trials. Coal entering the column is in lbs(mass)/hour and the total slurry is in gallons per hour (gph).

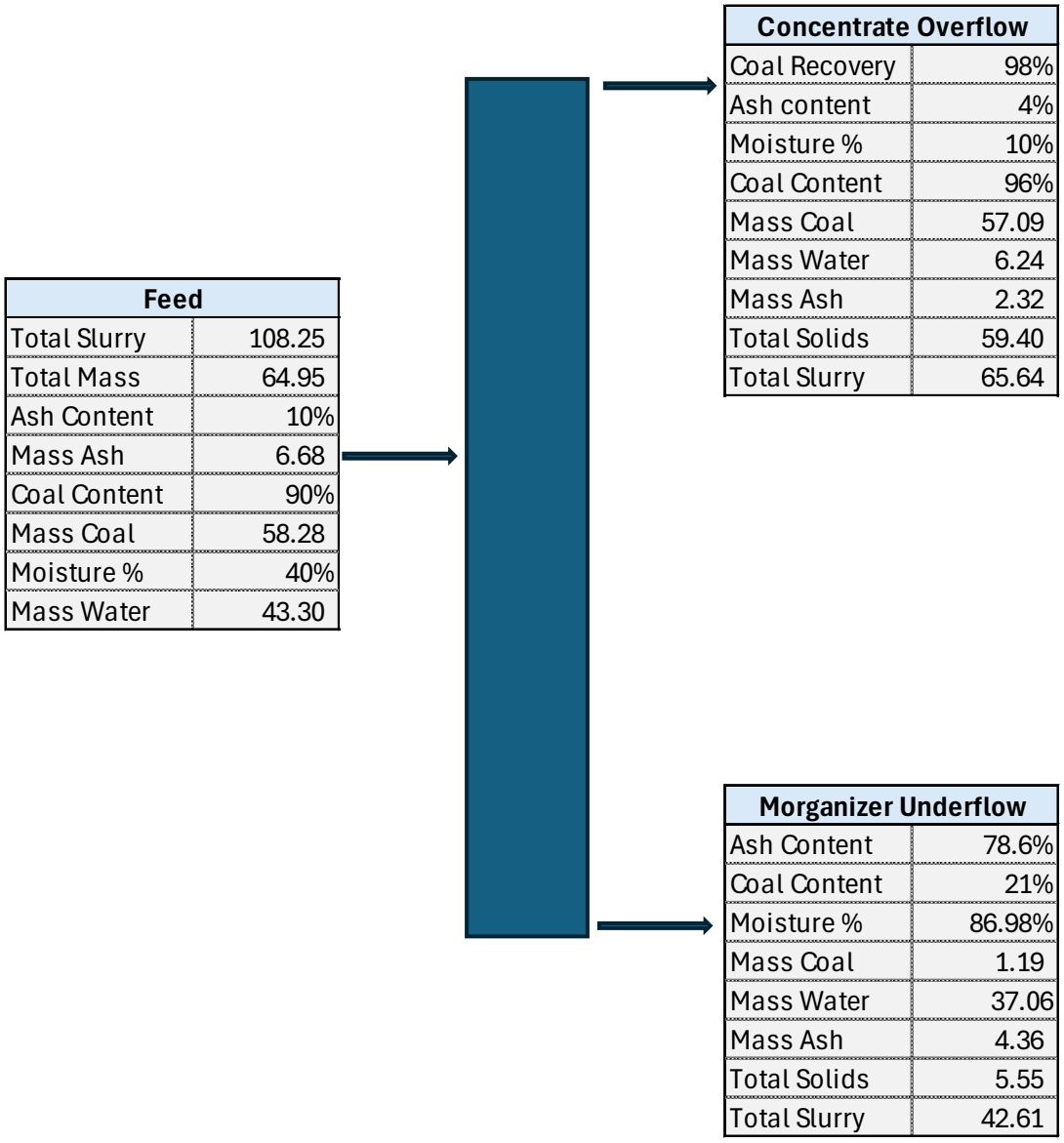


Figure 4-34: Material Balance for Column Type Morganizer as tested.

4.8. Theoretical Reactor Size Determination

In order to determine the necessary reactor diameter for a proposed process, several factors will need to be considered. These factors include the proposed mass flow rate into the reactor, desired % solids by volume of the product overflow, and max particle size in the proposed system.

The first step is to determine the volumetric flow rate based on the mass flow rate into the column.

Equation 4-12

$$Vol.Flow\ Rate = \frac{Mass\ Flow\ Rate}{Density\ of\ Solid}$$

$$Vol.Flow\ Rate\ (\frac{cm^3}{hr}) = \frac{57.09\ \frac{lb}{hr} * 453.592\ \frac{g}{lb}}{1.35\ \frac{g}{cm^3}}$$

$$Vol.Flow\ Rate\ (\frac{cm^3}{hr}) = 19{,}181$$

$$Vol.Flow\ Rate\ \left(\frac{in^3}{sec}\right) = 19{,}181\ \frac{cm^3}{hr} * \frac{0.061 cm^3/in^3}{60\ \frac{sec}{hr}}$$

$$Vol.Flow\ Rate\ \left(\frac{in^3}{sec}\right) = 19.51$$

After determining the volumetric flow rate, using the predicted % solids by volume in the overflow along with the upward velocity needed to carry the largest particle over the top, the necessary diameter of the reactor can be calculated.

Using a proposed 8% solids by volume in the overflow and the upward flow of 3.94 ft/min (0.788 in/sec) previously calculated by Stoke's Law for a particle size of 44 microns, Q = V * A can be used to solve for the diameter. Based on the density of the overflow, the solvent flow rate is calculated to be 29.42 in^3/sec.

Equation 4-13

$$Q = V * A$$

Equation 4-14

$$Q = V * \pi * (\frac{D}{2})^2$$

Solving Equation 4-14 for D

$$D = 2 * \sqrt{\frac{Q}{\pi * V}}$$

$$D(in) = 2 * \sqrt{\frac{29.42\ \frac{in^3}{sec}}{\pi * 0.788\ \frac{in}{sec}}}$$

$$D(in) = 6.89$$

4.9. Number of Discs Required for Necessary Hydrophilic Surface Area

From the trials conducted in the pilot plant, a figure was determined on the amount of surface area needed for the amount of mass processed per hour. For the column-type Morganizer this factor was calculated to be 0.0471 lb/hr/sqft (k). Using this factor combined with the estimated mass flow rate the amount of hydrophilic surface area necessary in the reactor could be calculated.

Equation 4-15

$$Total\ HP\ Surface\ Area\ (ft^2) = k\frac{\frac{lb}{hr}}{ft^2} * Mass\ Flow\ Rate\ (\frac{lb}{hr})$$

$$Total\ HP\ Surface\ Area\ (ft^2) = 0.0471\frac{\frac{lb}{hr}}{ft^2} * 57.09\ (\frac{lb}{hr})$$

$$Total\ HP\ Surface\ Area\ (ft^2) = 2.69$$

$$Total\ HP\ Surface\ Area\ (in^2) = 387.17$$

Additionally, from the trials conducted on the pilot plant two ratios were determined between the dimensions of the reactor itself. First is Height of Column to Diameter of Column (H/D) which is referred to as "R" for this evaluation. R was determined to be 18 with a column height of 72 inches and a diameter of 4 inches. Second is the Diameter of the discs to the Diameter of the Column (d/D) which is referred to as "S" for this evaluation. S was determined to be 0.625 with disc diameter of 2.5 inches and column diameter of 4 inches. With these ratios, the spacing between the discs (s) to achieve the proper surface area can be calculated.

Equation 4-16

$$Total\ HP\ Surface\ Area = \ \Pi * S + \frac{s}{2} * \Pi * \ R^2$$

Solving Equation 4-16 for s:

$$Disc\ Spacing\ (in) = 2 * \frac{HPSA * S}{R^2}$$

$$Disc\ Spacing\ (in) = 2 * \frac{387.17 * 0.625}{18^2}$$

$$Disc\ Spacing\ (in) = 0.76$$

Using ratio R to determine the proposed height of the column, the number of discs necessary to be evenly distributed.

Equation 4-17

$$\#\ of\ Discs = \frac{R * D}{Disc\ Spacing}$$

$$\#\ of\ Discs = \frac{18 * 6.89\ in}{0.757\ in}$$

$$\#\ of\ Discs = 164$$

The factor k used in the previous calculations was determined through the testing completed on the pilot plant utilizing the column Morganizer. This was determined by the total hydrophilic surface area of the column and the coal being fed into the column.

Equation 4-18

$$k = \frac{A_{total\ hydrophilic}}{MF}$$

$$k = \frac{3.059\ ft^2}{65\frac{lb}{hr}}$$

$$k = \frac{0.0471\frac{sqft}{lb}}{hr}$$

4.10. Power Required to Operate Column

Add in steps 11 & 12 and find power costs to calculate a $/lb or ton cost.

From the number of discs that are necessary within the column, the power necessary to lift/operate the Morganizer can be determined using P = F * V. Where F is the force that the motor has to lift, and V is the velocity at which the discs oscillate in the column. For this case since the discs are operating within a liquid, the force will be the summation of the force due to

their mass as well as the drag forces inside the solvent. For the weight of a disc, a factor will be applied to account for the amount of volume within the disc the perforations account for. Based on the design used to manufacture the discs, the perforations account for approximately 49% of the total disc volume.

First step is to calculate the weight of one disc:

Equation 4-19

$$Mass\ Disc\ (lb) = vol.of\ disc\ (in^3) * \ dens.of\ stainless\ steel\ \left(\frac{lb}{in^3}\right) * vol.space\ occupied\ by\ perf.$$

$$Mass\ Disc\ (lb) = \ \Pi * \ r^2 * h * \ \rho_{ss} * \%\ Vol_{perf.}$$

$$Mass\ Disc\ (lb) = \ \Pi * \ 2.155^2 * 0.265 * \ .49\%$$

$$Mass\ Disc\ (lb) = \ .24$$

Total mass of the discs:

Equation 4-20

$$Total\ Mass_{discs} = \ Mass_{disc} * \#\ of\ Discs$$

$$Total\ Mass_{discs} = \ .24\ lb * 164$$

$$Total\ Mass_{discs}(lb) = \ 38.89$$

Equation 4-21

$$Total\ Mass\ to\ lift\ (lb) = Mass\ Discs\ (lb) + Mass\ Shaft\ (lb)$$

$$Total\ Mass\ to\ lift\ (lb) = 38.89 + \Pi * (\frac{.25}{2})^2 * (18 * 6.89)$$

$$Total\ Mass\ to\ lift\ (lb) = 40.51$$

To find the lifting force for the mass, multiply the mass by the gravitational constant:

Equation 4-22

$$F_{lift}\left(\frac{ftlb}{sec^2}\right) = 40.51lb * 32.2\ \frac{ft}{sec^2}$$

$$F_{lift}\left(\frac{ftlb}{sec^2}\right) = 1304.30$$

Next piece of the total lifting is the drag force contributed by the liquid surrounding the oscillating internals:

Equation 4-23

$$F_d = \left(\frac{1}{2}\right) * \rho * V^2 * C_D * A$$

Where C_D is the drag coefficient (Engineer's Edge, 2024) of a flat disc and ρ is the density of the liquid.

Equation 4-24

$$F_{drag\ per\ disc} = \left(\frac{1}{2}\right) * 0.0229\left(\frac{lb}{in^3}\right) * \left(4\frac{in}{sec^2}\right)^2 * 1.12 * 14.58\ in^2$$

$$F_{drag\ per\ disc}\left(\frac{lbin}{sec^2}\right) = 2.99$$

$$F_{drag\ total}\left(\frac{lbin}{sec^2}\right) = 2.99 * 164$$

$$F_{drag\ total}\left(\frac{lbin}{sec^2}\right) = 491.52$$

Therefore, the total force needed to be moved is equal to the total of the drag force and force due to the mass.

Equation 4-25

$$Total\ Load = F_{mass} + F_{drag}$$

$$Total\ Load\ \left(\frac{lbin}{sec^2}\right) = 1304.30 + 491.52$$

$$Total\ Load\ \left(\frac{lbin}{sec^2}\right) = 1795.83$$

In order to determine the size of the motor necessary in addition to the load to be lifted, the shaft efficiency and the motor efficiency. In this evaluation, shaft efficiency is assumed to be 85% and motor efficiency is assumed to be 90%.

Equation 4-26

$$Motor\ (HP) = Total\ Load\ \left(\frac{lbin}{sec^2}\right) * V\ \left(\frac{ft}{sec}\right) * Eff_{shaft} * Eff_{motor}$$

$$Motor\ (HP) = 1795.83\ \left(\frac{lbin}{sec^2}\right) * 0.33\ \left(\frac{ft}{sec}\right) * .85 * .90$$

$$Motor\ (HP) = 1.423$$

With the size of the motor determined, an estimated cost to operate the column can be calculated. Since I HP is equal to 746 Watts, the motor in this example will have a wattage rating of:

Equation 4-27

$$P_{Watts} = P_{HP} * 746\ (\frac{Watts}{HP})$$

$$P_{Watts} = 1.423 * 746\ (\frac{Watts}{HP})$$

$$P_{Watts} = 1061.35$$

To determine the energy consumption over the period of one hour the following formula can be used:

Equation 4-28

$$kWh = (Watts * t)/1000$$

$$kWh = (1061.35 * 1)/1000$$

$$kWh = 1.06$$

Therefore, the motor used in the theoretical pilot plant will consume around 1.06 kW for each hour of operation. Given the rolling 12-month average industrial energy pricing of $0.0802/hWh the motor would only cost around $0.08/ hour to operate. With a mass flow into the column of 57/lbs. per hour, the column in the designed plant would cost approximately $2.81 per ton of to operate.

4.11. Scaling Parameters Determined from Pilot Plant Trials

This exercise shows that based on the parameters developed in the trials on the pilot plant, the theoretical plant would need a motor just under 1.5 HP. Based on the calculations determined here, several relationships can be developed that will aid in the design of a commercial size plant. The first is determining the diameter of the reactor to fit a commercial process. The second is to calculate the number of discs needed to produce the appropriate surface area to handle the organic load of the process. Finally, the third is to calculate the size of the motor necessary to operate the internals that are sized for the commercial process. Below defines these relationships.

4.11.1. Scale up #1: Reactor Diameter

The diameter of the reactor can be determined from the cross-sectional area of the column using the relationship of Q = V * A. In this application, V is the minimum value of the upward velocity needed to carry over the maximum particle size and Q is the volumetric flow of the liquid/solids moving upward through the column. Solving for A:

Equation 4-29

$$A = \frac{Q}{V}$$

The volumetric flow, Q, can be found using the mass flow (MF) and the density of the slurry moving upward through the column.

Equation 4-30

$$Q = \frac{MF}{\rho_{slurry}}$$

The density of the slurry can be found by using:

Equation 4-31

$$\rho_{slurry} = \frac{100}{((\frac{\%_{solids}}{SG_{solids}} + \left(100 - \frac{\%_{solids}}{SG_{liguid}}\right))}$$

Substituting Equation 4-31 into Equation 4-30:

$$Q = \frac{MF * ((\frac{\%_{solids}}{SG_{solids}} + \left(100 - \frac{\%_{solids}}{SG_{liguid}}\right))}{100}$$

The velocity can be determined using Stoke's law for the largest particle size.

Equation 4-32

$$V = \frac{d^2 * g * (\rho_{solid} - \rho_{liquid})}{18 * \mu}$$

Where d is the diameter of the largest particle size, g is the gravitational constant, and μ is the viscosity of the liquid. While agglomerate sizes are approximately 1mm in size, they become broken apart in the Morganizer and the resulting particles in the column are below 325 mesh allowing Stokes to be applicable. Substituting these in to solve for the Area gives:

Equation 4-33

$$A = \frac{MF * ((\frac{\%_{solids}}{SG_{solids}} + \left(100 - \frac{\%_{solids}}{SG_{liguid}}\right))}{100(\frac{d^2 * g(\rho_s - \rho_l)}{18\mu})}$$

Since the area is for a circular tube, the diameter of the reactor is:

Equation 4-34

$$A = \Pi * (\frac{D}{2})^2$$

Solving for the diameter:

$$D = 2 * \sqrt{\frac{A}{\Pi}}$$

Substituting the pieces together:

Equation 4-35

$$D = 2 * \sqrt{\frac{MF * ((\frac{\%_{solids}}{SG_{solids}} + \left(100 - \frac{\%_{solids}}{SG_{liguid}}\right))}{100\left(\frac{d^2 * g(\rho_s - \rho_l)}{18\mu}\right) * \pi}}$$

If the Mass Flow, the largest particle the column has to handle, and the % solids by volume in the overflow are known, the above formula will determine the diameter of the reactor needed to handle the material. From there, using the height to diameter relationship described earlier, the total height of the column can be determined.

4.11.2. Scale up #2: Number of plates needed within the column:

The number of plates needed in the column can be determined by finding the average spacing between the plates divided over the height of the column.

Equation 4-36

$$\#\ of\ plates = \frac{Column\ Height}{Ave.Spacing}$$

The column height can be determined with the height to diameter ratio (R) once the necessary reactor diameter (D) is found. The average spacing is found with the following formula solving for n:

Equation 4-37

$$Area_{required} = \pi * S + \frac{n}{2} * \pi * R^2$$

$$Area_{Required} = MF * k$$

Where MF is the mass flow that the column will need to handle, and k is a scaling factor of the hydrophilic surface area determined in the pilot plant testing.

Combining the equations gives:

Equation 4-38

$$MF * k = \pi * S + \frac{n}{2} * \pi * R^2$$

Where S is the ratio of the diameter of the column to the diameter of the plates.

Solving for n:

Equation 4-39

$$n = \frac{2(MF * k - \pi S)}{R^2 * \pi}$$

Therefore:

$$Equation\ 4\text{-}40 \#\ of\ plates = \frac{D*R}{\frac{2(MF*k-\pi S)}{R^2*\pi}}$$

Using this formula, the number of plates needed for configuration inside the column can be calculated.

4.11.3. Scale up #3: Motor HP rating necessary to operate column:

The power of the motor is calculated with 2 components, the weight of the internals being lifted and the drag force of the internals in the liquid inside the column.

For this, P = F * V will be used.

Equation 4-41

$$V = \frac{d_l}{2H_z}$$

Where d_l is the distance that the internals will travel during one period of oscillation in the column and H_z is the oscillating frequency of the internals.

Equation 4-42

$$F_{total} = F_{drag} + F_{weight}$$

$$F_{weight} = g * (Weight_{Discs} + Weight_{shaft})$$

$$F_{weight} = g * (\#_{discs} * Mass_{disc} + \pi r^2 h)$$

$$F_{weight} = g * (\#_{discs} * Mass_{disc} + \pi((\frac{D}{2})^2 DR)$$

$$F_{weight} = g * (\#_{discs} * Mass_{disc} + \pi((\frac{D}{2})^2 DR)$$

$$F_{weight} = g * (\#_{discs} * Mass_{disc} + \pi \frac{D^3}{4} R)$$

$$F_{drag} = \frac{1}{2}\rho_l V^2 \mu A$$

Therefore, the power necessary would be given by:

Equation 4-43

$$P_{necessary} = \left(\frac{1}{2}\rho_l V^2 \mu \pi \frac{D^2}{4}\right) + g(\#_{Discs} * Mass_{disc} + \pi \frac{D^3}{4} R)$$

Substituting in for Velocity

Equation 4-44

$$P_{necessary} = \left(\frac{1}{2}\rho_l V^2 \mu \pi \frac{D^2}{4}\right) + g(\#_{Discs} * Mass_{disc} + \pi \frac{D^3}{4} R)$$

Solving for the motor power:

Equation 4-45

$$P_{motor} = Eff_{shaft} * Eff_{motor} * P_{necessary}$$

$$P_{motor} = Eff_{shaft} * Eff_{motor} * (\left(\frac{1}{2}\rho_l V^2 \mu \pi \frac{D^2}{4}\right) + g\left(\#_{Discs} * Mass_{disc} + \pi \frac{D^3}{4} R\right))$$

Using this formula would allow for the proper size motor to be purchased when constructing a plant utilizing a column designed for the specific process.

4.12. Conclusions and Design Recommendations

The trials conducted for this project looked at two different types of Morganizer designed at dispersing coal agglomerates. Both types of columns utilized an upward flow of iso-hexane to carry the dispersed coal to the overflow. The structured packing column was a more mechanically simpler design that relied on the turbulence created by the liquid moving through the channels created by the strips of metal. The oscillating column relied on a stack of perforated discs that would pulse up and down creating the force necessary to disperse the agglomerates. Both types of columns performed well with the oscillating column beating the average product moisture of the packed column by one percent. However, the structured packing column was extremely prone to plugging especially when agglomerate formation was excellent. The oscillating column was not affected by plugging issues, so the remaining trials focused on improving the design.

Through a series of trials, the oscillating column was tested to not only be able to produce a low ash low moisture carbon product but also be able to be scaled up to a viable commercial scale plant. The results suggest that the disc spacing within the column does not need to be uniform. Rather a lesser number of discs can be used when the spacing is close around the feed inlet and wide in the lower portion of the column. This spacing allows the internals to disperse the agglomerates while keeping the coal particles from making it too far down the height of the column where they risk being lost in the tails. The trials were also a success in that the data collected allowed the design of a commercial scale plant that utilizes the HHS process to recover coal from decanter effluent that previously would have been sent to a waste impoundment.

Recommendations for potential research looking at this design would be to test the current column configuration with a variety of coal slurry samples with varying solids and ash content. Fine tuning the column to handle a wider spectrum of waste streams would make the process more attractive for adoption by other operators in and outside of the Central Appalachian Basin.

Chapter 5. Development of a Column Jig Type Morganizer

5.1. History of Jigging

The use of jigging in the coal cleaning process is one of the oldest methods that exists. In fact, jigging can trace its roots back to the 1560's when Agricola describes a jigging sieve used by miners at the time for separating metal ore from waste material (Agricola, Hoover, and Hoover 1912). The idea behind jigging is to achieve particle stratification through the alternating expansion and contraction of the particle bed. This can be achieved by utilizing a pulsing liquid flow within a bed of coarse ragging. Jigs were commonly used because they could handle large particles at very high capacities for single units. They have been known to handle particles up to 20 cm in size at a rate of 680 tons per hour (Daemen 2004). One of the more common jig types utilized in coal cleaning was the Baum jig. The Baum jig was introduced in the United States in 1928. By 1935, over one third of the clean coal produced in the US was done by a jig(Yancey et al. 1938). Prior to this, the primary jig used in US coal production was the piston type. This jig relied on the pulsation created by the injection and exhausting of air in the closed end of a U-shaped tube. This action would pulse the water through the particle bed suspended over a perforated plate (Daemen 2004). This perforated plate is typically covered by a layer of ragging material which is made of particles with a selected specific gravity. This bed of ragging material allows for the heavier particles to drop through and form the concentrate underflow while the remaining slurry and lighter particles report to the tailings overflow (Falconer 2003). The reason that the Baum jig became more widely used over the piston jig is that the use of air to create the puling motion allowed for easier modification of the separation characters. Piston jigs relied on eccentrics run by motors which were typically fixed (Yancey et al. 1938).

In addition to coal, as Agricola alluded to above, jigs have been used on a variety of mineral separation processes. One such industry is gold mining. Jigging is effective for gold separation is that it induces stratification of the material inside of the process. The denser gold particles will end up on the bottom of the jig and the light material will work their way to the top (Michaud 2016). Jigs can be effectively used in any process where the target material has a large differential in specific gravity versus the waste material. Figure 5-1 below shows a small scale two stage rectangular mineral jig.



Figure 5-1. Photo of a small two stage mineral jig (Michaud 2016).

While jigging has enjoyed a prominent role in coal and mineral processing over the past few centuries it has gradually been replaced. This has been due to the fact that more efficient methods for separating large and dense particles have been developed. However, over the jigs operational period one limitation always stood out with the method. Jigs from the onset struggled with fine particles. While jigs have been developed that have been able to capture particles down to 20 microns such as the Kelsey jig, they remain not widely adopted. Across the industry, jig use has dropped off almost to nothing in the US in favor of other separation technologies such as dense media separation, cyclones and spirals, and flotation. Other major coal production countries around the world including Australia are following this trend. Countries such as China and India are among the few where jigging still makes up a significant portion of the separation technology used (Phengsaart et al. 2023). Figure 5-2 below shows the usage of different coal cleaning technologies in the top five producing countries.

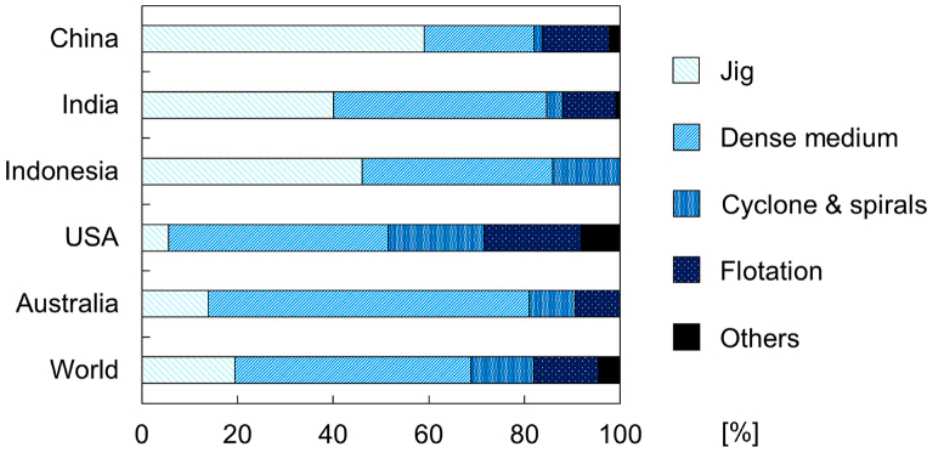


Figure 5-2. Coal cleaning technology use in the top 5 coal producing countries.

5.2. Use of Jig in the HHS process

While the jig has been primarily used as a gravity-based separation system in mineral processing recent developments have also shown that the jigging action has benefit in the de-emulsification step (or *Morganizer*) of the HHS process. The simplicity and effectiveness of a jig's pulsing motion in density separation made it attractive to look at for use in dispersion of coal emulsions. The pulsing mechanism generally was created by simple mechanical means which was an attractive trait of the jig for use in HHS. Replacing the more complex oscillating column internals with a pulsing mechanism would in theory lower the initial capital required to implement an HHS plant and lower the power costs necessary to run it. The lower capital and operating costs would lower the boundaries that would prevent a larger number of operators adopting it.

Previous laboratory versions of the Morganizer used column-based extractors relying on mechanical energy input by vibratory screens. Preliminary laboratory tests were conducted using a pulsing column with a ragging layer similar to a piston-style jig. This laboratory testing started with a one-inch glass tube unit with a launder top. The unit consisted of three sections. The top had an overflow launder which used tubing to direct overflow into a beaker. The middle section had a screen held in place whose function was to keep the ragging from falling out of the unit. Also, in this middle section there was a port where solvent could be pumped in to create an upward flow to carry freed carbon particles to the overflow. The bottom piece had a funnel type bottom with a valve. The valve could be opened to let out built up water released from

agglomerates in order to keep the interface level steady. Figure 5-3 below shows the actual lab jig Morganizer and the diaphragm metering pump used to create the pulse.



Figure 5-3. Laboratory jig Morganizer and diaphragm metering pump.

The bottom section included a port that was connected to a metering diaphragm pump. This metering pump was responsible for creating the pulsing motion within the unit. This was achieved by using Tygon tubing connected from the outlet of the pump to the jig. On the inlet side of the pump, a short piece of closed off Tygon tubing was connected. When the pump operated it would pump the liquid back and forth since the inlet was closed. The amount of tubing used could set how much stroke the pump produced and at its max it was capable of over 250 strokes per minute. Pump is shown in Figure 5-3 above.

The primary difference between this new type of jig and conventional jigs is how material moves through the unit. In conventional jigs, material is introduced on one end of the jig. Then by means of a sloped bed or some other mechanism the material travels laterally across the surface area with the light particles making their way to the top and the heavier particles sinking. The heavier particles can then be collected at the bottom on the lower end while the lighter particles can overflow the top of the lower end. In contrast the new jig relied on vertical movement of liquids and particles to do the separation. The test jig was fed by scooping agglomerates into the open top of the tube. The water laden particles would sink down to the ragging layer where the pulsing motion would drag them back in forth inside the glass beads.

This would break the agglomerates apart allowing the carbon particles to flow upward with the additional solvent being pumped in and allow the water to sink to go out with the tailings.

5.3. Materials and Methods

5.3.1. Pilot Scale Jig Scale Up and Design

Laboratory trials showed that a jig-type Morganizer could efficiently disperse agglomerates and recovery dry product at high capacity. Due to this success, a pilot scale jig Morganizer was designed, constructed, and tested. Initially, the team utilized a custom-modified laboratory jig supplied by 911 Metallurgist. See Figure 5-1 above for a representation of the jig purchased. Preliminary testing validated the laboratory results with a product ash of 2.72%; however, the small vertical liquid layer (<2 inches) caused substantial operational challenges associated with the automated control of the liquid-solvent interface.

To overcome this challenge, a larger column-type piston jig was designed and constructed. This unit utilized a piston unit driven by compressed air to generate a pulsing movement in a liquid column. The nominal inner diameter of the piping associated with this unit was six inches, corresponding to a potential max capacity commensurate with that of the other pilot-scale HHS process operations. Figure 5-4 shows the concept drawing for the new jig.

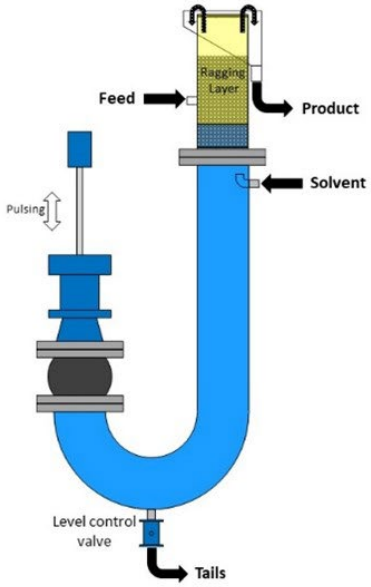


Figure 5-4. Concept drawing of U-tube pilot scale jig type Morganizer.

The piston jig was fabricated in 3 main parts. The largest piece of the equipment was a six-inch steel pipe section bent into a “U” shape. One side of the “U” was approximately two feet higher than the other side. The longer side had been drilled and tapped for sampling ports space along its length. Both ends of the section had a flange welded on for connection. The short side of the section was where the remaining two pieces of the unit bolted on. The first piece that bolted to the “U” was an enclosed four-inch diameter piston. An expansion flange was attached to the piston to take the four-inch diameter up to six inches to mate with the other sections. Between the piston and “U” section of pipe was a rubber buffer that was included to dampen vibration caused by the movement of the mechanical components on the rest of the jig. On the opposite side of the piston from the piping was a pneumatic cylinder connected to an actuator valve. This valve and cylinder used compressed air to both drive and pull the piston back and forth to create the pulsing motion. Figure 5-5 below shows the u-tube base for the new six-inch jig Morganizer and Figure 5-6 shows the finished jig installed on the pilot plant.



Figure 5-5. Completed base of U-tube pilot scale Morganizer.

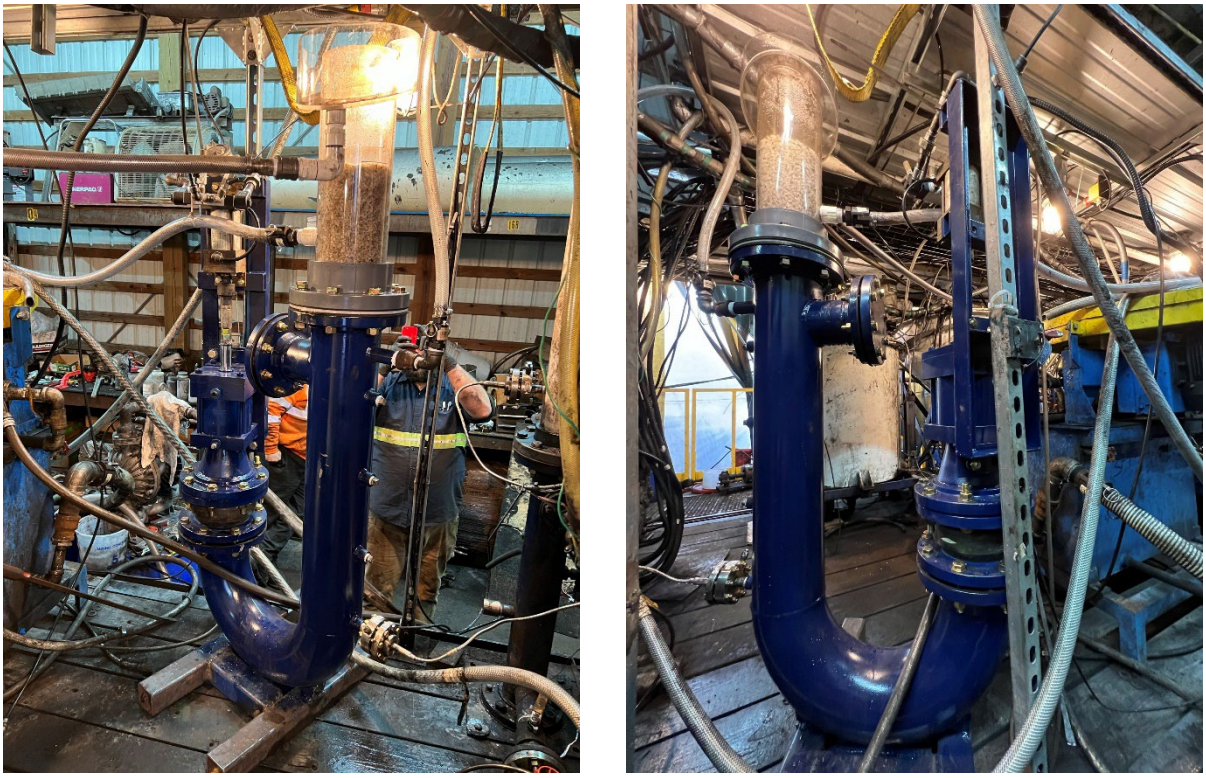


Figure 5-6. Completed pilot scale Morganizer installed on pilot plant.

Additional modifications to the original unit included adding one-inch feed ports to match the feed tubing originally attached to the oscillating column. A 3D printed flange disk was fabricated to hold a small mesh screen which would keep the ragging layer in the appropriate space within the liquid column. Figure 5-7 showing the 3D printed screen support.



Figure 5-7. 3D printed screen support.

Lastly, the actuating valve was plumbed into the compressed air system on the pilot plant and a regulator valve was installed to keep the pressure below the maximum of 80 psi the valve block recommended. The relays controlling the actuator valve were located in a control box which was installed in the utility side of the control room. The box was not explosion proof rated so it was moved into this room to keep it in a safe environment away from solvent fumes when powered up. Figure 5-8 showing the actuator valve.



Figure 5-8. Jig actuator valve.

5.3.2. Materials

Coal samples: All jig testing trials in the lab and on the pilot plant were conducted with coal samples collected from metallurgical operators in Southwestern Virginia and Alabama. These samples are low volatile bituminous sourced from screenbowl effluent and from flotation tailings. Additional details on these samples are provided in Chapter 3.

Ragging: The prior laboratory studies utilized 2 mm glass spheres for the jig ragging layer. In the pilot process, similar glass spheres were considered; however, they were deemed cost prohibitive due to the volume needed to fill the column. As an alternative, the team utilized coarse feldspar supplied by a standard commercial dealer. The feldspar was delivered with pieces averaging 1" x 2-3." This material was subsequently crushed (via hammer mill) to approximately ½" x ¾." In addition, a finder fraction of ¼" x ½" fraction was also retained to evaluate the influence of ragging size on jig performance.

Ina addition to the felspar, a second option for ragging was spherical ceramic media. This media was procured from a standard dealer with nominal size options being 2 mm and 6 mm. Each size was evaluated independently, and trials were not conducted using blended ragging.

5.3.3. Procedures

Testing of the jig was conducted by isolating the front end of the process. The pilot plant would operate as normal up through the Morganizer stage with the solvent recovery half of the plant idled. The typical trial started with feed slurry pumped in from the feed sump and processed through the agglomeration system. For all jig trials, the agglomeration step was operated with three minutes of retention time, one minute in the high shear tank and two minutes in the low shear tank. Retention time calculations were identical for the agglomeration step as in the column. The below formula shows how the retention time was derived. Agitation settings in the tanks were kept the same as prior testing with the oscillating column, the high shear tank was set at 0.50 KW and the low shear was set at 0.045 kW. The same sieve screen from the column trials was also used. Following agglomeration and screening, the well-formed agglomerates were pumped directly to the jig Morganizer. Throughout the tests, the water-solvent interface was controlled via PLC, and manual observation was used to ascertain overall operability. After reaching steady state (at least 3 jig retention times), feed, tailings, underflow, and overflow samples were collected and retained. Samples were analyzed for moisture using an A&D MF-50 moisture balance and for ash content using a Leco TGA 701. Final results showed product ash, product moisture, and jig overflow percent solids.

Equation 5-1

$$t\ (\text{min}) = \frac{TLV\ (gal)}{Flow\ Rate\ (gpm)}$$

TLV = Total Liquid Volume for the vessel at the outlet.

For an 8-inch diameter tank with a cone bottom with discharge port 10 inches from bottom of cylinder portion of tank:

Equation 5-2

$$TLV\ (gal) = Cylinder\ Volume\ (gal) + Cone\ Volume(gal)$$

$$TLV\ (gal) = \Pi * r^2 * h * 7.48\ \left(\frac{gal}{ft^3}\right) + \Pi *\ r^2 * \frac{h}{3} * 7.48\ (gal/ft^3)$$

$$TLV\ (gal) = 2.21$$

Substituting Equation 5-2 into Equation 5-1:

$$t\ (\text{min}) = \frac{2.21\ (gal)}{2\ (gpm)}$$

$$t\ (\text{min}) = 1.10$$

5.4. Results and Discussion

5.4.1. Laboratory Jig Results

A Selection of results from laboratory testing are shown below. Product moistures were extremely low for a majority of these tests which showed that the jig Morganizer could effectively dewater and disperse coal agglomerates. Product ash content was under 10% but higher than the upper limit of the super-clean specs being tested for carbon recovery. These results showed that the new type of Morganizer had potential to perform at least as well as the oscillating column which prompted further investigation of a larger scale unit. Table 19shows data for the laboratory jig Morganizer.

Table 19. Laboratory HHS jig Morganizer results.

Feed Ash (%)	Product Ash (%)	Product Moisture (%)	Tails Ash (%)	Yield to Concentrate (%)	Combustible Recover (%)
54.9	10.26	1.17	90.27	44.21	87.96
54.90	7.53	1.38	91.34	43.48	89.15
54.90	6.86	0.86	91	42.90	88.61
54.9	7.18	2.45	91	43.07	88.64
54.90	6.88	1.05	89.94	42.19	87.10
13.63	6.88	1.05	85.1	91.37	98.51
54.9	6.55	1.50	85.77	38.97	80.74
16.35	3.84	4.77	87.49	85.04	97.76

54.9	6.88	1.05	85.1	41.96	86.63

5.4.2. Evaluation of Ragging

Initial trials of the jig began with operating first with water to ensure the mechanism was working properly and that the feed and overflow ports functioned as designed. Ragging used in first round of testing was the smaller ¼" x ½" size class. A layer of approximately four inches was added to the jig. The laboratory jig was using a ratio of jig diameter to ragging height of 1:1. Using the same 1:1 relationship was how the original estimate to use four inches of ragging in the four-inch diameter jig was determined.

After confirmation, iso-hexane was added to simulate feed coming from the agglomeration portion of the process. For the beginning trials the pulse was set to be around 250-300 pulses per minute with a stroke length between 1/8" and ¼" which mimicked lab tests. Observations of these tests showed water becoming trapped on the top of the ragging layer. Analyzing the ragging layer revealed that the layer would shrink in thickness and compact over a short period of operating the pulsing mechanism. The pieces of ragging due to how the rock fractures tended to be elongated and flat on two sides. These elongated pieces would work sideways while in motion and eventually begin to lay flat on top of one another. As the entire ragging layer followed suit, it created an impermeable layer which prevented solvent from flowing up and through as well as water from dropping down through into the system's tails. Several trials were conducted to repeat confirm the ragging particles were behaving in this manner. The decision was made to move to the larger feldspar pieces with the thought that the larger pieces would not pack as tightly as the smaller pieces and allow pore space between for liquid to flow. However, after a few quick trials it was confirmed that the larger particles behave similarly to the smaller particles and would pack solid and not allow liquids to flow through. The final tests with the feldspar ragging were conducted with the layer reduced from approximately four inches to between one to two inches to see if thickness impacted the compaction. Similar to the previous tests, the thinner layers of feldspar ragging still compacted impeding flow.

Following the testing with feldspar ragging, spherical ceramic media was the next choice to be tested in the jig as ragging material. At the lab two sizes where available for testing; 2mm

and 6mm. The 2mm spheres were chosen for the first trials due to the spheres being the same size as the ones tested in the lab jig. It quickly became apparent that these small spheres suffered the same problem as the feldspar ragging. Despite their spherical shape, the ragging layer packed itself together with little pore space not allowing liquid to flow freely through. The final ragging layer trials were conducted with a one-inch layer of 6 mm ceramic spheres. Despite their larger size and weight over the 2mm spheres they did not compact and remained independent of other particles as the pulsing action continued. The free movement of the spheres allowed the iso-hexane to flow up and overflow from the jig and for water to flow down and out through the tails.

The change from the 2mm spheres to the 6mm spheres did not impact the amount of hydrophilic surface area inside the jig. Below shows the calculation for one inch of ragging's surface area in a six-inch diameter cylinder.

Volume of ragging zone (V_{rz}):

Equation 5-3

$$V(rz) = \pi * r^2 * h$$

$$V(rz) = \pi * 3^2 * 1$$

$$V(rz) = 28.27in\text{^}3$$

Volume of 6mm ragging sphere (V_{s6}):

Equation 5-4

$$V(6) = \frac{4}{3}\pi * r^2$$

$$V(6) = \frac{4}{3}\pi * .24^2$$

$$V(6) = 0.06\ in\text{^}3$$

Volume of 2mm ragging sphere (V_{s2}):

Equation 5-5

$$V(2) = \frac{4}{3}\pi * r^2$$

$$V(2) = \frac{4}{3}\pi * .04^2$$

$$V(2) = 0.0016\ in\text{^}3$$

Number of Spheres in ragging zone (n_s):

Equation 5-6

$$n(s) = V(rz)/V(s)$$

$$n(s6) = V(rz)/V(s6)$$

$$n(s6) = 358$$

$$n(s2) = 12899$$

Ragging surface area (R_{SA}):

Equation 5-7

$$A(R) = n(s) * SA(sphere)$$

$$A(R6) = 358 * 0.0175$$

$$A(R6) = 62.8\ in\text{^}2$$

$$A(R2) = 12899 * .005$$

$$A(R2) = 62.8\ in\text{^}2$$

As the above calculation shows the change from the smaller 2mm ragging sphere size to the larger 6mm size did not affect the total amount of surface area available to collect water separated from the agglomerates.

Figure 5-9 shows both types of ragging installed in the upper portion of the jig Morganizer prior to testing.



Figure 5-9. Images of feldspar ragging (L) and spherical ceramic ragging (R) in the Morganizer.

One important aspect of the ragging is that it separates when in motion to allow agglomerates to enter in the spaces between the media. This ensures that the entire surface area of the spheres is being effectively utilized. To get the media to separate, enough force must be applied to overcome the weight of the particles as well as the drag of them moving through the liquid. To overcome the weight of the particles, the force applied must be equal to or greater to the buoyancy force of the media. The below derivation shows how much force needs to be applied for spherical media in pilot jig.

The buoyancy force of the ragging layer (rl) will be a product of the buoyancy force of an individual ragging sphere and the total number of spheres in the ragging layer.

Equation 5-8

$$F_{rl} = \#_{spheres} * F_{sphere}$$

First to determine the buoyancy force of one sphere where g is the gravitational constant:

Equation 5-9

$$F_{sphere} = \rho_{sphere} * Vol_{sphere} * g$$

$$F_{sphere} = \rho_{sphere} * \frac{4}{3} \Pi r^3 * g$$

The number of spheres is determined by finding the volume of which the spheres will occupy in the jig and multiplying it by a factor (k) used to determine the number of spheres in a given volume.

Equation 5-10

$$\#_{spheres} = k * \frac{Vol_{rl}}{Vol_{sphere}}$$

$$\#_{spheres} = k * \frac{\Pi r^2 * h}{\frac{4}{3}\Pi r^3}$$

$$\#_{spheres} = k * \frac{3r^2 * h}{4r^3}$$

It is important to note that the radii shown in the formula above are not the same. The radius in the numerator is for the jig diameter and the radius in the denominator is for the ragging sphere.

Therefore, the buoyancy force of the ragging layer can be determined by:

Equation 5-11

$$F_{rl} = k\frac{3r^2 * h}{4r^3} * \rho_{sphere} * \frac{4}{3}\Pi r^3 * g$$

$$F_{rl} = \rho_{sphere} * g * k * r^2 * h * \Pi$$

The drag force on an individual piece of ragging caused by the surrounding solvent can be found by:

Equation 5-12

$$F_{drag} = \frac{1}{2} * v * \mu * A$$

Where v is the upward velocity of the particles, μ is the drag coefficient of a sphere, and A is the cross-sectional area of the ragging sphere. The total drag force on the ragging is given by:

Equation 5-13

$$F_{drag\ total} = \#_{spheres} * \frac{1}{2} * v * \mu * \Pi(\frac{d}{2})^2$$

Therefore, the force necessary to lift and separate the ragging material will be the summation of the total drag force and the total buoyancy force of the spheres. Solving this for the media used in the pilot plant gives the necessary force to lift the ragging layer to equal almost 6 Newtons. Therefore, the force needed to be applied by the pulsing mechanism has to be greater than 6 Newtons in order to lift and separate the media spheres.

5.4.3. Shakedown Trials

Using the procedure described above, shakedown trials were conducted using the ceramic ragging material. These first trials with coal were promising as the jig was able to break apart the agglomerates and send the majority of the water out with the tails. However, the product moisture taken from samples in these trials were higher than expected. They ranged from 15% up to almost 50% depending on agglomerate formation. The water present in the samples appeared to be micro sized droplets of free water that were carried up and out with the carbon material. Two theories were developed as to why the water droplets were accompanying the coal in the solvent. First was due to the material used to construct the upper portion of the jig. Clear Plexiglass was used so that visual observation could be made of what was occurring in the ragging layer, incoming feed, interface level, and proper flow direction of liquids. In contrast to the rest of the unit, the plexiglass was not hydrophilic like steel is. Figure 5-10 lists the contact angles water has with different material surfaces. Typically contact angles above 90 degrees, which is where the plastics fall are hydrophobic. Therefore, once the water made it past the ragging layer it had no surface to adhere to and coalesce before dropping back out of the solvent. Second, was due to the overall diameter of the jig. The fluid velocity within the six-inch plexiglass portion was theorized to be too slow to allow the coal particles to move fast enough with the solvent to fully separate from the water. Samples were not analyzed from these initial trials due to the large amounts of visible water in the overflow product. Visual observations estimated that the moisture contents were approximately 50% or above for each sample taken.

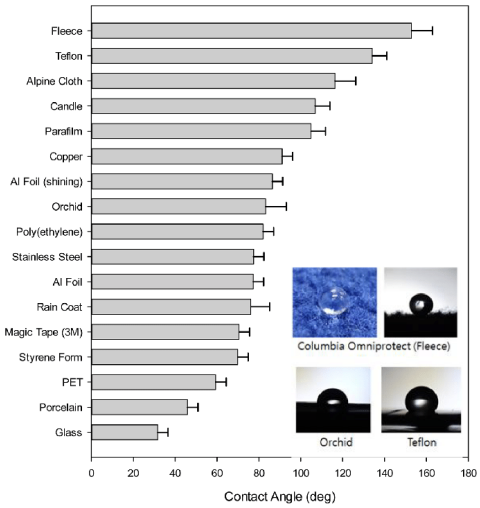


Figure 5-10: Contact angles of various materials with water.

To test these two theories, a modification was designed and fabricated in house that would simultaneously create a hydrophilic surface area for water to coalesce on as well as increase the fluid velocity within the top portion of the jig. The resulting modification consisted of a steel flanged cone reducing from six inches in diameter to four inches in diameter. The smaller diameter of the cone was connected to a length of four-inch thin-walled steel pipe as tall as the plexiglass column used in the previous trial. All of this was made to be inserted into the existing jig to make use of the already fabricated overflow launder. A 3D printed collar was attached to the top of the steel pipe to bridge the gap between the four inch and six-inch pipe. Figure 5-11 below shows the steel insert fabricated and the 3D printed flange.



Figure 5-11. Steel insert and 3D printed flange.

Trials resumed with the modified jig Morganizer utilizing the same ragging size and layer depth as previously tested. Samples taken from the product overflows showed much lower moisture values and were in line with results from the oscillating column Morganizer. Full analysis of the samples was not completed, however the moistures of these overflow products ranged from 4% to 8%. While this modification was proving to be successful at solving the product moisture issue, another issue was brought up by the research team. Since the internal tubing of jig was constructed of steel, visual confirmation of what was occurring within the jig could not be observed. Due to this a request was made for the jig to be remade out of glass. This would allow visual observation of the process as well as providing a hydrophilic surface for water droplets to adhere to.

5.4.4. Glass jig Testing

The glass redesign required the purchase of glass tubing that was not only the correct size but sturdy enough to withstand behind utilized on a pilot plant. Three sections of 4-inch glass tubing were purchased to ensure there was spare material in the event the jig fractured during fabrication or during use. The tubing had a nominal inside diameter of four inches and a wall

thickness of 3/8". The thickness gave the tubing enough cross-sectional area to be able to have feed ports or pipe fittings installed. The new design is shown below in Figure 5-12.

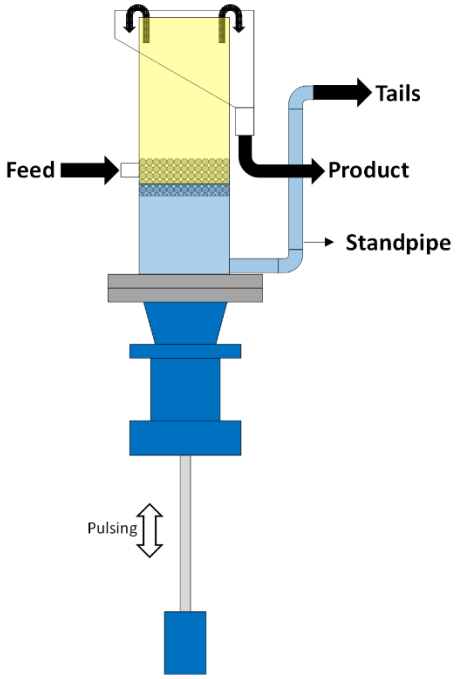


Figure 5-12. Concept design for new jig Morganizer.

The new design for the jig aimed to simplify the unit by reducing the size of the tubing and length of liquid the pulsing unit needed to move. It was observed while operating the previous jig configuration that the up stroke of the pulse was much slower than the down stroke. This was attributed to the weight of the water column that the unit had to push. The six-inch tubing combined with the "U" section meant that there was a significant amount of water inside the lower portion of the jig compared to the amount of solvent in the upper portion. Even after reducing the length of the six-inch pipe on the jig, the amount of water in the "U" section still inhibited the speed of the upward stroke. The new design would need to make the water column as minimal as possible to fully utilize the acceleration of the particles caused by the pulsing.

The 6-inch jig had a tube length of approximately 4 feet. The volume of water in this tube is determined as:

Equation 5-14

$$Vol_{jig} = \Pi * r^2 * h$$

$$Vol_{jig} = \Pi * (\frac{6}{24})^2 * 4$$

$$Vol_{jig} = \Pi * (\frac{3}{12})^2 * 4$$

$$Vol_{jig} = .785\ ft^3$$

Converting to gallons where 1 cubic foot = 7.48 gallons:

$$Vol_{jig} = 5.87\ gallons$$

Therefore, the weight of the water needed to be lifted by the pulsing mechanism is approximately 49.5 pounds.

Whereas the new 4-inch jig had a volume of 0.15 cubic feet and would only require the pulsing mechanism to lift approximately 9.6 pounds of water or around 20% of what the previous jig was requiring of the mechanism.

The final design resulted in the removal of the cone on the piston so the diameter throughout the jig would be consistent at four inches. The piston was then mounted on a plate that would serve as the base for the jig column. This plate was mounted to the top of a new stand which would also support the pneumatic cylinder and control valve. The support plates were then reinforced to resist flexing of the metal during operation. The jig was constructed in three pieces. The bottom two pieces were constructed of machined four-inch pipe pieces. The top consisted of glass tubing glued into a machine four-inch pipe collar. The concept behind using pipe fittings to construct the body of the jig was that it would allow for sturdy connections but at the same time be able to be taken apart for repairs and cleaning. In addition, three different lengths of glass tubing were cut to construct 3 versions of the jig top. The six-inch, nine-inch, and twelve-inch lengths of glass would allow for testing different jig heights by only needing to thread off the top and put a new one on. Only a few initial trials were conducted with the new jig Morganizer. Of those trials only one set of data was collected, and the results are below in Table 20.

Table 20. Results from limited trials with jig Morganizer.

Feed Ash (%)	Product Ash (%)	Product Moisture (%)	Tails Ash (%)	Yield to Concentrate (%)	Combustible Recover (%)
72.7	5.4	10	93.1	23.3	80.6



Figure 5-13. Modified jig pulsing mechanism (L) and new jig launder tops (R).



Figure 5-14. New jig Morganizer post fabrication (L) and jig Morganizer installed on pilot plant (R)

5.4.5. Material Balance for Jig Morganizer

Below in Figure 5-14 is the material balance for the Jig Type Morganizer based on the limited testing completed on the pilot plant. Feed used in the balance calculations was the same as used for the Column Type Morganizer. Coal entering the jig is in lbs(mass)/hour and the total slurry is in gallons per hour (gph).

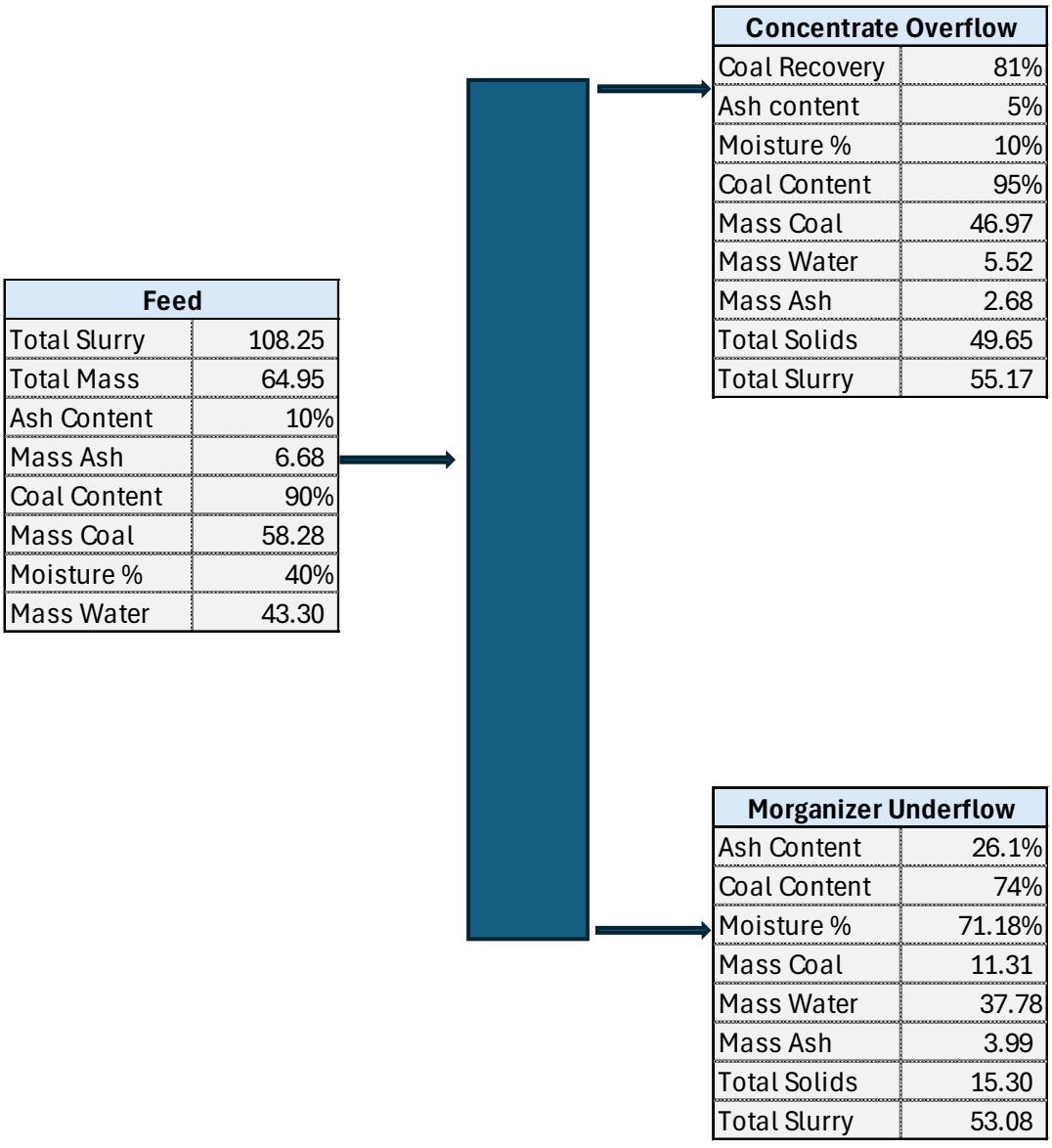


Figure 5-15: Material Balance for Jig Type Morganizer

5.4.6. Future Testing, Scale up, and Design Considerations

Initial testing of the pilot jig Morganizer showed favorable results with respect to product quality, solids loading in the overflow, and overall operability. These results confirm the prior

laboratory tests and suggest a jig type design may be favorable to a column type design. Design recommendations derived from this study include the following:

1. A column type jig, with a larger liquid height, is preferred over a horizontal-type jig. Control of the liquid-solvent interface is critical during operation, and the limitations of most commercial sensors suggest that minimal liquid height of 15 inches is needed to properly control the process.
2. Spherical ragging is recommended over types with flat sides. These flat sides can lead to ragging packing together and preventing liquid flow.
3. The ragging depth in the jig should be kept to a minimum based on the jig's diameter. For the six-inch jig a ragging depth of ¼ to 1/3 of the diameter allowed for enough surface area for dispersing. Ragging depths greater than this tended to be too heavy for the pulsing mechanism to lift properly and restricted the independent movement of the individual pieces.

   Calculating the surface area for the discs in the oscillating column and comparing it to the jig shows how much more surface area the ragging can add in the pilot plant.

Equation 5-15

$$SA_{Osc.Column} = SA_{Disc} * \#_{Discs}$$
$$SA_{Osc.Column} = 4.820in^2 * 36$$
$$SA_{Osc.Column} = 168.71in^2$$

For the jig in the pilot plant:

Equation 5-16

$$SA_{ragging} = SA_{sphere} * \#_{spheres}$$
$$SA_{ragging} = 0.196in^2 * 1280$$
$$SA_{ragging} = 251.2in^2$$

Even though the jig had one inch of ragging material in the four-inch column, it had nearly 1.5 times the surface area than the discs used in the six-foot section of the oscillating column where the discs were located.

4. The pulsing frequency and stroke length were tied together with the pulsing unit tested. As the stroke length grew, the number of strokes the unit was able to produce in a minute decreased. Based on lab results and observations from the limited trials, a

short stroke length of 1/8" to ¼" is preferred with a frequency above 250 strokes per minute.

5. Jig capacity was not fully tested, however initial observations showed that a 4" diameter jig could handle approximately double the solids capacity of the same diameter oscillating column. Since most waste streams would have solids contents equal to or greater than the one tested, it would be recommended to start the pilot plant size jig Morganizer at 4 inches.
6. Recommendations for future tests are shown below.

5.5. Planned future testing.

After initial functional testing, a test procedure was developed to systematically analyze the major parameters of operating the jig. These include the ragging later depth, jig column height, jig stroke frequency, and jig stroke length. The primary result indicator would be the ash content of the carbon product in the overflow as well as the ash content of the mineral matter in the tailings. The sample to be tested was the same low-vol metallurgical decanter effluent used in the used in testing the oscillating column. The goal of using this sample would be to directly compare the two Morganizer types and see which was more effective at producing a low ash coal sample. Additionally, the testing would compare the solids content loading to determine with Morganizer was capable of higher throughput of material.

The first rounds of testing of the jig column would look at the jig stroke frequency and the jig stroke length. Analyzing the data would determine the optimal configuration of stroke frequency and length. After this configuration is determined, it will be set for the next round of testing. Keeping this condition steady, the ragging layer depth and the height of the column would be varied. This portion of testing would determine at all how these two parameters affected the overall performance of the jig.

The data collected would be used to develop a relationship for scaling up the jig for commercial use. Using the scaling up information a unit cost based on size could also be determined. This information would be useful for potential adapters of the technology for investment consideration.

5.6. Jig Scaleup

Although there was limited data gathered from the pilot scale jig testing, a relationship for scaling the jig can be developed. Using a similar starting point to the column Morganizer scaleup, where the expected organic mass flow into the reactor is used to find the necessary hydrophilic surface area. From the required surface area, the diameter and height of the jig can be determined using relationships developed from the pilot testing.

From the column analysis:

Equation 5-17

$$SA_{req.} = MF * k$$

Where MF is the carbon mass flow expected into the reactor and k is the factor determined from testing for the amount of surface area per unit mass of coal per unit of time.

In the case of the jig, the required surface area will primarily be dictated by the hydrophilic media inside the reactor. The media is assumed to be spherical as tested in the lab and on the pilot plant.

Equation 5-18

$$SA_{req.} = \#_{spheres} * SA_{sphere}$$

The number of spheres will be determined by the volume of the reactor that the spheres take up (ragging layer, rl) and the volume of an individual sphere. In the case of the ragging spheres, r = d/2 where d is the diameter of the chosen ragging material.

Equation 5-19

$$Vol_{rl} = \Pi r^2 h$$

$$Vol_{Sphere} = \frac{4}{3}\Pi r^3$$

Utilizing a relationship developed for testing in the pilot plant h = .25 D where D is the diameter of the reactor.

Equation 5-20

$$Vol_{rl} = \Pi(\frac{D}{2})^2 * 0.25D$$

$$Vol_{rl} = \Pi \frac{D^2}{4} * 0.25D$$

$$Vol_{rl} = 0.0625\Pi D^3$$

The volume of the ragging layer is then divided by the volume of an individual ragging sphere.

Equation 5-21

$$\#_{spheres} = \frac{0.0625\Pi D^3}{\frac{4}{3}\Pi(\frac{d}{2})^3}$$

$$\#_{spheres} = \frac{0.1875D^3}{4(\frac{d}{2})^3}$$

Therefore, the required surface area of the ragging will be the product of the number of spheres and the surface area of an individual ragging sphere.

Equation 5-22

$$SA_{req.} = \frac{0.1875D^3}{4(\frac{d}{2})^3} * 4\Pi(\frac{d}{2})^2$$

$$SA_{req.} = \frac{0.1875D^3}{\frac{d}{2}} * \Pi$$

$$SA_{req.} = \frac{0.375\Pi D^3}{d}$$

Substituting Equation 5-22 into Equation 5-17 and solving for the diameter of the reactor gives.

$$SA_{req.} = MF * k$$

Equation 5-23

$$\frac{0.375\Pi D^3}{d} = MF * k$$

$$D = \sqrt{\frac{MF * k * d}{0.375 * \Pi}}$$

Therefore, given the expected mass flow of the carbon to be processed in the reactor and the size of the hydrophilic media to be used for the ragging layer, the appropriate reactor diameter can be determined.

5.7. Summary and Conclusions

Although the jig Morganizer was only able to run a few actual trials, it showed that the concept could work as a viable replacement for the oscillating column Morganizer. The limited data from coal samples produced from the jig were close in line with samples produced on the pilot plant with the oscillating column. If time had allowed further testing with the same source samples used with the oscillating column would have most likely proved it could produce low ash coal products at the same time taking up less physical space and employing a much simpler mechanism.

To fully vet the jig, it would be recommended to follow the above plans for testing to develop the jig and fully understand how the different parameters affect the process. Following these tests trials should resume using a variety of coal sources to ensure the jig Morganizer can handle different feed streams and still produce an on-spec product. Additionally, the jig has the potential to overcome the particle size limit and overall capacity of the oscillating column. Testing is recommended to find the actual limits of the jig's operating capacity as well as how large particles it can process. If the jig can operate at a higher capacity and handle larger particle sizes it will open the process to more source stream possibilities which would make it much more valuable to operators. This coupled with the smaller footprint inside the overall plant would provide for quicker returns on investments for those who adopt the technology.

Chapter 6. Preconcentration of Coal-Based Rare Earth Element Feedstocks using X-Ray Sorter Technology

C.M. Sechrist[1], S. Keles[1], C.A. Noble[1], G.H. Luttrell[1], R.Q. Honaker[2]

1: Department of Mining and Minerals Engineering
Virginia Tech
Blacksburg, VA 24061

2: University of Kentucky
Lexington, KY 40506

This chapter was published as an abstract-reviewed proceedings article in the 2018 International Technical Conference on Clean Energy. Sechrist's primary contributions include the experimental data collection, formal analysis, and manuscript writing.

Citation: Sechrist, Chad M., Serhat Keles, Aaron Noble, Gerald H. Luttrell, Rick Q. Honaker. (2018). "Preconcentration of Coal-Based Rare Earth Element Feedstocks Using X-Ray Sorter Technology," Proceedings, 43rd International Technical Conference on Clean Energy, Sheraton Sand Key, Clearwater, Florida, June 3-8, 2018, 8 pp, Preprint No. 113-2018.

6.1. Abstract

Recent reports by the U.S. Department of Energy indicate that many of the nation's coal seams contain rare earth elements (REEs) that are vital to industries involved in green energy production, high-tech manufacturing, and national security. Unfortunately, the local concentration of these critical elements in the natural environment is typically rare, which makes the development of cost-effective extraction systems very challenging. To address this problem, various low-cost methods have been evaluated for preconcentrating the REEs contained in low-grade resources. One very promising approach involves the use of electronic ore sorting technology to selectively segregate particles enriched in REEs for downstream processing systems. This article reviews the working principles of sorter technology and presents results from recent pilot-scale testing of this low-cost approach for REE preconcentration from coal-based sources.

6.2. Introduction

The U.S. Department of Energy (DOE) identified several rare earth elements (REEs) that are critical to the continued development of new technologies for generating, storing, transmitting, and conserving energy (DOE, 2010). As shown in Table 21, the list of REEs include 15 elements that appear together in the periodic table under the lanthanide series. Scandium and yttrium are also commonly included in this list. The Critical Materials Strategy Report published by DOE cited eight REEs that are particularly important for clean energy technology development (DOE, 2011). Five of these elements, specifically dysprosium, neodymium, terbium, yttrium, and europium, were cited as being highly vulnerable to shortages (Bauer et al., 2012). The identification of suitable replacements for these critical elements has also proven challenging due to their unique magnetic, electrochemical, and luminescent properties (Haque et al., 2014). In 2015, the global production of rare earth oxides was 124,000 tons (USGS, 2016). Domestic sales of REEs represent ~$4 billion in direct annual value and generate an additional ~$7 trillion in value-added goods and services (Kennedy, 2015; Barakos and Gutzmer, 2016). REEs are also critical for national security since they are needed to manufacture high-tech instruments used in the defense industry.

Table 21. List of Rare Earth Elements

	Chemical Element	Chemical Symbol	Atomic Number	Heavy REEs	Light REEs
	Scandium	Sc	21	x	
	Yttrium	Y	39	x	
Lanthanide Elements	Lanthanum	La	57		x
	Cerium	Ce	58		x
	Praseodymium	Pr	59		x
	Neodymium	Nd	60		x
	Promethium	Pm	61		x
	Samarium	Sm	62		x
	Europium	Eu	63		x
	Gadolinium	Gd	64	x	
	Terbium	Tb	65	x	
	Dysprosium	Dy	66	x	
	Holmium	Ho	67	x	
	Erbium	Er	68	x	
	Thulium	Tm	69	x	
	Ytterbium	Yb	70	x	
	Lutetium	Lu	71	x	

A growing number of articles have been published during the past several years suggesting that the nation's coal producers may be able to supply critical materials such as REEs as byproducts from their existing operations. For example, the USGS Coal Quality Database indicates that many U.S. coal seams contain elevated levels of REEs (Ekmann, 2012). According to USGS reports (USGS, 2016), the domestic coal industry has the potential to produce ~40,000 tons per year of rare earth oxides, which is nearly twice the current national consumption. Another study commissioned by the National Energy Technology Laboratory (NETL) suggests that U.S. coal and coal byproducts contain ~11 million metric tonnes of recoverable REEs (Bryan et al., 2015). Many experts believe that the key barrier that has to overcome to realize this potential opportunity is the lack of process technologies capable of converting low-grade (~250-300 ppm) coal-based feedstocks into salable products. In light of this need, researchers at

Virginia Tech and the University of Kentucky have begun to develop a new suite of REE extraction technologies under research programs sponsored by the U.S. Department of Energy. One technology being developed for this purpose is electronic ore sorting. This high-tech process first emerged as a significant player in the mineral processing industry in the late 1980s. The technology is essentially an automated version of the "hand sorting" technique used by early workers in the emerging coal and metals mining industries. This article reviews the working principles of modern sorter technology as applied to the preconcentration of coal-based sources of REEs. Recent test data from laboratory and pilot-scale trials are also presented that illustrate the potential of this approach.

6.2.1. Ore Sorter Technology

Electronic ore sorters were first introduced to the minerals processing industry in the late 1940s (Salter and Wyatt, 1991). Since that time, faster microprocessors, improved sensors, and lower equipment costs have allowed this unique technology to evolve and become commercially attractive for a variety of applications (Sivamohan and Forssberg, 1991). Recent estimates indicate that nearly 300 industrial-scale sorters are now used worldwide for ore concentration (Wills and Finch, 2015). As shown in Figure 6-1, electronic sorters utilize specially designed sensors, such as x-ray analyzers, to interrogate the quality of feed particles that are spread across a moving conveyor belt. High-speed microprocessors use sensor data to control pneumatic actuators located at the end of the conveyor. The pneumatic actuators are sequenced so that particles meeting the target quality are diverted into the product stream while non-specification particles pass along a normal trajectory. This system offers many benefits for coarse particle upgrading including mechanical simplicity, high capacity, low cost, and minimal environmental impacts (Wyman, 1985). Several commercial systems have been recently developed for specific applications in upgrading coal feedstocks (Honaker et al., 2006; Ketelhodt, 2010; Kiser et al., 2013; Ketelhodt and Bergmann, 2010). The compact size and low unit cost of sorter technology also makes this technology a potentially viable approach for separating REE-bearing rock from coal-based resources at remote locations at surface mines, preparation facilities and waste disposal areas.

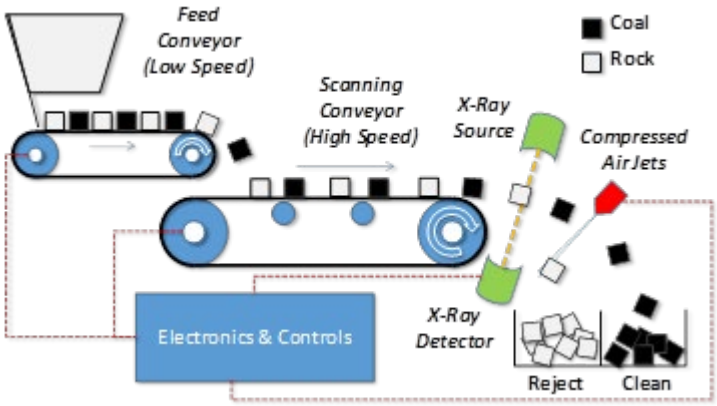


Figure 6-1. Schematic of the X-ray sorting process.

6.3. Experimental

6.3.1. Sample Collection

Two sets of coal-based feedstocks were collected for use in the sorter evaluation program. Both were collected from a major mining complex near Nebo, Kentucky, which mines coal from the West Kentucky No. 13 (Baker) seam. The first sample consisted of an underground channel sample cut by hand from the individual beds of strata within the coal seam. This procedure resulted in the collection of 35 individual layers of strata along the vertical seam height. The second sample collected for this study was obtained from the preparation plant refuse belt using an automated sweep sampler. The sample, which consisted of coarse (>1 mm) refuse solids rejected by the plant, contained ~280 ppm of total REEs. The coarse sample was screened to produce a plus 12 mm (1/2 inch) sample, which is an ideal feedstock for the x-ray sorting process evaluated in this study.

6.3.2. Channel Sample Evaluation

Several series of laboratory tests were conducted to visually assess the potential of x-ray analysis for distinguishing different beds within the coal seam. This assessment was conducted using a Smiths-Heimann 6040i X-Ray Inspection Scanner Figure 6-2, which is functions in a similar manner as an airport luggage scanner. During testing, samples to be interrogated were placed in a flat sample container and passed between an x-ray source and detector. The resultant scan provides an output image that is color-coded based on the amount of x-rays absorbed by the particles. The absorption is a function of elemental composition of the material. High atomic number materials absorb more (transmit less) x-rays, while low atomic number materials absorb

less (transit more). Because of this phenomenon, mineral matter impurities present in coal tend to absorb more x-rays since this class of material is richer in high atomic numbers like Al and Si than organic carbonaceous matter. One complication is that particle thickness can also impact x-ray transmission through a solid. This problem can be overcome by scanning with two wavelengths of x-rays, which provides data that can be deconstructed to reflect only the atomic numbers of the contained materials.



Figure 6-2. X-ray baggage scanner (L) and Pilot-scale DriJet^{tm} x-ray sorter system.

6.3.3. Coarse Refuse Preconcentration

The final series of tests performed as part of this study involved the actual separation of REE-bearing feedstocks using a pilot-scale sorter. A photograph of the x-ray sorter used in this work is shown in Figure 6-2. The pilot-scale unit was used to segregate coarse refuse material currently discarded at the mine site into fractions of higher and lower atomic number. The dual-scan x-ray sorter was supplied by Mineral Separation Technologies (MST), which commercially markets this technology to the coal industry under the tradename DriJet™ (Kiser et al., 2013). This particular unit interrogates airborne particles tossed from a high-speed conveyor and categorizes each object according to a composite atomic number. Based on this data, an integrated high-speed microprocessor actuates a horizontal array of pneumatic compressed air jets that selectively divert target particles into an “ejected” stream while allowing others to flow freely along a normal trajectory into a “passed” stream. Due to equipment constraints associated with the pilot-scale machine, the feed sample used in this part of the test program was sized into a 50 x 12 mm (2x1/2 inch) fraction prior to testing.

6.3.4. Sample Analysis

All of the samples generated in this study were analyzed for dry ash content using ASTM D3174-12. The ash residue was then acid digested and spectroscopically analyzed via ICP-MS according to protocols specified in ASTM D6357. The elements analyzed in this work have been listed previously in Table 1.

6.4. Results and Discussion

6.4.1. Channel Sample Results

Table 22 provides a listing of stratigraphic data obtained for the channel sample of the West Kentucky No. 13 seam. The seam, which was ~9.7 ft in total thickness, was subdivided by a qualified geologist into 35 distinct beds of strata (B1-B35). For ease of reference, the rows for coal strata (<45% ash) are colored in black shading, while rock strata (>75% ash) are colored in gray shading. The rock layers were found for the roof (B1-B2), floor (B34-B35) and five inter-seam partings (B6, B8, B15-B16, B32). All of these rock strata were identified as claystone lithology. Two of partings (B24, B27) were designated as coal (<45% ash), although the geologist identified the strata as beds containing significant mineralization (i.e., B24 contained mixed fusinite/pyrite and B27 containing mixed claystone/fusinite). Approximately 68% of the dry solid mass within the stratigraphic column was coal, while the remaining 32% was rock. The 26 layers of coal strata had ash contents that ranged from 4.42% to 44.07% ash. The combined ash content of these layers was calculated to be 14.74%. The 9 layers of rock strata, which had a combined dry ash content of 88.34%, all had ash values of 79% ash or higher.

Table 22. Stratigraphic data for the West Kentucky channel/core sample.

ID	Strata	Thick (ft)	Mass (%)	Ash (%)	TREE (ppm_a)	LREE (ppm_a)	HREE (ppm_a)	TREE (ppm_w)	LREE (ppm_w)	HREE (ppm_w)	HREE/ LREE
B1	Roof	0	4.6	92.12	259.5	218.2	41.3	239.1	201	38.1	0.19
B2	Roof	0.31	4.3	92.37	277.6	237.1	40.5	256.5	219	37.4	0.17
B3	Coal	0.6	2.4	9.47	457.5	270.4	187.1	43.3	25.6	17.7	0.69
B4	Coal	0.87	2.6	11.1	236	191.3	44.7	26.2	21.2	5	0.23
B5	Coal	1.17	2.7	21.29	179.7	140.4	39.3	38.3	29.9	8.4	0.28
B6	Parting	1.45	1.4	82.13	212.1	173.8	38.4	174.2	142.7	31.5	0.22
B7	Coal	1.55	0.8	22.24	390.4	341.6	48.7	86.8	76	10.8	0.14
B8	Parting	1.63	0.8	81.2	1143.9	988.8	155.2	928.9	802.9	126	0.16
B9	Coal	1.69	2.9	4.42	626.9	511.3	115.7	27.7	22.6	5.1	0.23
B10	Coal	2.04	2.1	6.52	179.8	141.6	38.2	11.7	9.2	2.5	0.27
B11	Coal	2.29	2.2	12.94	261.8	215.5	46.4	33.9	27.9	6	0.22
B12	Coal	2.54	3.9	8.78	231.1	155.7	75.4	20.3	13.7	6.6	0.48
B13	Coal	2.99	3.4	21.09	281	124.8	156.2	59.3	26.3	32.9	1.25
B14	Coal	3.35	2.1	23.59	222.9	146.3	76.6	52.6	34.5	18.1	0.52
B15	Parting	3.57	7.3	88.81	362.7	317.5	45.2	322.1	282	40.1	0.14
B16	Parting	4.07	5.8	87.38	456.2	394.7	61.5	398.6	344.9	53.8	0.16
B17	Coal	4.47	2.5	6.22	404.8	299.4	105.4	25.2	18.6	6.6	0.35
B18	Coal	4.77	2.5	9.17	295.9	244.5	51.4	27.1	22.4	4.7	0.21
B19	Coal	5.06	2.8	10.63	276.8	233.7	43.1	29.4	24.8	4.6	0.18
B20	Coal	5.38	2.6	8.12	213.7	172.9	40.9	17.4	14	3.3	0.24
B21	Coal	5.68	2.8	5.9	237.2	181.1	56.1	14	10.7	3.3	0.31
B22	Coal	6.01	2.2	6.27	283.2	212.3	70.9	17.8	13.3	4.4	0.33
B23	Coal	6.27	3.5	6.25	308.5	218.6	89.9	19.3	13.7	5.6	0.41
B24	Parting	6.68	4.6	44.07	190	166.1	23.9	83.8	73.2	10.5	0.14
B25	Coal	7.09	2.7	27.73	379.5	314.4	65.1	105.2	87.2	18.1	0.21
B26	Coal	7.36	2.9	9.89	348	278.8	69.2	34.4	27.6	6.8	0.25
B27	Parting	7.69	0.9	24.8	287	239.8	47.1	71.2	59.5	11.7	0.2
B28	Coal	7.78	3	8.99	275.7	224	51.7	24.8	20.1	4.6	0.23
B29	Coal	8.13	3.3	11.1	268.3	221.8	46.4	29.8	24.6	5.2	0.21
B30	Coal	8.5	2.2	23.17	486.3	364.1	122.2	112.7	84.4	28.3	0.34
B31	Coal	8.73	3.3	19.21	340.6	277.6	62.9	65.4	53.3	12.1	0.23
B32	Parting	9.08	1	79.21	334.5	287.5	47.1	265	227.7	37.3	0.16
B33	Coal	9.15	0.5	14.39	271.2	218.1	53.1	39	31.4	7.6	0.24
B34	Floor	9.21	4.3	85.87	389.8	286.2	103.6	334.7	245.8	89	0.36
B35	Floor	9.51	2.9	88.93	161.2	135.9	25.2	143.3	120.9	22.4	0.19
	Total Bed	--	100	38.56	332.1	274.4	57.7	128.1	105.8	22.2	0.21
	Coal Only*		67.6	14.74	282.9	217.5	65.4	57.5	45.2	12.3	0.27
	Rock Only*		32.4	88.34	349.2	294.2	55	308.5	259.9	48.6	0.19

**Coal Only = Strata<45% Ash; Rock Only = Strata>75% Ash Subscript Notation: a=ash basis; w=whole basis*

Table 22 also summarizes the total rare earth element (TREE) concentrations, including yttrium and scandium, contained in the various layers of strata. The total bed contained a

relatively low value of 128 ppm_w (332 ppm_a) of TREEs. However, most of the REE enrichment occurred in beds designated as rock (>75% ash), which collectively contained 349 ppm_w (309 ppm_a) of TREEs, 260 ppm_w (294 ppm_a) of LREEs, and 49 ppm_w (55 ppm_a) of HREEs. This data suggests that the TREE concentration could theoretically be increased from 128 to 309 ppm_w by separating the coal and rock fractions contained in this seam. In fact, the TREE concentration tended to track relatively well with ash content, as shown in Figure 6-3. This trend suggests that the REE enrichment for this particular channel sample is largely due to inorganic mineralization and that organic matter is a diluent to the REE content. Figure 6-3 also shows that the parting designated as B8 is particularly enriched, with nearly 929 ppm_w (1144 ppm_a) of TREEs. As such, the TREE content of a sorted product from this feedstock has the potential to be nearly tripled (from 309 to 929 ppm_w) by selectively segregating the B8 strata of "claystone parting" from other beds of rock contained within this seam.

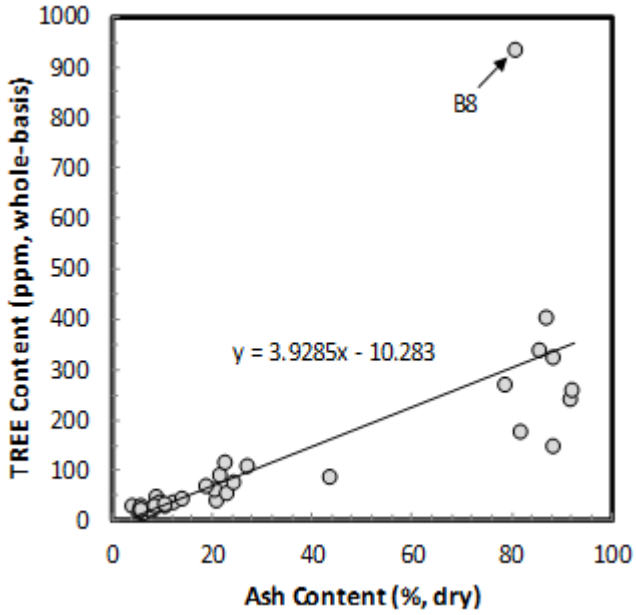


Figure 6-3. Correlation between ash content and TREE concentration for different layers of coal seam strata from a channel sample.

To further investigate the potential segregation of the various beds by x-ray sorting, powdered samples from each of the 35 stratigraphic layers was subjected to x-ray scans using the x-ray inspection scanner described above. Figure 6-4 shows the raw images obtained from this

procedure. As expected, the x-ray color-coding shows that the seam was comprised of many different layers of materials enriched in either carbonaceous matter (brown) or rock (green/blue).

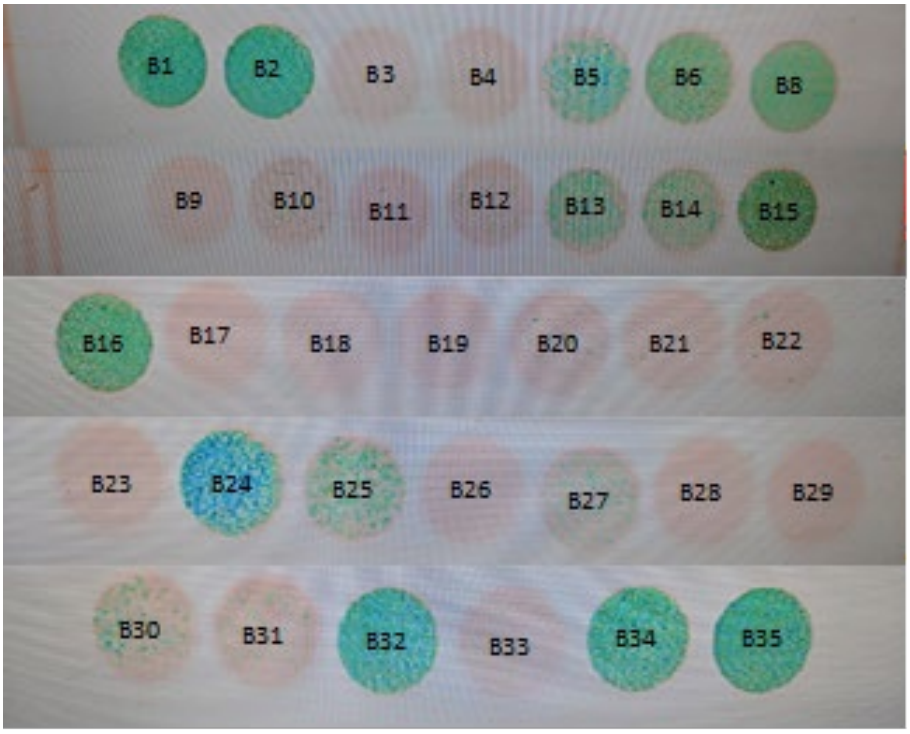


Figure 6-4. Images from an x-ray inspection scanner of powdered samples from different layers of coals seam strata.

For ease of comparison, the color-coding from these scans is replicated in Figure 6-5 along with the ash contents (left) and TREE concentrations (right) for each layer. The illustration shows that a good correlation was observed between layers containing elevated levels of ash and those enriched in REEs. More importantly, the color-coded x-ray scans shown in this illustration demonstrate that layers enriched in REEs can be readily distinguished by x-ray scanning technology.

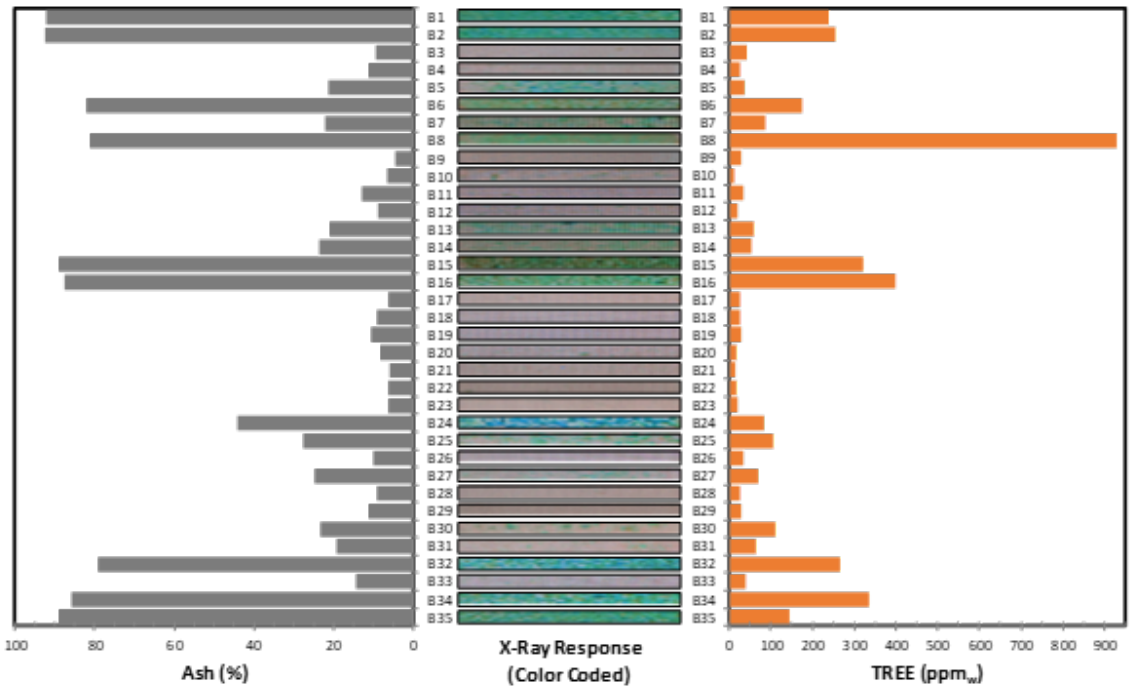


Figure 6-5. Associations of ash content, TREE concentration and x-ray response for different layers of strata from a coal seam channel sample.

6.4.2. Coarse Refuse Results

Based on the promising data obtained using the x-ray inspection scanner, a series of pilot-scale separation tests were conducted to better evaluate the potential of x-ray sorter technology for preconcentration of REEs. The sample of coarse refuse used in these tests was depleted of organic matter by the coal washing processes employed by the preparation plant where the sample was collected. This feed was initially passed through the separator to generate an ejected carbon-rich product (Product A). This non-ejected material was collected and repassed through the sorter at a higher separation set-point to generate a middlings product (Product B) and a final high-ash product (Product C).

Table 23. Pilot-scale sorter test data.

Product	Mass (%)	Ash (%)	TREE (ppm$_w$)	LREE (ppm$_w$)	HREE (ppm$_w$)
A (eject)	17.1	54.5	211.3	159.1	52.2
B (midds)	52.8	75.1	285.4	199	65.8
C (pass)	30.1	78.8	312.4	241.4	71.7
Total	100	72.7	280.8	204.9	65.3

Table 23 shows the results obtained from the preliminary series of pilot-scale sorter tests. The data shows that the first ejected product contained 54.5% ash, which was substantially lower than the 72.7% ash contained in the sized feed. This fraction was also found to contain considerably less REE enrichment in terms of total (211 vs. 281 ppm), light (159 vs. 205 ppm) and heavy (65 vs. 52 ppm) REEs. The most enriched stream was the final pass (non-ejected) product that was obtained after two stages of processing. As shown in Table 3, this stream surpassed the 300-ppm threshold for TREEs, which is often cited in DOE solicitations as the minimum allowable content of REEs for qualified feedstocks in federally funded projects. A comparison of the REE concentrations in the eject (A) and pass (C) products suggest that the sorter technology provided an upgrade ratio of about 1.5 for total REEs (i.e., 312.4/211.3 = 1.48). A slightly higher ratio was observed for the light REEs (241.4/159.1=1.52), and a slightly lower ratio was observed for the heavy REEs (71.7/52.2 = 1.38). Figure 6-6 shows the upgrade ratio for each individual element. The illustration suggests that the upgrade ratio varied considerably from a low of 1.15 for Europium (Eu) to a high of 1.98 for Lutetium (Lu). It should be noted that the high upgrade ratios observed for Sm, Ho and Lu may be unreliable due to the very low concentration of these elements present in the product samples.

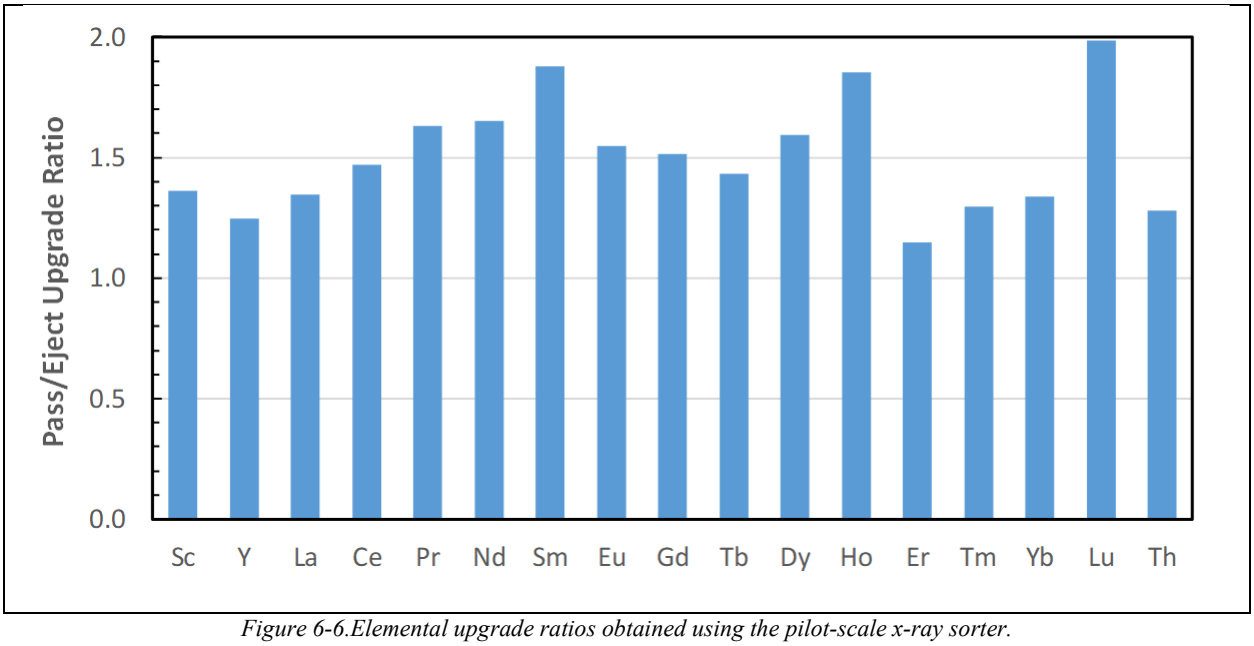


Figure 6-6.Elemental upgrade ratios obtained using the pilot-scale x-ray sorter.

6.5. Summary

Several series of tests were conducted to experimentally evaluate the potential of x-ray sorting technology for preconcentrating coal-based feedstocks containing rare earth elements (REEs). Laboratory data collected using an x-ray inspection scanner showed that this analysis technique can effectively distinguish between layers of strata within a coal seam containing different amounts of ash-bearing mineral matter. The strata containing elevated amounts of ash mineralization were also found to be most enriched in REEs, suggesting that x-ray sorting technology could be used to preconcentrate REE feedstocks for downstream separation processes. In light of this potential, a sample of coarse waste rejected by an industrial coal preparation plant was passed through a pilot-scale x-ray sorter. The experimental data from this test work showed that the feed material could be split into a carbonaceous product depleted with REEs and an inorganic product enriched in REEs. The upgrade ratio (UR), which is defined as the REE concentration in the enriched product divided by that in the depleted product, was approximately 1.5 for total REEs. The upgrade ratio for light REEs was slightly higher (UR=1.52) than that obtained for heavy REEs (UR=1.52). The upgrade ratio for each individual REE ranged from a high of 1.98 to a low of 1.15. Collectively, this data set suggests that x-ray sorting technology can indeed serve as a low-cost method for enhancing the concentration of REEs in coal-based feedstocks. Also, as a dry process, this approach avoids issues related to water usage and waste disposal that typically occur using traditional water-based separation processes. The compact footprint of this process may also allow the technology to be integrated into the flowsheet of existing coal processing facilities with minimal retrofit costs.

Chapter 7. Use of the HHS Process for Preconcentrating Coal-based Resources for Rare Earth Element Extraction

7.1. Introduction:

Need to write at least a paragraph here on the purpose of this work. One of the problems facing Rare Earth Elements (REEs) mining in the US is that there are virtually no concentrated minable sources of REE bearing minerals. However, these minerals have been discovered in low concentrations in waste materials connected to bituminous coal mining in the Appalachian basin. Recognizing this, the Department of Energy (DoE) has sponsored research to find viable methods to preconcentrate these materials prior to processing. The preconcentration would lower the volume of chemicals needed to extract the REEs from the host material and make the process economically feasible.

Two of these preconcentration methods involved using an x-rat sorter on coarse material and the HHS process on fine particles. The information presented below highlights the work looking at preconcentration completed with HHS.

7.2. Materials and Methods

7.2.1. Materials

Detailed testing of the mobile HHS platform was initiated using approximately 2,400 gallons of slurry obtained from the Leatherwood coal preparation plant. The test samples were obtained from the thickener underflow stream produced when the Leatherwood plant was treating primarily run-of-mine coal from the Fireclay seam. Samples were collected on two different occasions. The thickener underflow sample collected during the first sampling campaign contained a very high ash content of approximately 80% ash, while those collected during the second sampling campaign contained only about 66% ash. Five complete sets of test runs were conducted. Test runs 1 through 3 were run with the higher ash (80%) feed and test runs 4 and 5 were run with the lower ash (66%) feed.

7.2.2. Pilot Plant Modification and Operation.

The mobile pilot plant, described in Chapter 2, was used for the decarbonization testing. Additional design modifications and adaptations specific to this work are included herein.

1. Exploratory Testing

After the initial design and construction period, exploratory testing of the mobile HHS rig continued to evaluate potential operational and mechanical challenges. Brief descriptions of these problems and the subsequent corrective actions are given in the following paragraphs.

Large agglomerate formation: In the first step of the HHS process, coal agglomerates are formed by agitating the coal slurry with a hydrocarbon oil in both high-shear and low-shear mixing units. Next, these agglomerates are separated from the slurry that contains mineral matter using mechanical flotation machines. Then, coal agglomerates are sent to a phase inversion tank and subsequently to a Morganizer, where they are dispersed in an oil phase and are separated from any residual water. In most of the initial test runs, this circuit performed well for the first 20-30 minutes of a test run. In this initial period, the feed to the primary flotation machine contained properly formed agglomerates. However, after this initial period, the amount of well-formed agglomerates in the primary flotation machine started decreasing. This reduction in mass in turn affected the performance of the Morganizer, because poorly formed agglomerates would not break up and disperse in the oil phase. As a result, some of the residual water was not efficiently removed in this step. Consequently, the final product contained higher than desired moistures.



Figure 7-1. Large agglomerates

A close inspection of the low shear mixing tank after a poor test run revealed that the tank was full of large agglomerates with sizes up to an inch (Figure 7-1). Ideally, the agglomerate size is desired to be only a few millimeters. These agglomerates were too heavy to float. Thus, many of them sank and were not transferred downstream to the flotation cells. Only the poorly formed agglomerates were able to go to the flotation step. This explained the overall deterioration of the process performance during test runs.

The low shear mixing tank originally did not have any baffles to help with mixing. This design was thought to be the reason for the agglomerates to become so large. Once they formed,

the agglomerates would roll on the sides of the tank and would keep growing almost indefinitely. Based on this theory, four baffles were added to the inside of the tank. Further testing showed that baffles really did not help with decreasing the size of agglomerates. At the end, it was determined that the overall mixing time or retention time in the tank was too long, thus causing agglomerates to grow uncontrollably. Trials performed by bypassing the low shear tank and feeding the primary flotation machine directly from the high shear tank helped in reducing agglomerate sizes. While this approach helped with reducing the size of agglomerates, a low shear tank is still a necessity when processing coals that are more difficult to agglomerate. The current low shear tank has several different discharge ports at different heights for adjusting the retention time. However, even when using the lowest port, the retention time is too high at over six minutes. Whereas, no more than 2-3 minutes of retention time is needed for low shear mixing. As a result, a new low shear tank was designed and ordered to be built by a local fabricator. This new tank will allow for varying retention times between 1 and 3 minutes.

2. *Primary flotation launder plugging:*

In early test runs, the project team experienced difficulty in moving the agglomerates from the overflow of the flotation vessels. Initially, this issue was thought to be mitigated by using a bigger pump and overflowing more water with agglomerates. While this solution helped with the transfer of agglomerates, it did not completely resolve the issue. It was determined that the design of the flotation launder was not favorable for dry agglomerate transfer. The launder (Figure 7-2(a)) was too deep and too steep. Thus, even with the increased amount of water discharge, the agglomerates still stuck to the sides of the launder while letting most of the water pass through them. As a quick solution to this problem, a new bottom plate was added into the launder as shown in Figure 7-2(b). The plate greatly reduced the slope of the launder, which in turn let water carry solids over to the discharge port. Moreover, since more water is normally pushed out of the second cell, the modified launder is sloped from this cell towards the first cell. This way, the dry agglomerates overflowing from the first cell are carried to the discharge port with the help of water overflowing from the second cell. Lastly, a plexiglass window was installed on the launder to easily observe any plugging issues in the launder (Figure 7-2(c)).



Figure 7-2. New flotation launder design

3. Pumping air through the Morganizer

The Morganizer design relies on having consistent upward solvent flow to carry coal particles to an overflow port. The water and tailing particles that are too heavy to travel upwards would sink in the Morganizer and would be discarded as tailings. The upward velocity of the solvent has to be adjusted carefully based on the settling velocity difference between coal particles and water. If the solvent velocity is too high, then water would start traveling upwards instead of downwards. As a result, the Morganizer overflow stream would have a more than desired moisture content.

The diaphragm pump installed on the primary flotation launder is operated continually to keep the launder empty of any material. This action is done due to the tendency of agglomerates floating on water. On several occasions, it was observed that when any liquid level is kept in the launder, agglomerates would float and build up while all the new liquid overflowing from the flotation cell would go through these agglomerates and would be pumped away. Over time, the launder would become plugged up with solids. The one problem with running the launder pump in a continuous manner is that when the launder is empty, rather than liquid and solids would be pumped into the Morganizer. This result effectively decreases the liquid volume in the column, which causes the overall upward solvent velocity to increase. As such, high moisture carryover is observed as explained above.

In order to fix the issue, several different solutions including adding a new deaeration tank, using the phase inversion tank as a deaeration tank, etc. were considered. In the end, a simpler route was chosen; a tee connection was added at an elevated height to the Morganizer feed line. One side of the tee is connected to the common vent system. This configuration allows the tee to be a small deaeration device and to discard all the air pumped from the primary

flotation launder before it reaches the Morganizer. Preliminary tests conducted using just water showed that the tee was very effective with de-aerating the feed to the Morganizer.

4. Vacuum pump oil in the system:

The vacuum pump for the drum filter that was originally installed on the HHS trailer required a type of mineral vacuum oil to operate. Due to how the pump is designed, the vacuum oil was in continuous contact with solvent vapors coming from the drum filter during operation. This configuration caused the oil to be stripped away by the solvent, thus requiring the pump to be filled up with oil at least once during every process run. However, the vacuum oil continued accumulating in the overall HHS system over time. The Morganizer has a structured packing that is hydrophilic and would capture water while in operation. This is where the coal agglomerates are separated from the residual water. However, the vacuum oil accumulated on the packing, as well, and made the packing surface hydrophobic. Therefore, the residual water in the coal agglomerates did not have a chance to coalesce on the packing. This action, in turn, caused product moisture to increase. In order to resolve this issue, a new vacuum pump with a liquid ring seal was ordered and installed on the trailer. Initial tests indicated that this pump performed far better than the original vacuum pump.

7.2.3. Results and Discussion

5. Decarbonization Testing

The results obtained from the detailed tests are summarized in Table 24 The data is also plotted in Figure 7-3 for ease of comparison. The test data indicates that the HHS technology consistently produced a clean coal product with a marketable ash content regardless of which feed was treated by the HHS platform. For the higher ash feed, clean coal products containing 7.5-10% ash were generated in test runs 1 to 3, respectively. Unfortunately, the clean coal yield in the first test was very low (i.e., 0.8%), which resulted in a recovery of combustible matter of only 10.3%. The low yield was attributed to an operating issue that was resolved prior to conducting additional tests with the high ash feed. The two additional tests (runs 2 and 3) performed with the high ash feed achieved exceptional combustible recovery values of 99.9% and 98.8%, respectively, and generated marketable clean coal products containing 8.4% to 10.0% ash. Due to the large amount of ash-bearing material in the feed, the clean coal yields from these two test runs were still relatively low (i.e., 14.7% and 14.8%). As should be expected, the next two tests (runs 4 and 5) that were conducted using the lower ash (67%) feed provided

substantially higher clean coal yields of 27.4% and 29.7% and provided good combustible recoveries of 90-95%. The higher yields obtained in test runs 4 and 5 did not appear to diminish the quality of the clean coal product, which ranged from 7.4% to 9.3% ash when treating the lower ash feedstock. The only performance indicator that did not meet expectations during the detailed testing program was the product moisture content. The test data showed that the mobile HHS platform produced higher than desirable final moisture values ranging from a low of 16.6% in test run 3 to 23.3% moisture in test run 4. The root cause(s) of the higher moisture contents, which appear to be related to issues with agglomerate formation/dispersion, are currently being addressed by the project team.

Table 24. Decarbonization data from five series of detailed HHS test runs.

Test Run	Mass	Ash	Mineral	Moisture	Distribution (%)	
	(%, dry)	(%, dry)	(%, dry)	(%, ar)	Ash	Comb.
Run 1 (Higher Ash Feed)*						
ROM Feed	100	85.8	92.7	-	100	100
Coal Product	0.8	7.5	8.1	24.7	0.1	10.3
REE Product	99.2	86.5	93.4	-	99.9	89.7
Run 2 (Higher Ash Feed)						
ROM Feed	100	80.2	86.6	-	100	100
Coal Product	14.7	8.4	9.1	18.6	1.5	99.9
REE Product	85.3	92.6	100	-	98.5	0.1
Run 3 (Higher Ash Feed)						
ROM Feed	100	80.2	86.6	-	100	100
Coal Product	14.8	10	10.8	16.6	1.9	98.8
REE Product	85.2	92.4	99.8	-	98.1	1.2
Run 4 (Lower Ash Feed)						
ROM Feed	100	66.6	71.9	-	100	100
Coal Product	27.4	7.4	8	23.3	3.1	89.7
REE Product	72.6	88.9	96	-	96.9	10.3
Run 5 (Lower Ash Feed)						
ROM Feed	100	66.6	71.9	-	100	100
Coal Product	29.7	9.3	10	21.6	4.1	95
REE Product	70.3	90.7	98	-	95.9	5

**Note: Process experienced operational issues*

While the focus of the initial work with the HHS test rig was primarily to evaluate the capabilities of this technology for feedstock decarbonization, the data obtained from this portion of the test plan also indicated that the decarbonization step significantly increased the

concentrations of rare earth elements (REEs) in the remaining ash-rich product streams. The separation data for the REEs are summarized in Table 25.

Table 25.REE concentration data from five series of detailed HHS test runs.

Test Run	Mass (%, dry)	Ash (%, dry)	TREE (ppm_a)	TREE (ppm_w)	Distribution TREE
Run 1 (Higher Ash Feed)*					
ROM Feed	100	85.8	379.5	305.7	100
Coal Product	0.8	7.5	1442.4	108.2	2.3
REE Product	99.2	86.5	371.1	320.9	97.7
Run 2 (Higher Ash Feed)					
ROM Feed	100	80.2	376.8	302.2	100
Coal Product	14.7	8.4	1389.8	117	6.1
REE Product	85.3	92.6	359.4	332.7	93.9
Run 3 (Higher Ash Feed)					
ROM Feed	100	80.2	376.8	302.2	100
Coal Product	14.8	10	1220.3	122.5	68.4
REE Product	85.2	92.4	351.9	325.2	91.6
Run 4 (Lower Ash Feed)					
ROM Feed	100	66.6	412.2	274.4	100
Coal Product	27.4	7.4	1488.3	110.7	13.9
REE Product	72.6	88.9	366	325.4	86.1
Run 5 (Lower Ash Feed)					
ROM Feed	100	66.6	412.2	274.4	100
Coal Product	29.7	9.3	1239.6	115.3	13.1
REE Product	70.3	90.7	371	336.6	86.3

Some of the key performance data is also plotted in Figure 7-3 to make it easier to compare each test run. Note that the REE assay values are reported on both an ash-basis parts-per-million (ppm_a) and on a whole-basis parts-per-million (ppm_w). The results show that the overwhelming vast majority of REEs contained in this particular feedstock reported to the ash rich REE product stream and very little reported to the clean coal stream Figure 7-3. For example, test run 2 recovered 93.9% of the REEs in the ash-rich stream, while allowing only 6.1% of the REEs to be lost with the carbon-rich clean coal product. The resulting REE enrichment appears to be largely due to the removal of organic/carbonaceous matter that serves to dilute the REE concentration. This suggestion is supported by the data plotted in Figure 7-4 to Figure 7-6, which shows that the whole-sample REE concentrations are linearly related to the

dry ash contents of the product samples. Since the intercept of this linear plot is non-zero, the ash based REE content increases sharply as the ash content approaches zero.

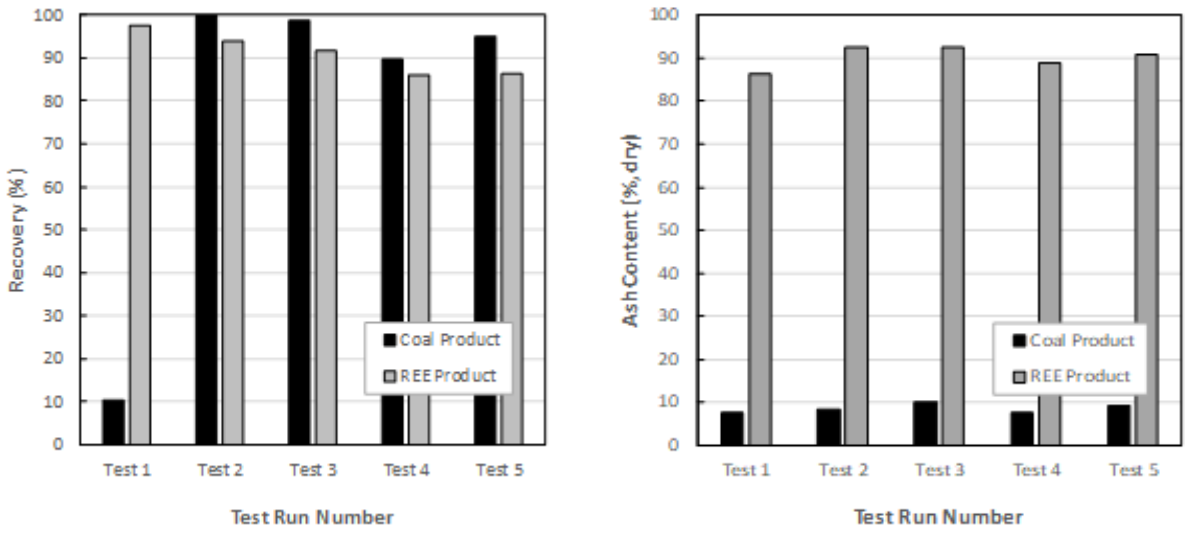


Figure 7-3. Recovery of combustible matter to the clean product and REEs to the REE product (high-ash tails) (L) and Ash contents of the clean product and REE product (high-ash tails) (R)

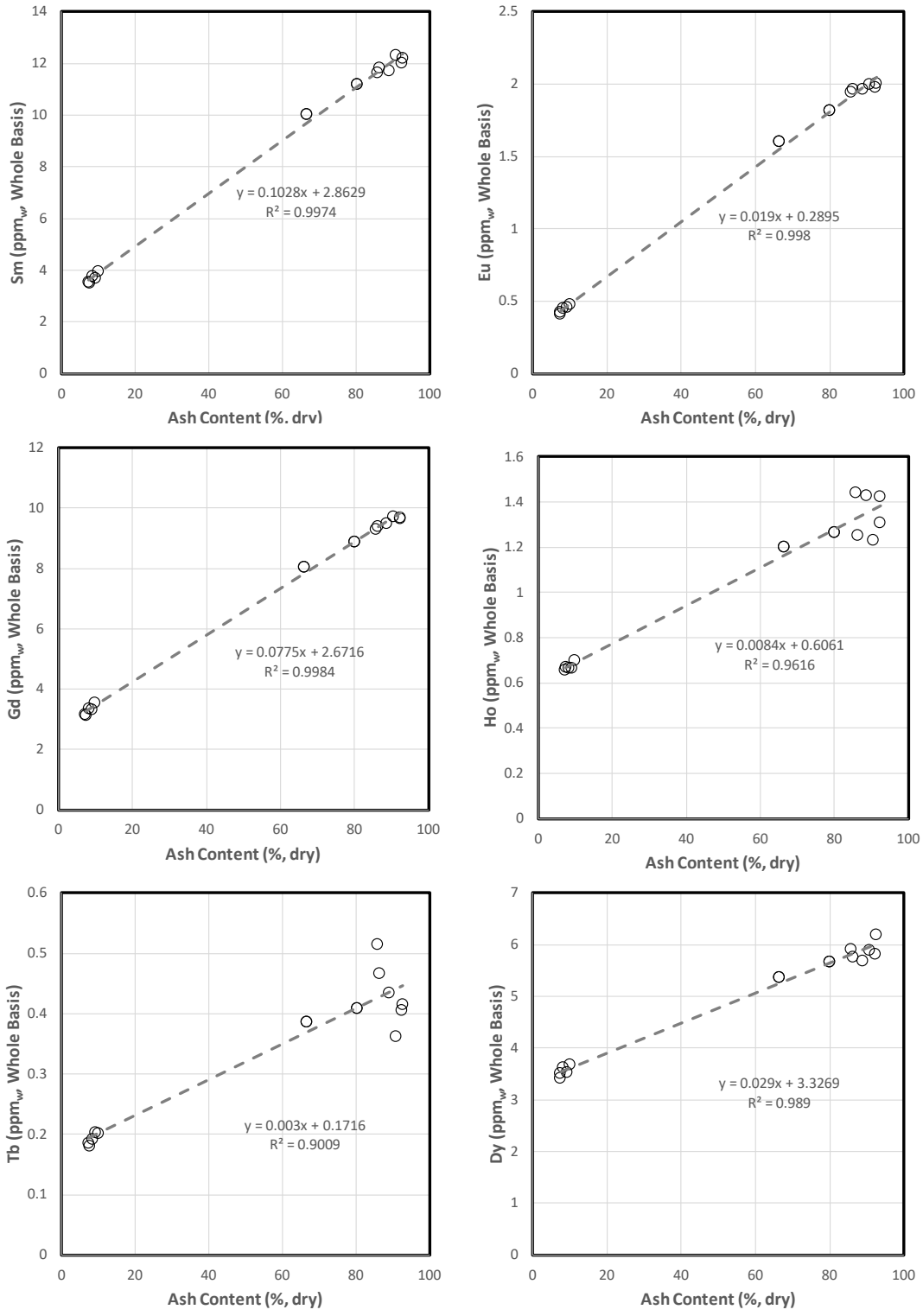


Figure 7-4. Element concentration versus ash content for selected elements.

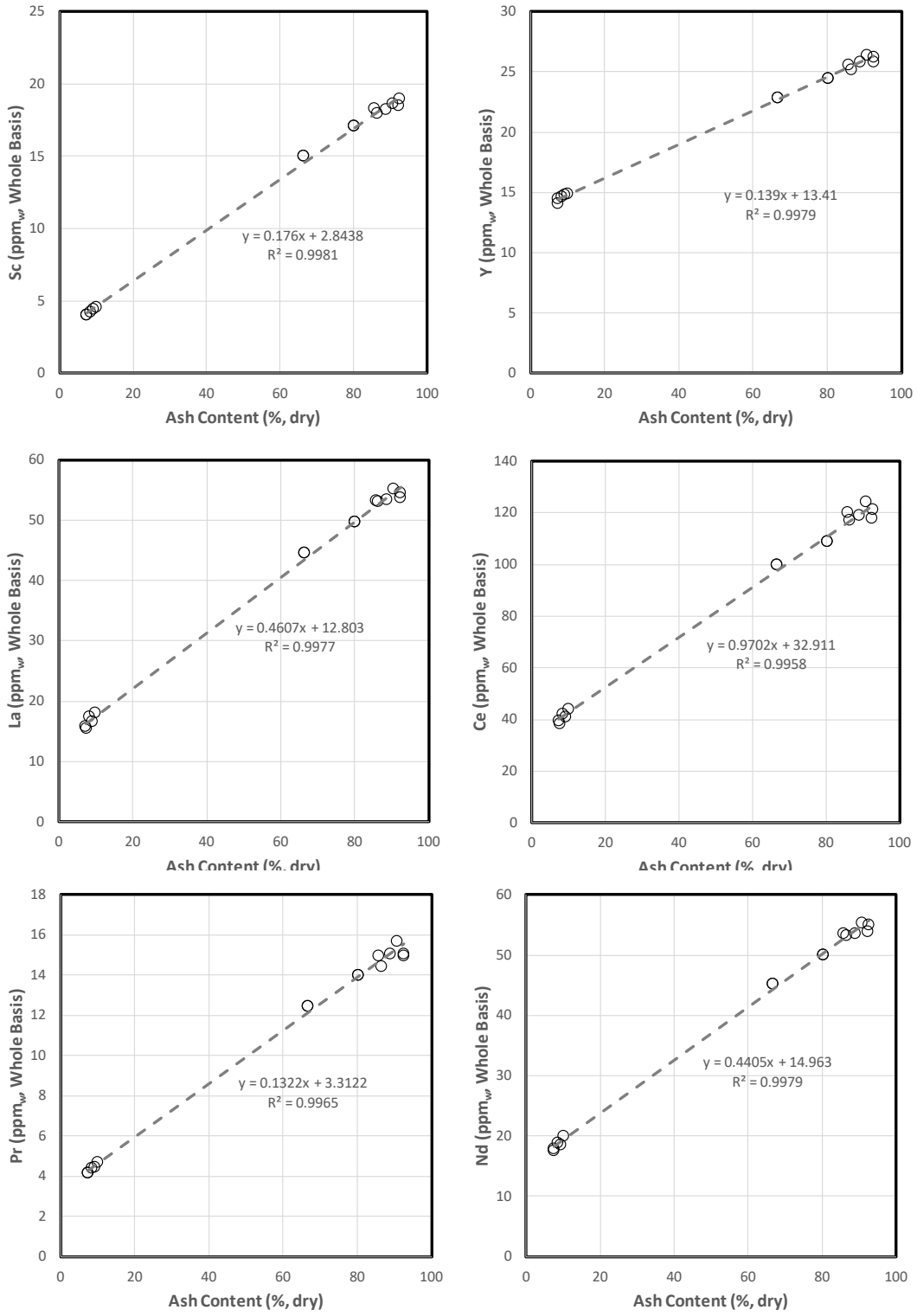


Figure 7-5. Element concentration versus ash content for selected elements.

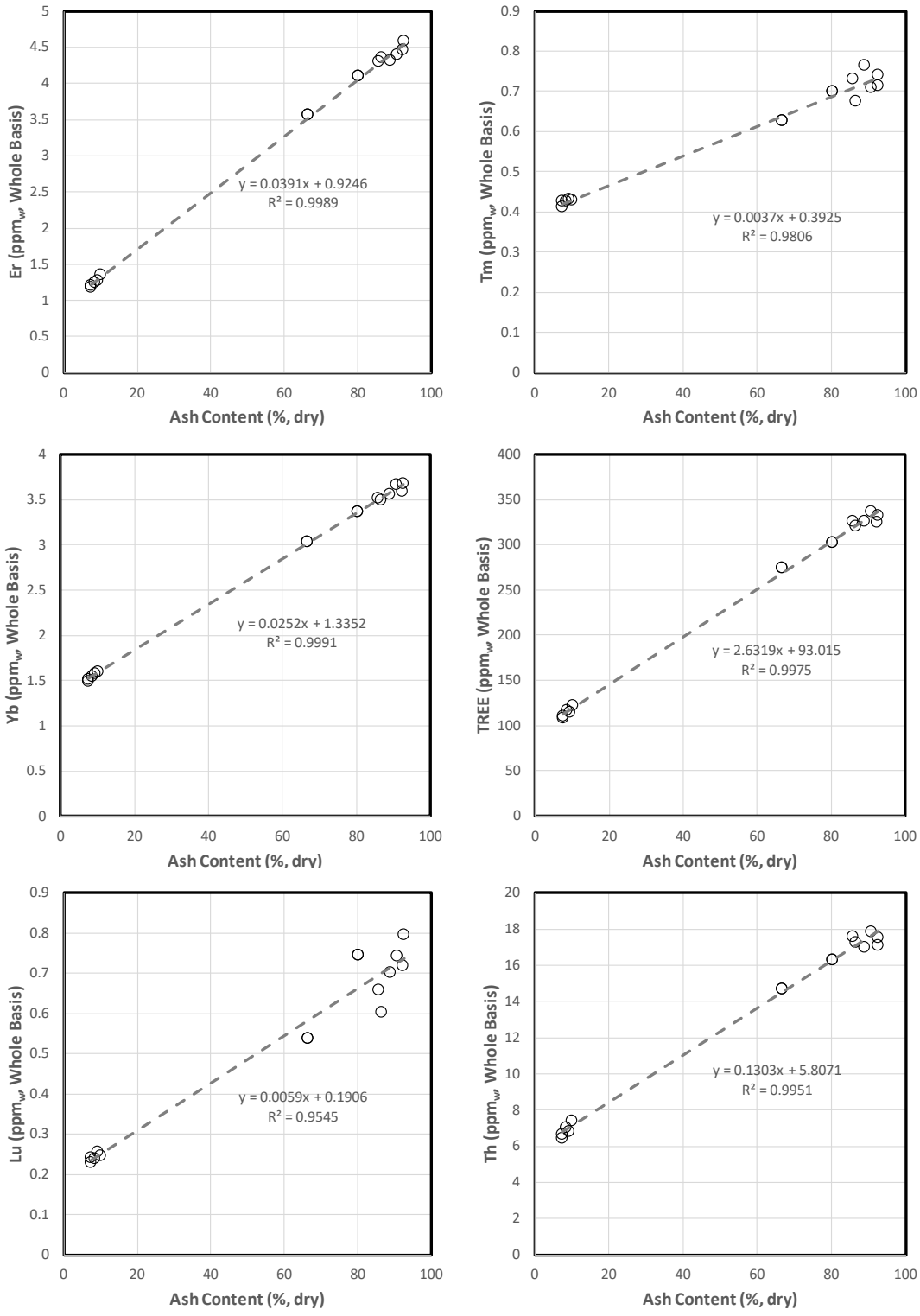


Figure 7-6. Element concentration versus ash content for selected elements.

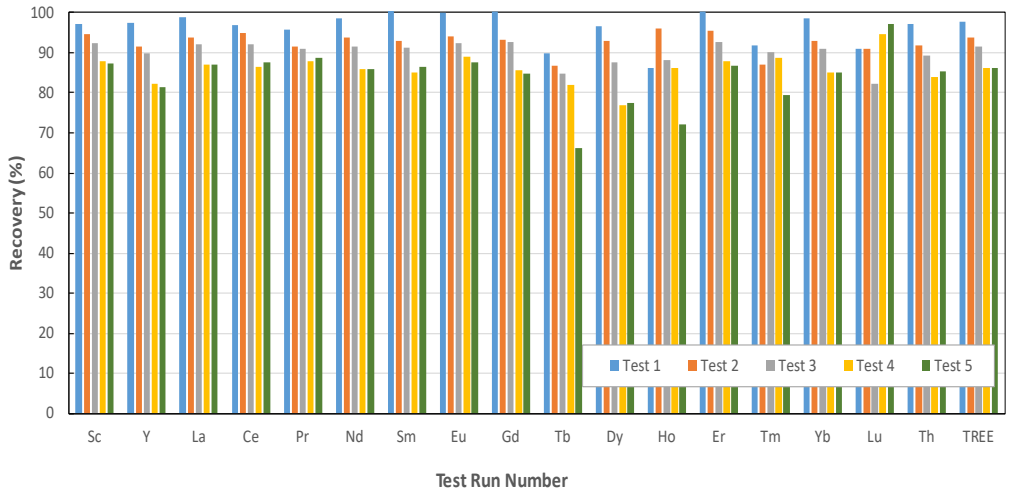


Figure 7-7. Element-by-element recoveries achieved during decarbonization testing.

A final noteworthy observation from the data collected from the detailed testing of the HHS process is that the recoveries of individual REEs to the ash-rich product stream remained very high in all test runs. Element-by-element recoveries, which are plotted in Figure 7-7 for each of the five test runs, show that >85-90% recoveries of REEs were achieved for every element during the decarbonization step. As a result, the total concentration of REEs were all well above 300 ppm_w (whole basis) after HHS processing.

7.2.4. Discussion/Comparisons with X-ray sorting

The X-ray sorter and the HHS pilot plant both proved to be able to preconcentrate REEs from coal waste stocks. The primary difference between the two is that the X-ray sorter was a dry process using compressed air and primarily focused on coarse particles. The HHS pilot plant concentrated on coal waste slurries and targeted coal particles passing a 100-mesh screen or less than 150 microns. Both processes were able to produce a preconcentrated product above 300 ppm which was the lower threshold that the DoE was looking for the source to be considered economically potential. The difference between the processes in achieving this upgrade result was in the process efficiency. To reach a product upgrade over 300 ppm the X-ray sorter needed three passes through the scanner and Drijet with the non-ejected material being the stream sent back through for the subsequent passes. In contrast, the HHS pilot plant was able to reach a 300-ppm target after one pass of the feed sample through the process. Additionally, the HHS process

was able to achieve recoveries of 85 – 90% for each REE in the test spectrum. This is most likely due to the process treating fine particles which means the carbon and mineral particles are highly liberated due to the small size.

7.3. Summary and Conclusions

Preconcentration of REEs using the HHS process has shown very promising results in treating coal waste streams. While other processes are capable of concentrating the elements, they have shortcomings that limit their effectiveness. The X-ray sorter, while able to reach the potential grade threshold, is limited by the feed stocks it can process. It is a dry process so went particles can cause issues by coating the sensor with mud and debris after passing the jets. The wet particles also hold the potential to allow smaller particles to bypass the eject bin by sticking to the surface of larger particles. The main limitation to this process is then the particle size that it can process. The process has a lower size threshold that precludes its use on many circuits.

The HHS process currently has its own size limitation that inhibits what particles it can process. However, with it being a wet process it is able to handle a variety of waste streams within a plant such as thickener underflow, decanter effluent, and flotation tailings. The results from the pilot plant tests mirror tests completed in the laboratory where samples were subjected to the HHS process and achieved very high concentrations of REEs. One thickener underflow sample showed a REE enrichment of over 5,000% (B. Li and Luttrell 2019) with just decarbonization and HHS agglomeration. The decarbonization process is essential as it removes excess carbon before HHS which allows it to be more effective and removing carbon lowers reagent consumption during post processing. This decarbonization can be accomplished by flotation prior to HHS which allows the two steps to be seamlessly integrated into existing plants and allows for preconcentration to be completed in one pass through the units.

Chapter 8. Conclusions and Recommendations

The current technology used in coal cleaning has for many years been effective in producing products that meet the purity and quantity demands from the downstream markets. However, there has been a lower limit to the size of coal particles that modern processing plants can effectively clean. Particles below this limit typically report to waste streams and end up in impoundments causing higher and higher potential for environmental hazards. The past few decades researchers have come up with methods that were successful in cleaning these ultra-fine particles but being able to efficiently scale the methods up to commercial scale has not been met with success. The HHS process was one of the methods developed to recover these fine particles and proved to be very effective at cleaning and dewatering. Further investigation was initiated into further developing the process and scaling up the technology into a commercial scale application.

This document provides a summary of the work completed to adapt HHS to commercial-scale implementations. Laboratory tests were conducted first to provide a base for the coal samples being tested. From there parameters were developed to be able to scale up the test to a pilot scale trial on a newly constructed pilot plant that would implement the latest advancements in HHS and agglomeration. The trials conducted on the pilot plant would cover all aspects of the process but would specifically focus on the agglomeration and dispersion portions. Efficient agglomeration on a larger scale was achieved through the use of high-speed mixing technology. This method was able to produce better results while using the same power consumption as previous methods. The beneficial aspect of this to a commercial design is that the method at which the energy is applied through a mixer to the slurry is easier to scale up than increasingly larger pumps. The Morganizer is a piece of HHS technology previously developed, but during this project it was evaluated on many parameters necessary for scaling. From the results of this research project, a full commercial scale plant was able to be designed and constructed.

This opened the door to the possibility that HHS technology could be further improved upon and pieces such as the Morganizer could evolve. This evolution would mean that the technology could be more easily adapted by a variety of operators. Additionally, the evolved versions of the technology designed in this research would require less space in the process and

be smaller in size with less mechanical parts. This would relate to the cost of adaptation being lowered and the process more attractive to investors.

While the research was successful in generating data that could lead to the commercial scale up of the HHS process, there is still room for improvement. Some of the recommendations based on the information gathered in the research are as follows.

- Test the pilot plant thoroughly with a wide range of coal samples ranging from steam, met, low vol, high vol, anthracite, etc. The process showed in the lab that it could handle a variety of samples and even though multiple sample sources were used in this testing, it does not definitively show that the plant as configured will work with every source.
- Continue development of the column type jig Morganizer. Initial testing with the pilot plant unit showed it could be as capable or better than the oscillating column Morganizer. Further testing to find the optimal operating parameters should be able to confirm its ability to clean and dewater coal using a more mechanically simple process while occupying a smaller space.
- Further investigation of the remaining portions of the process to find where improvements could be made to overall energy use and the footprint of the plant. Being able to reduce the overall size of the plant as well as reducing operational costs would aid in removing additional barriers to adoption of the process.

The author recognizes the following original and distinct contributions that can be attributed to this work.

1. The first pilot plant for the HHS process was built as a continuous process that was capable of producing low ash and low moisture content products from both bituminous and anthracite coal sources.
2. Developed design criteria for agglomeration and column Morganizer that facilitate the ability to scale to a commercial scale and would be implemented in the design of the first commercial HHS plant constructed in the US.
3. Developed a design for a column type jig Morganizer that will be able to replace the oscillating column by producing the same spec products but in a smaller and more economically scalable size. Though more testing is required on this unit, preliminary results indicate promising performance.

4. Presented “Production of High-Value Carbon Products from Waste Coals Using the Hydrophobic-Hydrophilic Separation Process” at 2022 SME Annual Meeting in Salt Lake City, UT.
5. Presented “Production of High-Value Carbon Products from Waste Coals Using the Hydrophobic-Hydrophilic Separation Process” at Metallurgical Coal Producer's Association 13th Annual Professional Engineering Mining Seminar, March 31, 2022, Southwest Virginia Community College in Cedar Bluff, Va.
6. Published and presented “The Hydrophobic-Hydrophilic Separation (HHS) Process for Ultrafine Coal Recovery” at CoalProTec 2022 Conference and Exhibition, April 25-27, Lexington, Kentucky. The article was also published in the Coal Processing Technology journal, published by CPSA.
7. Published “Preconcentration of Coal- Based Rare Earth Element Feedstocks Using X-Ray Sorter Technology” at the Clearwater Clean Energy Conference, June 3-8, 2018, Clearwater, Florida, Paper 113.
8. Additionally, work from this research contributed to the following publications:
    1. Keles S., C. Sechrist, N. Gupta, B. Li, K. Huang, G.H. Luttrell, R-H. Yoon, A. Jones, and J. Reyher. The Hydrophobic-Hydrophilic Separation (HHS) Process for the Recovery and Dewatering of Ultrafine Mineral and Coal Fines. IMPC Eurasia Conference 2019, Antalya, Turkey, November 1, 2019.
    2. Roos C., C. Sechrist, S. Keles, W. Zhang, A. Noble, R. Honaker. The Economic Impact of X-ray Sorting Applications in Coal Production. CoalProTech 2020, Lexington, KY. April 21-22, 2020.
    3. Reyher J., T. Jones, C. Sechrist, S. Keles, N. Gupta, P. Bethell, J. Luttrell, R-H. Yoon. Commercial Application of the Hydrophobic-Hydrophilic Separation (HHS) process for the Recovery of Ultrafine Coal from Thicker Underflows. CoalProTech 2020, Lexington, KY. April 21-22, 2020.
    4. Noble, A., C.M. Sechrist, S. Keles, G.H. Luttrell, and R.Q. Honaker, 2019. Utilization of X-Ray Sorter Technology to Enhance the Economic Viability of Recovering Rare Earth Elements from Coal-Based Feedstocks, 2019 SME Annual Conference and Exhibit, Denver, CO, February 25-27, 2019.

References

Agricola, Georgius, Herbert Hoover, and Lou Hoover. 1912. *De Re Metallica*. London: The Mining Magazine.

Baeyens, J., D. van Gauwbergen, and I. Vinckier. 1995. "Pneumatic Drying: The Use of Large-Scale Experimental Data in a Design Procedure." *Powder Technology* 83(2): 139–48. doi:10.1016/0032-5910(94)02945-K.

Baird, M H I. 1976. *Axial Dispersion in a Reciprocating Plate Extract Ion Column*.

Banerjee, Chandrachur, Vimal Kumar Chandaliya, and Pratik Swarup Dash. 2021. "Recent Advancement in Coal Tar Pitch-Based Carbon Fiber Precursor Development and Fiber Manufacturing Process." *Journal of Analytical and Applied Pyralysis* 158.

Black, Sara. 2017. "Coal as an Avenue to Low-Cost Carbon Fibers." *CompositeWorlds.com*. https://www.compositesworld.com/articles/coal-as-an-avenue-to-low-cost-carbon-fibers (October 12, 2021).

Calvo, Guiomar, Gavin Mudd, Alicia Valero, and Antonio Valero. 2016. "Decreasing Ore Grades in Global Metallic Mining: A Theoretical Issue or a Global Reality?" *Resources* 5(4): 1–14. doi:10.3390/resources5040036.

Chang, M. C. Oliver, Judith C. Chow, John G. Watson, Philip K. Hopke, Seung Muk Yi, and Glenn C. England. 2004. "Measurement of Ultrafine Particle Size Distributions from Coal-, Oil-, and Gas-Fired Stationary Combustion Sources." *Journal of the Air and Waste Management Association* 54(12): 1494–1505. doi:10.1080/10473289.2004.10471010.

Critchley, Liam. 2020. "Using Waste to Cost-Effectively Produce Graphene." *Azo Nano*. https://www.azonano.com/article.aspx?ArticleID=5589 (October 12, 2021).

Daemen, Jaak J K. 2004. *History of Coal Industry*. Reno, Nevada.

Dagle, Robert A., Vanessa Dagle, Mark D. Bearden, Jamelyn D. Holladay, Theodore R. Krause, and Shabbir Ahmed. 2017. "An Overview of Natural Gas Conversion Technologies for Co-Production of Hydrogen and Value-Added Solid Carbon Products." *(No. PNNL-26726; ANL-17/11). Pacific Northwest National Lab. (PNNL), Richland, WA (United States); Argonne National Lab.(ANL), Argonne, IL (United States).*: 65.

Daud, Wan Ramli Wan. 2008. “Fluidized Bed Dryers - Recent Advances.” *Advanced Powder Technology* 19(5): 403–18. doi:10.1163/156855208X336675.

E V Manlapig, C Green, J W Parkinson, and A S Murphy. 2001. “The Technology and Economic Incentives for Recovering Coal from Tailings Impoundments.” *Society of Mining, Metallurgy and Exploration: Littleton, Colorado,*: 26–28.

EIA. 2020. “Coal Prices and Outlook.” *Coal explained*. https://www.eia.gov/energyexplained/coal/prices-and-outlook.php (October 12, 2021).

EIA. 2022. “Electricity Explained - Electricity Generation, Capacity, and Sales in the United States.”

Engineer’s Edge. “Circular Flat Disc Drag Coefficient and Drag Equations”. *Air Flow Drag, Drag Coefficient Equation and Calculators Fluid design and Engineering Data*. https://www.engineersedge.com/fluid_flow/circular_flat_disk_drag_coefficient_14035.htm. 2024.

Falconer, Andrew. 2003. “Gravity Separation: Old Technique/New Methods.” *Physical Separation in Science and Engineering* 12(1): 31–48. doi:10.1080/1478647031000104293.

Freeland, Chad L, Roe-hoan Yoon Co-chair, Gregory T Adel, and Chad L Freeland. 2010. “Low Temperature Drying of Ultrafine Coal.”

Gagarin, H., S. Sridhar, I. Lange, and M. D. Bazilian. 2020. “Considering Non-Power Generation Uses of Coal in the United States.” *Renewable and Sustainable Energy Reviews* 124(May 2019): 109790. doi:10.1016/j.rser.2020.109790.

Geim, A K. 2009. “Graphene : Status and Prospects.” *Science* 324(June): 1530–35.

Glatz, Don, and Brendan Cross. 2020. *DESIGNING LIQUID-LIQUID EXTRACTION COLUMNS*.

Greaves, Joshua, and Sons Ltd. 2023. “What Are High Speed Dispersers?”

Gupta, N., B. Li, G. Luttrell, R. H. Yoon, R. Bratton, and J. Reyher. 2016. “Hydrophobic-Hydrophilic Separation (HHS) Process for the Recovery and Dewatering of Ultrafine Coal.” *2016 SME Annual Conference and Expo: The Future for Mining in a Data-Driven World*: 706–9.

Gupta, Nikhil, Gerald H Luttrell, Roe-hoan Yoon, Gregory T Adel, and Stanley C Suboleski. 2014. “Development of a Novel Fine Coal Development of a Novel Fine Coal.”

Hennis, Mark. 2017. “Industrial Mixers: System Consideration Basics.” *manfacturing.net*. https://www.manufacturing.net/operations/article/13195273/industrial-mixers-system-consideration-basics#:~:text=An impeller to tank diameter,66 or higher. (April 12, 2022).

Honaker, R. Q., R. H. Yoon, and G. H. Luttrell. 2005. “Ultrafine Coal Cleaning Using Selective Hydrophobic Coagulation.” *International Journal of Coal Preparation and Utilization* 25(1): 81–97. doi:10.1080/07349340590927413.

IEA. 2021. “The Role of Critical Minerals in Clean Energy Transitions.”

IEA. 2022. “World Total Coal Production, 1971-2020.” *Coal Information*.

James, Brian. 2012. “Mixing 101: Baffled by Baffles?” *dynamixinc.com*. https://dynamixinc.com/baffled-by-baffles/ (April 12, 2022).

James, Brian. 2015. “Understanding How Tank Design Affect Mixing.” *dynamixinc.com*. https://dynamixinc.com/optimal-tank-design/ (April 12, 2022).

Jones, Alan W, Roe-hoan Yoon, and Aaron Noble. 2019. “Advancement of the Hydrophobic-Hydrophilic Separation Process.”

Karr, A. E. 1980. “Design, Scale-Up, and Applications of the Reciprocating Plate Extraction Column.” *Separation Science and Technology* 15(4): 877–905. doi:10.1080/01496398008076276.

Karr, A. E., W. Gebert, and M. Wang. 1980. “Extraction of Whole Fermentation Broth with Karr Reciprocating Plate Extraction Column.” *The Canadian Journal of Chemical Engineering* 58(2): 249–52. doi:10.1002/cjce.5450580217.

Karr, Andrew E. 1959. *Performance of a Reciprocating-Plate Extraction Column*.

Karthikeyan, Muthusamy, Wu Zhonghua, and Arun S. Mujumdar. 2009. “Low-Rank Coal Drying Technologies - Current Status and New Developments.” *Drying Technology* 27(3): 403–15. doi:10.1080/07373930802683005.

Keboletse, K. P., F. Ntuli, and O. P. Oladijo. 2021. “Influence of Coal Properties on Coal Conversion Processes-Coal Carbonization, Carbon Fiber Production, Gasification and

Liquefaction Technologies: A Review." *International Journal of Coal Science and Technology* 8(5): 817–43. doi:10.1007/s40789-020-00401-5.

Keles, Serhat, Gerald H Luttrell, Roe-Hoan Yoon, Gregory T Adel, and Ricky Q Honaker. 2010. "Fine Coal Dewatering Using Hyperbaric Filter Centrifugation."

Keller, D. V. Jr. 1982. "Otisca T-Process: A New Coal Beneficiation Approach for the Preparation of Coal Slurries." In *9th Annual International Conference on Coal Gasification, Liquefaction, and Conversion to Electricity Proceedings*, ed. K.W. Couch. , 14.

Kolstad, Charles. 2017. "What Is Killing the US Coal Industry?" *Stanford-Institute for Economic Policy Research*.

Lee, Seul Yi, and Roop L. Mahajan. 2021. "A Facile Method for Coal to Graphene Oxide and Its Application to a Biosensor." *Carbon* 181: 408–20. doi:10.1016/j.carbon.2021.05.007.

Lee, Seul-Yi, and Roop Mahajan. 2021. "A Facile Method for Coal to Graphene Oxide and Its Application to a Biosensor." *Carbon* 181: 408–20.

Li, Biao, and Gerald H Luttrell. 2019. "Hydrophobic-Hydrophilic Separation Process for the Recovery of Ultrafine Particles Hydrophobic-Hydrophilic Separation Process for the Recovery of Ultrafine Particles."

Li, Kuo, Susan M. Rimmer, and Qinfu Liu. 2018. "Geochemical and Petrographic Analysis of Graphitized Coals from Central Hunan, China." *International Journal of Coal Geology* 195: 267–79. doi:10.1016/j.coal.2018.06.009.

Liu, Junjun, Rui Li, and Bai Yang. 2020. "Carbon Dots: A New Type of Carbon-Based Nanomaterial with Wide Applications." *ACS Central Science* 6(12): 2179–95. doi:10.1021/acscentsci.0c01306.

Lukianov, E. S., S. Yu Lozovaya, and N. M. Lozovoy. 2018. "Modeling of Thermal Mode of Drying Special Purposes Ceramic Products in Batch Action Chamber Dryers." *IOP Conference Series: Materials Science and Engineering* 327(2). doi:10.1088/1757-899X/327/2/022043.

Mankosa, Michael J., Jaisen N. Kohmuench, Lance Christodoulou, and Gerald H. Luttrell. 2016. "Recovery of Values from a Porphyry Copper Tailings Stream." *IMPC 2016 - 28th International Mineral Processing Congress* 2016-Septe(i).

McSpirit, Stephanie, Shaunna Scott, Duane Gill, Sharon Hardesty, and Dewayne Sims. 2007. "Risk Perceptions After a Coal Waste Impoundment Failure: A Survey Assessment." *Journal of Rural Social Sciences* 22(2): 12–31. https://egrove.olemiss.edu/cgi/viewcontent.cgi?article=1312&context=jrss.

Michaud, David. 2016. "Gold Jig & Mineral Processing Jigs." *Gold Extraction, Gravity Concentration*. https://www.911metallurgist.com/blog/gold-mineral-processing-jigs (April 13, 2023).

Nikolopoulos, Nikolaos, Ioannis Violidakis, Emmanouil Karampinis, Michalis Agraniotis, Christian Bergins, Panagiotis Grammelis, and Emmanouil Kakaras. 2015. "Report on Comparison among Current Industrial Scale Lignite Drying Technologies (A Critical Review of Current Technologies)." *Fuel* 155: 86–114. doi:10.1016/j.fuel.2015.03.065.

Northern Graphite Pricing. 2021. "How Is Graphite Priced?" *Graphite Pricing*. https://www.northerngraphite.com/about-graphite/graphite-pricing/ (October 12, 2021).

Olney, Matt. 2020. "A Brief History of Energy – Coal." *Dyball Associates Limited*.

Osman, H., S. V. Jangam, J. D. Lease, and Arun S. Mujumdar. 2011. "Drying of Low-Rank Coal (LRC)-A Review of Recent Patents and Innovations." *Drying Technology* 29(15): 1763–83. doi:10.1080/07373937.2011.616443.

Othmer, Donald, M.H.I Baird, and Rama Rao. 1991. "The Reciprocating Plate Column - Development and Applications." *Chemical Engineering Communications* 116(1): 67–68.

Phengsaart, Theerayut, Palot Srichonphaisan, Chinawich Kertbundit, Natatsawas Soonthornwiphat, Somthida Sinthugoot, Nutthakarn Phumkokrux, Onchanok Juntarasakul, et al. 2023. "Conventional and Recent Advances in Gravity Separation Technologies for Coal Cleaning: A Systematic and Critical Review." *Heliyon* 9(2). doi:10.1016/j.heliyon.2023.e13083.

Qiao, Rui, Noble, Aaron, Yoon, Roe-hoan. 2021. "UCFER Final Technical Report." 4200(003137015).

Richardson, Gary H, and ; J Derle Thorpe. 1995. “United States Patent (19) Richardson et al. 54). APPARATUS AND METHODS FOR MEASURING MELK COAGULATION TIME AND RIGIDITY IN THE MANUFACTURE OF FERMENTED DARY PRODUCTS.”

Roe-Hoan Yoon; Gerald H. Luttrell. 1995. “METHOD FOR DEWATERING FINE COAL.” : 9.

Rubio, J., and A. M. Marabini. 1987. “Factors Affecting the Selective Flocculation of Hydroxyapatite from Quartz and/or Calcite Mixtures.” *International Journal of Mineral Processing* 20(1–2): 59–71. doi:10.1016/0301-7516(87)90017-2.

Sambaer, Wannes, Martin Zatloukal, and Dusan Kimmer. 2012. “3D Air Filtration Modeling for Nanofiber Based Filters in the Ultrafine Particle Size Range.” *Chemical Engineering Science* 82: 299–311. doi:10.1016/j.ces.2012.07.031.

Shama, Rao, A Simha, T, G, P Rao, K, and V Kumar, Ravi, G, V. 2018. “Carbon Composites Are Becoming Competitive and Cost Effective.” *Infosys Limited*: 1–12. https://www.infosys.com/engineering-services/white-papers/Documents/carbon-composites-cost-effective.pdf.

Smith, Kara E. 2008. “Cleaning and Dewatering Fine Coal Using Hydrophobic Displacement.” *Master Thesis*.

Smith, Kathryn H., Tim Bowser, and Geoffrey W. Stevens. 2008. “Performance and Scale-Up of Karr Reciprocating Plate Extraction Columns.” *Industrial and Engineering Chemistry Research* 47(21): 8368–75. doi:10.1021/ie800581u.

Smith, Sarah Ann. 2012. “Methods of Improving Oil Agglomeration.”

Trahar, W. J., and L. J. Warren. 1976. “The Flotability of Very Fine Particles - A Review.” *International Journal of Mineral Processing* 3(2): 103–31. doi:10.1016/0301-7516(76)90029-6.

Turner, John. 2021. “What Can We Learn from the Role of Coal in the Industrial Revolution?” *Lessons from History*.

Yancey, H F, M R Geer, R E Shinkoskey, and / M R Geer. 1938. *Performance of a Pulsator-Type Coal-Washing Jig*.

Yoon, R. H., and G. H. Luttrell. 1989. “The Effect of Bubble Size on Fine Particle Flotation.” *Mineral Processing and Extractive Metallurgy Review* 5(1–4): 101–22. doi:10.1080/08827508908952646.

Yoon, R. H., G. H. Luttrell, and R. Asmatulu. 2002. “Extending the Upper Particle Size Limit for Coal Flotation.” *Journal of The South African Institute of Mining and Metallurgy* 102(7): 411–15.

Yoon, Roe-Hoan, Nikhil Gupta, Gerald Luttrell, Li Biao, Stanley Suboleski, and Robert C. Bratton. 2016. “HHS Process: A New Approach for Recovering Fine Illinois Basin Coals.” *Proceedings of International Coal Preparation Conference* (April): 25–27.

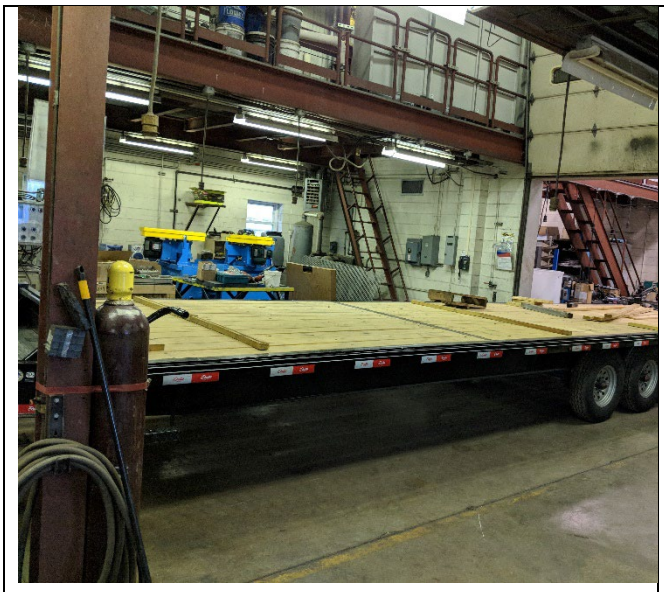
Zhang, Wencai, Mohammad Rezaee, Abhijit Bhagavatula, Yonggai Li, John Groppo, and Rick Honaker. 2015. “A Review of the Occurrence and Promising Recovery Methods of Rare Earth Elements from Coal and Coal By-Products.” *International Journal of Coal Preparation and Utilization* 35(6): 281–94. doi:10.1080/19392699.2015.1033097.

Zhu, Y, C Zhao, Y Xu, C Hu, and X Zhao. 2019. “Preparation and Characterization of Coal Pitch-Based Needle Coke (Part 1): The Effects of Aromatic Index in Refine Coal Pitch.” *Energy and Fuels* 33(4): 3456–64.

Appendix

This Appendix includes various images of the pilot plant through its different stages of construction. Also included are images of the individual process pieces and images of improvements made to specific units.

Trailer purchased for Pilot Plant.	Initial framing of control room.



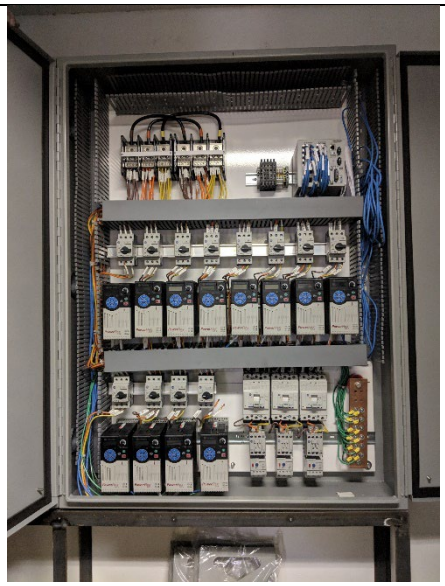
Electronic panels installed in ctrl room.

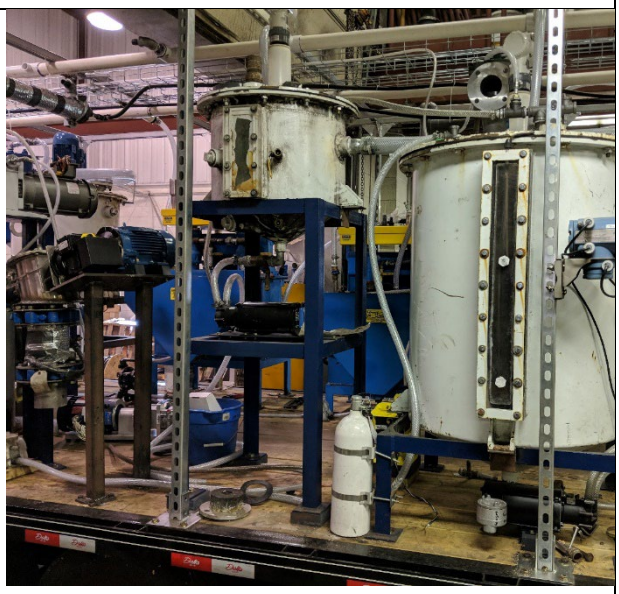
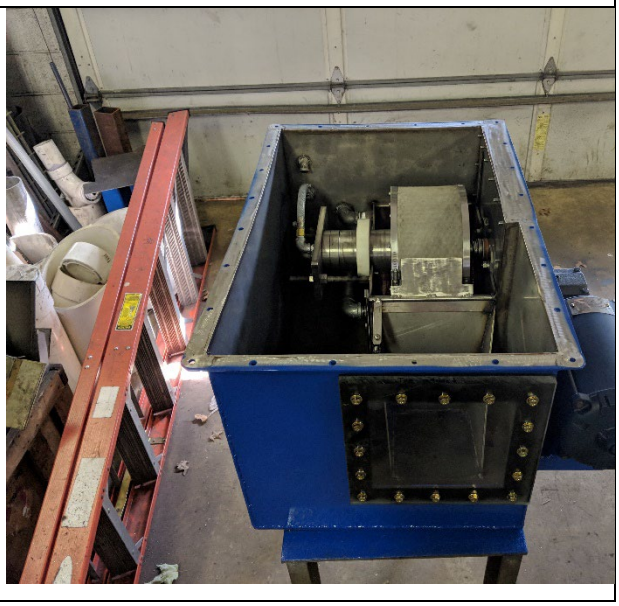


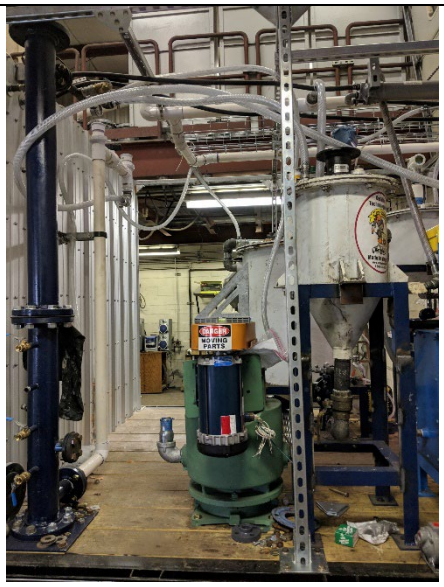
Completed siding on control room.

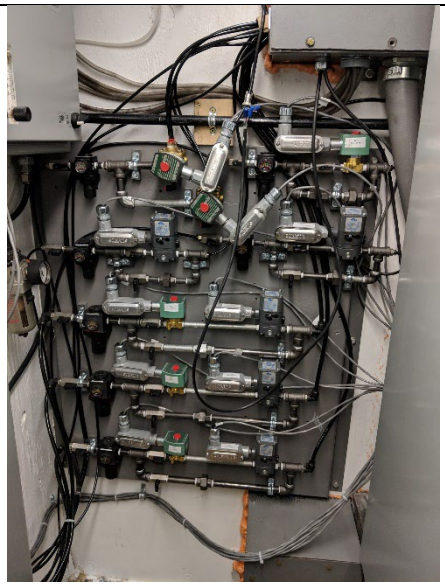


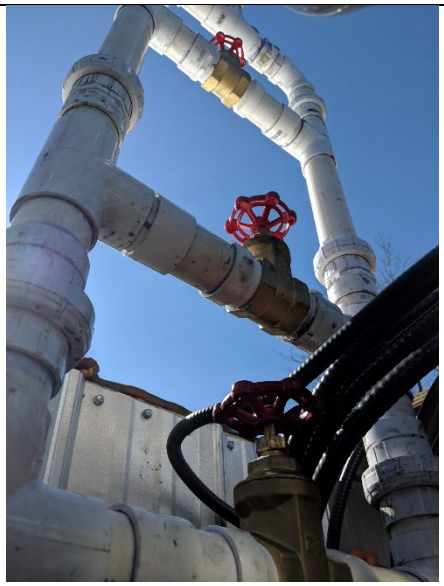


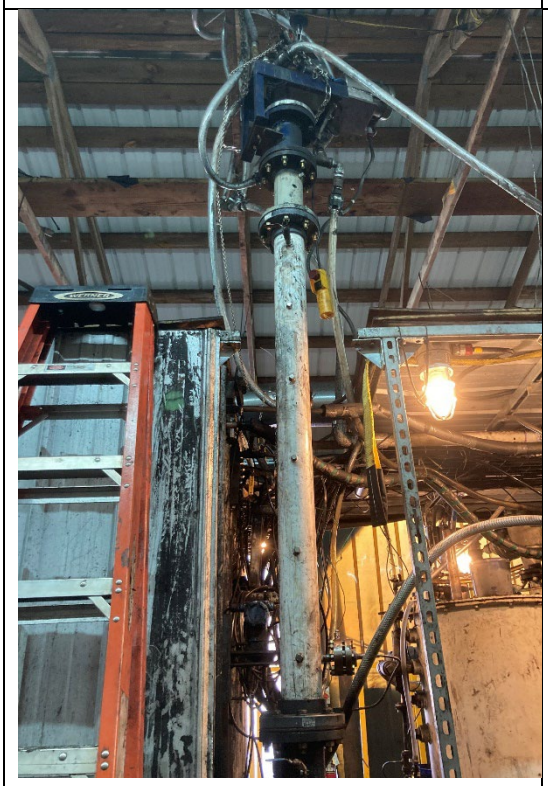
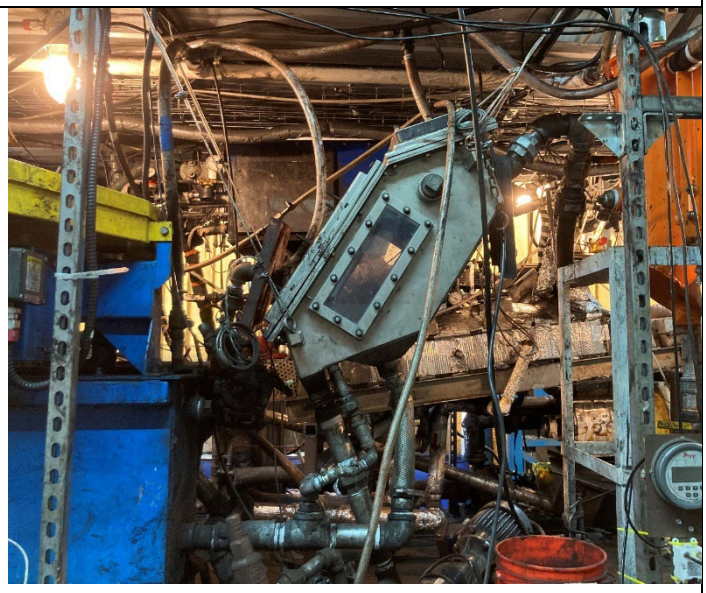
Utility room with air generators.	PLC units.
	
Power supply from PLC to motors.	Firewall between process and PLC/utility
	

Initial agglomeration setup.	Initial thickener unit.
	
Flotation cells installed.	Finished drum filter.
	

Installation of thermal dryer.	Hot oil piping installed.
	
Tailings pump installed.	Rear view of process after installation.
	

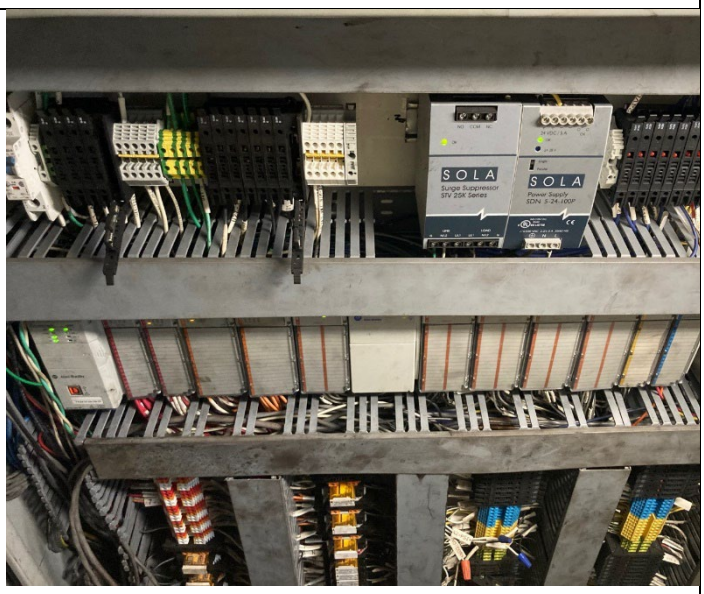
Post installation of major components.	Pneumatic control bank.
	
Touch PLC control screen.	Initial pilot plant setup.
	

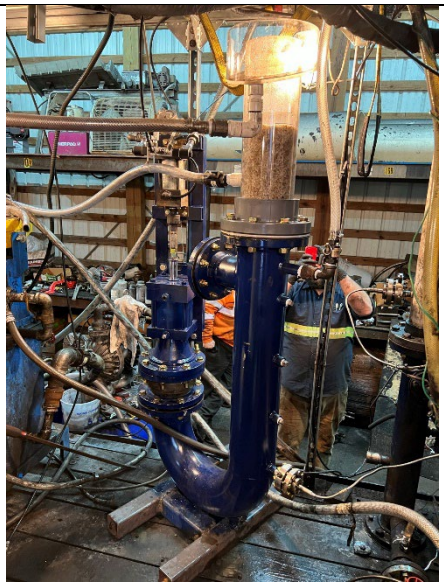
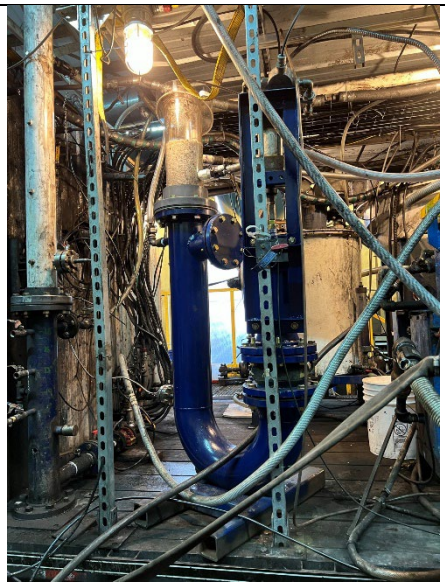
PVC standpipe.	Column underflow control valve.
	
Initial spring trials.	Final testing facility.
	

PVC oscillating column.	New high shear pump.
	
New low shear tank.	Sieve screen installed.
	

Oscillating disc stack.	New high shear mixer.
	
Vertical column baffles.	4” structured packing.
	

Iso-hexane area monitor.	Conspec control box.
	
Nitrogen generator.	Chiller unit.
	

Closeup of VFD.	Fuse bank.
	
Oil heater control box.	Onboard fire extinguisher bottle.
	

New jig U-tube base.	New jig base installed on pilot plant.
	
New jig installed on pilot plant.	New jig installed on pilot plant.
	

3D printed screen holder for jig.	Screen holder after use.
	
Revised column jig Morganizer.	Revised Morganizer being built.
	